

University of Groningen

Players in glioma progression

de Almeida Galatro, Thais

IMPORTANT NOTE: You are advised to consult the publisher's version (publisher's PDF) if you wish to cite from it. Please check the document version below.

Document Version

Publisher's PDF, also known as Version of record

Publication date:

2017

[Link to publication in University of Groningen/UMCG research database](#)

Citation for published version (APA):

de Almeida Galatro, T. (2017). *Players in glioma progression: Genomic exploration of glioma cell compartments*. [Thesis fully internal (DIV), University of Groningen]. University of Groningen.

Copyright

Other than for strictly personal use, it is not permitted to download or to forward/distribute the text or part of it without the consent of the author(s) and/or copyright holder(s), unless the work is under an open content license (like Creative Commons).

The publication may also be distributed here under the terms of Article 25fa of the Dutch Copyright Act, indicated by the "Taverne" license. More information can be found on the University of Groningen website: <https://www.rug.nl/library/open-access/self-archiving-pure/taverne-amendment>.

Take-down policy

If you believe that this document breaches copyright please contact us providing details, and we will remove access to the work immediately and investigate your claim.

Downloaded from the University of Groningen/UMCG research database (Pure): <http://www.rug.nl/research/portal>. For technical reasons the number of authors shown on this cover page is limited to 10 maximum.

Players in glioma progression

Genomic exploration of glioma cell
compartments

Thais Fernanda de Almeida Galatro

ISBN/EAN: 978-94-6182-790-6
NUR-code: 870
NUR-omschrijving: Geneeskunde algemeen

Sponsors: Fundação de Amparo à Pesquisa do Estado de São Paulo (Fapesp),
Fundação Faculdade de Medicina, BCN.



university of
 groningen

Players in glioma progression

Genomic exploration of glioma cell compartments

PhD thesis

to obtain the degree of PhD at the
 University of Groningen
 on the authority of the
 Rector Magnificus Prof E. Sterken
 in accordance with
 the decision by the College of Deans

This thesis will be defended in public on

26th of April 2017 at 14:30 hours

by

Thais Fernanda de Almeida Galatro

born on 8th of June 1986
 in Santos, Brazil

Promoters

Prof. dr. B.J.L. Eggen

Prof. dr. H.W.G.M. Boddeke

Prof. dr. S.K.N. Marie

Assessment committee

Prof. dr. F. A. E. Kruyt

Prof. dr. U. L. M. Eisel

Prof. dr. H. Kettenmann

Content

Chapter 1	6
<i>General introduction</i>	
Chapter 2	28
<i>Differential expression of ID4 and its association with TP53 mutation, SOX2, SOX4 and OCT-4 expression levels</i>	
Chapter 3	54
<i>Current state-of-the-art in molecular stratification of GBM and characterization of a Brazilian cohort.</i>	
Chapter 4	71
<i>Characterization of inhibitors of differentiation (ID) 1-4 expression in human gliomas</i>	
Chapter 5	93
<i>Isolation of microglia and immune infiltrates from mouse and primate central nervous system</i>	
Chapter 6	108
<i>The human microglia transcriptome and age-associated changes in actin dynamics and cell function</i>	
Chapter 7	146
<i>Microglia molecular signature in diffuse gliomas</i>	
Chapter 8	182
<i>Summary and general discussion</i>	
Chapter 9	200
<i>Nederlandse samenvatting</i>	
Acknowledgements	211

CHAPTER 1

GENERAL INTRODUCTION

Tumors of the Central Nervous System

Central Nervous System (CNS) tumors are relatively rare, with the world incidence of primary brain tumors affecting 7 individuals in 100,000 inhabitants per year (Ostrom et al., 2015). They represent a vastly heterogeneous group of neoplasias originating from intracranial tissues and meninges. They vary according to their tissue of origin, location, dissemination pattern, clinical history, age of occurrence and diagnosis (Chen et al., 2016; Collins, 2004). CNS tumors are quite aggressive, and the percentage of a 5 years' overall survival after diagnosis can be as low as 6.0% (Ostrom et al., 2015). The World Health Organization (WHO) recognizes over 120 forms of brain tumors (Louis et al., 2007, 2016) of which gliomas are the most frequent.

Gliomas are a heterogeneous group of primary neuroectodermal tumors, originating from glial cells – such as astrocytes and oligodendrocytes, or their progenitor cells. Previous classifications (Louis et al., 2007) subdivided gliomas in different grades of malignancy (grade I-IV) based mainly on histological and clinical features, along with tumor growing pattern. The current classification associates previous information with mutational data, specifically *IDH1/2* mutations, whose alterations occur early in diffuse glioma tumorigenesis (both from astrocytic and oligodendrocytic origins) (Louis et al., 2016; Parsons et al., 2008). As a consequence, classification has become more complete, grouping prognostic markers and helping guide the treatment for gliomas that are biologically and genetically similar. Figure 1 displays the new classification.

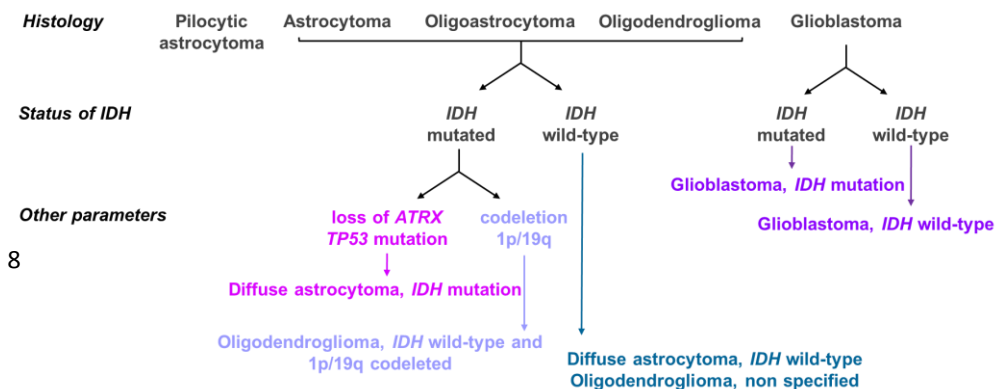


Figure 1: 2016 WHO grade classification of gliomas

Pilocytic astrocytoma

Grade I pilocytic astrocytomas (AGI) occur mainly in the cerebellum of children (Collins, 2004). In contrast to other gliomas, AGI are slow growing, circumscribed tumors. If surgical resection is possible, the prognosis is relatively good (Ichimura et al., 2004).

The genetic association of the neurofibromatosis type I gene, *NF1*, and AGI is well established (Reis and Tihan, 2015). *NF1* is a transcriptional suppressor that negatively regulates *RAS* oncogene expression. When constitutively activated, *RAS* protein leads to the subsequent activation of the mTOR signaling pathway and of associated cell proliferation transcription factors.

The fusion between *KIAA1549* and *BRAF* genes and a copy number gain of 1.9MB in chromosome 7q34, are also involved in the pathology of AGI. This is the most frequent genetic alteration in this type of tumor (Deshmukh et al., 2008; Pfister et al., 2008). The consequence of such fusion is the loss of the amino terminal domain of *BRAF* protein, constitutively activating its kinase activity and increasing cell proliferation.

Diffuse gliomas

Diffuse gliomas (classified as grade II-IV by WHO (Louis et al., 2016)) are infiltrative CNS tumors. Astrocytomas, oligodendrogliomas and glioblastomas (GBM) are included in this classification. Due to their invasive nature, complete surgical resection of these tumors is very difficult to achieve. The presence of residual tumor cells results in recurrence and malignant progression, albeit at different intervals. Part of lower grade tumors will either recur or progress to a GBM within months, while others will remain stable for years; the same is true for GBMs, with recurrence occurring at different rates (Cancer Genome Atlas Research Network et al., 2015;

Ceccarelli et al., 2016; Foote et al., 2015; Kamoun et al., 2016). The determining factors for one behavior or another are not yet completely understood.

Diffuse astrocytomas

Grades II and III of astrocytoma (AGII and AGIII, respectively) occur mostly in adults. Their main feature, invasiveness, is what makes their prognosis worse, as that hampers complete surgical resection (Ichimura et al., 2015). Both tumors can progress to higher grade malignancies (Furnari et al., 2007), a process of high clinical relevance, since AGII patients present an overall survival (OS) of 7 years; this time is reduced by 50% in the case of AGIII and to less than 15 months in the case of grade IV tumors (glioblastomas, GBMs) (Binder et al., 2016).

Diffuse astrocytomas present molecular particular features identified in high performance genetic studies completed in the past few years (Cancer Genome Atlas Research Network et al., 2015; Ceccarelli et al., 2016). IDH1/2 mutations are present in most of the cases, and were recently listed as crucial for the diagnosis of AGII by the WHO (Louis et al., 2016). Mutations that inactivate the functions of both ATRX and TP53 are also frequent, with the first being essential to differentiate between astrocytic and oligodendrocytic tumors. Epigenetic alterations, such as methylation of CpG islands (G-CIMP) are present in 55% of cases (Ceccarelli et al., 2016).

Oligodendrogliomas

Oligodendrogliomas (OD) constitute less than 10% of all gliomas (Ostrom et al., 2015). ODs mainly occur in young adults and, although more delimited than astrocytomas, ODs also can infiltrate the surrounding normal brain tissue. In approximately 50% of the cases there is the presence of calcification, a feature that has been useful for clinical diagnosis (Wesseling et al., 2015). High-throughput molecular studies (Cancer Genome Atlas Research Network et al., 2015; Ceccarelli et al., 2016) identified the co-deletion of chromosomes 1p/9q arms and mutation in TERT and FUBP1 genes as genetic markers of oligodendrogliomas.

OD patients have a better prognosis than astrocytoma patients, and their mean OS ranges between 12-14 years. The tumor can remain silent for many years. However, in a selected number of cases, the development of tumors with clinical and histological

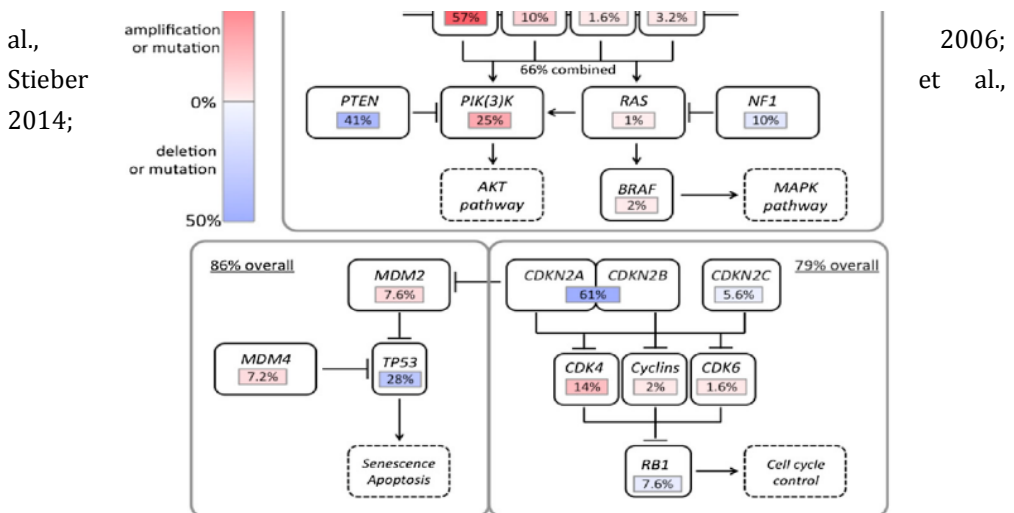
features of high malignancies (either grade III or even grade IV), occurs (Louis et al., 2016).

Glioblastomas

Glioblastomas (GBM) are extremely aggressive, highly malignant, and the most frequent of gliomas. Their main features include high mitotic and vascular proliferation rates, necrosis and resistance to both chemotherapy and radiotherapy treatments (Cloughesy et al., 2014). GBMs occur mainly in adults and can originate *de novo* (primary), without any previous history of a lower grade tumor, or through the malignant transformation of pre-existing tumors, which occurs in around 5% of the cases (Ohgaki and Kleihues, 2013).

Recent advances in integrated large scale strategies allowed the identification of genetic alterations singular to GBM's genesis and progression (Brennan et al., 2013; Cancer Genome Atlas Research Network et al., 2015; Ceccarelli et al., 2016; Phillips et

Figure 2: Main molecular alterations and signaling pathways in glioblastomas. Adapted from (Brennan et al., 2013).



Verhaak et al., 2010) (Figure 2).

These genetic studies have identified four molecular subtypes of GBM: Proneural, Classical, Neural and Mesenchymal. The proneural subtype is characterized

by alterations in *IDH1/2*, *TP53* and *PDGFRA* genes. The prognosis for patients with this type of GBM is better, since it has been previously shown that alterations in *IDH1/2* genes are an independent better prognosis factor (Yan et al., 2009). There are no specific genetic alterations detected in the neural subtype. This subtype is mainly defined by the overexpression of normal neural markers, such as *GABRA1* and *SYT1*, as well as *MBP* and *SNCG* (Verhaak et al., 2010). The other two subtypes, Classical and Mesenchymal, present distinct molecular features, albeit similar clinical outcomes and prognosis – and both have a worse prognosis than Proneural GBM. The identity of the Classical subtype is defined by amplifications in chromosome 7 and deletions in chromosome 10, corresponding to *EGFR* mutations/amplifications, such as the oncogenic variant *EGFRVIII* (Thorne et al., 2016), and loss of the *Ink4a/ARF* locus, respectively. The deletion of *CDKN2A* gene happens in around 95% of Classical GBM cases (Verhaak et al., 2010). Finally, 57% of the Mesenchymal subtype carries mutations in the *NF1* gene, mutations/deletion of *RB1* gene in 13% of cases and overexpression of *CHI3L1* and *MET*, genes associated to epithelial-to-mesenchymal transition and of a worse prognosis (Phillips et al., 2006; Verhaak et al., 2010).

Despite being prevalent in a specific subgroup, we can observe in Figure 3 that the molecular alterations associated to each GBM subtype are not exclusive. It is also worthwhile to remember that very few of these alterations happen in *hotspots* – regions with an accumulation of mutations (Rogozin and Pavlov, 2003) – as is the case of *IDH1* (R132H mutation) and the oncogenic variant *EGFRVIII*. Therefore, to achieve precise molecular classification of GBMs one would need a global analysis of its genetic alterations.

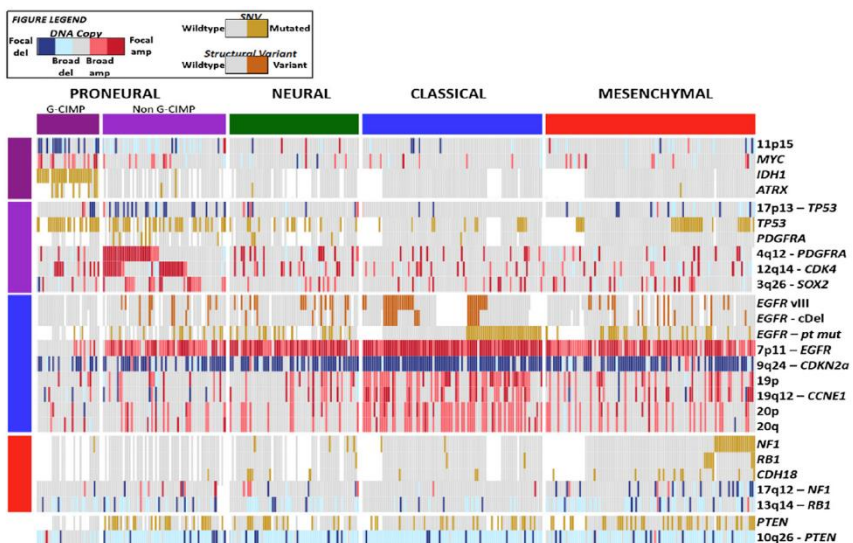


Figure 3: *The molecular subtypes of glioblastomas.* Adapted from (Brennan et al., 2013).

Despite further elucidating the biology of GBMs and their complex intrinsic heterogeneity, these findings also hinder treatment options, given the plethora of possible therapeutic targets.

Glioma microenvironment

Glioma tumorigenicity is not exclusively the result of its genetic alterations. The crosstalk between tumor cells and the surrounding microenvironment plays a crucial role in modulating glioma growth and aggressiveness. Cells that constitute this microenvironment include cancer stem cells, endothelial cells, pericytes and normal CNS cells, such as glial cells, neurons and microglia (Charles et al., 2011). The distribution of such cells leads to the formation of specific niches, rendering the glioma microenvironment vastly heterogeneous. The consequence is the maintenance of tumor growth and resistance to immune system attacks and to treatment (Hambardzumyan and Bergers, 2015). The most abundant, non-neoplastic cells in this microenvironment belong to the myeloid lineage, comprising of CNS-resident microglia, and infiltrating tumor associated monocytes/macrophages (further called iTAMs) originating in the bone marrow (Hambardzumyan et al., 2015). A recent study showed that myeloid immune cells are the first to respond during the early phases of gliomagenesis (Chen et al., 2015).

Microglia, origin and development

Microglia the resident immune cells of the CNS with a unique ontogeny and are crucially shaped by their local CNS environment (Salter and Beggs, 2014). They represent around 10% of all brain cells (Ransohoff and El Khoury, 2016). Microglia were first described by the work of R o Ortega, early in the 20th century (Tremblay et al., 2015), where he detailed microglia cell morphology: a small cell body highly branched ramifications. During development, microglia are implicated in neuronal network formation by synaptic pruning. This monitoring function continues into adulthood and

is essential for the maintenance of homeostasis (Davalos et al., 2005; Nimmerjahn et al., 2005).

Fate mapping studies showed that microglia have a different ontogeny than other tissue macrophages (Hoeffel et al., 2015). Microglia originate from erythro-myeloid progenitors in the yolk sac and exert an assortment of functions, like antigen-presentation, phagocytosis, neural support and are implicated in shaping neural networks, further described on the next topic (Hoeffel et al., 2015; Kierdorf et al., 2013; Schulz et al., 2012). Genome-wide transcriptome and epigenome studies of mouse microglia showed that microglia cluster very differently from other tissue macrophages and other glial cells (Butovsky et al., 2014; Chiu et al., 2013; Hickman et al., 2013; Zhang et al., 2014). In mice, microglia develops from one progenitor cell, an erythro-myeloid progenitor from the yolk sac, and migrate to the brain very early in development, contrary to what happens with other tissue resident macrophages, that develop later and go through to the fetal liver before migrate to their specific tissues (Ginhoux and Williams, 2016; Ginhoux and Prinz, 2015; Kierdorf et al., 2013; Schulz et al., 2012). These studies also revealed that microglia genesis is dependent on the signaling of colony stimulating factor 1 receptor (*CSF1R*) and transcription factors *PU.1* and *IRF8* (Kierdorf et al., 2013).

After infiltrating the brain, these cells develop, become self-sufficient and, in homeostatic conditions, there is no infiltration from circulating monocytes/macrophages (Perdiguero and Geissmann, 2016; Ransohoff, 2011). Recent study (Elmore et al., 2014), in which there was depletion of microglial cells from the mouse brain using *CSF1R* inhibitors, this population was replaced by new microglia within a week after inhibition was stopped. This study revealed the existence of a Nestin-positive microglia population. Another study (Bruttger et al., 2015), using genetic ablation of microglia, showed that these cells form clusters of proliferative cells that express high levels of *IL1R1*, and that these cells are responsible for the repopulation of the mouse brain.

Microglia function

The role of microglia in monitoring the brain during homeostasis is well established, along with its function in the defense of CNS in the advent of bacterial and viral infections, lesions, neurodegenerative and auto-immune diseases (Shemer et al., 2015). During homeostasis, microglia have a small cell body and extended ramifications

in order to monitor the surrounding environment and to connect itself to synaptic and extra-synaptic regions (Tremblay et al., 2010). When activated by stimuli, whether they are physiological or pathological, microglia retracts their ramifications and become amoeboid. This process is quite fast and dynamic, and is reversible at any stage (Colton et al., 2000; Karperien et al., 2013).

Microglia express receptors on their membrane capable of measuring synaptic activity, underlying a role for these cells in the removal of “weak” synapses (synaptic pruning) (Kettenmann et al., 2011; Paolicelli et al., 2011; Schafer et al., 2012). At the same time, other studies suggested the participation of microglia in processes such as the formations of synapses, neuronal survival and axonal growth (Parkhurst et al., 2013; Ueno et al., 2013; Wu et al., 2015).

As CNS phagocytes, microglial cells are responsible for the identification and removal of apoptotic cells, as well as acting as the first line of defense against pathogens (Ransohoff and El Khoury, 2016). Through the fractalkine receptor (CX3CR1), they are able to respond to phagocytosis stimuli sent from cells entering apoptosis, in addition to controlling the number of neurons, even being able to induce programmed cell death to those cells (Brown and Neher, 2014; Sokolowski et al., 2014). All of these mechanisms maintain the homeostatic state in the brain and confer to microglia the title of “guardian of the CNS” (Figure 4).

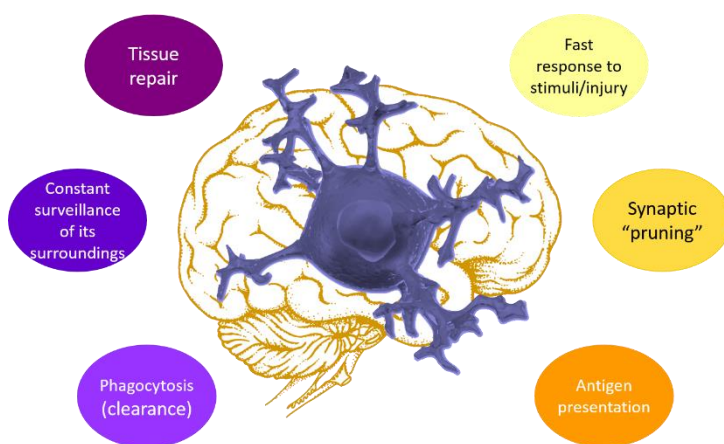


Figure 4: *Microglia function as “guardians of the CNS”.*

Microglia under pathological conditions

The role of microglia in neurodegenerative diseases, such as Alzheimer's Disease (Heppner et al., 2015) and Parkinson's Disease (Sanchez-Guajardo et al., 2015), as well as in auto-immune diseases, such as multiple sclerosis (Mahad et al., 2015), has been thoroughly studied. Upon the onset of glioma, microglia respond to its stimuli as it does to any other injury. However, this interaction has raised controversy, as there is no consensus whether microglia responses to glioma are always the same, beneficial to tumor growth, or what are their variations. The focus of this work is how microglia changes in the advent of glioma, and we will present current literature on the matter in the next sections.

Infiltrated monocytes and macrophages

While the only myeloid cell in the normal brain is microglia, under neuropathological conditions, blood brain barrier integrity is affected and allows infiltration of myeloid cells from the periphery. Monocytes that infiltrate the brain originate from hematopoietic stem-cells in the bone marrow (Shi and Pamer, 2011) and are, therefore, ontogenetically different from microglia. However, to differentiate between these two cell types in the diseased brain has always been arduous, since there is a lack of specific markers and previous reports suggested that circulating monocytes can remain in the CNS after inflammation is resolved, and acquire microglia-like features further hampering distinction between resident microglia and infiltrated myeloid cells (Flügel et al., 2001; Hickey and Kimura, 1988; Massengale et al., 2005). This last hypothesis was contradicted by murine parabiosis experiments, where it was demonstrated that infiltrated cells disappear from the CNS when the disease enters remission (Ajami et al., 2011). For mice, it is possible to identify infiltrated monocytes using the LY-6C marker. For human, so far there is no reliable marker known to make the same differentiation.

Activation of microglia and iTAMs and their role in glioma

As mentioned before, innate immune cells such as microglia and iTAMs are major components of the glioma microenvironment, constituting to up to 40% of the tumor mass. There are conflicting studies regarding the role of such cells in tumor progression. While some claim better outcomes for patients with high rates of immune

cells, either by infiltration or from the resident tissue, many others have assessed the same phenomena to be related to poorer prognosis (reviewed by Fridman *et al* (Fridman et al., 2012)). Such divergence in results seems to arise from the different functional and activation states innate immune cells can adopt within the same tumor and at different time points. Considering their ability to respond readily to stimuli, changes the microenvironment can lead both to anti or pro-tumoral responses.

Historically, microglia and iTAMs activation has been classified as classic (M1) and alternative (M2) (Galdiero et al., 2013; Hao et al., 2012; Mantovani et al., 2002). Classical activation corresponds to a pro-inflammatory phenotype, and its features include the production of iNOS, free radicals and inflammatory cytokines such as TNF-alpha and IL1-beta. The anti-inflammatory phenotype (M2, alternative) is particular to tissue repair, in which there is an increased production of arginase 1, of cell surface receptor CD163, and the release of growth factors such as TGF-beta and the hepatocyte growth factor. Gamma interferon and microbial products induce classic activation, while interleukin 4 or even TGF-beta lead to a M2 phenotype. Due to the fast way both microglia and iTAMs respond to stimuli, there is high controversy regarding the M1/M2 polarization. However, this classification still is broadly used and corresponds to clinical alterations (Ellert-Miklaszewska et al., 2013; Gabrusiewicz et al., 2015; Ghoochani et al., 2016; Nakagawa and Chiba, 2014).

Studies have demonstrated that iTAMs promote tumor growth using mechanisms that are solely immunological, but also non-immunological mechanisms; and that in the majority of cases, they present an anti-inflammatory phenotype (Mantovani et al., 2008; Pollard, 2009; Solinas et al., 2009). The same is true for microglia (Glass and Synowitz, 2014). The secreted factors in this activation phenotype promote, for instance, increased tumor angiogenesis (Brandenburg et al., 2016; Muramatsu et al., 2010), increased glioma cell motility and invasion (Bettinger et al., 2002), as well as interactions with cancer stem-cells, enhancing tumor proliferative capacity and resistance to therapy (Sarkar et al., 2014; Ye et al., 2012; Zhou et al., 2015).

Immune evasion – characterized by the ability tumor cells have to manipulate the immune system via secretion of cytokines and growth factors, and one of the hallmarks of cancer (Hanahan, 2014) to promote tumor progression and escape destruction –, is crucially dependent on the crosstalk between these two types of cells. In the scope of glioma, with such high heterogeneity rates found in tumor cells, targeting non-neoplastic cells, particularly microglia and iTAMs, seems to be a more

effective gambit to understand and overcome the mechanisms associated with recurrence and therapeutic resistance.

Despite all the evidence just cited, the great majority of the studies was done in mice, where it is possible to differentiate between microglia and iTAMs. Another aspect that hampers the extrapolation of murine results to humans is the fact that mice gliomas are not very similar to human gliomas regarding their cell of origin and molecular alterations (Szatmári et al., 2006). Different molecular subtypes of GBM have varied clinical behavior (Li et al., 2015; Natesh et al., 2015; Steed et al., 2016), and might interact differently with the microenvironment. Besides, the evaluation of expression of microglia activation markers in human gliomas needs a control population for comparison. In most cases, samples from epilepsy surgeries are used in human studies. Microglia associated to epilepsy displays an intrinsic inflammatory status that differs from normal, homeostatic microglia (Devinsky et al., 2013; Eyo et al., 2016). The use of post-mortem brain tissue is a useful alternative, provided the protocols and the characterization of the material is through.

Aims of this thesis

The main goal of this thesis is to study the status and phenotype of microglia in human gliomas and to delineate the human microglia gene expression profile. Microglia are essential for the homeostasis and protection of the CNS. Because of their plasticity, microglia readily respond to stimuli and become activated, exerting their functional roles. Gliomas, the most common of brain tumors, possess high percentages of those cells, along with iTAMs. The intrinsic heterogeneity of gliomas results in different responses to the microenvironment, depending on the type of tumor. Advances in large scale genetic studies have enabled the identification and characterization of different molecular subtypes of gliomas. However, there is little progress in treatment options so far. Understanding the dynamics between tumor and myeloid cells and the correlation between oncogenic molecular alterations in the tumor and the changes leading to pro-tumorigenic activation of innate immunity cells would elucidate potential treatment alternatives.

Outline of thesis

In this **Chapter 1**, we reviewed the current literature on glioma biology, classification and molecular subtyping. We also explored the knowledge in the function of cells belonging to glioma microenvironment innate immune compartment, namely microglia and iTAMs.

In **Chapter 2**, we analyzed the expression and correlation of genes associated with stemness and glioma stem cells (*ID4*, *SOX4* and *OCT-4*), an association that imparts shorter overall survival in primary GBM patients.

In **Chapter 3**, we applied NGS technology to classify a Brazilian cohort of GBM samples. We assessed the correlation of our molecular findings using a more feasible proteomic immunohistochemistry-based approach. Our results indicate the need for a genetic approach to further classify GBMs, particularly the Mesenchymal subtype.

In **Chapter 4**, we explored the role of a family of transcription factors, inhibitors of differentiation (IDs) in gliomas from different origins (astrocytic and oligodendrocytic) and grades (I-IV), as well as the different GBM subtypes classified in Chapter 3. We show an association between IDs and the proneural subtype of GBM, as well as their usefulness in differentiating between astrocytomas and oligodendrogliomas.

In **Chapter 5**, we describe a protocol for *ex vivo* isolation of pure populations of microglia and myeloid infiltrates from the CNS, based on mechanical dissociation followed by FACS-sorting.

In **Chapter 6**, we identified the human microglia transcriptome and assessed how the aging process affects these cells. Aside from stipulating a core of genes responsible for human microglia identity, we also demonstrated that genes related to actin modulation are affected during aging, possibly hampering cell motility.

Finally, in **Chapter 7**, we report the differences found in the transcriptome of glioma and normal human microglia, as well as the differences between microglia derived from lower grade gliomas and glioblastomas. We propose a transcriptional network of regulators responsible for the proliferative and motility changes we found, as well as related the extracellular matrix genes overexpression to the most malignant subtypes of GBMs (Mesenchymal).

In **Chapter 8**, a summary and discussion of the principal findings from this thesis are presented, as well as an overview of possible future direction on experiments involving the cells that play an important role in glioma progression.

REFERENCES

- Ajami, B., Bennett, J.L., Krieger, C., McNagny, K.M., and Rossi, F.M.V. (2011). Infiltrating monocytes trigger EAE progression, but do not contribute to the resident microglia pool. *Nat. Neurosci.* *14*, 1142–1149.
- Bettinger, I., Thanos, S., and Paulus, W. (2002). Microglia promote glioma migration. *Acta Neuropathol. (Berl.)* *103*, 351–355.
- Binder, D.C., Davis, A.A., and Wainwright, D.A. (2016). Immunotherapy for cancer in the central nervous system: Current and future directions. *Oncoimmunology* *5*, e1082027.
- Brandenburg, S., Müller, A., Turkowski, K., Radev, Y.T., Rot, S., Schmidt, C., Bungert, A.D., Acker, G., Schorr, A., Hippe, A., et al. (2016). Resident microglia rather than peripheral macrophages promote vascularization in brain tumors and are source of alternative pro-angiogenic factors. *Acta Neuropathol. (Berl.)* *131*, 365–378.
- Brennan, C.W., Verhaak, R.G.W., McKenna, A., Campos, B., Noushmehr, H., Salama, S.R., Zheng, S., Chakravarty, D., Sanborn, J.Z., Berman, S.H., et al. (2013). The somatic genomic landscape of glioblastoma. *Cell* *155*, 462–477.
- Brown, G.C., and Neher, J.J. (2014). Microglial phagocytosis of live neurons. *Nat. Rev. Neurosci.* *15*, 209–216.
- Bruttger, J., Karram, K., Wörtge, S., Regen, T., Marini, F., Hoppmann, N., Klein, M., Blank, T., Yona, S., Wolf, Y., et al. (2015). Genetic Cell Ablation Reveals Clusters of Local Self-Renewing Microglia in the Mammalian Central Nervous System. *Immunity* *43*, 92–106.
- Butovsky, O., Jedrychowski, M.P., Moore, C.S., Cialic, R., Lanser, A.J., Gabriely, G., Koeglsperger, T., Dake, B., Wu, P.M., Doykan, C.E., et al. (2014). Identification of a unique TGF- β -dependent molecular and functional signature in microglia. *Nat. Neurosci.* *17*, 131–143.
- Cancer Genome Atlas Research Network, Brat, D.J., Verhaak, R.G.W., Aldape, K.D., Yung, W.K.A., Salama, S.R., Cooper, L.A.D., Rheinbay, E., Miller, C.R., Vitucci, M., et al. (2015). Comprehensive, Integrative Genomic Analysis of Diffuse Lower-Grade Gliomas. *N. Engl. J. Med.* *372*, 2481–2498.
- Ceccarelli, M., Barthel, F.P., Malta, T.M., Sabedot, T.S., Salama, S.R., Murray, B.A., Morozova, O., Newton, Y., Radenbaugh, A., Pagnotta, S.M., et al. (2016). Molecular

Profiling Reveals Biologically Discrete Subsets and Pathways of Progression in Diffuse Glioma. *Cell* 164, 550–563.

Charles, N.A., Holland, E.C., Gilbertson, R., Glass, R., and Kettenmann, H. (2011). The brain tumor microenvironment. *Glia* 59, 1169–1180.

Chen, R., Cohen, A.L., and Colman, H. (2016). Targeted Therapeutics in Patients With High-Grade Gliomas: Past, Present, and Future. *Curr. Treat. Options Oncol.* 17, 42.

Chen, Y.-H., McGowan, L.D., Cimino, P.J., Dahiya, S., Leonard, J.R., Lee, D.Y., and Gutmann, D.H. (2015). Mouse low-grade gliomas contain cancer stem cells with unique molecular and functional properties. *Cell Rep.* 10, 1899–1912.

Chiu, I.M., Morimoto, E.T.A., Goodarzi, H., Liao, J.T., O’Keeffe, S., Phatnani, H.P., Muratet, M., Carroll, M.C., Levy, S., Tavazoie, S., et al. (2013). A neurodegeneration-specific gene-expression signature of acutely isolated microglia from an amyotrophic lateral sclerosis mouse model. *Cell Rep.* 4, 385–401.

Cloughesy, T.F., Cavenee, W.K., and Mischel, P.S. (2014). Glioblastoma: from molecular pathology to targeted treatment. *Annu. Rev. Pathol.* 9, 1–25.

Collins, V.P. (2004). Brain tumours: classification and genes. *J. Neurol. Neurosurg. Psychiatry* 75 *Suppl* 2, ii2-11.

Colton, C.A., Chernyshev, O.N., Gilbert, D.L., and Vitek, M.P. (2000). Microglial contribution to oxidative stress in Alzheimer’s disease. *Ann. N. Y. Acad. Sci.* 899, 292–307.

Davalos, D., Grutzendler, J., Yang, G., Kim, J.V., Zuo, Y., Jung, S., Littman, D.R., Dustin, M.L., and Gan, W.-B. (2005). ATP mediates rapid microglial response to local brain injury in vivo. *Nat. Neurosci.* 8, 752–758.

Deshmukh, H., Yeh, T.H., Yu, J., Sharma, M.K., Perry, A., Leonard, J.R., Watson, M.A., Gutmann, D.H., and Nagarajan, R. (2008). High-resolution, dual-platform aCGH analysis reveals frequent HIPK2 amplification and increased expression in pilocytic astrocytomas. *Oncogene* 27, 4745–4751.

Devinsky, O., Vezzani, A., Najjar, S., Lanerolle, N.C.D., and Rogawski, M.A. (2013). Glia and epilepsy: excitability and inflammation. *Trends Neurosci.* 36, 174–184.

Ellert-Miklaszewska, A., Dabrowski, M., Lipko, M., Sliwa, M., Maleszewska, M., and Kaminska, B. (2013). Molecular definition of the pro-tumorigenic phenotype of glioma-activated microglia. *Glia* 61, 1178–1190.

Elmore, M.R.P., Najafi, A.R., Koike, M.A., Dagher, N.N., Spangenberg, E.E., Rice, R.A., Kitazawa, M., Matusow, B., Nguyen, H., West, B.L., et al. (2014). Colony-stimulating

factor 1 receptor signaling is necessary for microglia viability, unmasking a microglia progenitor cell in the adult brain. *Neuron* *82*, 380–397.

Eyo, U.B., Murugan, M., and Wu, L.-J. (2016). Microglia-Neuron Communication in Epilepsy. *Glia*.

Flügel, A., Bradl, M., Kreutzberg, G.W., and Graeber, M.B. (2001). Transformation of donor-derived bone marrow precursors into host microglia during autoimmune CNS inflammation and during the retrograde response to axotomy. *J. Neurosci. Res.* *66*, 74–82.

Foote, M.B., Papadopoulos, N., and Diaz, L.A. (2015). Genetic Classification of Gliomas: Refining Histopathology. *Cancer Cell* *28*, 9–11.

Fridman, W.H., Pagès, F., Sautès-Fridman, C., and Galon, J. (2012). The immune contexture in human tumours: impact on clinical outcome. *Nat. Rev. Cancer* *12*, 298–306.

Furnari, F.B., Fenton, T., Bachoo, R.M., Mukasa, A., Stommel, J.M., Stegh, A., Hahn, W.C., Ligon, K.L., Louis, D.N., Brennan, C., et al. (2007). Malignant astrocytic glioma: genetics, biology, and paths to treatment. *Genes Dev.* *21*, 2683–2710.

Gabrusiewicz, K., Hossain, M.B., Cortes-Santiago, N., Fan, X., Kaminska, B., Marini, F.C., Fueyo, J., and Gomez-Manzano, C. (2015). Macrophage Ablation Reduces M2-Like Populations and Jeopardizes Tumor Growth in a MAFIA-Based Glioma Model. *Neoplasia N. Y. N* *17*, 374–384.

Galdiero, M.R., Garlanda, C., Jaillon, S., Marone, G., and Mantovani, A. (2013). Tumor associated macrophages and neutrophils in tumor progression. *J. Cell. Physiol.* *228*, 1404–1412.

Ghoochani, A., Schwarz, M.A., Yakubov, E., Engelhorn, T., Doerfler, A., Buchfelder, M., Bucala, R., Savaskan, N.E., and Eyüpoglu, I.Y. (2016). MIF-CD74 signaling impedes microglial M1 polarization and facilitates brain tumorigenesis. *Oncogene*.

Ginhoux, F., and Guilliams, M. (2016). Tissue-Resident Macrophage Ontogeny and Homeostasis. *Immunity* *44*, 439–449.

Ginhoux, F., and Prinz, M. (2015). Origin of microglia: current concepts and past controversies. *Cold Spring Harb. Perspect. Biol.* *7*, a020537.

Glass, R., and Synowitz, M. (2014). CNS macrophages and peripheral myeloid cells in brain tumours. *Acta Neuropathol. (Berl.)* *128*, 347–362.

Hambardzumyan, D., and Bergers, G. (2015). Glioblastoma: Defining Tumor Niches. *Trends Cancer* *1*, 252–265.

Hambardzumyan, D., Gutmann, D.H., and Kettenmann, H. (2015). The role of microglia and macrophages in glioma maintenance and progression. *Nat. Neurosci.* *19*, 20–27.

Hanahan, D. (2014). Rethinking the war on cancer. *Lancet Lond. Engl.* *383*, 558–563.

Hao, N.-B., Lü, M.-H., Fan, Y.-H., Cao, Y.-L., Zhang, Z.-R., and Yang, S.-M. (2012). Macrophages in tumor microenvironments and the progression of tumors. *Clin. Dev. Immunol.* *2012*, 948098.

Heppner, F.L., Ransohoff, R.M., and Becher, B. (2015). Immune attack: the role of inflammation in Alzheimer disease. *Nat. Rev. Neurosci.* *16*, 358–372.

Hickey, W.F., and Kimura, H. (1988). Perivascular microglial cells of the CNS are bone marrow-derived and present antigen in vivo. *Science* *239*, 290–292.

Hickman, S.E., Kingery, N.D., Ohsumi, T.K., Borowsky, M.L., Wang, L., Means, T.K., and El Khoury, J. (2013). The microglial sensome revealed by direct RNA sequencing. *Nat. Neurosci.* *16*, 1896–1905.

Hoeffel, G., Chen, J., Lavin, Y., Low, D., Almeida, F.F., See, P., Beaudin, A.E., Lum, J., Low, I., Forsberg, E.C., et al. (2015). C-Myb(+) erythro-myeloid progenitor-derived fetal monocytes give rise to adult tissue-resident macrophages. *Immunity* *42*, 665–678.

Ichimura, K., Ohgaki, H., Kleihues, P., and Collins, V.P. (2004). Molecular pathogenesis of astrocytic tumours. *J. Neurooncol.* *70*, 137–160.

Ichimura, K., Narita, Y., and Hawkins, C.E. (2015). Diffusely infiltrating astrocytomas: pathology, molecular mechanisms and markers. *Acta Neuropathol. (Berl.)* *129*, 789–808.

Kamoun, A., Idbaih, A., Dehais, C., Elarouci, N., Carpentier, C., Letouzé, E., Colin, C., Mokhtari, K., Jouvét, A., Uro-Coste, E., et al. (2016). Integrated multi-omics analysis of oligodendroglial tumours identifies three subgroups of 1p/19q co-deleted gliomas. *Nat. Commun.* *7*, 11263.

Karperien, A., Ahammer, H., and Jelinek, H.F. (2013). Quantitating the subtleties of microglial morphology with fractal analysis. *Front. Cell. Neurosci.* *7*, 3.

Kettenmann, H., Hanisch, U.-K., Noda, M., and Verkhratsky, A. (2011). Physiology of microglia. *Physiol. Rev.* *91*, 461–553.

Kierdorf, K., Erny, D., Goldmann, T., Sander, V., Schulz, C., Perdiguero, E.G., Wieghofer, P., Heinrich, A., Riemke, P., Hölscher, C., et al. (2013). Microglia emerge from erythromyeloid precursors via Pu.1- and Irf8-dependent pathways. *Nat. Neurosci.* *16*, 273–280.

Li, R., Li, H., Yan, W., Yang, P., Bao, Z., Zhang, C., Jiang, T., and You, Y. (2015). Genetic and clinical characteristics of primary and secondary glioblastoma is associated with differential molecular subtype distribution. *Oncotarget* 6, 7318–7324.

Louis, D.N., Ohgaki, H., Wiestler, O.D., Cavenee, W.K., Burger, P.C., Jouvet, A., Scheithauer, B.W., and Kleihues, P. (2007). The 2007 WHO classification of tumours of the central nervous system. *Acta Neuropathol. (Berl.)* 114, 97–109.

Louis, D.N., Perry, A., Reifenberger, G., von Deimling, A., Figarella-Branger, D., Cavenee, W.K., Ohgaki, H., Wiestler, O.D., Kleihues, P., and Ellison, D.W. (2016). The 2016 World Health Organization Classification of Tumors of the Central Nervous System: a summary. *Acta Neuropathol. (Berl.)* 131, 803–820.

Mahad, D.H., Trapp, B.D., and Lassmann, H. (2015). Pathological mechanisms in progressive multiple sclerosis. *Lancet Neurol.* 14, 183–193.

Mantovani, A., Sozzani, S., Locati, M., Allavena, P., and Sica, A. (2002). Macrophage polarization: tumor-associated macrophages as a paradigm for polarized M2 mononuclear phagocytes. *Trends Immunol.* 23, 549–555.

Mantovani, A., Allavena, P., Sica, A., and Balkwill, F. (2008). Cancer-related inflammation. *Nature* 454, 436–444.

Massengale, M., Wagers, A.J., Vogel, H., and Weissman, I.L. (2005). Hematopoietic cells maintain hematopoietic fates upon entering the brain. *J. Exp. Med.* 201, 1579–1589.

Muramatsu, M., Yamamoto, S., Osawa, T., and Shibuya, M. (2010). Vascular endothelial growth factor receptor-1 signaling promotes mobilization of macrophage lineage cells from bone marrow and stimulates solid tumor growth. *Cancer Res.* 70, 8211–8221.

Nakagawa, Y., and Chiba, K. (2014). Role of microglial m1/m2 polarization in relapse and remission of psychiatric disorders and diseases. *Pharm. Basel Switz.* 7, 1028–1048.

Natesh, K., Bhosale, D., Desai, A., Chandrika, G., Pujari, R., Jagtap, J., Chugh, A., Ranade, D., and Shastry, P. (2015). Oncostatin-M differentially regulates mesenchymal and proneural signature genes in gliomas via STAT3 signaling. *Neoplasia N. Y. N* 17, 225–237.

Nimmerjahn, A., Kirchhoff, F., and Helmchen, F. (2005). Resting microglial cells are highly dynamic surveillants of brain parenchyma in vivo. *Science* 308, 1314–1318.

Ohgaki, H., and Kleihues, P. (2013). The definition of primary and secondary glioblastoma. *Clin. Cancer Res. Off. J. Am. Assoc. Cancer Res.* 19, 764–772.

Ostrom, Q.T., Gittleman, H., Fulop, J., Liu, M., Blanda, R., Kromer, C., Wolinsky, Y., Kruchko, C., and Barnholtz-Sloan, J.S. (2015). CBTRUS Statistical Report: Primary Brain and Central Nervous System Tumors Diagnosed in the United States in 2008-2012. *Neuro-Oncol.* *17 Suppl 4*, iv1-iv62.

Paolicelli, R.C., Bolasco, G., Pagani, F., Maggi, L., Scianni, M., Panzanelli, P., Giustetto, M., Ferreira, T.A., Guiducci, E., Dumas, L., et al. (2011). Synaptic pruning by microglia is necessary for normal brain development. *Science* *333*, 1456–1458.

Parkhurst, C.N., Yang, G., Ninan, I., Savas, J.N., Yates, J.R., Lafaille, J.J., Hempstead, B.L., Littman, D.R., and Gan, W.-B. (2013). Microglia promote learning-dependent synapse formation through brain-derived neurotrophic factor. *Cell* *155*, 1596–1609.

Parsons, D.W., Jones, S., Zhang, X., Lin, J.C.-H., Leary, R.J., Angenendt, P., Mankoo, P., Carter, H., Siu, I.-M., Gallia, G.L., et al. (2008). An integrated genomic analysis of human glioblastoma multiforme. *Science* *321*, 1807–1812.

Perdiguerro, E.G., and Geissmann, F. (2016). The development and maintenance of resident macrophages. *Nat. Immunol.* *17*, 2–8.

Pfister, S., Janzarik, W.G., Remke, M., Ernst, A., Werft, W., Becker, N., Toedt, G., Wittmann, A., Kratz, C., Olbrich, H., et al. (2008). BRAF gene duplication constitutes a mechanism of MAPK pathway activation in low-grade astrocytomas. *J. Clin. Invest.* *118*, 1739–1749.

Phillips, H.S., Kharbanda, S., Chen, R., Forrest, W.F., Soriano, R.H., Wu, T.D., Misra, A., Nigro, J.M., Colman, H., Soroceanu, L., et al. (2006). Molecular subclasses of high-grade glioma predict prognosis, delineate a pattern of disease progression, and resemble stages in neurogenesis. *Cancer Cell* *9*, 157–173.

Pollard, J.W. (2009). Trophic macrophages in development and disease. *Nat. Rev. Immunol.* *9*, 259–270.

Ransohoff, R.M. (2011). Microglia and monocytes: 'tis plain the twain meet in the brain. *Nat. Neurosci.* *14*, 1098–1100.

Ransohoff, R.M., and El Khoury, J. (2016). Microglia in Health and Disease. *Cold Spring Harb. Perspect. Biol.* *8*, a020560.

Reis, G.F., and Tihan, T. (2015). Therapeutic targets in pilocytic astrocytoma based on genetic analysis. *Semin. Pediatr. Neurol.* *22*, 23–27.

Rogozin, I.B., and Pavlov, Y.I. (2003). Theoretical analysis of mutation hotspots and their DNA sequence context specificity. *Mutat. Res.* *544*, 65–85.

Salter, M.W., and Beggs, S. (2014). Sublime Microglia: Expanding Roles for the Guardians of the CNS. *Cell* *158*, 15–24.

Sanchez-Guajardo, V., Tentillier, N., and Romero-Ramos, M. (2015). The relation between α -synuclein and microglia in Parkinson's disease: Recent developments. *Neuroscience* 302, 47–58.

Sarkar, S., Döring, A., Zemp, F.J., Silva, C., Lun, X., Wang, X., Kelly, J., Hader, W., Hamilton, M., Mercier, P., et al. (2014). Therapeutic activation of macrophages and microglia to suppress brain tumor-initiating cells. *Nat. Neurosci.* 17, 46–55.

Schafer, D.P., Lehrman, E.K., Kautzman, A.G., Koyama, R., Mardinly, A.R., Yamasaki, R., Ransohoff, R.M., Greenberg, M.E., Barres, B.A., and Stevens, B. (2012). Microglia sculpt postnatal neural circuits in an activity and complement-dependent manner. *Neuron* 74, 691–705.

Schulz, C., Gomez Perdiguero, E., Chorro, L., Szabo-Rogers, H., Cagnard, N., Kierdorf, K., Prinz, M., Wu, B., Jacobsen, S.E.W., Pollard, J.W., et al. (2012). A lineage of myeloid cells independent of Myb and hematopoietic stem cells. *Science* 336, 86–90.

Shemer, A., Erny, D., Jung, S., and Prinz, M. (2015). Microglia Plasticity During Health and Disease: An Immunological Perspective. *Trends Immunol.* 36, 614–624.

Shi, C., and Pamer, E.G. (2011). Monocyte recruitment during infection and inflammation. *Nat. Rev. Immunol.* 11, 762–774.

Sokolowski, J.D., Chabanon-Hicks, C.N., Han, C.Z., Heffron, D.S., and Mandell, J.W. (2014). Fractalkine is a “find-me” signal released by neurons undergoing ethanol-induced apoptosis. *Front. Cell. Neurosci.* 8, 360.

Solinas, G., Germano, G., Mantovani, A., and Allavena, P. (2009). Tumor-associated macrophages (TAM) as major players of the cancer-related inflammation. *J. Leukoc. Biol.* 86, 1065–1073.

Steed, T.C., Treiber, J.M., Patel, K., Ramakrishnan, V., Merk, A., Smith, A.R., Carter, B.S., Dale, A.M., Chow, L.M.L., and Chen, C.C. (2016). Differential localization of glioblastoma subtype: implications on glioblastoma pathogenesis. *Oncotarget*.

Stieber, D., Golebiewska, A., Evers, L., Lenkiewicz, E., Brons, N.H.C., Nicot, N., Oudin, A., Bougnaud, S., Hertel, F., Bjerkvig, R., et al. (2014). Glioblastomas are composed of genetically divergent clones with distinct tumorigenic potential and variable stem cell-associated phenotypes. *Acta Neuropathol. (Berl.)* 127, 203–219.

Szatmári, T., Lumniczky, K., Désaknai, S., Trajcevski, S., Hídvégi, E.J., Hamada, H., and Sáfrány, G. (2006). Detailed characterization of the mouse glioma 261 tumor model for experimental glioblastoma therapy. *Cancer Sci.* 97, 546–553.

Thorne, A.H., Zanca, C., and Furnari, F. (2016). Epidermal growth factor receptor targeting and challenges in glioblastoma. *Neuro-Oncol.* 18, 914–918.

Tremblay, M.-È., Lowery, R.L., and Majewska, A.K. (2010). Microglial interactions with synapses are modulated by visual experience. *PLoS Biol.* *8*, e1000527.

Tremblay, M.-È., Lecours, C., Samson, L., Sánchez-Zafra, V., and Sierra, A. (2015). From the Cajal alumni Achúcarro and Río-Hortega to the rediscovery of never-resting microglia. *Front. Neuroanat.* *9*, 45.

Ueno, M., Fujita, Y., Tanaka, T., Nakamura, Y., Kikuta, J., Ishii, M., and Yamashita, T. (2013). Layer V cortical neurons require microglial support for survival during postnatal development. *Nat. Neurosci.* *16*, 543–551.

Verhaak, R.G.W., Hoadley, K.A., Purdom, E., Wang, V., Qi, Y., Wilkerson, M.D., Miller, C.R., Ding, L., Golub, T., Mesirov, J.P., et al. (2010). Integrated genomic analysis identifies clinically relevant subtypes of glioblastoma characterized by abnormalities in PDGFRA, IDH1, EGFR, and NF1. *Cancer Cell* *17*, 98–110.

Wesseling, P., van den Bent, M., and Perry, A. (2015). Oligodendroglioma: pathology, molecular mechanisms and markers. *Acta Neuropathol. (Berl.)* *129*, 809–827.

Wu, Y., Dissing-Olesen, L., MacVicar, B.A., and Stevens, B. (2015). Microglia: Dynamic Mediators of Synapse Development and Plasticity. *Trends Immunol.* *36*, 605–613.

Yan, H., Parsons, D.W., Jin, G., McLendon, R., Rasheed, B.A., Yuan, W., Kos, I., Batinic-Haberle, I., Jones, S., Riggins, G.J., et al. (2009). IDH1 and IDH2 mutations in gliomas. *N. Engl. J. Med.* *360*, 765–773.

Ye, X., Xu, S., Xin, Y., Yu, S., Ping, Y., Chen, L., Xiao, H., Wang, B., Yi, L., Wang, Q., et al. (2012). Tumor-associated microglia/macrophages enhance the invasion of glioma stem-like cells via TGF- β 1 signaling pathway. *J. Immunol. Baltim. Md 1950* *189*, 444–453.

Zhang, Y., Chen, K., Sloan, S.A., Bennett, M.L., Scholze, A.R., O’Keefe, S., Phatnani, H.P., Guarnieri, P., Caneda, C., Ruderisch, N., et al. (2014). An RNA-Sequencing Transcriptome and Splicing Database of Glia, Neurons, and Vascular Cells of the Cerebral Cortex. *J. Neurosci. Off. J. Soc. Neurosci.* *34*, 11929–11947.

Zhou, W., Ke, S.Q., Huang, Z., Flavahan, W., Fang, X., Paul, J., Wu, L., Sloan, A.E., McLendon, R.E., Li, X., et al. (2015). Periostin secreted by glioblastoma stem cells recruits M2 tumour-associated macrophages and promotes malignant growth. *Nat. Cell Biol.*

CHAPTER 2

Differential expression of *ID4* and its association with *TP53* mutation, *SOX2*, *SOX4* and *OCT-4* expression levels

Thais F. A. Galatro¹, Miyuki Uno^{1,2}, Sueli M. Oba-Shinjo^{1,2}, Antonio N. Almeida¹, Manoel J. Teixeira¹, Sérgio Rosemberg³, and Suely K. N. Marie^{1,2}

¹Department of Neurology, School of Medicine, University of São Paulo, São Paulo/SP, Brazil.

²Center of Translational Oncology, Instituto do Câncer do Estado de São Paulo (ICESP), São Paulo/SP, Brazil.

³Department of Pathology, School of Medicine, University of São Paulo, São Paulo/SP, Brazil

SUMMARY

Inhibitor of DNA Binding 4 (ID4) is a member of the helix-loop-helix ID family of transcription factors, mostly present in the central nervous system during embryonic development, that has been associated with *TP53* mutation and activation of *SOX2*. Along with other transcription factors, *ID4* has been implicated in the tumorigenic process of astrocytomas, contributing to cell dedifferentiation, proliferation and chemoresistance. In this study, we aimed to characterize the *ID4* expression pattern in human diffusely infiltrative astrocytomas of World Health Organization (WHO) grades II to IV of malignancy (AGII-AGIV); to correlate its expression level to that of *SOX2*, *SOX4*, *OCT-4* and *NANOG*, along with *TP53* mutational status; and to correlate the results with the clinical end-point of overall survival among glioblastoma patients. Quantitative real time PCR (qRT-PCR) was performed in 130 samples of astrocytomas for relative expression, showing up-regulation of all transcription factors in tumor cases. Positive correlation was found when comparing *ID4* relative expression of infiltrative astrocytomas with *SOX2* ($r=0.50$; $p<0.005$), *SOX4* ($r=0.43$; $p<0.005$) and *OCT-4* ($r=0.39$; $p<0.05$). The results from *TP53* coding exon analysis allowed comparisons between wild-type and mutated status only in AGII cases, demonstrating significantly higher levels of *ID4*, *SOX2* and *SOX4* in mutated cases ($p<0.05$). This pattern was maintained in secondary GBM and further confirmed by immunohistochemistry, suggesting a role for *ID4*, *SOX2* and *SOX4* in early astrocytoma tumorigenesis. Combined hyperexpression of *ID4*, *SOX4* and *OCT-4* conferred a much lower (6 months) median survival than did hypoexpression (18 months). Because both *ID4* alone and a complex of *SOX4* and *OCT-4* activate *SOX2* transcription, it is possible that multiple activation of *SOX2* impair the prognosis of GBM patients. These observational results of associated expression of *ID4* with *SOX4* and *OCT-4* may be used as a predictive factor of prognosis upon further confirmation in a larger GBM series.

INTRODUCTION

Inhibitor of DNA Binding (ID) proteins (ID1-4) belong to the helix-loop-helix (HLH) superfamily of transcription factors and exert their functions through the highly conserved HLH dimerization domain. Due to the lack of a DNA binding domain, IDs sequester and inhibit the activity of their specific target proteins, playing important roles in cell cycle control, growth, differentiation, angiogenesis and tumorigenesis (Benezra et al., 1990a, 1990b; Iavarone and Lasorella, 2004; Perk et al., 2005). In healthy organisms, *ID* expression is up-regulated in stem and progenitor cells, maintaining self-renewal capacity, pluripotency and an undifferentiated state. However, *ID* expression declines to basal values when cells differentiate towards the destined specific lineage (Iavarone and Lasorella, 2006; Norton, 2000). The expression of ID1-3 proteins is widespread, while the ID4 expression pattern is restricted to the developing brain, particularly in neural progenitor cells (Yun et al., 2004). The overexpression of IDs in tumor cells has been suggested to induce reversion to an embryonic-like state, with high rates of proliferation, migration and neo-angiogenesis facilitating tumor formation (Perk et al., 2005).

Astrocytomas are the most common primary brain tumors. World Health Organization (WHO) classifies the astrocytomas into four grades: grade I or pilocytic astrocytoma, grade II, or low-grade astrocytoma (AGII), grade III, or anaplastic astrocytoma (AGIII) and grade IV astrocytoma or glioblastoma (AGIV or GBM) (Louis et al., 2007). Diffusely infiltrative astrocytomas (AGII-GBM) invade the surrounding normal brain tissue, hampering tumor resection. GBM is the most malignant and frequent brain tumor in adults and they can be divided into two subgroups: primary GBM, which arise de novo, and secondary GBM, which results from the progression of a lower grade astrocytoma (Ohgaki and Kleihues, 2011, 2012). The malignant transformation of astrocytomas, is associated with augmented ID expression (Iavarone and Lasorella, 2004), particularly ID4 (Kuzontkoski et al., 2010; Zeng et al., 2010). Interestingly, the up-regulation of *ID4* has been associated with *TP53* mutation status (Dell'Orso et al., 2010; Fontemaggi et al., 2009), which is an early event in astrocytoma progression; additionally, *TP53* mutation is more related to secondary GBM (Ohgaki and Kleihues, 2011). Moreover, hyperexpression of *ID4* was found to be a key regulator of malignant transformation of *Ink4a/Arf*^{-/-} (cyclin-dependent kinase inhibitor 2A, isoform 4) murine astrocytes in *in vivo* experiments, resulting in formation of high grade gliomas according to clinical and histological analysis (Jeon et al., 2008). These

results may be consistent with astrocyte dedifferentiation to an immature progenitor-like state. It has also been demonstrated that ID4 protein activates SRY (sex determining region Y)-box 2 (*SOX2*) transcription in GBM and glioma stem cells (Jeon et al., 2011). Similarly, SOX4 and POU class 5 homeobox 1 (*OCT-4*) proteins were also shown to activate *SOX2* transcription in glioma initiating cells (Ikushima et al., 2011), (Lin et al., 2010). Along with Nanog homeobox (*NANOG*), these transcription factors are highly expressed in embryonic, progenitor, and tumor stem cells, in contrast to the low levels of expression that are found in differentiated cells (Boiani and Schöler, 2005; Chambers and Tomlinson, 2009; Qu and Shi, 2009).

This study aimed to characterize the *ID4* expression pattern in human astrocytomas of grades II to IV of malignancy; to correlate its expression level to that of *SOX2*, *SOX4*, *OCT-4* and *NANOG*, along with *TP53* mutational status; and to correlate the results with the clinical end-point of overall survival among GBM patients. In parallel, expression of the neural and brain tumor stem cell marker *CD133* was assessed to better evaluate the progenitor cell condition (Holmberg et al., 2011; Ma et al., 2008; Marie et al., 2008).

MATERIALS AND METHODS

Tissue samples and ethical statement

One hundred and thirty diffusely infiltrative astrocytomas (grades II to IV) were obtained during therapeutic surgery of patients treated by the Neurosurgery Group of the Department of Neurology at Hospital das Clínicas at the School of Medicine of the University of São Paulo, in the period of 2000 to 2007. The cases were categorized according to the WHO grading system (Louis et al., 2007) by neuropathologists from the Division of Pathological Anatomy of the same institution. The studied series consisted of 26 AGII, 18 AGIII, 86 GBM, and 22 non-neoplastic (NN) brain anonymized cases from epilepsy patients subjected to temporal lobectomy. Demographic data of the studied cases is presented in Table 1, and the clinical findings are presented in Table S1. Samples were macrodissected and immediately snap-frozen in liquid nitrogen upon surgical removal. A 4 μ m-thick cryosection of each sample was analyzed under a light microscope after hematoxylin-eosin staining for assessment of necrotic, cellular debris and non-neoplastic areas (in tumor samples), followed by removal from the frozen block by microdissection prior to DNA and RNA extractions (Marie et al., 2008; Oba-Shinjo et al., 2005). Eighty-one GBM patients (94.2%) presented with onset of clinical symptoms within 3 months prior to diagnostic surgical intervention and were classified as presenting primary GBM. Five GBM patients (5.8%) presented a tumor which was resected over one year after a lower grade astrocytoma (grade II or III), and were designated as secondary GBM cases. Written informed consent was obtained from all patients according to the ethical guidelines approved by the Department of Neurology, School of Medicine, University of São Paulo (0599/10).

Table 1. Demographic data from patients analyzed in this study

Total of cases	Morphology ^a	Mean age at diagnosis (years) ^b	Gender ^c
22	NN	38 \pm 7.6	12F, 10M
26	AGII	34 \pm 8.1	11F, 15M
18	AGIII	35 \pm 12.3	7F, 11M
86	GBM	54 \pm 13.9	28F, 58M

^aNN, non-neoplastic; AGII, low-grade astrocytoma; AGIII, anaplastic astrocytoma; GBM, glioblastoma

^bAge at diagnosis was calculated from date of birth to date of surgery

^cM, male; F, female

Sample preparation

Total RNA was extracted from frozen tissues (tumor and non-neoplastic) using an RNeasy Mini Kit (Qiagen, Hilden, Germany). Evaluation of RNA concentration and purity were carried out by measuring absorbance at 260 and 280 nm. Ratios of 260/280 measures ranging from 1.8 to 2.0 were considered satisfactory for purity standards. Denaturing agarose gel electrophoresis was used to assess the quality of the samples. A conventional reverse transcription reaction was performed to yield single-stranded cDNA. The first strand of cDNA was synthesized from 1 µg of total RNA previously treated with 1 unit of DNase I (FPLC-pure, GE Healthcare, Uppsala, Sweden) using random and oligo (dT) primers, RNase inhibitor, and SuperScript III reverse transcriptase according to the manufacturer's recommendations (Life Technologies, Carlsbad, USA). The resulting cDNA was subsequently treated with 1 unit of RNase H (GE Healthcare, Uppsala, Sweden), diluted with TE buffer, and stored at -20°C until later use.

Quantitative real time PCR (qRT-PCR)

The relative expression level of *ID4*, *SOX2*, *SOX4*, *OCT-4*, *NANOG* and *CD133* were analyzed by qRT-PCR, using the SYBR Green approach. Quantitative data were normalized in relation to the geometric mean of three housekeeping genes, suitable for the analysis: hypoxanthine phosphoribosyltransferase (*HPRT*), glucuronidase beta (*GUSB*) and TATA box binding protein (*TBP*), as previously demonstrated by our group (Valente et al., 2009). The primers were designed to amplify 80–120 bp amplicons, with a melting temperature of 60°C and were synthesized by IDT (Integrated DNA Technologies, Coralville, USA) as follows (5' to 3'): *ID4* F: TGAACAAGCAGGGCGACAG, *ID4* R: CCCTCTCTAGTGCTCCTGGCT; *SOX2* F: AAGAGAACACCAATCCCATCCA, *SOX2* R: AGTCCCCCAAAAAGAAGTCCA; *SOX4* F: CAGAAGGGAGGGGAAACATA, *SOX4* R: GAATCGGCACTAAGGAGTTGGT; *NANOG* F: GCAAGAACTCTCCAACATCCTGA, *NANOG* R: CATTGCTATTCTTCGGCCAGTT; *OCT-4* F: CGTGAAGCTGGAGAAGGAGA, *OCT-4* R: CTTGGCAAATTGCTCGAGTT; *CD133* F: TCGGAAACTGGCAGATAGCAA, *CD133* R: GTGAACGCCTTGTCCCT; *HPRT* F: TGAGGATTTGGAAAGGGTGT, *HPRT* R: GAGCACACAGAGGGCTACAA; *GUSB* F: GAAAATACGTGGTTGGAGAGCTCATT, *GUSB* R: CCGAGTGAAGATCCCCTTTTAA; *TBP* F: AGGATAAGAGAGCCACGAACCA, *TBP* R: CTTGCTGCCAGTCTGGACTGT. The minimum primer concentrations necessary were

determined to give the lowest threshold cycle (Ct) and maximum amplification efficiency, while minimizing non-specific amplification. Primer concentrations used were 150 nM for *ID4*, 200 nM for *HPRT*, *TBP*, *SOX2*, *SOX4* and *OCT-4*, and 400 nM for *GUSB*, *NANOG* and *CD133*. Standard curve was established to ensure amplification efficiency and analysis of melting curves demonstrated a single peak for all PCR products. Additionally, agarose gel electrophoresis was employed to check the size of the PCR product amplified. SYBR Green I amplification mixtures (12 μ l) contained 3 μ l of cDNA, 6 μ l of 2X Power SYBR Green I Master Mix (Life Technologies, Carlsbad, USA) and forward and reverse primers. PCR reactions were run on an ABI Prism 7500 sequence detector (Life Technologies, Carlsbad, USA) as follows: 2 min at 50°C, 10 min of polymerase activation at 95°C, and 40 cycles of 15 s at 95°C and 1 min at 60°C. All the reactions were performed in duplicate. The following equations were applied to calculate gene relative expression according to primer efficiency (E) in tumor samples versus the mean of non-neoplastic tissues: $2^{-\Delta\Delta Ct}$ (Livak and Schmittgen, 2001) for *SOX2*, *SOX4*, *OCT-4* and *CD133*; and $1+E^{-\Delta\Delta Ct}$ (Pfaffl, 2001) for *ID4* and *NANOG*, where ΔCt = Ct specific gene- geometric mean Ct of housekeeping genes and $\Delta\Delta Ct$ = ΔCt tumor - mean ΔCt non-neoplastic. For statistical analysis, gene expression status was scored as high or low expression in relation to the median relative expression value at each grade of astrocytoma.

DNA extraction and *TP53* mutational analyses

DNA extraction was performed from frozen tumor tissues using All Prep DNA/RNA Mini Kit (Qiagen, Hilden, Germany), and peripheral leukocyte DNA was extracted by a salting-out procedure (Miller et al., 1988).

Whole coding *TP53* exons (2 to 11) analysis was performed using the polymerase chain reaction single-strand conformation polymorphism (PCR-SSCP) assay and DNA sequencing, as previously reported (Uno et al., 2005, 2006).

Immunohistochemistry

For immunohistochemical detection, tissue sections were routinely processed and subjected to antigen retrieval. Briefly, slides were immersed in 10 mM citrate buffer, pH 6.0 and incubated at 122°C for 3 min using an electric pressure cooker (BioCare Medical, Walnut Creek, USA). Specimens were then blocked and further

incubated with the following antibodies raised against human ID4 (rabbit polyclonal, ab20988, Abcam, Cambridge, UK, 1:100), SOX2 (mouse clone 6, S1451, Sigma Aldrich, St. Louis, USA, 1:100), SOX4 (rabbit polyclonal, S7318, Sigma Aldrich, St. Louis, USA, 1:800) at 16-20°C for 16 hours. Development of the reaction was performed with a commercial kit (Novolink; Novocastra, Newcastle-upon-Tyne, UK) at room temperature, using diaminobenzidine and Harris hematoxylin for nuclear staining. Optimization using positive controls suggested by the manufacturer of each antibody (breast carcinoma for ID4 and SOX4 antibodies, and normal esophagus for SOX2), was performed in order to obtain optimal dilution. Staining intensity of tissue sections was evaluated independently by two observers (SKNM and TFAG). A semi-quantitative score system considering both intensity of staining and percentage of cells was applied as follows: for intensity of staining, 0=negative, 1=weak, 2=moderate and 3=strong; for cell percentage, 0=no cells stained, 1=10–25%, 2 =26–50%, 3=51–75% and 4 = 76–100%. Only cases with positive cell staining with scores ≥ 2 were considered as positive. Digital photomicrographs of representative fields were captured and processed using Picasa 3 (Google, Mountain View, USA).

Statistical analysis

The statistical analysis of relative gene expression in different grades of astrocytoma was assessed using the Kolmogorov-Smirnov normality test, and the non-parametric Kruskal-Wallis and Dunn tests. Correlation between relative gene expression values was assessed using the non-parametric Spearman-rho correlation test and the parametric Pearson's correlation test. The Mann-Whitney test was used to compare *TP53* mutational status and relative gene expression. The Kaplan-Meier survival curve was analyzed using the *log-rank* (Mantel Cox) test and multivariate analysis using the Cox proportional hazards model. The logistic regression model included the following parameters: age at diagnosis, gender (female *versus* male), degree of tumor surgical resection (gross total resection (GTR) *versus* partial resection (PR) and gene expression status (hyper or hypoexpression). Differences were considered statistically significant when $p < 0.05$. Calculations were performed using SPSS, version 15.0 (IBM, Armonk, USA).

RESULTS

Relative expression levels in diffusely infiltrative astrocytomas

Gene expression analysis by qRT-PCR for *ID4* showed higher median expression levels in all diffusely infiltrative astrocytoma cases (AGII to GBM) relative to the NN cases, and comparison among the groups was statistically significant (Figure 1A, $p < 0.0005$, Kruskal-Wallis test). Although the *ID4* median expression level in GBM cases was lower than in AGII and AGIII, there was a variability of these expression values, with cases presenting both higher and lower values than the other grades. Similar variability of *ID4* expression was also observed in AGII and AGIII (Figure 1A). A multivariate Cox regression model (which considered age at diagnosis, gender, degree of tumor surgical resection, and *ID4* expression status) showed that *ID4* expression (hyper or hypoeexpression) alone had no impact on patient's prognosis. Only age at diagnosis was an independent prognostic factor (hazard ratio=1.02, $p=0.02$). *SOX2*, *SOX4*, *OCT-4*, *NANOG*, and *CD133* also showed higher mRNA levels in AGII-GBM cases in comparison to NN, as shown in Figure 1B-1F. *SOX2* expression levels were compared to *ID4* levels to verify the degree of their co-expression in human diffusely infiltrative astrocytomas. Interestingly, the correlation analysis of *SOX2* showed mRNA levels similar to *ID4*, with positive correlation found in AGII ($r=0.731$; $p=0.00002$), AGIII ($r=0.671$; $p=0.006$) and GBM ($r=0.334$; $p=0.0006$). Next, *SOX4*, *OCT-4*, *NANOG* and *CD133* expression levels were also evaluated. *SOX4* expression levels were similar to those of *ID4*, although positive correlation was only found in AGII ($r=0.568$; $p=0.002$) and GBM ($r=0.414$; $p=0.00009$). *OCT-4* relative expression correlated positively with *ID4* in AGIII ($r=0.551$; $p=0.02$) and GBM ($r=0.364$; $p=0.01$). In contrast to the other analyzed genes, several GBM cases exhibited very low expression levels of *NANOG*, and no correlation was found between *ID4* and *NANOG* expression levels. *ID4* and *CD133* expressions did neither not correlate. An overview of the results of analyzed correlations is shown in Figure 2.

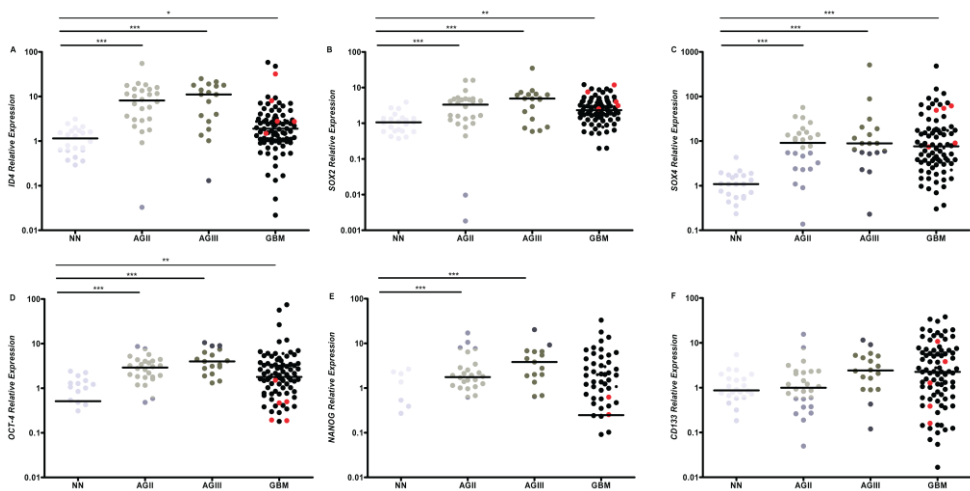


Figure 1: Expression levels of genes in diffusely infiltrative astrocytomas (AGII to GBM). Transcript levels of *ID4* (A), *SOX2* (B), *SOX4* (C), *OCT-4* (D), *NANOG* (E) and *CD133* (F) were determined in 26 low-grade astrocytomas (AGII), 18 anaplastic astrocytomas (AGIII) and 86 GBM cases relative to 22 non-neoplastic (NN) by quantitative real-time PCR. Relative expression values were calculated based on the geometric mean of *HPRT*, *GUSB* and *TBP* expression levels of each sample and non-neoplastic brain values. The following equations were applied to calculate gene relative expression according to primer efficiency (E) in tumor samples versus the mean of non-neoplastic tissues: $2^{-\Delta\Delta Ct}$ (Livak and Schmittgen, 2001) for *SOX2*, *SOX4*, *OCT-4* and *CD133*; and $1+E^{-\Delta Ct}$ (Pfaffl, 2001) for *ID4* and *NANOG*, where $\Delta Ct = Ct$ specific gene - mean Ct of housekeeping genes and $\Delta\Delta Ct = \Delta Ct$ tumor - mean ΔCt non-neoplastic. Red dots represent the secondary GBM cases. Horizontal bars show the median of each group and the values are presented in Table 2. *NANOG* expression in 15 NN and 40 GBM cases was very low and, as a result, the horizontal bar for NN does not appear in the graphic (median=0). The difference of relative gene expressions among the groups were statistically significant ($p < 0.0005$ for *ID4*, *SOX2*, *SOX4*, *OCT-4* and *NANOG*; and $p < 0.05$ for *CD133*, Kruskal-Wallis test). A pair-based comparison was assessed using Dunn test. The p value results are shown, where *** $p < 0.0005$, ** $p < 0.005$ and * $p < 0.05$.

Table 2. Median of relative expression levels of the analyzed genes in astrocytomas, according to morphology

Morphology ^a	<i>ID4</i>	<i>SOX2</i>	<i>SOX4</i>	<i>OCT-4</i>	<i>NANOG</i>	<i>CD133</i>
NN	1.15	1.06	1.09	0.51	0	0.87
AGII	8.12	3.32	9.12	2.92	1.77	1
AGIII	11.1	4.9	8.86	4	3.84	2.43
GBM	1.89	2.32	7.63	1.79	0.25	2.26

^aNN, non-neoplastic; AGII, low-grade astrocytoma; AGIII, anaplastic astrocytoma; GBM, glioblastoma

It is interesting to note that secondary GBM cases (red dots on Figure 1) exhibited a higher median expression level for *ID4* (2.78) than did primary GBM cases (1.84). Similar results were obtained for *SOX2* (3.96 for secondary and 2.26 for primary GBM) and *SOX4* (48.99 for secondary and 6.74 for primary). In contrast, the median of OCT-4 expression was 0.47 in secondary GBM and 2.03 in primary GBM; the median of *NANOG* expression level in secondary GBM was 0.13 while 0.35 in primary GBM, and the median of CD133 expression level was 1.28 for secondary GBM and 2.26 for primary GBM. To further investigate the factors contributing to these differences, the expression values were analyzed according to *TP53* mutation status.

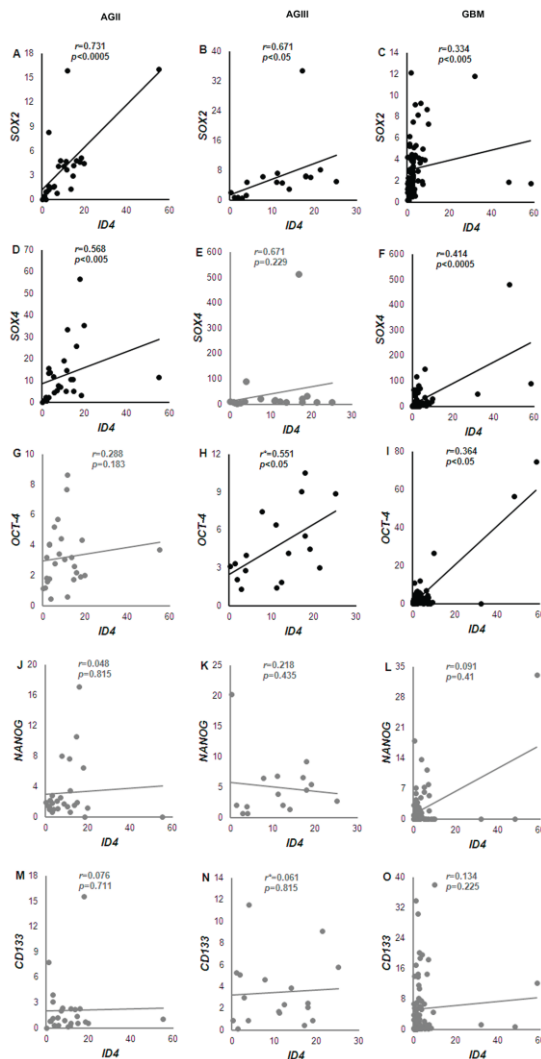


Figure 2: Correlation between *ID4* and *SOX2*, *SOX4*, *OCT-4*, *NANOG* and *CD133* expression levels in diffusely infiltrative astrocytomas. Correlation was assessed in AGII (A, D, G, J, M), AGIII (B, E, H, K, N) and GBM (C, F, I, L, O) cases. *ID4* expression level was correlated to *SOX2* (A-C), *SOX4* (D-F), *OCT-4* (G-I), *NANOG* (J-L) and *CD133* (M-O) expression levels. The significant correlations are shown in black and the non-significant in grey. r correlation coefficient assessed by Spearman-rho test, and r^* by Pearson's correlation test.

Association between *ID4*, *SOX2*, *SOX4*, and *NANOG* mRNA expressions and *TP53* mutation status

The frequency of *TP53* mutation was 11.6% in GBM (10 out of 86), 16.6% in AGIII (3 out of 18) and 50% in AGII (13 out of 26), as described in our previous studies (Uno et al., 2005, 2006) (Table S1). Our GBM series is composed mainly by primary GBMs, which explains the low frequency of *TP53* mutation and corroborates the classification based on clinical presentation. The low frequency of *TP53* mutations in GBM and AGIII cases did not permit statistical analyses of the proposed parameters; however, this analysis was feasible among AGII cases. Interestingly, *TP53*-mutated AGII cases showed higher relative expression of *ID4* when compared to AGII cases with wild-type *TP53* ($p=0.048$) (Figure 3A). Also, *SOX2* ($p=0.044$), *SOX4* ($p=0.004$) and *NANOG* ($p=0.025$) relative expressions were higher in mutated than in wild-type *TP53* in AGII cases (Figure 3B, 3C and 3E respectively). No difference was found for *OCT-4* relative expression between wild-type and mutated *TP53* cases (Figure 3D). Despite the fact that *TP53*-mutated AGII cases displayed slightly higher relative expression of *CD133*, the difference was not statistically significant (Figure 3F). No difference in expression was found regarding the different types of *TP53* mutations (whether missense, nonsense or in splicing sites). Mann-Whitney test was applied for all the above statistical analysis. Moreover, no significant impact was observed in the overall survival time or in the progression free survival time in AGII cases, concerning either relative expression levels of *ID4*, *SOX2*, *SOX4*, *OCT4*, *NANOG*, and *CD133* or *TP53* mutational status (results presented Table S2). Although *TP53* mutated AGII cases presented a median of 40 months of overall survival time compared to a median of 51 months of wild-type *TP53* AGII cases, it did not reach statistical significance because of the small number of cases in each group (Figure 3, white lozenges for deceased AGII patients).

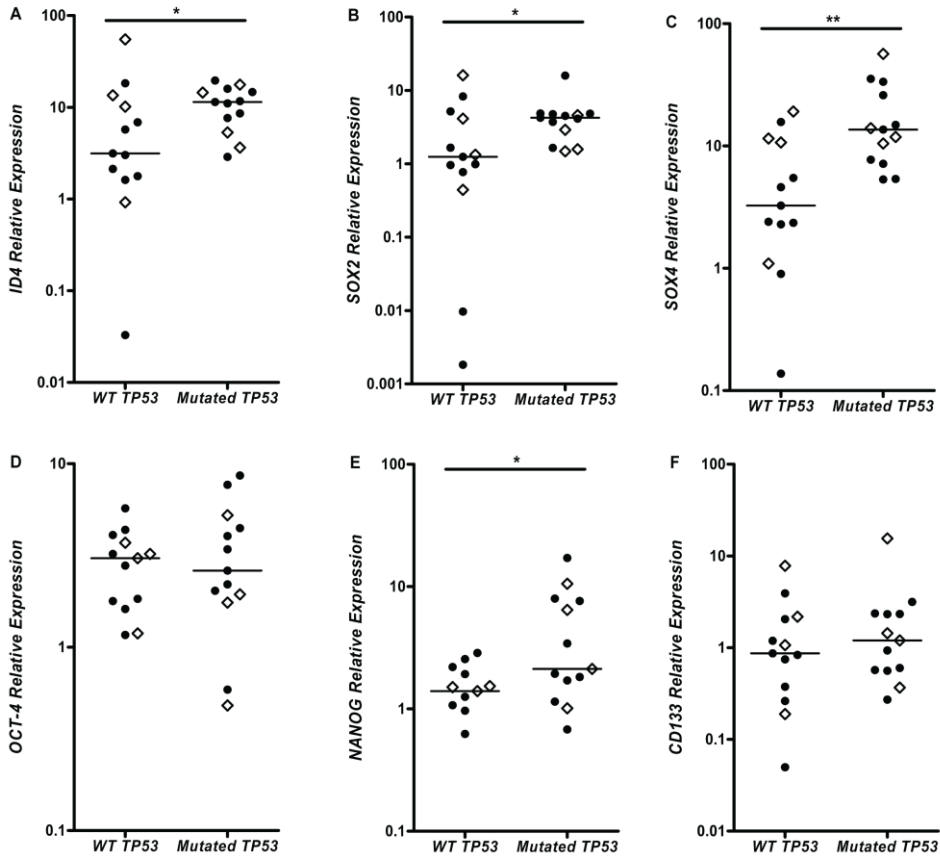


Figure 3: Comparison of gene expression levels between the wild-type *TP53* (*WT TP53*) and the mutated *TP53* (*Mutated TP53*) in AGII cases. Higher expressions of *ID4* (A), *SOX2* (B), *SOX4* (C) and *NANOG* (E) were observed on the mutated *TP53* AGII cases. No difference was found for *OCT-4* (D) and *CD133* (F) relative expression between the two groups. White lozenges represent the deceased patients. The *p* values are: **p* < 0.05 and ***p* < 0.005, Mann-Whitney test.

Associated expression of *ID4*, *SOX2* and *SOX4* with *TP53* mutational status was further confirmed at the protein level by immunohistochemistry. The wild type *TP53* AGII cases (Figure 4A-4C) showed weak or no staining for the three targets in comparison to the *TP53*-mutated cases (Figure 4D-4F), as did the primary GBM cases (Figure 4G-4I) when compared to the secondary GBM (Figure 4J-4L) cases.

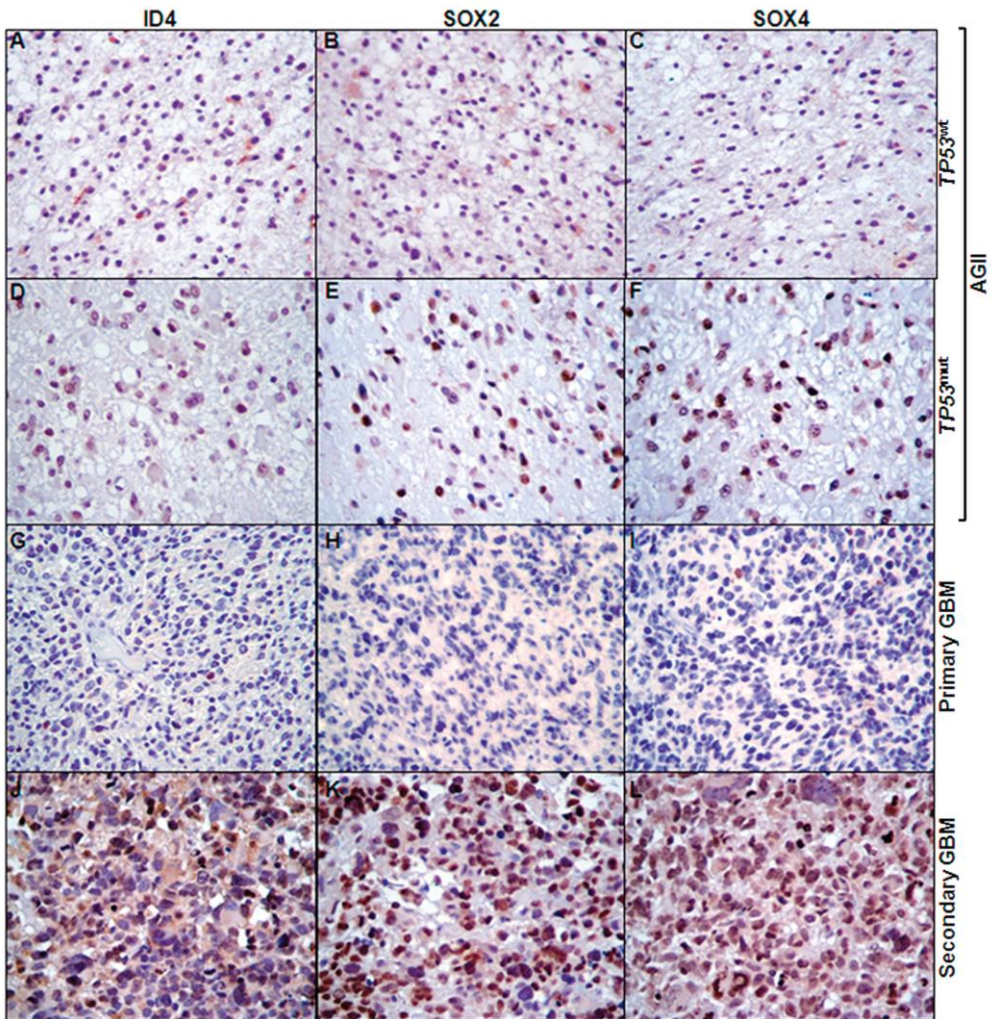


Figure 4: ID4, SOX2 and SOX4 immunohistochemistry. Representative cases of wild-type *TP53* AGII (A-C), mutated *TP53* AGII (D-F), primary GBM (G-I) and secondary GBM (J-L) stained for ID4, SOX2 and SOX4 are demonstrated. Both mutated AGII and secondary GBM cases showed stronger and larger number of nuclear stained cells (score 3 for intensity and $\geq 75\%$ of positive cells) for ID4, SOX2 and SOX4. Comparatively, wild-type *TP53* AGII and primary GBM presented score 1 for intensity and $< 25\%$ of positive cells. The reaction was performed in paraffin embedded tissue sections with a commercial polymer kit (Novolink; Novocastra, UK), using diaminobenzidine as developer and Harris hematoxylin for nuclear counterstaining. 200x magnification for all images.

The overview of *TP53* mutation status, relative gene expression for AGII, and expression differences among AGII, AGIII, primary and secondary GBM are displayed as heat map in Figure 5.

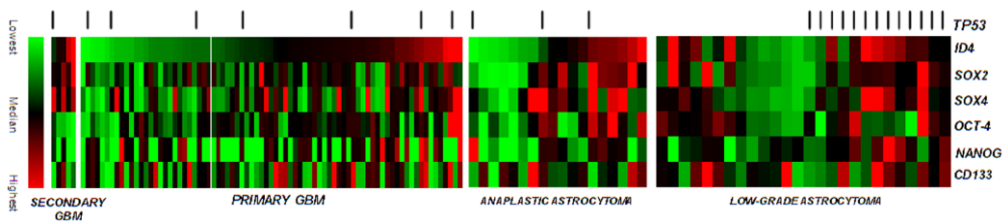


Figure 5: Heatmap displaying the relative gene expressions in low-grade astrocytoma (AGII), anaplastic astrocytoma (AGIII) and GBM cases according to *TP53* mutation status. The *TP53* mutated cases are represented by side dashes. The mutated *TP53* AGII cases showed more elevated expression levels of *ID4*, *SOX2*, *SOX4* and *NANOG*. *CD133* expressions were more heterogeneous among the cases. *SOX2* and *SOX4* showed similar expression levels to *ID4*. Similarly, secondary GBM cases also presented higher *ID4*, *SOX2*, *SOX4* expression levels. *OCT-4*, *NANOG* and *CD133* expression levels were heterogeneous among secondary GBM cases, and *OCT-4* presented higher mRNA levels in primary GBM.

Impact of *ID4*, *SOX4* and *OCT-4* expression levels on clinical outcome for GBM patients

Considering the variability of the relative expression values found in GBM cases, we evaluated the impact of up-regulation of the analyzed genes on overall patient survival. For the evaluation, conditions were determined for high and low gene expression. Secondary GBM cases were excluded from this analysis due to the small number of cases. None of the genes had an impact on overall survival, either on their own or when grouped in pairs for the determined conditions (Figure S1). However, there was a significant difference when comparing GBM cases with high *ID4*, *SOX4* and *OCT-4* expressions (median survival of 6 months) with cases with low expressions for the three genes (median survival of 18 months) (*log-rank* $p=0.014$), as shown on the Kaplan-Meier survival curve in Figure 6.

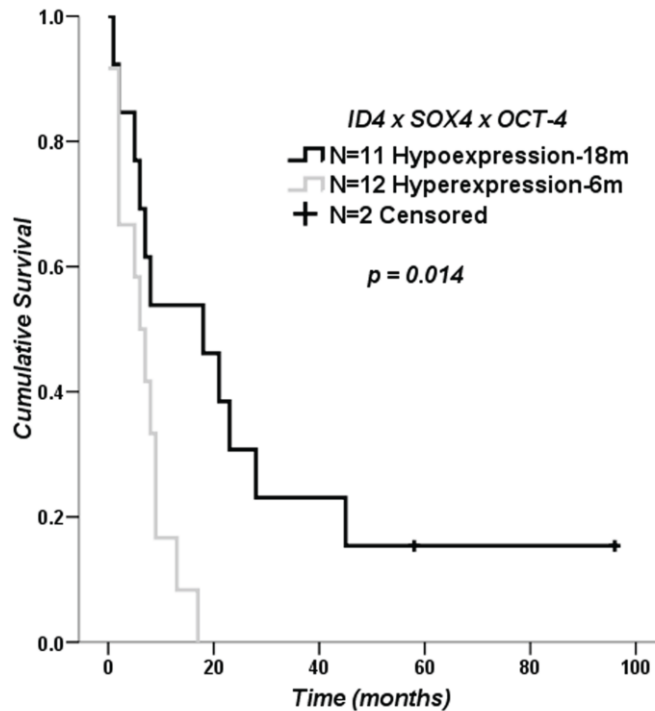


Figure 6: Survival curve of GBM patients. Twenty-five GBM cases out of 86 GBM cases presented concomitant high or low *ID4*, *SOX4* and *OCT-4* relative expression levels (12 GBM cases presenting high expressions and 13 low expressions for the three genes). The survival time difference between the two groups was statistically significant (*log rank p-value*=0.014), presenting median survival time of 6 months for GBM cases presenting concomitant high expressions for the three genes compared to 18 months for GBM cases with low expressions.

DISCUSSION

We have demonstrated a differential expression of *ID4* in human diffusely infiltrative astrocytoma cases demonstrating association with *TP53* mutation status, as well as to *SOX2*, *SOX4* and *OCT-4* mRNA expression levels.

***ID4* mRNA levels are elevated in astrocytomas in comparison to non-neoplastic brain tissue**

Our study demonstrated significantly higher mRNA expression levels of *ID4* in astrocytomas when compared to non-neoplastic brain tissue. Similar results have also been described for ID1-3 proteins in astrocytomas, with higher expression levels in tumors than in non-neoplastic white-matter (Vandeputte et al., 2002). A previous immunohistochemical report has shown stronger ID4 expression in GBM compared to AGII, AGIII and normal brain tissue (Zeng et al., 2010). Such association was not significant in our study, most probably due to a larger number of cases analyzed herein, and also to the heterogeneity inherent to GBM, here corroborated by the widespread *ID4* mRNA expression among the studied GBM cases. Nevertheless, the increased *ID4* expression level in diffusely infiltrative astrocytoma is in accord with the tumor re-expression model of IDs (Perk et al., 2005), postulating *ID4* as an additional marker of astrocytoma progression in malignancy.

A recent report (Martini et al., 2012) has shown that *ID4* promoter methylation was an independent factor on patient's prognosis, and that association of *ID4* promoter methylation and *MGMT* methylation status conferred significantly longer overall survival to GBM patients. We assessed the correlation between *ID4* hypoexpression and the *MGMT* methylation status in GBM, previously reported by our group (Uno et al., 2011). The Cox regression model showed only *MGMT* status as an independent factor for prognosis (hazard ratio = 4.684, $p=0.014$), differing from the previous report. Further studies on *ID4* promoter methylation are needed in the present GBM series.

***ID4* hyperexpression is driven by mutated *TP53* in AGII**

Here we demonstrate a significant difference in *ID4* expression between AGII cases harboring *TP53* mutation versus wild-type, mutated cases showing significant increase in *ID4* expression. Other studies in breast cancer models have demonstrated *in*

in vitro *ID4* up-regulation driven by the mutated p53 protein (Dell'Orso et al., 2010; Fontemaggi et al., 2009). *TP53* mutations, present in 50% of AGII cases, are considered one of the earliest events in astrocytoma formation (Ohgaki and Kleihues, 2011). The significant association shown here between *TP53* mutation and *ID4* expression could possibly classify *ID4* hyperexpression as an early event in astrocytoma formation. The analysis of AGII patients OS time in *TP53* mutated and wild-type cases showed that the mutated cases had a shorter survival by eleven months in comparison to the wild-type group. Considering the low number of cases, further studies are necessary to confirm statistically this result. The great majority of *TP53* mutations are missense, localized in specific gene domains (“hot spots”) that do not inactivate protein function. On the contrary, these alterations stabilize the mutated protein and enhance its oncogenic activity by increasing the transcription of target genes, recruiting other transcription factors and co-factors (recently reviewed in (Freed-Pastor and Prives, 2012)). However, no difference of the analyzed gene expressions were found compared to the different types of *TP53* mutation in the current AGII series, and it remains to be elucidated if the cases harboring inactivating nonsense mutations present alternative activation for *ID4*, *SOX2* and *SOX4*.

Associated expression of *ID4* with *SOX2* and *SOX4* and with mutated *TP53*

SOX2 also proved to be significantly augmented and correlated to *ID4* in *TP53* mutated AGII cases. *SOX2* overexpression driven by inactivation of p53 in mouse embryonic fibroblasts has been demonstrated (Kawamura et al., 2009), although the mechanism remains unknown. One possible explanation is that *ID4* up-regulation activates *SOX2* through inhibition of a microRNA, mir-9*, which is a direct negative regulator of *SOX2*, as shown in glioma cell lines (Jeon et al., 2011). Our findings of *ID4* up-regulation associated to *TP53* mutated status and to *SOX2* hyperexpression in human astrocytoma specimens corroborate these previous observations in cell lines. Taken together, these data suggest that *ID4* and *SOX2* act jointly post-*TP53* mutation in promoting astrocytoma tumorigenesis.

The association between *SOX4* and p53 has also been reported (Hur et al., 2010; Pan et al., 2009), with *SOX4* stabilizing p53 protein and inhibiting its induction of the apoptotic pathway. In our study, *SOX4* expression was increased in *TP53* mutated cases, in a similar pattern to *ID4*. It remains to be elucidated what role the observed

association between *SOX4* and mutated *TP53* plays in the process of astrocytic tumor formation.

Our results showed a significant increase in *NANOG* expression in *TP53* mutated AGII cases. It is known that p53 is a direct negative regulator of *NANOG* (Lin et al., 2005) and that the absence of a functional p53 protein augments *NANOG* expression. *NANOG* levels did not correlate to any of the other analyzed targets, and its expression pattern in GBM cases was random, enabling us to speculate that *NANOG* works differently to contribute to astrocytoma formation. *CD133* levels were not significantly different when *TP53* mutated and wild-type AGII cases were compared, and GBM cases also displayed a random pattern, suggesting that *CD133* also works differently in the tumorigenic process of astrocytomas.

OCT-4 relative expression was not influenced by *TP53* mutational status and did not correlate with *ID4* expression in AGII cases. However, the expression pattern of GBM cases was strikingly different: secondary GBM exhibited very low *OCT-4* mRNA levels in comparison to primary GBM. Together with the positive correlation between *OCT-4* and *ID4* found in both AGIII and GBM cases, these data indicate a role for this target in the most malignant grades of astrocytoma. These results prompted us to further investigate the combined expression of *ID4*, *SOX4* and *OCT-4*.

Impact of *ID4*, *SOX4* and *OCT-4* mutual hyperexpression on primary GBM patients' overall survival

The expression level variability among GBM cases was present for all analyzed genes (Figure 1), with some cases exhibiting very high mRNA levels in contrast to low levels found in others. Again, this phenomenon may be due to the extensive heterogeneity found in GBM at both the cellular and molecular levels (Bonavia et al., 2011), contributing to difficulties in eradicating these tumors. Thus, we believed it was necessary to ascertain whether patients bearing tumors with higher mRNA levels of the analyzed genes showed worse overall survival. When we grouped *ID4*, *SOX4* and *OCT-4* together, patients hyperexpressing these genes exhibited much lower survival time. In bladder cancers, both *ID4* and *SOX4* were amplified and overexpressed heterogeneously (Wu et al., 2005), similar to astrocytomas, and contributed to the variable biological and clinical behavior of the tumors. As previously mentioned, *OCT-4* and *SOX4* proteins form a transcription complex and induce *SOX2* expression, increasing the tumorigenicity of glioma cells. Although decreased survival was

demonstrated in mice inoculated with GBM cells hyperexpressing *OCT-4*, we observed that *OCT-4* alone had no impact on our patients' overall survival (Figure S1D). Because *ID4* alone, as well as the *SOX4* and *OCT-4* complex, activates *SOX2*, and because chemoresistance is associated with both *SOX2* and *ID4* augmented expression, it is possible to speculate that multiple *SOX2* activation events in GBM may impair patient prognosis. *SOX2* and *OCT-4*, are considered masters of pluripotency in embryonic stem cells (Mallanna and Rizzino, 2012). This role is maintained in cancer stem cells (CSC), a subset of tumor cells regarded as possessing traits such as therapeutic resistance, tumor angiogenesis and recurrence (Sampieri and Fodde, 2012). *ID4* has also shown to play an important role in CSC biology, its expression being imperative to the formation and maintenance of CSC population (Park et al., 2011). In GBM stem cells (Galli et al., 2004; Singh et al., 2003, 2004; Yuan et al., 2004), *ID4* has been postulated as an important target in the dedifferentiation process, as shown in the *in vitro* reports (Jeon et al., 2008, 2011). Moreover, the re-expression of embryonic stem cells genes in tumors, including gliomas, has been associated with a more aggressive phenotype (Ben-Porath et al., 2008; Guo et al., 2011; Holmberg et al., 2011). It is possible that this is the cause for the worse clinical end-point of overall survival among GBM patients found in our study. However, because of the low number of GBM cases (n=25) in which this finding was demonstrated, the present result should be validated in an independent study sample containing a higher number of GBM patients.

In this scenario, *ID4* seems to be a promising target for further studies in order to better understand its role in tumorigenesis and its potential use in therapeutics.

Acknowledgments

We sincerely thank the doctors and residents of the Discipline of Neurosurgery of the Department of Neurology at Hospital das Clínicas of School of Medicine, University of São Paulo, for the therapeutic and diagnostic procedures of all patients included in this study, and the doctors and technicians at the Division of Pathological Anatomy of the same institution for the WHO grade classification of tumor samples and tissue section processing. We also thank the Psychiatry Institute for the logistic help in the surgical therapy.

There are no conflicts of interest to declare in relation to the work described herein.

REFERENCES

Benezra, R., Davis, R.L., Lassar, A., Tapscott, S., Thayer, M., Lockshon, D., and Weintraub, H. (1990a). Id: a negative regulator of helix-loop-helix DNA binding proteins. Control of terminal myogenic differentiation. *Ann. N. Y. Acad. Sci.* *599*, 1–11.

Benezra, R., Davis, R.L., Lockshon, D., Turner, D.L., and Weintraub, H. (1990b). The protein Id: a negative regulator of helix-loop-helix DNA binding proteins. *Cell* *61*, 49–59.

Ben-Porath, I., Thomson, M.W., Carey, V.J., Ge, R., Bell, G.W., Regev, A., and Weinberg, R.A. (2008). An embryonic stem cell-like gene expression signature in poorly differentiated aggressive human tumors. *Nat. Genet.* *40*, 499–507.

Boiani, M., and Schöler, H.R. (2005). Regulatory networks in embryo-derived pluripotent stem cells. *Nat. Rev. Mol. Cell Biol.* *6*, 872–884.

Bonavia, R., Inda, M.-M., Cavenee, W.K., and Furnari, F.B. (2011). Heterogeneity maintenance in glioblastoma: a social network. 4055–4060.

Chambers, I., and Tomlinson, S.R. (2009). The transcriptional foundation of pluripotency. *Development* *136*, 2311–2322.

Dell'Orso, S., Ganci, F., Strano, S., Blandino, G., and Fontemaggi, G. (2010). ID4: a new player in the cancer arena. 48–58.

Fontemaggi, G., Dell'Orso, S., Trisciuglio, D., Shay, T., Melucci, E., Fazi, F., Terrenato, I., Mottolese, M., Muti, P., Domany, E., et al. (2009). The execution of the transcriptional axis mutant p53, E2F1 and ID4 promotes tumor neo-angiogenesis. 1086–1093.

Freed-Pastor, W.A., and Prives, C. (2012). Mutant p53: one name, many proteins. *Genes Dev.* *26*, 1268–1286.

Galli, R., Binda, E., Orfanelli, U., Cipelletti, B., Gritti, A., De Vitis, S., Fiocco, R., Foroni, C., Dimeco, F., and Vescovi, A. (2004). Isolation and characterization of tumorigenic, stem-like neural precursors from human glioblastoma. *Cancer Res.* *64*, 7011–7021.

Guo, Y., Liu, S., Wang, P., Zhao, S., Wang, F., Bing, L., Zhang, Y., Ling, E.-A., Gao, J., and Hao, A. (2011). Expression profile of embryonic stem cell-associated genes Oct4, Sox2 and Nanog in human gliomas. *Histopathology* *59*, 763–775.

Holmberg, J., He, X., Peredo, I., Orrego, A., Hesselager, G., Ericsson, C., Hovatta, O., Oba-Shinjo, S.M., Marie, S.K.N., Nistér, M., et al. (2011). Activation of neural and

pluripotent stem cell signatures correlates with increased malignancy in human glioma. e18454.

Hur, W., Rhim, H., Jung, C.K., Kim, J.D., Bae, S.H., Jang, J.W., Yang, J.M., Oh, S.-T., Kim, D.G., Wang, H.J., et al. (2010). SOX4 overexpression regulates the p53-mediated apoptosis in hepatocellular carcinoma: clinical implication and functional analysis in vitro. *Carcinogenesis* 31, 1298–1307.

Iavarone, A., and Lasorella, A. (2004). ID proteins in neural cancer. *Cancer Lett.* 204, 189–196.

Iavarone, A., and Lasorella, A. (2006). ID proteins as targets in cancer and tools in neurobiology. *Trends Mol. Med.* 12, 588–594.

Ikushima, H., Todo, T., Ino, Y., Takahashi, M., Saito, N., Miyazawa, K., and Miyazono, K. (2011). Glioma-initiating cells retain their tumorigenicity through integration of the Sox axis and Oct4 protein. *J. Biol. Chem.* 286, 41434–41441.

Jeon, H.-M., Jin, X., Lee, J.-S., Oh, S.-Y., Sohn, Y.-W., Park, H.-J., Joo, K.M., Park, W.-Y., Nam, D.-H., DePinho, R.A., et al. (2008). Inhibitor of differentiation 4 drives brain tumor-initiating cell genesis through cyclin E and notch signaling. *Genes Dev.* 22, 2028–2033.

Jeon, H.-M., Sohn, Y.-W., Oh, S.-Y., Oh, S.-Y., Kim, S.-H., Beck, S., Kim, S., and Kim, H. (2011). ID4 imparts chemoresistance and cancer stemness to glioma cells by derepressing miR-9*-mediated suppression of SOX2. *Cancer Res.* 71, 3410–3421.

Kawamura, T., Suzuki, J., Wang, Y.V., Menendez, S., Morera, L.B., Raya, A., Wahl, G.M., and Izpisua Belmonte, J.C. (2009). Linking the p53 tumour suppressor pathway to somatic cell reprogramming. *Nature* 460, 1140–1144.

Kuzontkoski, P.M., Mulligan-Kehoe, M.J., Harris, B.T., and Israel, M.A. (2010). Inhibitor of DNA binding-4 promotes angiogenesis and growth of glioblastoma multiforme by elevating matrix GLA levels. *Oncogene* 29, 3793–3802.

Lin, B., Madan, A., Yoon, J.-G., Fang, X., Yan, X., Kim, T.-K., Hwang, D., Hood, L., and Foltz, G. (2010). Massively parallel signature sequencing and bioinformatics analysis identifies up-regulation of TGFBI and SOX4 in human glioblastoma. *PloS One* 5, e10210.

Lin, T., Chao, C., Saito, S. 'ichi, Mazur, S.J., Murphy, M.E., Appella, E., and Xu, Y. (2005). p53 induces differentiation of mouse embryonic stem cells by suppressing Nanog expression. *Nat. Cell Biol.* 7, 165–171.

Livak, K.J., and Schmittgen, T.D. (2001). Analysis of relative gene expression data using real-time quantitative PCR and the 2(-Delta Delta C(T)) Method. 402–408.

Louis, D.N., Ohgaki, H., Wiestler, O.D., Cavenee, W.K., Burger, P.C., Jouvett, A., Scheithauer, B.W., and Kleihues, P. (2007). The 2007 WHO classification of tumours of the central nervous system. 97–109.

Ma, Y.-H., Mentlein, R., Knerlich, F., Kruse, M.-L., Mehdorn, H.M., and Held-Feindt, J. (2008). Expression of stem cell markers in human astrocytomas of different WHO grades. *J. Neurooncol.* 86, 31–45.

Mallanna, S.K., and Rizzino, A. (2012). Systems biology provides new insights into the molecular mechanisms that control the fate of embryonic stem cells. *J. Cell. Physiol.* 227, 27–34.

Marie, S.K.N., Okamoto, O.K., Uno, M., Hasegawa, A.P.G., Oba-Shinjo, S.M., Cohen, T., Camargo, A.A., Kosoy, A., Carlotti, C.G., Jr, Toledo, S., et al. (2008). Maternal embryonic leucine zipper kinase transcript abundance correlates with malignancy grade in human astrocytomas. *Int. J. Cancer* 122, 807–815.

Martini, M., Cenci, T., D'Alessandris, G.Q., Cesarini, V., Cocomazzi, A., Ricci-Vitiani, L., De Maria, R., Pallini, R., and Maria Larocca, L. (2012). Epigenetic silencing of *Id4* identifies a glioblastoma subgroup with a better prognosis as a consequence of an inhibition of angiogenesis. *Cancer*.

Miller, S.A., Dykes, D.D., and Polesky, H.F. (1988). A simple salting out procedure for extracting DNA from human nucleated cells. *Nucleic Acids Res.* 16, 1215.

Norton, J.D. (2000). ID helix-loop-helix proteins in cell growth, differentiation and tumorigenesis. *J. Cell Sci.* 113 (Pt 22), 3897–3905.

Oba-Shinjo, S.M., Bengtson, M.H., Winnischofer, S.M.B., Colin, C., Vedoy, C.G., de Mendonça, Z., Marie, S.K.N., and Sogayar, M.C. (2005). Identification of novel differentially expressed genes in human astrocytomas by cDNA representational difference analysis. *Brain Res. Mol. Brain Res.* 140, 25–33.

Ohgaki, H., and Kleihues, P. (2011). Genetic profile of astrocytic and oligodendroglial gliomas. 177–183.

Ohgaki, H., and Kleihues, P. (2012). The Definition of Primary and Secondary Glioblastoma. *Clin. Cancer Res. Off. J. Am. Assoc. Cancer Res.*

Pan, X., Zhao, J., Zhang, W.-N., Li, H.-Y., Mu, R., Zhou, T., Zhang, H.-Y., Gong, W.-L., Yu, M., Man, J.-H., et al. (2009). Induction of *SOX4* by DNA damage is critical for p53 stabilization and function. *Proc. Natl. Acad. Sci. U. S. A.* 106, 3788–3793.

Park, S.-J., Kim, R.-J., and Nam, J.-S. (2011). Inhibitor of DNA-binding 4 contributes to the maintenance and expansion of cancer stem cells in 4T1 mouse mammary cancer cell line. *Lab. Anim. Res.* 27, 333–338.

Perk, J., Iavarone, A., and Benezra, R. (2005). Id family of helix-loop-helix proteins in cancer. 603–614.

Pfaffl, M.W. (2001). A new mathematical model for relative quantification in real-time RT-PCR. *e45*.

Qu, Q., and Shi, Y. (2009). Neural stem cells in the developing and adult brains. *J. Cell. Physiol.* *221*, 5–9.

Sampieri, K., and Fodde, R. (2012). Cancer stem cells and metastasis. *Semin. Cancer Biol.* *22*, 187–193.

Singh, S.K., Clarke, I.D., Terasaki, M., Bonn, V.E., Hawkins, C., Squire, J., and Dirks, P.B. (2003). Identification of a cancer stem cell in human brain tumors. *Cancer Res.* *63*, 5821–5828.

Singh, S.K., Hawkins, C., Clarke, I.D., Squire, J.A., Bayani, J., Hide, T., Henkelman, R.M., Cusimano, M.D., and Dirks, P.B. (2004). Identification of human brain tumour initiating cells. *Nature* *432*, 396–401.

Uno, M., Oba-Shinjo, S.M., de Aguiar, P.H., Leite, C.C., Rosemberg, S., Miura, F.K., Junior, R.M., Scaff, M., and Nagahashi Marie, S.K. (2005). Detection of somatic TP53 splice site mutations in diffuse astrocytomas. 321–327.

Uno, M., Oba-Shinjo, S.M., Wakamatsu, A., Huang, N., Ferreira Alves, V.A., Rosemberg, S., de Aguiar, P., Leite, C., Miura, F., Marino, R.J., et al. (2006). Association of TP53 mutation, p53 overexpression, and p53 codon 72 polymorphism with susceptibility to apoptosis in adult patients with diffuse astrocytomas. 50–57.

Uno, M., Oba-Shinjo, S.M., Camargo, A.A., Moura, R.P., Aguiar, P.H. de, Cabrera, H.N., Begnami, M., Rosemberg, S., Teixeira, M.J., and Marie, S.K.N. (2011). Correlation of MGMT promoter methylation status with gene and protein expression levels in glioblastoma. *Clin. São Paulo Braz.* *66*, 1747–1755.

Valente, V., Teixeira, S.A., Neder, L., Okamoto, O.K., Oba-Shinjo, S.M., Marie, S.K.N., Scrideli, C.A., Paçó-Larson, M.L., and Carlotti, C.G., Jr (2009). Selection of suitable housekeeping genes for expression analysis in glioblastoma using quantitative RT-PCR. 17.

Vandeputte, D.A.A., Troost, D., Leenstra, S., Ijlst-Keizers, H., Ramkema, M., Bosch, D.A., Baas, F., Das, N.K., and Aronica, E. (2002). Expression and distribution of id helix-loop-helix proteins in human astrocytic tumors. 329–338.

Wu, Q., Hoffmann, M.J., Hartmann, F.H., and Schulz, W.A. (2005). Amplification and overexpression of the ID4 gene at 6p22.3 in bladder cancer. *Mol. Cancer* *4*, 16.

Yuan, X., Curtin, J., Xiong, Y., Liu, G., Waschmann-Hogiu, S., Farkas, D.L., Black, K.L., and Yu, J.S. (2004). Isolation of cancer stem cells from adult glioblastoma multiforme. *Oncogene* 23, 9392–9400.

Yun, K., Mantani, A., Garel, S., Rubenstein, J., and Israel, M.A. (2004). Id4 regulates neural progenitor proliferation and differentiation in vivo. *Dev. Camb. Engl.* 131, 5441–5448.

Zeng, W., Rushing, E.J., Hartmann, D.P., and Azumi, N. (2010). Increased inhibitor of differentiation 4 (id4) expression in glioblastoma: a tissue microarray study. 1-5.

CHAPTER 3

Current state-of-the-art in molecular stratification of GBM and characterization of a Brazilian cohort.

Galatro TF^{1,2}, Moretti IF¹, Galdeno VF¹, Sola P¹, Oba-Shinjo SM¹, Marie SKN^{1,3}, Lerario AM^{4,5,6}

¹Department of Neurology, Laboratory of Molecular and Cellular Biology, LIM15, School of Medicine, University of São Paulo, São Paulo, Brazil.

²Department of Neuroscience, Section Medical Physiology, University Medical Center Groningen, University of Groningen, Groningen, The Netherlands.

³Center for Studies of Cellular and Molecular Therapy (NAP-NETCEM-NUCEL), University of São Paulo, São Paulo, Brazil.

⁴Departments of Cell & Developmental Biology, Pathology, Molecular & Integrative Physiology, Internal Medicine, University of Michigan, Ann Arbor, MI 48109, USA.

⁵University of Michigan Comprehensive Cancer Center, University of Michigan, Ann Arbor, MI 48109, USA.

⁶Bioinformatics coordinator of SELA (NGS facility core), School of Medicine, University of São Paulo.

Submitted

SUMMARY

Glioblastoma (GBM), the most common and lethal brain tumor, is one of the most difficult forms of CAN malignancy to treat. Integrated genomic analysis to unravel the molecular architecture of GBM, revealed a new sub classification and promising precision in the care for patients with specific genetic alterations. Here, we present the classification of a Brazilian GBM cohort into the main molecular subtypes; proneural, classical and mesenchymal, using high-throughput DNA sequencing. We tested the possible use of the overexpression of EGFR and CHI3L1 through immunohistochemistry for the identification of the Classical and mesenchymal subtypes, respectively. Our results show that genetic identification of GBM subtypes is not possible based on single targeted mutations, particularly in the case of the mesenchymal subtype. Also, it is not possible to single out mesenchymal cases through CHI3L1 expression. Our data indicate that the mesenchymal subtype, the most malignant subtype of GBM, needs further extensive research to allow for genetic identification/stratification.

INTRODUCTION

Glioblastoma multiforme (GBM) is the most common and most malignant brain tumor in adults. GBMs are part of the glioma group of tumors. The World Health Organization (WHO)(Louis et al., 2016) classifies gliomas according to their resemblance to their cell of origin, along with histological and molecular features. GBMs, the most prevalent of gliomas, are considered highly aggressive grade IV tumors, exhibiting high mitotic rates, micro-vascular proliferation and necrosis. GBMs also present the poorest prognosis, with a median survival of 15 months from the time of diagnosis(Wen and Kesari, 2008). Due to their invasive nature, complete surgical resection is very difficult to achieve. The presence of residual tumor cells results in recurrence and malignant progression, albeit at different intervals.

GBMs can be further divided into two subgroups: primary GBM, which arise *de novo*, and secondary GBM, which results from the progression of a lower grade tumor(Ohgaki and Kleihues, 2013). These two clinical forms of GBM have different and extensively characterized molecular features (reviewed by Ohgaki & Kleihues, 2013(Ohgaki and Kleihues, 2013)). The past decade has seen the rise of high-throughput sequencing techniques, which has provided in-depth knowledge of molecular alterations in tumor cells. GBM has been one of the most molecularly profiled tumors by several groups, including The Cancer Genome Atlas (TCGA) Networks(Brennan et al., 2013; Cancer Genome Atlas Research Network et al., 2015; Ceccarelli et al., 2016; Parsons et al., 2008; Phillips et al., 2006; Stieber et al., 2014; Verhaak et al., 2010). These studies have singled out specific determinant mutations of the newly identified subtypes: proneural, neural, classical and mesenchymal (Figure 2). Proneural tumors present alterations in *IDH1*, *PDGFRA* and *TP53*; classical tumors display mainly *EGFR* mutation/amplification and the presence of *EGFRvIII* oncogenic variant; and mesenchymal tumors show *RB1* and *NF1* mutations as the main feature. The neural subtype presents overexpression of neural markers, not displaying any specific genetic alteration. Overall patient survival was also correlated with GBM molecular subtypes, with the mesenchymal subtype presenting the worst prognosis. However, the reproducibility, clinical relevance, and functional basis of these subclasses remain to be established.

In this study, we have developed a NGS-based gene panel to interrogate several genes commonly mutated in GBM. We classified a series of Brazilian GBM cases based on the somatic mutation signatures previously established for the three main subtypes:

proneural, classical and mesenchymal. We validated our genetic findings with orthogonal methods and immunohistochemistry. In this multi-institution cohort of Brazilian patients, GBM subtype distribution and associated patient outcomes corroborate previously published results and further validates the clinical relevance of GBM subtyping. NGS-based approaches for GBM classification are fast, reliable, and therefore, may have value as a diagnostic tool that may add in the clinical decision making process.

MATERIALS AND METHODS

GBM samples and ethical statement

One hundred and ten GBM samples were obtained during therapeutic surgery of patients treated by the Neurosurgery Group of the Department of Neurology at Hospital das Clínicas at the School of Medicine of the University of São Paulo, in the period of 2000 to 2014. GBM diagnosis was confirmed by neuropathologists from the Division of Pathological Anatomy of the same institution, according to the WHO grading system. Patient information and clinical findings are presented in Supplemental Table 1. Samples were macrodissected and immediately snap-frozen in liquid nitrogen upon surgical removal. A 4µm-thick cryosection of each sample was analyzed under a light microscope after hematoxylin-eosin staining for assessment of necrotic, cellular debris and non-neoplastic areas, followed by removal from the frozen block by microdissection prior to DNA extractions. Written informed consent was obtained from all patients according to the ethical guidelines approved by the Ethical Committee of Hospital das Clínicas, School of Medicine, University of São Paulo (0599/10).

Targeted gene panel sequencing

Based on previous literature assessing GBM molecular sub classification (Brennan et al., 2013; Phillips et al., 2006; Verhaak et al., 2010), 40 genes were targeted for capture and deep sequencing. This customized panel included genes such as *NF1*, *RB1*, *EGFR*, *TP53*, *PTEN*, *IDH1* and *PDGFRA*, whose alterations have all been previously associated with the three main GBM subtypes: proneural, classical and mesenchymal. Using the SureDesign tool (Agilent Technologies Inc., USA), the targeted RNA capture enrichment baits were designed to include coding exon regions and 50 bp from both 3' end and 5' end of the flanking intronic sequence. The purpose was to incorporate possible splicing site mutations in our analysis. A total of 973 regions from the 40 genes were targeted for a final capture size of 2.79 Mb.

Target-enrichment DNA library was constructed using the Agilent SureSelect XT Target Enrichment Kit (Agilent Technologies Inc.), following the recommended protocol. Two hundred nanograms of tumor DNA was sheared using a E220 focused-ultrasonicator (Covaris, USA) to generate DNA fragments with a mean peak around 150bp. Indexed and adaptor-ligated libraries were multiplexed and paired-end

sequenced on Illumina NextSeq 500 platform (Illumina, USA). An additional library was built from peripheral blood DNA from all the patients pooled in equal amounts.

Bioinformatics analysis

Sequencing data was generated as 150-bp paired-end reads using the Illumina Next-Seq platform. Raw data was aligned to the hg38 assembly of the human genome using *bwa*(Li and Durbin, 2009). Aligned reads were coordinate-sorted with the *bamsort* tool from *Biobambam2*(Tischler and Leonard, 2014). Variant calling was performed simultaneously in all the tumor samples with *Platypus*(2014), and in the germline pool with *freebayes*, with the parameters properly set to call pooled data (--pooled-discrete and ploidy parameter set to 132, which corresponds to the number of alleles present in the pool). The resulting VCFs file were annotated with *SnEff* and *SnSIFT*(Cingolani et al., 2012).

Tissue microarray (TMA) construction and Immunohistochemistry

Two representative areas of each tumor were chosen by neuropathologists and marked both on HE sections and on the original paraffin block. Each of the 0.6 mm-diameter three cores of tumor tissue was extracted from the marked area of each donor block using an arraying machine (MTA-1, Beecher Instruments Inc., USA). The cores were inserted into a TMA recipient block in predetermined sites. Sections of 3 μ m-thickness were cut from the TMA block. A representative TMA section was initially stained for HE to assess the suitability of each core, and all other sections were paraffin coated and stored at -20°C until use.

For immunohistochemical detection, serial TMA sections were deparaffinized, rehydrated, treated for endogenous peroxidase blocking and subjected to antigen retrieval. Briefly, slides were immersed in 10 mM citrate buffer, pH 6.0 and incubated at 122°C for 3 min using an electric pressure cooker (BioCare Medical, USA). Specimens were then blocked and further incubated anti-human CHI3L1 (mouse monoclonal, clone AT4A3; abcam, United Kingdom) and anti-human EGFR (mouse monoclonal, clone 31G7; Thermo Fisher Scientific, USA) at 16-20°C for 16 hours. Development of the reaction was performed with a commercial kit (Novolink; Novocastra, United Kingdom) at room temperature, using diaminobenzidine and Harris hematoxylin for nuclear staining. Optimization using positive controls suggested by the manufacturer of each

antibody was performed in order to obtain optimal dilution. Two observers (SKNM and TFAG) evaluated staining intensity of tissue sections independently. A semi-quantitative score system considering both intensity of staining and percentage of cells was applied as follows: for intensity of staining and cell percentage, 0=no cells stained, 1=10–25%, 2 =26–50%, 3=51–75% and 4=76–100%. Only cases with positive cell staining with scores ≥ 2 were considered as positive. Digital photomicrographs of representative fields were captured and processed using Picasa 3 (Google, USA).

Statistical analysis

Survival data was assessed by comparing the Kaplan-Meier survival curves using the log-rank (Mantel Cox) test. A p-value < 0.05 was considered statistically significant. For this analysis, we included 77 cases with complete clinical follow-up. Calculations were performed using SPSS, version 23.0 (IBM, USA).

RESULTS

Molecular classification of GBM

We used the mutational profile derived from our targeted gene panel to classify tumors into three major molecular subtypes: proneural, classical, and mesenchymal. We defined the proneural subtype by the presence of *IDH1*, *PDGFRA*, and *TP53* mutations. The classical subtype was defined by *EGFR* alterations (amplification and mutations), *PTEN* mutations, and the presence of the oncogenic variant *EGFRV8*. *EGFR* amplification results was based on a previous publication from our group (Carvalho et al., 2014). Finally, for the definition of the mesenchymal subtype, we used mutations in *NF1* and *RB1* as a mean for classification. For each patient, we used DNA from blood leukocytes for germline alterations subtraction. None of the found alterations were present in this germline controls. Aside from this control, we considered in this analysis a) known pathogenic mutations, such as the *IDH1* R132H, b) variants that were not present in populational databases (1000kg/ExAC), c) variants with predicted pathogenicity (nonsense or frameshift, or a missense mutation with high SIFT and polyphen scores), d) variants not present in our germline pool. All the tumors which did not carry a mutation in the genes described above and meet the defined criteria were classified as “others”. Hence, given the lack of a specific genetic profile that defines the neural subtype, we were not able to identify this subclass in our dataset. The complete list of genetic alteration can be found in Supplemental Table 2.

The targeted NGS analysis was performed on 110 GBM samples (Supplemental Table 1). A 20x coverage was achieved in ~97% of the targeted regions of the GBM samples. The mean coverage of the germline pool was 6063.67x.

Following the proposed criteria, we were able to classify 90 of the 110 analyzed GBM samples within the three major subtypes. Corroborating data from previous studies, genetic alteration singular to the classical subtype were more prevalent, corresponding to 45.9% of the classified cases. Samples with alterations inherent of the mesenchymal subtype corresponded to 19.3% of the cases; finally, 17.4% of the cases showed alterations particular to the proneural subtype (Figure 1).

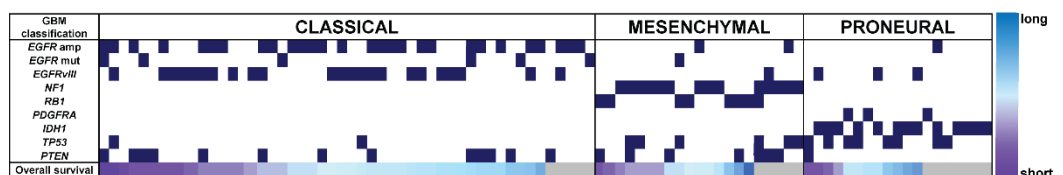
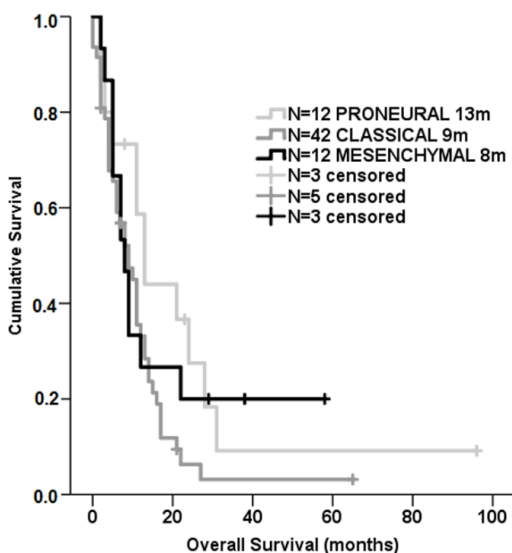


Figure 1. Representation of the molecularly classified data across the spectrum of the genetic alterations of the cases molecularly classified in our GBM cohort. Classification was achieved using a customized gene panel, followed by exome sequencing. The gradient depicts patient overall survival, further explored in the Kaplan-Meier in Figure 2. The gray squares represent the cases without a complete clinical follow-up. amp, amplification; mut,

We next evaluated the overall survival of GBM patients according to our molecular classification. As shown in Figure 2, patients classified as mesenchymal GBM had a slightly shorter overall survival in comparison to other subgroups (medians of 8, 9, and 13 months for the mesenchymal, classical, and proneural, respectively; log-rank $p < 0.05$).



Molecular classification of GBM does not correlate with immunohistochemical markers to differentiate between classical and mesenchymal subtypes

Concomitant with the molecular classification of GBMs, we also assessed the protein expression level of CHI3L1 (YKL-40) and EGFR. CHI3L1 is associated with the mesenchymal subtype of GBM, while EGFR overexpression is a known characteristic of the classical subtype (Phillips et al., 2006; Verhaak et al., 2010). Immunohistochemistry staining was performed in a subset of our molecularly classified samples, comprising a cohort of 40 cases (8 mesenchymal, 9 proneural, 20 classical and 3 other). Figure 3 shows the results and Figure 4 depicts examples of stained tissue microarray sections.

Figure 2: Survival curve of the molecularly classified GBM cases. Kaplan-Meier of 77 GBM cases detailing survival (log rank test) times according to our molecular classification. Patients alive at the time of the last clinical follow-up were censored from this analysis. N, number of cases; m, months.

While in only one of the mesenchymal samples CHI3L1 was not detected, cases positive for CHI3L1 (scoring above 2) were present in all three subtypes (6 mesenchymal, 6 proneural and 10 classical cases were positive for CHI3L1). For EGFR, all proneural and 6 mesenchymal cases prove to be negative for this marker (staining score ≤ 1). Despite presenting genetic characteristics of classical subtypes, 4 of these cases did not express detectable levels of EGFR. A complete listing of immunohistochemistry scores is provided in Supplemental Table 1.

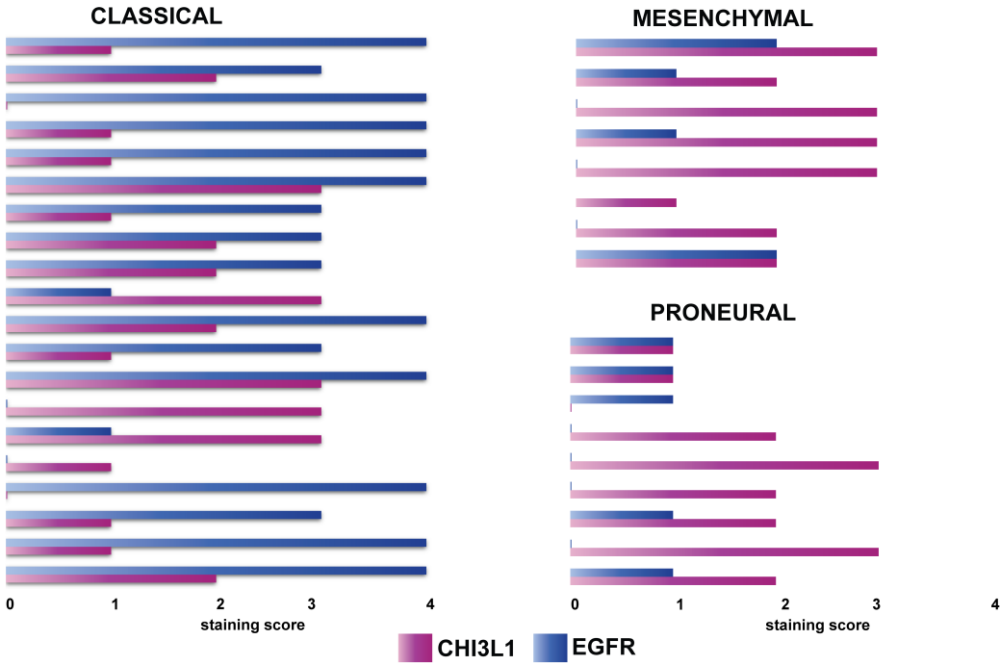
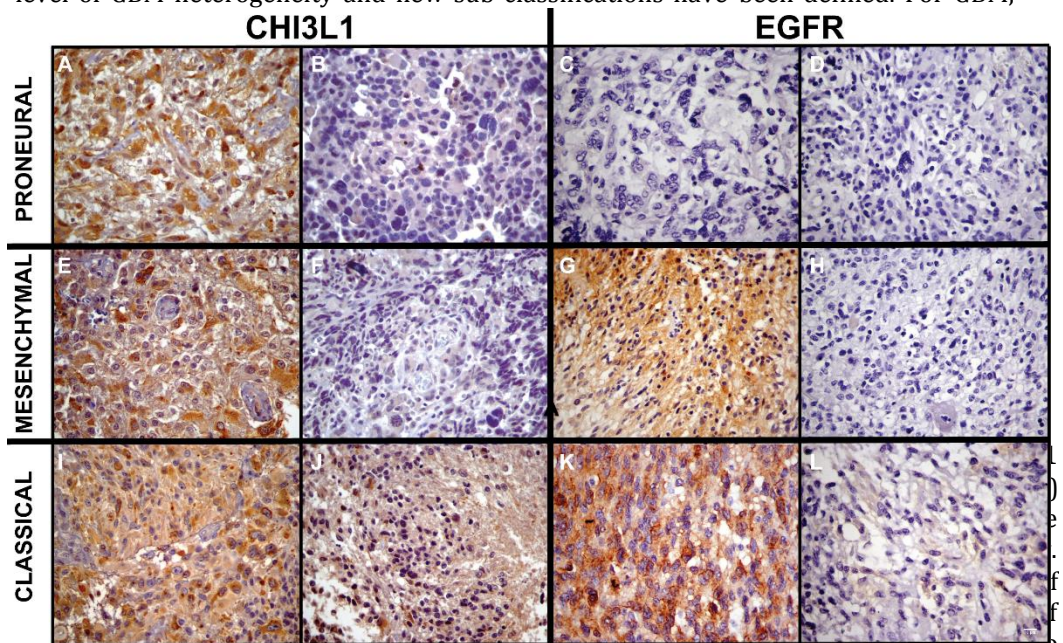


Figure 3: Scoring of immunohistochemical analysis of CHI3L1 and EGFR in GBM cases. Each GBM sample, previously classified with the molecular approach, was scored for the classical (EGFR, blue) and mesenchymal (CHI3L1, pink) immunohistochemical markers. Scoring ranged from 0-4, in which 0=no cells stained, 1=10–25%, 2 =26–50%, 3=51–75% and 4=76–100%. EGFR staining was prevalent in classical samples, although classical cases did not present significant staining of the marker, while other mesenchymal samples presented comparable levels of EGFR. CHI3L1 was present in high levels in cases from all three GBM subtypes.

DISCUSSION

The advent of next generation sequencing and large-scale molecular analysis in the last decade revealed that molecular alterations predict GBM patients' response to treatment, overall survival and clinical outcome. A new light has been shed on the high level of GBM heterogeneity and new sub classifications have been defined. For GBM,



CHI3L1 marker. Despite being negative in proneural cases (B), EGFR overexpression failed to differentiate between mesenchymal and classical cases, with both groups showing positive and negative cases. The reaction was performed in paraffin embedded tissue sections with a commercial polymer kit (Novolink; Novocastra, UK), using diaminobenzidine as developer and Harris hematoxylin for nuclear counterstaining. 400x magnification for all images. Scale bar 10µm

several studies have singled out specific determinant mutations of the main, newly identified subtypes: proneural, classical and mesenchymal (Figure 1)(Brennan et al., 2013; Cancer Genome Atlas Research Network et al., 2015; Ceccarelli et al., 2016; Parsons et al., 2008; Phillips et al., 2006; Stieber et al., 2014; Verhaak et al., 2010). Their potential to aid the choice of better treatment options is a step forward to precision medicine.

We have performed a somatic mutation analysis in our GBM cohort using a customized gene panel that contains all the coding and splicing regions of the genes

most commonly mutated in GBM. Our NGS panel allowed us to classify ~85% of our samples according to the molecular subtype using a single assay, which would be very laborious and time-consuming with the traditional methods, such as Sanger sequencing. The results we obtained, regarding the percentage of each GBM subtype, as well as their association with overall patient survival, is in accordance with what has been published in literature so far (Brennan et al., 2013; Ceccarelli et al., 2016; Phillips et al., 2006; Stieber et al., 2014; Verhaak et al., 2010).

Since its first documentations, in the late 2000's, molecular subclasses of GBMs have proven to be fundamental for new discoveries that ultimately will lead to better clinical approaches and precision medicine. For instance, Davis *et al* (Davis et al., 2016) have used the classification to compare genetic alterations in cultured brain-tumor initiating cells, important as a model system to study treatment options and GBM biology, to their original tumors, validating such cells for future studies. Natash *et al* (Natash et al., 2015) explored the role of a cytokine present in the microenvironment of GBM, oncostatin, and its signaling pathway, associated with poor prognosis, to be related to the aggressive nature associated with features found in the mesenchymal GBM subtype. Chen and Xu (Chen and Xu, 2016) have recently developed an algorithm that matches FDA approved drugs to the molecular subtype of GBMs, based on the genetic alterations of each subtype. Hence, it is important to specifically differentiate mesenchymal and classical GBMs, as for the latter specific tyrosine kinase inhibitors and adjuvant antibodies are available (reviewed by Padfield *et al* (Padfield et al., 2015)), while for the former currently only one drug is introduced in phase one clinical trial (clinical trial identifier: NCT02272270). New practical proposals, more suitable for big diagnostic centers, have been looked for. The exemplified studies highlight the usefulness of GBM classification in improving current knowledge, biological understanding and diagnosis and treatment options for this tumor.

However, since the basis for such classification is the genetic approach, requiring the implementation of molecular biology techniques, other more feasible methodologies have been searched. A recent study revealed that MRI derived quantitative volumetric tumor phenotype features only moderately predict the molecular GBM subtypes, suggesting that subtypes do not generally alter the size composition of tumor areas (Grossmann et al., 2016). Therefore, the more feasible proteomic IHC-based approach, still based on the reported molecular findings, has been the preferred technique for GBM classification.

Both proneural and classical GBM subtypes present genetic point mutations or alterations (*IDH1* R132H and *EGFRvIII*, respectively) have led to the development of specific antibodies to achieve a cheaper and more suitable to large diagnostic centers approach (Gupta et al., 2010; Kato, 2015). Nonetheless, *EGFRvIII* alterations were detected in only 28.4% of our GBM cohort, while classical cases corresponded to 45.9% of all cases. For those extra cases, EGFR protein overexpression still excluded 4 out of 23 samples with a classical genetic subtype.

The mesenchymal subtype presents a high heterogeneity of alterations within the usually mutated genes of this subtype (*NF1* and *RB1*). CHI3L1, or YKL-40, is a secreted lectin, related to the regulation of hypoxia-induced injury response and that has been previously associated with the mesenchymal subtype of GBM (Phillips et al., 2006; Verhaak et al., 2010). Previous studies have proposed CHI3L1 as an additional marker to be used as a diagnostic tool using the immunohistochemical approach for the sub classification of GBMs (Conroy et al., 2014; Joseph et al., 2015). Yet, our results indicate that higher CHI3L1 expression is not an event exclusive of the mesenchymal cases, with high percentages of both proneural and classical samples expressing such high levels.

Our results indicate the need for a genetic approach to further classify GBMs, so higher number of patients can profit from the precision such classifications provides in treatment options.

ACKNOWLEDGEMENTS

The authors sincerely thank the doctors and residents from the Discipline of Neurosurgery of the Department of Neurology at Hospital das Clínicas of School of Medicine, University of São Paulo, from the Neurosurgery group at Sírio Libanês Hospital and, particularly, Drs André M Bianco and Egmond Alves, for the therapeutic and diagnostic procedures of all patients included in this study. We also thank the physicians and technicians at the Division of Pathological Anatomy of the same institutions, particularly Dr Sergio Rosemberg, for the histological classification of tumor samples and tissue section processing. The authors thank São Paulo Research Foundation (FAPESP), grants #2013/07704-3, #2013/06315-3, #2013/02162-8, #2014-50137-5 and #2016/15652-1, CAPES-NUFFIC (062/15), Conselho Nacional de Pesquisa (CNPq 305730/2015-0) and Fundação Faculdade de Medicina (FFM) for financial support.

REFERENCES

Brennan, C.W., Verhaak, R.G.W., McKenna, A., Campos, B., Noushmehr, H., Salama, S.R., Zheng, S., Chakravarty, D., Sanborn, J.Z., Berman, S.H., et al. (2013). The somatic genomic landscape of glioblastoma. *Cell* 155, 462–477.

Cancer Genome Atlas Research Network, Brat, D.J., Verhaak, R.G.W., Aldape, K.D., Yung, W.K.A., Salama, S.R., Cooper, L.A.D., Rheinbay, E., Miller, C.R., Vitucci, M., et al. (2015). Comprehensive, Integrative Genomic Analysis of Diffuse Lower-Grade Gliomas. *N. Engl. J. Med.* 372, 2481–2498.

Carvalho, P.O., Uno, M., Oba-Shinjo, S.M., Rosemberg, S., Wakamatsu, A., da Silva, C.C., Teixeira, M.J., and Marie, S.K.N. (2014). Activation of EGFR signaling from pilocytic astrocytomas to glioblastomas. *Int. J. Biol. Markers* 29, e120-128.

Ceccarelli, M., Barthel, F.P., Malta, T.M., Sabedot, T.S., Salama, S.R., Murray, B.A., Morozova, O., Newton, Y., Radenbaugh, A., Pagnotta, S.M., et al. (2016). Molecular Profiling Reveals Biologically Discrete Subsets and Pathways of Progression in Diffuse Glioma. *Cell* 164, 550–563.

Chen, Y., and Xu, R. (2016). Drug repurposing for glioblastoma based on molecular subtypes. *J. Biomed. Inform.* 64, 131–138.

Cingolani, P., Patel, V.M., Coon, M., Nguyen, T., Land, S.J., Ruden, D.M., and Lu, X. (2012). Using *Drosophila melanogaster* as a Model for Genotoxic Chemical Mutational Studies with a New Program, SnpSift. *Front. Genet.* 3, 35.

Conroy, S., Kruyt, F.A.E., Joseph, J.V., Balasubramaniyan, V., Bhat, K.P., Wagemakers, M., Enting, R.H., Walenkamp, A.M.E., and den Dunnen, W.F.A. (2014). Subclassification of Newly Diagnosed Glioblastomas through an Immunohistochemical Approach. *PLoS ONE* 9.

Davis, B., Shen, Y., Poon, C.C., Luchman, H.A., Stechishin, O.D., Pontifex, C.S., Wu, W., Kelly, J.J., Blough, M.D., and Terry Fox Research Institute Glioblastoma Consortium (2016). Comparative genomic and genetic analysis of glioblastoma-derived brain tumor-initiating cells and their parent tumors. *Neuro-Oncol.* 18, 350–360.

Grossmann, P., Gutman, D.A., Dunn, W.D., Holder, C.A., and Aerts, H.J.W.L. (2016). Imaging-genomics reveals driving pathways of MRI derived volumetric tumor phenotypic features in Glioblastoma. *BMC Cancer* 16, 611.

Gupta, P., Han, S.-Y., Holgado-Madruga, M., Mitra, S.S., Li, G., Nitta, R.T., and Wong, A.J. (2010). Development of an EGFRvIII specific recombinant antibody. *BMC Biotechnol.* 10, 72.

Joseph, J.V., Conroy, S., Pavlov, K., Sontakke, P., Tomar, T., Eggens-Meijer, E., Balasubramaniyan, V., Wagemakers, M., Dunnen, W.F.A. den, and Kruyt, F.A.E. (2015). Hypoxia enhances migration and invasion in glioblastoma by promoting a mesenchymal shift mediated by the HIF1 α -ZEB1 axis. *Cancer Lett.* 359, 107–116.

Kato, Y. (2015). Specific monoclonal antibodies against IDH1/2 mutations as diagnostic tools for gliomas. *Brain Tumor Pathol.* 32, 3–11.

Li, H., and Durbin, R. (2009). Fast and accurate short read alignment with Burrows-Wheeler transform. *Bioinforma. Oxf. Engl.* 25, 1754–1760.

Louis, D.N., Perry, A., Reifenberger, G., von Deimling, A., Figarella-Branger, D., Cavenee, W.K., Ohgaki, H., Wiestler, O.D., Kleihues, P., and Ellison, D.W. (2016). The 2016 World Health Organization Classification of Tumors of the Central Nervous System: a summary. *Acta Neuropathol. (Berl.)* 131, 803–820.

Natesh, K., Bhosale, D., Desai, A., Chandrika, G., Pujari, R., Jagtap, J., Chugh, A., Ranade, D., and Shastry, P. (2015). Oncostatin-M differentially regulates mesenchymal and proneural signature genes in gliomas via STAT3 signaling. *Neoplasia N. Y. N* 17, 225–237.

Ohgaki, H., and Kleihues, P. (2013). The definition of primary and secondary glioblastoma. *Clin. Cancer Res. Off. J. Am. Assoc. Cancer Res.* 19, 764–772.

Padfield, E., Ellis, H.P., and Kurian, K.M. (2015). Current Therapeutic Advances Targeting EGFR and EGFRvIII in Glioblastoma. *Front. Oncol.* 5, 5.

Parsons, D.W., Jones, S., Zhang, X., Lin, J.C.-H., Leary, R.J., Angenendt, P., Mankoo, P., Carter, H., Siu, I.-M., Gallia, G.L., et al. (2008). An integrated genomic analysis of human glioblastoma multiforme. *Science* 321, 1807–1812.

Phillips, H.S., Kharbanda, S., Chen, R., Forrest, W.F., Soriano, R.H., Wu, T.D., Misra, A., Nigro, J.M., Colman, H., Soroceanu, L., et al. (2006). Molecular subclasses of high-grade glioma predict prognosis, delineate a pattern of disease progression, and resemble stages in neurogenesis. *Cancer Cell* 9, 157–173.

Stieber, D., Golebiewska, A., Evers, L., Lenkiewicz, E., Brons, N.H.C., Nicot, N., Oudin, A., Bougnaud, S., Hertel, F., Bjerkvig, R., et al. (2014). Glioblastomas are composed of genetically divergent clones with distinct tumorigenic potential and variable stem cell-associated phenotypes. *Acta Neuropathol. (Berl.)* 127, 203–219.

Tischler, G., and Leonard, S. (2014). biobambam: tools for read pair collation based algorithms on BAM files. *Source Code Biol. Med.* 9, 13.

Verhaak, R.G.W., Hoadley, K.A., Purdom, E., Wang, V., Qi, Y., Wilkerson, M.D., Miller, C.R., Ding, L., Golub, T., Mesirov, J.P., et al. (2010). Integrated genomic analysis

identifies clinically relevant subtypes of glioblastoma characterized by abnormalities in PDGFRA, IDH1, EGFR, and NF1. *Cancer Cell* 17, 98–110.

Wen, P.Y., and Kesari, S. (2008). Malignant gliomas in adults. *N. Engl. J. Med.* 359, 492–507.

(2014). Platypus, a reference genome-free algorithm that rapidly calls variants in clinical sequencing data. *SciBX Sci.-Bus. Exch.* 7.

CHAPTER 4

Characterization of inhibitors of differentiation (ID) 1-4 expression in human gliomas

Galatro TF^{1,2}, Lerario AM^{3,4}, Sola P¹, Oba-Shinjo SM¹, Marie SKN^{1,5}

¹Department of Neurology, Laboratory of Molecular and Cellular Biology, LIM15, School of Medicine, University of São Paulo, São Paulo, Brazil

²Department of Neuroscience, section Medical Physiology, University of Groningen, University Medical Center Groningen, Groningen, 9713 AV, The Netherlands.

³Departments of Cell & Developmental Biology, Pathology, Molecular & Integrative Physiology, Internal Medicine, University of Michigan, Ann Arbor, MI 48109, USA

⁴University of Michigan Comprehensive Cancer Center, University of Michigan, Ann Arbor, MI 48109, USA

⁵Center for Studies of Cellular and Molecular Therapy (NETCEM) University of Sao Paulo, São Paulo, Brazil

SUMMARY

Diffuse gliomas are primary brain tumors characterized by infiltrative growth and high heterogeneity, which renders the disease mostly incurable. Glioblastoma multiforme (GBM) is the most common and malignant form of glioma in adults. ID proteins (ID1-4) are dominant negative transcription factors that belong to the basic helix-loop-helix family (bHLH), a group of proteins that play crucial roles in cellular process ranging from cell cycle control, differentiation and tumorigenesis.

We have previously assessed *ID4* expression in diffuse astrocytomas. In the current work, we expanded our study, further looking into the expression pattern of all ID family members in astrocytomas ranging from grade I-IV. Furthermore, we used a targeted gene panel for mutation and exome sequencing to subclassify GBM samples and explore the distribution of ID1-4 along the three main subtypes of GBM with more defined gene mutation profile: proneural, classical and mesenchymal. A correlation with overall patient survival and a clinical endpoint for these GBM patients was also determined. Finally, we compared IDs expression in low-grade gliomas from both astrocytic and oligodendrocytic origin, evaluating how IDs expression varies between the two types of gliomas.

INTRODUCTION

Inhibitor of Differentiation (ID) proteins (ID1-4) are dominant negative transcription factors that belong to the basic helix-loop-helix family (bHLH), a highly evolutionarily conserved group of proteins that play crucial roles in cellular process ranging from cell cycle control, differentiation and tumorigenesis (Benezra et al., 1990; Lasorella et al., 2014). While other members of bHLH family retain a DNA binding region in their structure, ID proteins lack such region and sequester target proteins, forming inactive heterodimers and negatively regulating transcription. During embryonic development, ID proteins increase cellular proliferation while maintaining the undifferentiated state. After cellular differentiation is completed, ID levels decline to basal. It is no surprise, then, that their overexpression in cancer is associated with increased aggressiveness and a poorer prognosis (Lee et al., 2016; Weiler et al., 2015; Xu et al., 2016).

Diffuse gliomas are primary brain tumors characterized by infiltrative growth and high heterogeneity, which renders the disease mostly incurable. Glioblastoma multiforme (GBM) is the most common and most malignant form of glioma in adults. World Health Organization (WHO) (Louis et al., 2016) classifies gliomas according to their resemblance to their cell of origin, along with histological and immunohistochemical features. GBMs are considered grade IV tumors, exhibiting high mitotic rates, micro-vascular proliferation and necrosis. They can be further divided into two subgroups: primary GBM, which arise *de novo*, and secondary GBM, which results from the progression of a lower grade (Ohgaki and Kleihues, 2013). These two clinical forms of GBM have different and extensively characterized molecular features. The past decade has seen the rise of high-throughput sequencing techniques, which has provided in-depth knowledge of molecular alterations in tumor cells. GBM has been one of the most molecularly profiled tumors by several groups, including The Cancer Genome Atlas (TCGA) Networks (Brennan et al., 2013a; Cancer Genome Atlas Research Network et al., 2015; Ceccarelli et al., 2016; Parsons et al., 2008; Phillips et al., 2006; Stieber et al., 2014; Verhaak et al., 2010). Aside from the primary and secondary clinical classification, there are currently three major molecular GBM subtypes: proneural, with alterations in *IDH1*, *PDGFRA* and *TP53*; classic, displaying mainly *EGFR* mutation/amplification and the presence of *EGFRvIII* oncogenic variant; and mesenchymal, with *RB1* and *NF1* mutations as the main feature. The neural subtype does not present any specific genetic features and instead is classified by the

overexpression of normal neural genes. Patient overall survival also correlate with GBM molecular subtypes, with the mesenchymal subtype presenting the worst prognosis.

We have previously assessed *ID4* expression in diffuse astrocytomas (Galatro et al., 2013), demonstrating its association with *TP53* mutation and the impact of its co-expression with *SOX4* and *OCT-4* has on GBM patient overall survival. In the current work, we expanded our study, further looking into the expression pattern of all ID family members in astrocytomas ranging from grade I-IV. Furthermore, we used a targeted gene panel for mutation and exome sequencing to subclassify GBM samples and explore the distribution of ID1-4 along the three main subtypes of GBM with more defined gene mutation profile: proneural, classical and mesenchymal. A correlation with overall patient survival and clinical endpoint for these GBM patients was also made. Finally, we compared IDs expression in low-grade gliomas from both astrocytic and oligodendrocytic origins, evaluating how IDs expression varies between the two types of gliomas.

MATERIALS AND METHODS

Tissue samples and ethical statement

One hundred and eighty gliomas (grades I to IV) were obtained during therapeutic surgery of patients treated by the Neurosurgery Group of the Department of Neurology at Hospital das Clínicas at the School of Medicine of the University of São Paulo, in the period of 2000 to 2007. The cases were categorized according to the WHO grading system (Louis et al., 2016) by neuropathologists from the same institution. The studied series consisted of 153 astrocytomas (23 AGI, 26 AGII, 18 AGIII, 86 GBM), 27 low-grade oligodendrogliomas (OGII) and 22 non-neoplastic (NN) brain anonymized cases from epilepsy patients subjected to temporal lobectomy. Further data corresponding to patient clinical history is presented in Supplemental Table 1. Samples were collected, macrodissected and immediately snap-frozen in liquid nitrogen upon surgical removal. A 4µm-thick cryosection of each sample was analyzed under a light microscope after hematoxylin-eosin staining for assessment of necrotic, cellular debris and non-neoplastic areas (in tumor samples), followed by removal from the frozen block by microdissection prior to RNA extractions (Marie et al., 2008; Oba-Shinjo et al., 2005). Written informed consent was obtained from all patients according to the ethical guidelines approved by the Department of Neurology, School of Medicine, University of São Paulo (0599/10).

Sample preparation

Total DNA and RNA was extracted from frozen tissue (tumor and non-neoplastic) using an AllPrep Mini Kit (Qiagen, Hilden, Germany). Evaluation of concentration and purity were carried out by measuring absorbance at 260 and 280 nm. Ratios of 260/280 measures ranging from 1.8 to 2.0 were considered satisfactory for purity standards. Denaturing agarose gel electrophoresis was used to assess the quality of the samples. For RNA, a conventional reverse transcription reaction was performed to yield single-stranded cDNA. The first strand of cDNA was synthesized from 1 µg of total RNA previously treated with 1 unit of DNase I (FPLC-pure, GE Healthcare, Uppsala, Sweden) using random and oligo (dT) primers, RNase inhibitor, and SuperScript III reverse transcriptase according to the manufacturer's recommendations (Thermo Fischer Scientific, Carlsbad, CA, USA). The resulting cDNA

was subsequently treated with 1 unit of RNase H (GE Healthcare), diluted with TE buffer, and stored at -20°C until later use.

Quantitative real time PCR (qPCR)

Relative expression level of *ID1*, *ID2*, *ID3* and *ID4* was analyzed by qPCR, using the SYBR Green approach. Quantitative data was normalized in relation to the geometric mean of three housekeeping genes, suitable for the analysis: hypoxanthine phosphoribosyltransferase (*HPRT*), glucuronidase beta (*GUSB*) and TATA box binding protein (*TBP*), as previously demonstrated by our group (Valente et al., 2009). Primers were designed to amplify 80–130 bp amplicons, with an annealing temperature of 60°C and were synthesized by IDT (Integrated DNA Technologies, Coralville, USA) as follows (5' to 3'): *ID1* F: TCGCATCTTGTGTCGCTGA; *ID1* R: ATCGGTCTTGTCTCCCTCAGA; *ID2* F: CCACCTCAACACGGATATCA, *ID2* R: AACACCGTTATTCAGCCACA; *ID3* F: TACAGCGCTCATCGACTACA, *ID3* R: CTCGGCTGTCTGGATGGGA; *ID4* F: TGAACAAGCAGGGCGACAG, *ID4* R: CCCTCTCTAGTGCTCCTGGCT; *HPRT* F: TGAGGATTTGGAAAGGGTGT *HPRT* R: GAGCACACAGAGGGCTACAA; *GUSB* F: GAAAATACGTGGTTGGAGAGCTCATT, *GUSB* R: CCGAGTGAAGATCCCCTTTTAA; *TBP* F: AGGATAAGAGAGCCACGAACCA, *TBP* R: CTTGCTGCCAGTCTGGACTGT. The minimum primer concentrations necessary to give the lowest threshold cycle (Ct) and maximum amplification efficiency were determined, while minimizing non-specific amplification. Primer concentrations used were 150 nM for *ID4*, 200 nM for *HPRT*, *TBP*, *ID1*, *ID2* and *ID3*, and 400 nM for *GUSB*. Standard curve was established to ensure amplification efficiency and analysis of melting curves demonstrated a single peak for all PCR products. Additionally, agarose gel electrophoresis was employed to check the size of the PCR product amplified. SYBR Green I amplification mixtures (12 µl) contained 3 µl of cDNA, 6 µl of 2X Power SYBR Green I Master Mix (Thermo Fischer Scientific) and forward and reverse primers. PCR reactions were run on an ABI Prism 7500 sequence detector (Thermo Fischer Scientific) as follows: 2 min at 50°C, 10 min of polymerase activation at 95°C, and 40 cycles of 15 s at 95°C and 1 min at 60°C. All the reactions were performed in duplicate. The following equations were applied to calculate gene relative expression according to primer efficiency (E) in tumor samples versus the mean of non-neoplastic tissues: $2^{-\Delta Ct}$ (Livak and Schmittgen, 2001) for *ID1*; and $1+E^{-\Delta Ct}$ (Pfaffl, 2001) for *ID2*, *ID3* and *ID4*, where $\Delta Ct = Ct$ specific gene- geometric mean Ct of housekeeping genes. For statistical analysis, gene expression status was scored as high

or low expression in relation to the median relative expression value at each grade of astrocytoma.

Targeted gene panel for GBM molecular classification

Based on previous literature assessing GBM molecular subclassification (Brennan et al., 2013a; Phillips et al., 2006; Verhaak et al., 2010), 40 genes were targeted for capture and deep sequencing. This customized panel included genes such as *NF1*, *RB1*, *EGFR*, *TP53*, *PTEN*, *IDH1* and *PDGFRA*, whose alterations have all been previously associated with the three main GBM subtypes: proneural, classical and mesenchymal. Using the SureDesign tool (Agilent Technologies Inc., Santa Clara, CA, USA), the targeted RNA capture enrichment baits were designed to include coding exon regions and 50 bp from both 3' end and 5' end of the flanking intronic sequence. The purpose was to incorporate possible splicing site mutations in our analysis. A total of 973 regions from the 40 genes were targeted for a final capture size of 2.79 Mb.

Target-enrichment DNA library was constructed using the Agilent SureSelect XT Target Enrichment Kit (Agilent Technologies Inc.), following the recommended protocol. Two hundred ng of genomic DNA was sheared using a E220 focused-ultrasonicator (Covaris, Woburn, MA, USA) to generate DNA fragments with a mean peak around 150bp. Indexed and adaptor-ligated libraries were multiplexed and paired-end sequenced on Illumina NextSeq 500 platform (Illumina, San Diego, CA, USA). The full description of the analysis was presented in on our previous work *Current state-of-the-art in molecular stratification of GBM and characterization of a Brazilian cohort* (Galatro et al, *submitted*. Refer to **Chapter 3**).

Immunohistochemistry

For immunohistochemical detection, tissue sections were routinely processed and subjected to antigen retrieval. Briefly, slides were immersed in 10 mM citrate buffer, pH 6.0 and incubated at 122°C for 3 min using an electric pressure cooker (BioCare Medical, Walnut Creek, CA, USA). Specimens were then blocked and further incubated with the following antibodies raised against human ID1 (mouse monoclonal, Clone 2456C1a, ab66495, Abcam, Cambridge, UK, 1:25) , ID2 (mouse monoclonal, Clone 10C3, ab90055, Abcam, 1:400), ID3 (rabbit polyclonal, ab41834, Abcam, 1:200) ID4 (rabbit polyclonal, ab20988, Abcam, 1:100) at 16-20°C for 16 hours. Development of

the reaction was performed with a commercial kit (Novolink; Novocastra, Newcastle-upon-Tyne, UK) at room temperature, using diaminobenzidine and Harris hematoxylin for nuclear staining. Optimization using positive controls suggested by the manufacturer of each antibody (breast carcinoma for ID1, ID3 and ID4 antibodies, and normal testis for ID2), was performed in order to obtain optimal dilution. Staining intensity of tissue sections was evaluated independently by two observers (SKNM and TFAG). A semi-quantitative score system considering both intensity of staining and percentage of cells was applied as follows: for intensity of staining, 0=negative, 1=weak, 2=moderate and 3=strong; for cell percentage, 0=no cells stained, 1=10–25%, 2 =26–50%, 3=51–75% and 4 = 76–100%. Only cases with positive cell staining with scores ≥ 2 were considered as positive. Digital photomicrographs of representative fields were captured and processed using Picasa 3 (Google, Mountain View, CA,USA).

Statistical analysis

The statistical analyses of relative gene expression in different grades of astrocytoma were assessed using the Kolmogorov-Smirnov normality test, and the non-parametric Kruskal-Wallis and Dunn tests. Correlation between relative gene expression values was assessed using the non-parametric Spearman-rho correlation test and the parametric Pearson's correlation test. The Kaplan-Meier survival curve was analyzed using the *log-rank* (Mantel Cox) test. Differences were considered statistically significant when $p < 0.05$. Calculations were performed using SPSS, version 23.0 (IBM, Armonk, NY, USA).

RESULTS

Relative expression levels of IDs in human astrocytoma

Gene expression analysis by qPCR for *ID1*, *ID3* and *ID4* showed higher median expression levels in all astrocytoma cases (AGI to GBM) relative to the NN cases, and comparison among the groups was statistically significant (Figure 1, $p < 0.05$, Kruskal-Wallis test). Although the median expression level in GBM cases was lower than in AGII and AGIII, there was a clear variability of these expression values, with cases presenting both higher and lower expression than other grades. Similar variability of expression was also observed in AGII and AGIII, which further confirms the heterogeneity of the tumors. Despite showing a similar pattern in expression, *ID2* relative expression only showed statistical significant difference when comparing NN and AGIII samples (Figure 1B, $p < 0.05$, Kruskal Wallis test).

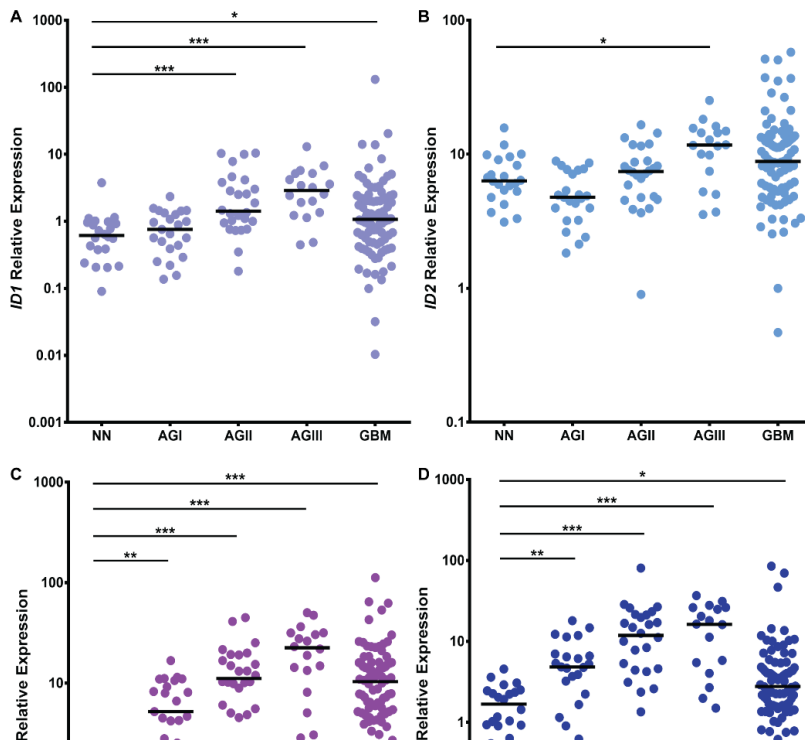


Figure 1: Expression levels of *ID* genes in astrocytomas (AGI to GBM). Transcript levels of *ID1* (A), *ID2* (B), *ID3* (C) and *ID4* (D) were determined in 22 non-neoplastic (NN) cases, 23 pilocytic astrocytoma (AGI), 26 low-grade astrocytomas (AGII), 18 anaplastic astrocytomas (AGIII) and 86 GBM cases by quantitative real-time PCR. Relative expression values were calculated based on the geometric mean of *HPRT*, *GUSB* and *TBP* expression levels of each sample. The equation $2^{-\Delta Ct}$ was applied to calculate gene relative expression according to primer efficiency (E) in tumor samples (Livak and Schmittgen, 2001), where $\Delta Ct = Ct$ specific gene – mean Ct of housekeeping genes. Horizontal bars show the median of each group. The difference of relative gene expressions among the groups were statistically significant ($p < 0.05$, Kruskal-Wallis test) for *ID1-4*. A pair-based comparison was assessed using Dunn test. The p value results are shown, where *** $p < 0.0005$, ** $p < 0.005$ and * $p < 0.05$.

*ID*s relative expression levels were compared among themselves to assess the degree of their co-expression in human astrocytoma samples. The results are displayed in Figure 2. All members of *ID* family were highly correlated ($p < 0.0005$, Spearman's correlation test) in tumor samples.

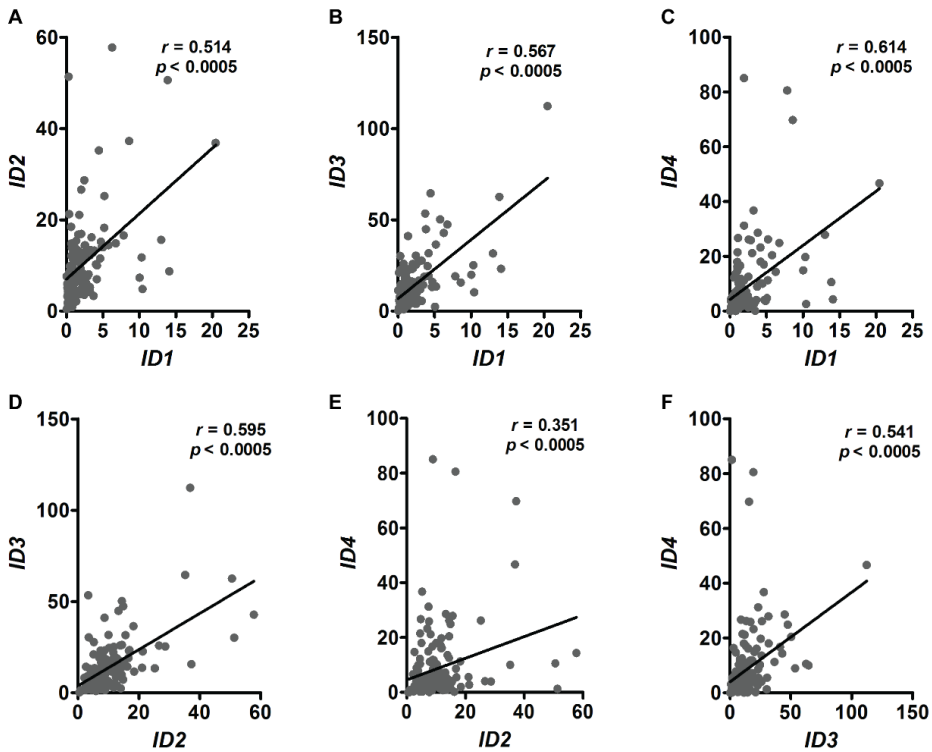


Figure 2: Correlation between *ID1*, *ID2*, *ID3* and *ID4* expression levels in astrocytomas. Correlation was assessed in all 153 astrocytoma samples. We compared the expression levels of *ID1* and *ID2* (A), *ID1* and *ID3* (B), *ID1* and *ID4* (C), *ID2* and *ID3* (D), *ID2* and *ID4* (E) and *ID3* and *ID4* (F). All members of *ID* family were highly correlated ($p < 0.0005$, Spearman-rho correlation test) in tumor samples. r , correlation coefficient assessed by Spearman-rho test.

Five samples of each astrocytoma grade and five samples of the NN samples were stained for *ID1-4* through immunohistochemistry to assess protein subcellular localization. *ID1* staining was only present in the nuclei of GBM samples. *ID2* presented a more homogeneous staining pattern, present in both cytoplasm and nucleus of NN and tumor samples. *ID3* showed positive staining in NN samples (mostly cytoplasm) and was strongly positive in the nucleus of tumor cells in AGII-IV samples. *ID4* showed similar staining pattern as *ID3* (Figure 3).

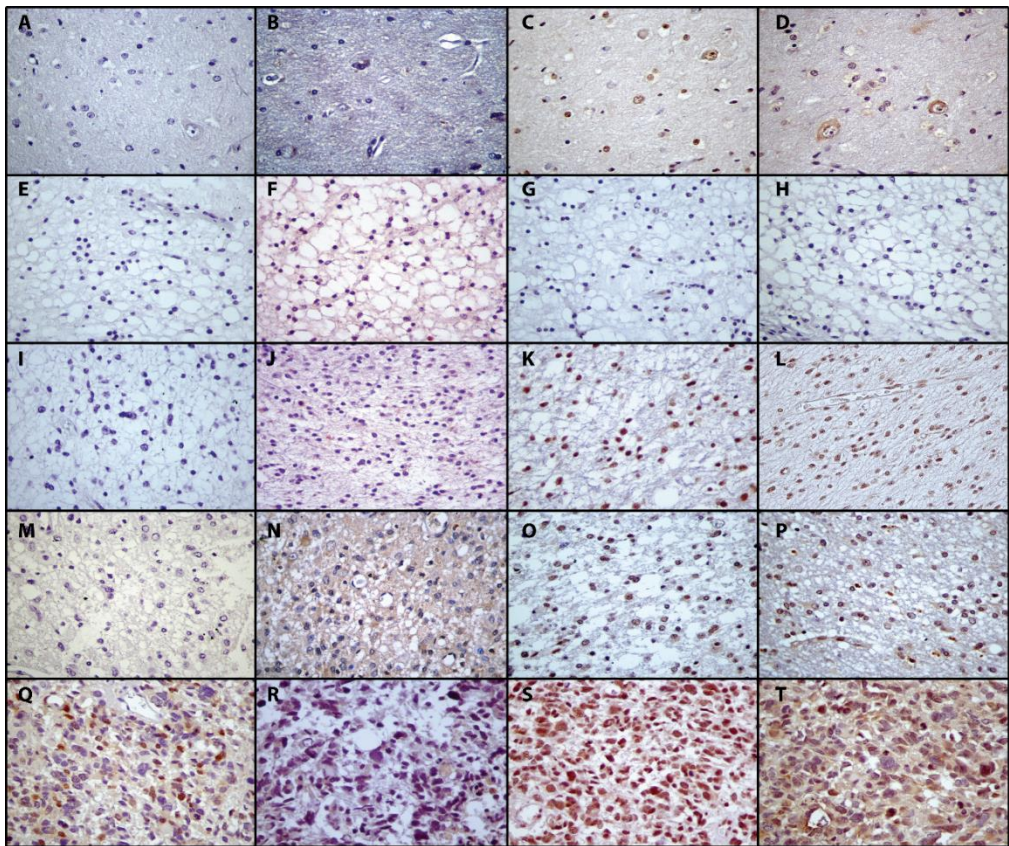


Figure 3: ID1-4 immunohistochemistry in non-neoplastic brain tissues and astrocytoma cases. Representative cases of each NN cases (A-D) and each astrocytoma grade – AGI (E-H), AGII (I-L), AGIII (M-P) and GBM (Q-T) – were stained for ID1 (A, E, I, M, Q), ID2 (B, F, J, N, R), ID3 (C, G, K, O, S) and ID4 (D, H, L, P, T). GBM cases showed stronger and larger number of nuclear stained cells (score 3 for intensity and $\geq 75\%$ of positive cells) for ID1, ID3 and ID4, while ID2 staining was restricted to the cytoplasm. For lower grade tumor cases, ID3 and ID4 showed higher levels of stained cells ($\geq 75\%$ of positive cells). The reaction was performed in paraffin embedded tissue sections with a commercial polymer kit (Novolink; Novocastra, UK), using diaminobenzidine as developer and Harris hematoxylin for nuclear counterstaining. 400x magnification for all images.

GBM sub classification and *ID*s differential gene expression

Given the high heterogeneity levels found in *ID*s expression in GBM and the genetic studies that further identified subclasses of GBM (Brennan et al., 2013b; Phillips et al., 2006; Verhaak et al., 2010), we performed exome sequencing of a targeted gene panel comprising the hallmark genes related to the subclassification of GBMs. For the proneural subtype, we used *IDH1* and *TP53* mutation and *PDGFRA* mutation for classification. For classical subtype, we used *EGFR* alterations (amplification and mutations), *PTEN* mutation and the presence of the oncogenic variant *EGFRvIII*. *EGFR* amplification results was based on a previous publication from our group (Carvalho et al., 2014). For the mesenchymal subtype, we used mutations in *NF1* and *RB1* as a mean for classification. Given the lack of a specific genetic profile that defines the neural subtype, this subclass was not included in our analysis and, instead, was included in the “others” category. The complete gene panel and results can be found in Supplemental Table 2.

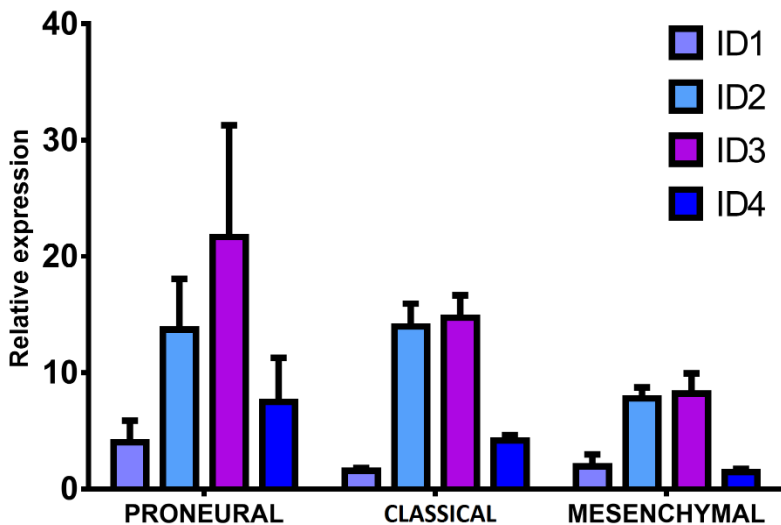


Figure 4: *ID*s expression distribution among GBM subclasses. GBM samples were subclassified as proneural, classical and mesenchymal using a customized gene panel and deep sequencing (see text and Supplemental Table 2 for details). Next, we evaluated *ID*s gene expression distribution among GBM subclasses. The mesenchymal subtype had the lowest expression of *ID* genes, while proneural had the highest. Only *ID4* gene expression (dark blue), diminishing from proneural to mesenchymal, was statistically different ($p < 0.05$, Kruskal Wallis test).

Figure 4 depicts *IDs* expression distribution among GBM molecular subclasses. The mesenchymal subtype had the lowest expression of *ID* genes, while proneural had the highest. The differential expression of *ID4*, diminishing from proneural to mesenchymal, was statistically different ($p < 0.05$, Kruskal Wallis test). *ID3* expression showed a similar pattern, albeit with no statistical difference. *ID2* expression was similar in proneural and classical subtypes, but declined in mesenchymal. Although higher in proneural subtype, *ID1* expression was the lowest among *ID* genes in GBM subtypes.

Next, we evaluated the impact of up-regulation of the analyzed genes on GBM patients' overall survival. For this analysis, conditions were determined for high and low gene expression. Recurrent GBM cases were excluded from this analysis. Given the low number of proneural and mesenchymal subtypes, it was not possible to analyze survival according to GBM sub-classification. Although no significant statistical difference was found when comparing the high *ID* expression group versus the low *ID* expression group ($\log rank p = 0.214$), the survival rate was of 20.8 ± 6.05 months in *ID^{low}* cases and of 11.3 ± 3.2 months in *ID^{high}* GBM cases.

***IDs* expression in Astro x Oligo low-grade tumors**

Proneural GBMs are characterized by molecular alterations also shared by low-grade diffuse gliomas, both of astrocytic and oligodendrocytic origin. Considering this, along with the high levels of *ID3-4* expression found in this GBM subtype, we evaluated *IDs* mRNA levels in a set of low-grade oligodendroglioma samples and compared them to our low-grade astrocytoma cohort. Whereas *ID1* expression remained similar between the two groups, *ID2-4* expression showed significant statistical differences. *ID2* levels were surprisingly higher in oligodendroglioma ($p < 0.0005$, *t*-test), while *ID3-4* expression analysis showed opposite results, with higher levels in low-grade astrocytoma ($p < 0.0005$, Mann-Whitney test). Figure 5 summarizes the results found. Immunohistochemical staining corroborated mRNA findings, with higher levels of *ID2* in oligodendroglioma samples compared to astrocytic ones, and *ID3-4* higher levels in astrocytoma cases, as demonstrated by Figure 6.

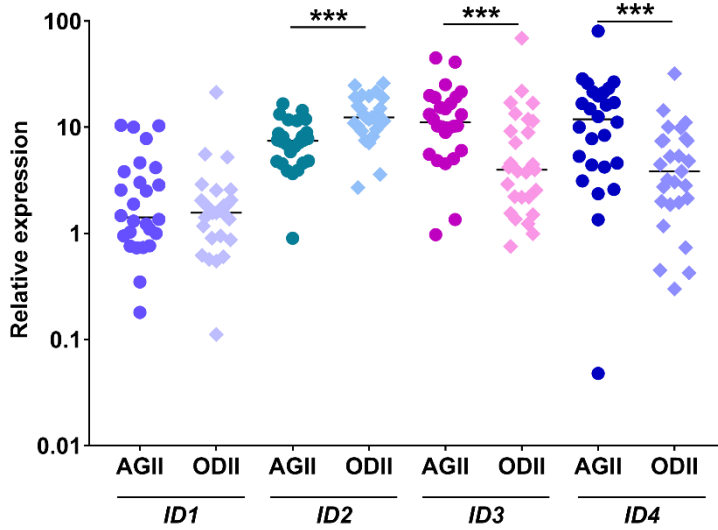


Figure 5: Expression levels of *ID* genes in low-grade gliomas. Relative expression of *IDs* was assessed in 27 cases of low-grade oligodendrogliomas (ODII) cases, and compared to the previously analyzed 26 low-grade astrocytomas (AGII) cases. *ID2* levels were higher in ODII cases ($p < 0.0005$, t-test), while *ID3-4* expression analysis showed opposite results, with higher levels in AGII samples ($p < 0.0005$, Mann-Whitney test). Horizontal bars show the median of each group. *** $p < 0.0005$.

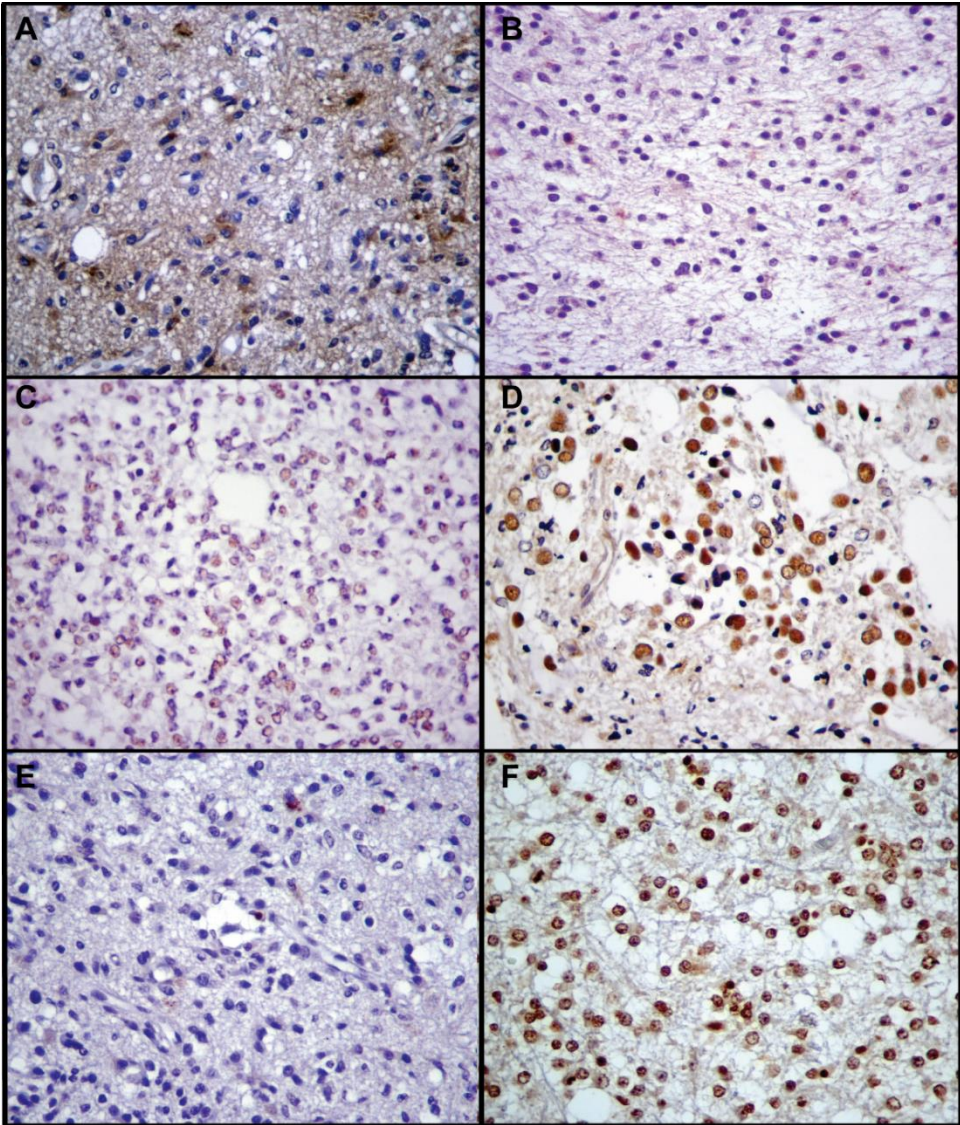


Figure 6: Immunohistochemistry of ID2-4 in low-grade glioma cases. ODII (A, C and E) and AGII (B, D and E) representative sections were stained for ID2 (A, B), ID3 (C, D) and ID4 (E, F). ODII cases showed high levels of ID2 staining ($\geq 75\%$ of positive cells) and very little cells positive for ID3-4, while AGII samples showed opposite results. The reaction was performed in paraffin embedded tissue sections with a commercial polymer kit (Novolink; Novocastra, UK), using diaminobenzidine as developer and Harris hematoxylin for nuclear counterstaining. 400x magnification for all images.

DISCUSSION

In this study, we have evaluated the distribution of *ID1-4* gene expression in human gliomas ranging from grade I-IV. ID proteins mainly act to inhibit cell differentiation and promote stemness, as it happens in the early phases of the developing brain, where IDs are important to prevent premature cell fate determination (Lyden et al., 1999; Niola et al., 2012). In cancer, IDs overexpression has been associated with disease aggressiveness and poorer prognosis. Previous studies have shown high levels of IDs in glioma cases, particularly in GBM (Jeon et al., 2011; Lee et al., 2016; Soroceanu et al., 2013; Vandeputte et al., 2002). Our study, however, revealed that the IDs expression levels were quite variable among GBMs, and the highest levels of *IDs* were among the proneural subtype, an association that has been made only in mice studies (Havrda et al., 2014; Rahme et al., 2016).

We and others previously showed an association between *IDs* and *SOX* genes (Galatro et al., 2013; Jung et al., 2010; Phi et al., 2010). Studies that characterized GBMs subtypes have classified *SOX* genes as hallmarks of the proneural cases (Phillips et al., 2006; Verhaak et al., 2010). Our findings of higher expression levels of *IDs*, particularly *ID2-4*, in the proneural subtype are in accordance with the previous works showing co-expression between these genes. Among *ID* genes, *ID1* showed the lowest expression amid GBM cases. Previous report (Barrett et al., 2012) has identified *ID1* as a marker to single-out stem-like glioma cells in a murine model. Glioma initiating cells represent a small population within tumors, which might explain the low levels of *ID1* found in our cohort.

Next, we observed differential expression of *IDs* comparing astrocytic and oligodendrocytic gliomas. While *ID1* levels remained similar between them, *ID2* levels were surprisingly higher in oligodendroglioma cases, whereas *ID3* and *ID4* showed opposite results, with much higher levels in grade II astrocytoma cases. *ID2* has been previously associated with the inhibition of OLIG2, a transcription factor responsible for the maturation of oligodendrocytes (Samanta and Kessler, 2004; Wang et al., 2001). A previous immunohistochemical study, performed in rats, associated *ID2* presence with the oligodendrocytic lineage and markers (Chen et al., 2007), proposing this protein was involved in oligodendrocyte terminal maturation. However, Havrda and colleagues (Havrda et al., 2014), while assessing the tumorigenicity of *ID2*, have shown that *ID2* first enhances OLIG2 expression, leading neural progenitor cells (NPC) to an oligodendroglial precursor cells phenotype, and then inhibit OLIG2 activity, hampering

maturation and, when re-expressed in mature cells, gives rise to gliomas. Our observations of higher levels of *ID2* in oligodendroglioma cases corroborate these findings. *ID3-4* have been previously deemed important for astrocyte lineage commitment (Bohrer et al., 2015; Samanta and Kessler, 2004) and glioma formation (Jin et al., 2011; Kuzontkoski et al., 2010). Recent study has shown that *ID3* is necessary for adult neural stem/precursor cells differentiation into astrocytes, highlighting its importance in the adult brain (Bohrer et al., 2015). We have previously postulated *ID4* as being associated with glioma progression (Galatro et al., 2013) and, in the current study, demonstrate the role of *ID3-4* as markers that differentiate low-grade gliomas of astrocytic origins from those of oligodendrocytic ones. It is noteworthy that tumors with oligodendroglial features have historically been associated with more sensitivity to treatment and a better prognosis than astrocytic ones (recently reviewed by Otani and collaborators (Otani et al., 2016). In this sense, we can propose *ID2-4* as markers to assist in the diagnosis and differentiation between these two types of gliomas and possibly aid the future treatment decision.

Our findings further stratify the distribution of *IDs* expression pattern in gliomas, pointing out the new association of these targets with the proneural GBM subtype, and as potential markers to differentiate tumors of astrocytoma and oligodendroglioma origin.

REFERENCES

Barrett, L.E., Granot, Z., Coker, C., Iavarone, A., Hambardzumyan, D., Holland, E.C., Nam, H., and Benezra, R. (2012). Self-renewal does not predict tumor growth potential in mouse models of high-grade glioma. *Cancer Cell* 21, 11–24.

Benezra, R., Davis, R.L., Lockshon, D., Turner, D.L., and Weintraub, H. (1990). The protein Id: a negative regulator of helix-loop-helix DNA binding proteins. *Cell* 61, 49–59.

Bohrer, C., Pfurr, S., Mammadzada, K., Schildge, S., Plappert, L., Hils, M., Pous, L., Rauch, K.S., Dumit, V.I., Pfeifer, D., et al. (2015). The balance of Id3 and E47 determines neural stem/precursor cell differentiation into astrocytes. *EMBO J.* 34, 2804–2819.

Brennan, C.W., Verhaak, R.G.W., McKenna, A., Campos, B., Noushmehr, H., Salama, S.R., Zheng, S., Chakravarty, D., Sanborn, J.Z., Berman, S.H., et al. (2013a). The somatic genomic landscape of glioblastoma. *Cell* 155, 462–477.

Brennan, C.W., Verhaak, R.G.W., McKenna, A., Campos, B., Noushmehr, H., Salama, S.R., Zheng, S., Chakravarty, D., Sanborn, J.Z., Berman, S.H., et al. (2013b). The somatic genomic landscape of glioblastoma. *Cell* 155, 462–477.

Cancer Genome Atlas Research Network, Brat, D.J., Verhaak, R.G.W., Aldape, K.D., Yung, W.K.A., Salama, S.R., Cooper, L.A.D., Rheinbay, E., Miller, C.R., Vitucci, M., et al. (2015). Comprehensive, Integrative Genomic Analysis of Diffuse Lower-Grade Gliomas. *N. Engl. J. Med.* 372, 2481–2498.

Carvalho, P.O., Uno, M., Oba-Shinjo, S.M., Rosemberg, S., Wakamatsu, A., da Silva, C.C., Teixeira, M.J., and Marie, S.K.N. (2014). Activation of EGFR signaling from pilocytic astrocytomas to glioblastomas. *Int. J. Biol. Markers* 29, e120-128.

Ceccarelli, M., Barthel, F.P., Malta, T.M., Sabedot, T.S., Salama, S.R., Murray, B.A., Morozova, O., Newton, Y., Radenbaugh, A., Pagnotta, S.M., et al. (2016). Molecular Profiling Reveals Biologically Discrete Subsets and Pathways of Progression in Diffuse Glioma. *Cell* 164, 550–563.

Chen, X.-S., Zhou, D.-S., and Yao, Z.-X. (2007). The inhibitor of DNA binding 2 is mainly expressed in oligodendrocyte lineage cells in adult rat brain. *Neurosci. Lett.* 428, 93–98.

Galatro, T.F. de A., Uno, M., Oba-Shinjo, S.M., Almeida, A.N., Teixeira, M.J., Rosemberg, S., and Marie, S.K.N. (2013). Differential expression of ID4 and its association with TP53 mutation, SOX2, SOX4 and OCT-4 expression levels. *PloS One* 8, e61605.

Havrda, M.C., Paoletta, B.R., Ran, C., Jering, K.S., Wray, C.M., Sullivan, J.M., Nailor, A., Hitoshi, Y., and Israel, M.A. (2014). Id2 mediates oligodendrocyte precursor cell maturation arrest and is tumorigenic in a PDGF-rich microenvironment. *Cancer Res.* *74*, 1822–1832.

Jeon, H.-M., Sohn, Y.-W., Oh, S.-Y., Oh, S.-Y., Kim, S.-H., Beck, S., Kim, S., and Kim, H. (2011). ID4 imparts chemoresistance and cancer stemness to glioma cells by derepressing miR-9*-mediated suppression of SOX2. *Cancer Res.* *71*, 3410–3421.

Jin, X., Yin, J., Kim, S.-H., Sohn, Y.-W., Beck, S., Lim, Y.C., Nam, D.-H., Choi, Y.-J., and Kim, H. (2011). EGFR-AKT-Smad signaling promotes formation of glioma stem-like cells and tumor angiogenesis by ID3-driven cytokine induction. 7125–7134.

Jung, S., Park, R.-H., Kim, S., Jeon, Y.-J., Ham, D.-S., Jung, M.-Y., Kim, S.-S., Lee, Y.-D., Park, C.-H., and Suh-Kim, H. (2010). Id proteins facilitate self-renewal and proliferation of neural stem cells. *Stem Cells Dev.* *19*, 831–841.

Kuzontkoski, P.M., Mulligan-Kehoe, M.J., Harris, B.T., and Israel, M.A. (2010). Inhibitor of DNA binding-4 promotes angiogenesis and growth of glioblastoma multiforme by elevating matrix GLA levels. 3793–3802.

Lasorella, A., Benezra, R., and Iavarone, A. (2014). The ID proteins: master regulators of cancer stem cells and tumour aggressiveness. *Nat. Rev. Cancer* *14*, 77–91.

Lee, S.B., Frattini, V., Bansal, M., Castano, A.M., Sherman, D., Hutchinson, K., Bruce, J.N., Califano, A., Liu, G., Cardozo, T., et al. (2016). An ID2-dependent mechanism for VHL inactivation in cancer. *Nature* *529*, 172–177.

Livak, K.J., and Schmittgen, T.D. (2001). Analysis of relative gene expression data using real-time quantitative PCR and the 2(-Delta Delta C(T)) Method. 402–408.

Louis, D.N., Perry, A., Reifenberger, G., von Deimling, A., Figarella-Branger, D., Cavenee, W.K., Ohgaki, H., Wiestler, O.D., Kleihues, P., and Ellison, D.W. (2016). The 2016 World Health Organization Classification of Tumors of the Central Nervous System: a summary. *Acta Neuropathol. (Berl.)* *131*, 803–820.

Lyden, D., Young, A.Z., Zagzag, D., Yan, W., Gerald, W., O'Reilly, R., Bader, B.L., Hynes, R.O., Zhuang, Y., Manova, K., et al. (1999). Id1 and Id3 are required for neurogenesis, angiogenesis and vascularization of tumour xenografts. *Nature* *401*, 670–677.

Marie, S.K.N., Okamoto, O.K., Uno, M., Hasegawa, A.P.G., Oba-Shinjo, S.M., Cohen, T., Camargo, A.A., Kosoy, A., Carlotti, C.G., Jr, Toledo, S., et al. (2008). Maternal embryonic leucine zipper kinase transcript abundance correlates with malignancy grade in human astrocytomas. *Int. J. Cancer J. Int. Cancer* *122*, 807–815.

Niola, F., Zhao, X., Singh, D., Castano, A., Sullivan, R., Lauria, M., Nam, H.-S., Zhuang, Y., Benezra, R., Di Bernardo, D., et al. (2012). Id proteins synchronize stemness and anchorage to the niche of neural stem cells. *Nat. Cell Biol.* *14*, 477–487.

Oba-Shinjo, S.M., Bengtson, M.H., Winnischofer, S.M.B., Colin, C., Vedoy, C.G., de Mendonça, Z., Marie, S.K.N., and Sogayar, M.C. (2005). Identification of novel differentially expressed genes in human astrocytomas by cDNA representational difference analysis. *Brain Res. Mol. Brain Res.* *140*, 25–33.

Ohgaki, H., and Kleihues, P. (2013). The definition of primary and secondary glioblastoma. *Clin. Cancer Res. Off. J. Am. Assoc. Cancer Res.* *19*, 764–772.

Otani, R., Uzuka, T., and Ueki, K. (2016). Classification of adult diffuse gliomas by molecular markers—a short review with historical footnote. *Jpn. J. Clin. Oncol.*

Parsons, D.W., Jones, S., Zhang, X., Lin, J.C.-H., Leary, R.J., Angenendt, P., Mankoo, P., Carter, H., Siu, I.-M., Gallia, G.L., et al. (2008). An integrated genomic analysis of human glioblastoma multiforme. *Science* *321*, 1807–1812.

Pfaffl, M.W. (2001). A new mathematical model for relative quantification in real-time RT-PCR. *e45*.

Phi, J.H., Kim, J.H., Eun, K.M., Wang, K.-C., Park, K.H., Choi, S.A., Kim, Y.Y., Park, S.-H., Cho, B.-K., and Kim, S.-K. (2010). Upregulation of SOX2, NOTCH1, and ID1 in supratentorial primitive neuroectodermal tumors: a distinct differentiation pattern from that of medulloblastomas. *J. Neurosurg. Pediatr.* *5*, 608–614.

Phillips, H.S., Kharbanda, S., Chen, R., Forrest, W.F., Soriano, R.H., Wu, T.D., Misra, A., Nigro, J.M., Colman, H., Soroceanu, L., et al. (2006). Molecular subclasses of high-grade glioma predict prognosis, delineate a pattern of disease progression, and resemble stages in neurogenesis. *Cancer Cell* *9*, 157–173.

Rahme, G.J., Zhang, Z., Young, A.L., Cheng, C., Bivona, E.J., Fiering, S.N., Hitoshi, Y., and Israel, M.A. (2016). PDGF Engages an E2F-USP1 Signaling Pathway to Support ID2-Mediated Survival of Proneural Glioma Cells. *Cancer Res.* *76*, 2964–2976.

Samanta, J., and Kessler, J.A. (2004). Interactions between ID and OLIG proteins mediate the inhibitory effects of BMP4 on oligodendroglial differentiation. *4131–4142*.

Soroceanu, L., Murase, R., Limbad, C., Singer, E., Allison, J., Adrados, I., Kawamura, R., Pakdel, A., Fukuyo, Y., Nguyen, D., et al. (2013). Id-1 is a key transcriptional regulator of glioblastoma aggressiveness and a novel therapeutic target. *Cancer Res.* *73*, 1559–1569.

Stieber, D., Golebiewska, A., Evers, L., Lenkiewicz, E., Brons, N.H.C., Nicot, N., Oudin, A., Bougnaud, S., Hertel, F., Bjerkgvig, R., et al. (2014). Glioblastomas are

composed of genetically divergent clones with distinct tumorigenic potential and variable stem cell-associated phenotypes. *Acta Neuropathol. (Berl.)* 127, 203–219.

Valente, V., Teixeira, S.A., Neder, L., Okamoto, O.K., Oba-Shinjo, S.M., Marie, S.K.N., Scrideli, C.A., Paçó-Larson, M.L., and Carlotti, C.G., Jr (2009). Selection of suitable housekeeping genes for expression analysis in glioblastoma using quantitative RT-PCR. 17.

Vandeputte, D.A.A., Troost, D., Leenstra, S., Ijlst-Keizers, H., Ramkema, M., Bosch, D.A., Baas, F., Das, N.K., and Aronica, E. (2002). Expression and distribution of id helix-loop-helix proteins in human astrocytic tumors. 329–338.

Verhaak, R.G.W., Hoadley, K.A., Purdom, E., Wang, V., Qi, Y., Wilkerson, M.D., Miller, C.R., Ding, L., Golub, T., Mesirov, J.P., et al. (2010). Integrated genomic analysis identifies clinically relevant subtypes of glioblastoma characterized by abnormalities in PDGFRA, IDH1, EGFR, and NF1. *Cancer Cell* 17, 98–110.

Wang, S., Sdrulla, A., Johnson, J.E., Yokota, Y., and Barres, B.A. (2001). A role for the helix-loop-helix protein Id2 in the control of oligodendrocyte development. 603–614.

Weiler, S., Ademokun, J.A., and Norton, J.D. (2015). ID helix-loop-helix proteins as determinants of cell survival in B-cell chronic lymphocytic leukemia cells in vitro. *Mol. Cancer* 14, 30.

Xu, K., Wang, L., Feng, W., Feng, Y., and Shu, H.-K. (2016). Phosphatidylinositol-3 kinase-dependent translational regulation of Id1 involves the PPM1G phosphatase. *Oncogene*.

CHAPTER 5

Isolation of microglia and immune infiltrates from mouse and primate central nervous system

Thais F. Galatro^{1,2*}, Ilia D. Vainchtein^{1*}, Nieske Brouwer¹, Erik W.G.M. Boddeke¹ and Bart J.L. Eggen¹

¹Department of Neuroscience, section Medical Physiology, University of Groningen, University Medical Center Groningen, Groningen, 9713 AV, The Netherlands.

²Department of Neurology, Laboratory of Molecular and Cellular Biology, LIM15, School of Medicine, University of São Paulo, São Paulo, Brazil

**shared first authorship, listed in alphabetical order*

SUMMARY

Microglia are the innate immune cells of the central nervous system (CNS) and play an important role in the maintenance of tissue homeostasis, providing neural support and neuroprotection. Microglia constantly survey their environment and quickly respond to homeostatic perturbations. Microglia are increasingly implicated in neuropathological and neurodegenerative conditions, such as Alzheimer's disease, Parkinson's disease and glioma progression. Here, we describe a detailed isolation protocol for microglia and immune infiltrates, optimized for large amounts of *post mortem* tissue from human and rhesus macaque, as well as smaller tissue amounts from mouse brain and spinal cord, that yield a highly purified microglia population (up to 98% purity). This acute isolation protocol is based on mechanical dissociation and a two-step density gradient purification, followed by fluorescence-activated cell sorting (FACS) to obtain pure microglia and immune infiltrate populations.

INTRODUCTION

Microglia are the macrophages of the central nervous system (CNS), originating from erythro-myeloid progenitors in the yolk sac (Hoeffel et al., 2015). Microglia are highly specialized and adapted to their CNS environment, involved in CNS development and homeostasis (Aloisi, 2001; Prinz et al., 2014; Ransohoff and Perry, 2009). Although microglia and other tissue macrophages, like liver Kupffer cells and skin Langerhans cells, arise from erythro-myeloid progenitors, they differ in their developmental programs and their respective tissue environment plays a major role in determining their unique gene expression profiles and functions (Gosselin et al., 2014; Hoeffel et al., 2015; Lavin et al., 2014).

Under healthy conditions, microglia are the only immune cells present in the CNS parenchyma. However, under neuropathological and neurodegenerative conditions, various other immune and antigen-presenting (AP) cells, such as macrophages and dendritic cells, infiltrate the CNS tissues (Brendecke and Prinz, 2015; Chinnery et al., 2010; McMenamin et al., 2003), where they modulate further immune cell infiltration and phenotypes. To elucidate the role of such immune cells in both normal conditions and disease, it is crucial to obtain sizable cell numbers and purity. Here, we present a fluorescence-activated cell sorting (FACS)-based protocol yielding highly pure immune cell populations from the CNS of mammals. The flexibility of this procedure allows diversity in sample origin (mouse, human and non-human primates) and tissue type (brain or spinal cord).

Contrary to enzymatic dissociation protocols, mechanical dissociation does not require a 37°C incubation, hence maintaining the cell surface markers integrity and allowing for phenotype investigation (Olah et al., 2012). The isolation procedure described here consists of 3 main steps: 1) mechanical dissociation of the tissue to obtain a single-cell suspension; 2) separation of cells from debris and myelin using Percoll gradient centrifugation; and 3) purification of immune cell types based on cell surface marker expression using FACS sorting (Figure 1).

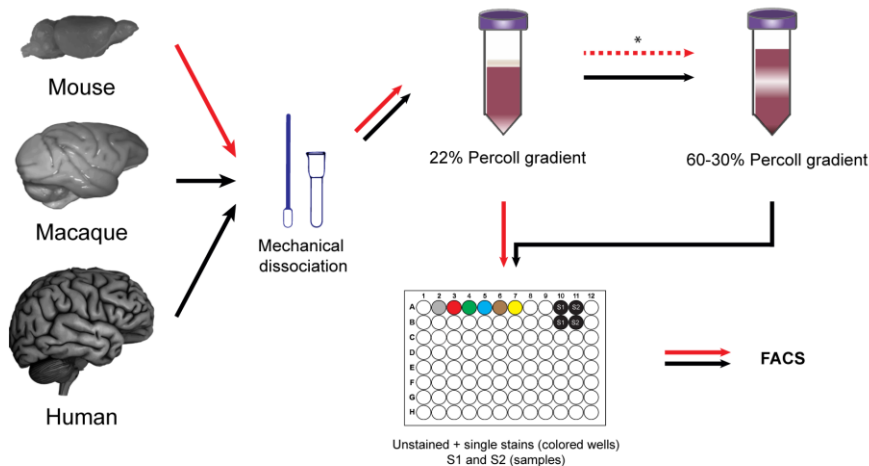


Figure 1: Isolation protocol for microglia and immune infiltrates of the CNS.

Step 1: mince brain tissue and dissociate with a glass tissue homogenizer until a homogeneous suspension is obtained. Step 2: myelin and cell debris are removed by Percoll gradient centrifugation. For small amounts of starting tissue, a single Percoll gradient is used (22%) and the resulting pellet is used for the next step. For larger amounts and myelin-rich starting tissue, a second Percoll gradient separation is applied (60-30%). In that case, the interphase between the two Percoll layers is used. Step 3: resulting cell suspension is blocked to reduce non-specific antibody binding, then stained for the desired membrane markers. The cell suspension is then filtered in a FACS tube and FACS sorted (Beckman Coulter MoFlo Astrios/XDP). * Optional: for functional assays perform the 60-30% Percoll gradient separation and continue from there.

SAMPLES

The origin and condition of the tissue sample is crucial for the end result of the isolation protocol. We have applied this optimized protocol to the following:

Mouse

Preferably, mice are perfused with 0.9% physiological saline solution prior to removal of CNS tissue to avoid contamination of CNS-immune cells with blood immune cells. Microglia have been successfully isolated from brain and spinal cord of several

experimental conditions and molecular backgrounds, such as aged mice (Holtman et al., 2015) and aging models (*mTerc*^{-/-}; *Ercc1*^{Δ/-}) (Raj et al., 2014, 2015), EAE (experimental autoimmune encephalomyelitis) (Vainchtein et al., 2014), GL261 glioma injected brains and Alzheimer's disease models (*APP23*, *5xFAD*).

Human and non-human primate samples

Human and non-human primate (Rhesus macaque; *Macaca mulatta*) brain samples have been collected under the course of full body autopsies. Donor age (increased cell-death and auto fluorescence with age), neuropathological condition (Alzheimer, Parkinson, and multiple sclerosis), CSF pH (pH≤6.5 results in poor RNA quality) and *post mortem* interval (up to 24 h) varied between these samples, which affected cell yields. Microglia have also been successfully isolated from surgical biopsies collected after tumor resection (glioma) or temporal lobectomy of epilepsy surgeries.

MATERIALS AND SOLUTIONS

Materials

1. 50 and 15 mL tubes
2. 5, 10, and 25 mL pipettes
3. 1 mL, 200 μ L, 20 μ L and 10 μ L pipettes and tips
4. 800 mL beaker glass with 106 and 300 μ m sieve on top
5. 70 μ m cell-strainer
6. round bottom 96-wells microplate
7. 5 mL polystyrene round-bottom tube with cell-strainer cap 12 x 75 mm style, referred to as "FACS tube"
8. 1.7 mL siliconized Eppendorf tubes
9. 5 cm³ or 15 cm³ glass homogenizers
10. centrifuge with controllable acceleration and brake

Solutions:

1. **Isolation medium with phenol red (iMed+)** (this medium is not suitable for FACS, due to phenol red interference): 500 mL of HBSS (1x) with phenol red; 7.5 mL HEPES 1 M (f.c. 15 mM); 6.5 mL glucose 45% (f.c. 0.6%).
2. **Isolation medium without phenol red (iMed-)**: 50 ml of HBSS (1x) without phenol red; 750 μ L HEPES 1 M (f.c. 15 mM); 650 μ L glucose 45% (f.c. 0.6%); 100 μ L 0.5 M EDTA pH=8.0 (f.c. 1 mM).
3. **Myelin gradient buffer**: prepare 1.5 L of NaH₂PO₄·H₂O (0.78 g/L; f.c. 5.6 mM), solution 1. Prepare 1.5 L of Na₂HPO₄ 2H₂O (3.56 g/L; f.c. 20 mM), solution 2. Adjust solution 1 to pH 7.4 with solution 2. Measure the final volume and add: 8 g/L NaCl (f.c. 140 mM); 0.4 g/L KCl (f.c. 5.4 mM); 2 g/L glucose (f.c. 11 mM). Autoclave and keep sterile at 4 °C.
4. **22% Percoll gradient solution**: 110 mL Percoll; 12 mL NaCl 1,5 M; 378 mL myelin gradient buffer.
5. **30%/60% Percoll solution**: prepare 100% Percoll solution by mixing 27 ml Percoll with 3 ml 10x HBSS. For 60% Percoll solution take 18 ml and add 12 ml PBS, or for 30% Percoll solution take 9 ml and add 21 ml PBS.
6. Virkon®S
7. DAPI (200 μ g/ml)
8. RNAlater
9. RLT plus

METHODS

The whole procedure is conducted on ice and all centrifugation steps are performed at 4 °C. When dealing with primate samples, steps 1-5 are carried out in a laminar flow due to potential biohazard risk. Waste is collected in 1% Virkon®S solution, stored for 24 h and autoclaved.

Preparation of a single-cell brain tissue homogenate

1. Weigh tissue, place it in a petri dish with iMed+ and cut it into 2 mm³ pieces with a scalpel.
2. Transfer the minced tissue to a glass tissue homogenizer with iMed+ and homogenize until a uniform solution is obtained. When using a 5 cm³ glass tissue homogenizer, transfer up to 1 gram of tissue each time, if a 15 cm³ glass tissue homogenizer is used, portions of 4 grams can be transferred. Repeat the procedure until all tissue is homogenized (see Note 1).
3. For small amounts of tissue, use a pre-wetted (with 1 mL of iMed+) 70 µm cell-strainer on top of a 50 mL tube and filter the tissue homogenate. For larger amounts of tissue, put 106 µm and 300 µm sieves on top of an 800 mL beaker glass and filter the solution.
4. For large (primate) samples, divide the tissue homogenate over several 50 mL tubes, no more than 1.5 g starting material per 50 mL tube (for example: 7.5 g of tissue results in 5 tubes).
5. Rinse glass homogenizer and beaker glass with extra iMed+ and add to the tissue homogenate after passing it through the sieve.
6. Centrifuge at 220 g, 10 min (brake and acceleration: 9).
7. Carefully remove supernatant by pipetting.
8. Resuspend the cell pellet in 1 mL of 22% Percoll solution. Add 19 mL 22% Percoll solution to the 50 mL tube and mix well (or add 10 mL when using 15 mL tubes).
9. Carefully (without mixing) place 3 mL of PBS on top of the 22% Percoll solution.
10. Separate cells and myelin by centrifugation: 20 min, 950 g (acceleration 4; brake 0).

11. Carefully remove the myelin layer by pouring it off (or pipetting). Leave the cell pellet undisturbed. For functional assays with vital mouse cells (i.e. chemotaxis and phagocytosis), continue with step 12, otherwise continue with step 20.
12. Resuspend the cell pellet in 1 mL 60% Percoll using 1 mL pipette tip.
13. Add 14 mL of 60% Percoll solution (per 50 mL tube) to the suspension and homogenize.
14. Carefully place 14 mL of 30% Percoll on top of the 60% Percoll layer.
15. Carefully layer 3 mL PBS on top of the 30% Percoll. Centrifuge for 25 min, 800 g (acceleration 4; brake 0)
16. Collect the 60%-30% interphase with a pre-wetted (with 1 mL iMed+) glass pipette and transfer to a 50 mL tube containing iMed+.
17. Add two volumes of iMed+ equivalent to the collected cell-rich interphase.
18. Pellet cells by centrifugation: 600 g, 10 min (brake and acceleration: 9).
19. Remove as much medium as possible (optional: place tube upside down).
20. Resuspend cell pellet in 100 μ L iMed- (the cells can be used for functional assays).
21. To prevent aspecific binding of antibodies perform a blocking step. Incubate samples for 15 min on ice with the following blocking solution (Table 1):

Table 1: Blocking reagents

Sample origin	Blocking reagent	Supplier	Amount
human / macaque	FcR-blocking	eBioscience	10 μ L / 100 μ L cell suspension
mouse	anti-mouse CD16/CD32	eBioscience	1 μ L / 100 μ L cell suspension

Settings of FACS sorting machine:

In order to facilitate fluorochrome compensation and settings of the FACS machine, unstained and single stained reference samples should be made. A small volume of the sample(s) can be used for such purpose (further referred to as FACS

setting solution), but keep in mind some of the markers are only lowly expressed in the brain. Preferably, beads can be used, or in case of mouse samples, splenocytes can be used for the settings (see Note 2). If a FACS setting solution is used, continue with step 22.

22. Transfer 5 μ L of the sample to a separate tube for the settings. In case of multiple samples, take 5 μ L of each sample and pool.

23. For primate samples fill the tube up to 300 μ L with iMed-, mouse samples up to 600 μ L with iMed-.

24. In a 96-well microplate, pipet 3x100 μ L of FACS setting solution in 3 wells (unstained, CD11b PE single stain, CD45 FITC single stain) in case of primate samples; or 6x100 μ L of FACS setting solution in 6 wells (unstained, CD11b PE single stain, CD45 FITC single stain; Ly-6C APC single stain, Ly-6G APC/Cy7 single stain, CD3 PE/Cy7 single stain) for mouse samples.

Antibody incubation procedure:

25. Add antibodies to the single stains in the 96-well microplate as indicated in Table 2 below, keep on ice for 20-30 min, in the dark.

26. Prepare and add antibody mix to the samples (human: 1,2; macaque: 1,3; mouse: 4-8) in the falcon tubes as indicated in Table 2 below, keep on ice for 20-30 min, in the dark.

Table 2: Antibody dilution

Sample origin	Antibody	Clone	Isotype	Supplier	Dilution
1. Human / Macaque	CD11b PE	ICRF44	Mouse IgG1, κ	Biolegend	1:25
2. Human	CD45 FITC	HI30	Mouse IgG1	Biolegend	1:25
3. Macaque	CD45 FITC	MB4-6D6	Mouse IgG1	Miltenyi Biotec	1:25

4.	Mouse	CD11b PE	M1/70	Rat IgG2b, κ	eBioscience	1:170
5.	Mouse	CD45 FITC	30- F11	Rat IgG2b, κ	eBioscience	1:250
6.	Mouse	Ly-6C APC	HK1.4	Rat IgG2c, κ	Biolegend	1:130
7.	Mouse	Ly-6G APC- Cy7	1A8	Rat IgG2a, κ	Biolegend	1:100
8.	Mouse	CD3 PE/Cy7	17A2	Rat IgG2b, κ	Biolegend	1:100

27. After incubation, divide the sample solution over several wells (100 μ L in each well of a 96 well microplate). Wash the tube with an extra 100 μ L of iMed- and pipet in a separate well. Add 100 μ L of iMed- to all wells (single stains and samples).

28. Spin the cells down for 3 min at 300 g.

29. Remove supernatant and add 100 μ L of iMed- to each well.

30. Transfer each single stain to an individual FACS tube by filtering it through the pre-wetted (50-100 μ L of iMed-) filter.

31. Combine each divided sample into an individual pre-wetted (50-100 μ L of iMed-) FACS tube.

32. Collect the remaining cells with iMed- (100 – 150 μ L) from the 96 well microplate and add it to the corresponding FACS tubes.

FACS isolation myeloid cells

33. 1-2 min before starting the FACS procedure add 0.5 μ L of DAPI.

34. First, gate on all the events/cells (SSC^{height} vs FSC^{height}, to gate out cell debris), second gate on singlets (first gate in SSC^{width} vs FSC^{height} followed by FSC^{width} vs FSC^{height}) (single cells 1 and 2; Fig. 2).

35. Select the live, single cells by gating against DAPI (DAPI vs FSC^{height}).

36. For primate samples, plot for SSC^{height} vs a fluorochrome that is not in the panel (for example PE/Cy7 for primate samples) and gate for non-autofluorescent cells.

37. Then plot for CD11b vs CD45, the CD11b^{pos} CD45^{int} cells are the microglia. In case mouse samples are used, the microglia gate 1 can be plotted for SSC^{height} vs Ly-6C, as microglia are Ly-6C^{neg}. A pure microglia population can be sorted (CD11b^{pos} CD45^{int} Ly-6C^{neg}; Fig. 2).

38. In the CD11b vs CD45 plot, the CD11b^{high}CD45^{int-high} cells (myeloid gate) are the infiltrates, consisting of macrophages and neutrophils that can be separated in mouse samples by gating for Ly-6G and Ly-6C (macrophages are Ly-6C^{pos} Ly-6G^{neg} and neutrophils are Ly-6C^{int} Ly-6G^{pos}).

39. In mouse samples, the CD45^{high} CD11b^{neg} fraction (lymphoid gate) in the CD11b vs CD45 plot can be plotted for SSC^{height} vs CD3 and a T-lymphocyte population can be sorted.

40. During sorting, cells should be collected in siliconized tubes filled with the following, depending on desired downstream application:

- 350 µL RNAlater, in case of RNA/DNA isolation for gene expression profiling.
- 350 µL iMed-, for other applications such as protein isolation and chromatin immunoprecipitation.

41. Collection of cells by centrifugation will depend on downstream application. I.e., for RNA/DNA isolation purposes, centrifuge 10 min, 5000 RCF; carefully remove RNAlater and lyse (invisible) cell pellet in 350 µL RLTplus and store at -80°C.

42. If cells are collected in iMed-, centrifuge for 10 min at 500 RCF, remove supernatant and resuspend pellet in the appropriate buffer.

Notes

Fig. 2: FACS sorting strategy. To isolate pure populations of microglia and different immune infiltrates (macrophages, neutrophils and T-lymphocytes), cells are first separated from cell debris and the remaining myelin by a gate in the SSC^{height} vs FSC^{height} . Single cells are selected in the SSC^{width} vs FSC^{height} followed by FSC^{width} vs FSC^{height} gates (single cells 1 and 2 gate). To obtain high quality RNA/DNA samples, live cells can be gated as $DAPI^{\text{neg}}$ ($DAPI$ vs FSC^{height}). Depending on the experimental condition in mice, three well identifiable cell populations can be distinguished using $CD11b$ vs $CD45$ plotting. From the microglia gate 1, microglia can be identified as $Ly-6C^{\text{neg}}$ when plotting for SSC^{height} vs $Ly-6C$. The myeloid gate contains two main populations when plotting for $Ly-6G$ vs $Ly-6C$; macrophages are $Ly-6C^{\text{pos}}$ $Ly-6G^{\text{neg}}$ and neutrophils $Ly-6C^{\text{int}}$ $Ly-6G^{\text{pos}}$. T-lymphocytes ($CD3^+$) can be sorted when gating for SSC^{height} vs $CD3$ in the lymphoid gate. For the primate samples, after the live cells gate, the autofluorescent cells should be removed by gating on the non-autofluorescent (AFS) cells (SSC^{height} vs a fluorochrome that is not used, preferably APC or PE/Cy7). This has to be performed for human samples, but is not obligatory for macaque due to less autofluorescence. In the $CD11b$ vs $CD45$ plot, microglia can be identified as $CD11b^{\text{pos}}$ $CD45^{\text{int}}$.

1. It is advised to use a 5 cm³ glass tissue homogenizer for low myelin content samples (i.e. mouse brain, spinal cord, glioma tissue) and a 15 cm³ glass tissue homogenizer for higher amounts of starting material or samples with high myelin content (primates).

2. Mouse splenocyte isolation: conduct steps 1-7 as described above. Resuspend the pellet in 1 mL of lysis buffer (ammonium chloride 155 mmol/L, potassium bicarbonate 10 mmol/L, sodium edetate 0.1 mmol/L) to remove red blood cells and incubate on ice for 5 min. Fill to 15 mL with iMed+ and perform step 7 again. Carefully pour off (or pipet) supernatant and resuspend pellet in 1 mL of iMed-. Use this cell suspension for the calibration and settings of FACS sorting machine and continue with step 24.

REFERENCES

Aloisi, F. (2001). Immune function of microglia. *Glia* 36, 165–179.

Brendecke, S.M., and Prinz, M. (2015). Do not judge a cell by its cover-diversity of CNS resident, adjoining and infiltrating myeloid cells in inflammation. *Semin. Immunopathol.*

Chinnery, H.R., Ruitenber, M.J., and McMenamin, P.G. (2010). Novel characterization of monocyte-derived cell populations in the meninges and choroid plexus and their rates of replenishment in bone marrow chimeric mice. *J. Neuropathol. Exp. Neurol.* 69, 896–909.

Gosselin, D., Link, V.M., Romanoski, C.E., Fonseca, G.J., Eichenfield, D.Z., Spann, N.J., Stender, J.D., Chun, H.B., Garner, H., Geissmann, F., et al. (2014). Environment drives selection and function of enhancers controlling tissue-specific macrophage identities. *Cell* 159, 1327–1340.

Hoeffel, G., Chen, J., Lavin, Y., Low, D., Almeida, F.F., See, P., Beaudin, A.E., Lum, J., Low, I., Forsberg, E.C., et al. (2015). C-Myb(+) erythro-myeloid progenitor-derived fetal monocytes give rise to adult tissue-resident macrophages. *Immunity* 42, 665–678.

Holtman, I.R., Raj, D.D., Miller, J.A., Schaafsma, W., Yin, Z., Brouwer, N., Wes, P.D., Möller, T., Orre, M., Kamphuis, W., et al. (2015). Induction of a common microglia gene expression signature by aging and neurodegenerative conditions: a co-expression meta-analysis. *Acta Neuropathol. Commun.* 3, 31.

Lavin, Y., Winter, D., Blecher-Gonen, R., David, E., Keren-Shaul, H., Merad, M., Jung, S., and Amit, I. (2014). Tissue-resident macrophage enhancer landscapes are shaped by the local microenvironment. *Cell* 159, 1312–1326.

McMenamin, P.G., Wealthall, R.J., Deverall, M., Cooper, S.J., and Griffin, B. (2003). Macrophages and dendritic cells in the rat meninges and choroid plexus: three-dimensional localisation by environmental scanning electron microscopy and confocal microscopy. *Cell Tissue Res.* 313, 259–269.

Olah, M., Raj, D., Brouwer, N., De Haas, A.H., Eggen, B.J.L., Den Dunnen, W.F.A., Biber, K.P.H., and Boddeke, H.W.G.M. (2012). An optimized protocol for the acute isolation of human microglia from autopsy brain samples. *Glia* 60, 96–111.

Prinz, M., Tay, T.L., Wolf, Y., and Jung, S. (2014). Microglia: unique and common features with other tissue macrophages. *Acta Neuropathol. (Berl.)* 128, 319–331.

Raj, D.D.A., Jaarsma, D., Holtman, I.R., Olah, M., Ferreira, F.M., Schaafsma, W., Brouwer, N., Meijer, M.M., de Waard, M.C., van der Pluijm, I., et al. (2014). Priming of

microglia in a DNA-repair deficient model of accelerated aging. *Neurobiol. Aging* 35, 2147–2160.

Raj, D.D.A., Moser, J., van der Pol, S.M.A., van Os, R.P., Holtman, I.R., Brouwer, N., Oeseburg, H., Schaafsma, W., Wesseling, E.M., den Dunnen, W., et al. (2015). Enhanced microglial pro-inflammatory response to lipopolysaccharide correlates with brain infiltration and blood-brain barrier dysregulation in a mouse model of telomere shortening. *Aging Cell*.

Ransohoff, R.M., and Perry, V.H. (2009). Microglial physiology: unique stimuli, specialized responses. *Annu. Rev. Immunol.* 27, 119–145.

Vainchtein, I.D., Vinet, J., Brouwer, N., Brendecke, S., Biagini, G., Biber, K., Boddeke, H.W.G.M., and Eggen, B.J.L. (2014). In acute experimental autoimmune encephalomyelitis, infiltrating macrophages are immune activated, whereas microglia remain immune suppressed. *Glia* 62, 1724–1735.

CHAPTER 6

The human microglia transcriptome and age-associated changes in actin dynamics and cell function

Thais F. Galatro^{1,2*}, Inge R. Holtman^{1*}, Antonio M. Lerario³, Ilia D. Vainchtein¹, Nieske Brouwer¹, Paula Sola², Mariana Veras⁴, Tulio Pereira^{5,6}, Renata Leite⁴, Thomas Möller⁷, Paul D. Wes⁷, Mari C. Sogayar⁵, Jon D. Laman¹, Wilfred den Dunnen⁸, Carlos A. Pasqualucci⁴, Sueli M. Oba-Shinjo², Erik W.G.M. Boddeke¹, Suely K. N. Marie^{2,5**}, Bart J.L. Eggen^{1**}

¹*Department of Neuroscience, Section Medical Physiology, University of Groningen, University Medical Center Groningen, Groningen, The Netherlands*

²*Department of Neurology, Laboratory of Molecular and Cellular Biology, LIM15, School of Medicine, University of São Paulo, São Paulo, Brazil*

³*Department of Internal Medicine, Division of Metabolism, Endocrinology, and Diabetes, University of Michigan, Ann Arbor, Michigan 48109, USA*

⁴*Brazilian Aging Brain Study Group, LIM22, School of Medicine, University of São Paulo, São Paulo, Brazil*

⁵*Center for Studies of Cellular and Molecular Therapy (NAP-NETCEM-NUCEL), University of São Paulo, São Paulo, Brazil*

⁶*Chemistry Institute, Department of Biochemistry, University of São Paulo, São Paulo, Brazil*

⁷*Neuroinflammation Disease Biology Unit, Lundbeck Research USA, Paramus, New Jersey 07652, USA*

⁸*Department of Pathology, University of Groningen, University Medical Center Groningen, Groningen, The Netherlands*

** shared first authors*

*** shared last authors*

Submitted

SUMMARY

Microglia are essential for central nervous system (CNS) homeostasis and innate neuroimmune function, and play important roles in neurodegeneration and brain aging. Their CNS-tailored functions and ontogeny distinguish microglia from other tissue-resident macrophages in mice. Here, we present the gene expression profile of pure cortical human microglia and corresponding unsorted cortical tissue samples. Microglia were isolated from the parietal cortex of 39 autopsy samples of humans with intact cognition and RNA sequenced. Overall, genes expressed by human microglia are similar to mouse microglia, such as established microglia genes *CX3CR1*, *P2YR12*, and *ITGAM/CD11b*. Interestingly, a number of immune genes, not identified as mouse microglia signature genes, were abundantly expressed in human microglia. These included *TLR*, *Fc-γ* and *SIGLEC* receptors as well as *TAL1* and *IFI16*, regulators of proliferation and cell cycle. Age-associated changes in human microglia were enriched for genes involved in cell adhesion, axonal guidance, cell surface receptor expression and actin (dis)assembly, suggesting these functions alter during aging. A very limited overlap was observed in genes with an age-associated change in expression between mice and humans, suggesting that human and mouse microglia age differently. The effect of post-mortem delay on human microglia gene expression was very limited, an observation further supported by gene expression profiles generated using biopsy samples obtained during epilepsy surgery. This data is the first comprehensive pure human microglia gene expression profile; human microglia clearly differ from mouse microglia, especially with respect to age-induced changes in gene expression.

INTRODUCTION

Microglia are highly specialized cells with a unique ontogeny and are crucially shaped by their local central nervous system (CNS) environment (Salter and Beggs, 2014). Fate mapping studies showed that microglia have a different ontogeny than other tissue macrophages (Hoeffel et al., 2015). Microglia originate from erythromyeloid progenitors in the yolk sac via *Csf1r*-, *Pu.1/Spi-1*- and *Irf8*-dependent pathways (Hoeffel et al., 2015; Kierdorf et al., 2013a; Schulz et al., 2012). Genome-wide transcriptome and epigenome studies of mouse microglia showed that microglia are very different from other tissue macrophages and other glial cell types (Butovsky et al., 2014; Buttgereit et al., 2016; Chiu et al., 2013; Gosselin et al., 2014; Hickman et al., 2013; Lavin et al., 2014; Zhang et al., 2014). These studies identified *Cx3cr1*, *Trem2*, *Tyrobp*, *Cd33*, *Sall1*, and *P2ry12* as genes specifically expressed in mouse microglia. This microglia gene expression profile is regulated by factors like $\text{Tgf-}\alpha$ in the CNS microenvironment and is likely also partially determined by their ontogeny (Butovsky et al., 2014; Gosselin et al., 2014).

Microglia are plastic cells that adopt different phenotypes under varying circumstances in the CNS, such as aging and neurodegeneration (Hanisch and Kettenmann, 2007). An increased inflammatory signature characterizes the aging and neurodegenerative mouse brain in which microglia obtain a sensitized, primed phenotype (Cribbs et al., 2012; Loerch et al., 2008; Perry and Holmes, 2014). Several studies report isolation of microglia from mouse models for these diseases and described age- and neurodegeneration-associated microglia expression profiles (Chiu et al., 2013; Hickman et al., 2008; Orre et al., 2014b, 2014a). In a recent meta-analysis, we identified a core expression profile of primed microglia that was preserved in different mouse models with neurodegenerative and aging conditions. This consensus profile was enriched for general immune gene ontology categories and more specific phagosome and lysosome KEGG pathways. In aging mice, microglia gene expression was also enriched for an Interferon Type-I and a ribosome signature (Holtman et al., 2015).

There is considerable debate on the similarity of microglia in different species (Smith and Dragunow, 2014). So far, pure microglia gene expression profiles were almost exclusively generated using murine microglia. It is unclear to what degree these findings can be extrapolated to human microglia and several arguments have been raised that suggest divergence between species. First, differences in the CNS

microenvironment between species have been identified with respect to CNS gene expression (Hawrylycz et al., 2015; Konopka et al., 2012; Miller et al., 2010), the lipidome (Bozek et al., 2015) and the proteome (Bayés et al., 2012). Second, it has been proposed that the immune system is an evolutionary hotspot with considerable cross-species divergence in microglia function¹⁹. Third, the validity of mouse models for neurodegenerative diseases has recently been re-examined (Burns et al., 2015). Mouse neurodegeneration models rarely mimic the expression profiles of corresponding human neurodegenerative conditions. Therefore, identification of the (dis)similarities between human and mouse microglia expression profiles and associated biological properties in physiological, aging and neurodegenerative conditions is important in view of the potential clinical or therapeutic implications of these differences.

To address these issues, human microglia samples from the right parietal cortex were collected and RNA-sequenced. We report a human microglia core gene expression profile, validated at the protein level, that contains many previously identified mouse microglia regulators and markers, as well as genes that were not identified in any of the previously identified mouse signatures. During aging, human microglia gene expression is characterized by changes in cell adhesion molecules; cell surface receptors and genes involved in Actin cytoskeleton dynamics, suggesting diminished cell motility during aging. This signature shared very little overlap with previously generated gene expression profiles of aging cortical mouse microglia.

MATERIALS AND METHODS

Human Brain Tissue

Human brain tissue was collected from the right parietal cortex during the course of full body autopsy. Samples were acquired from both the Human Brain Bank of the Department of Pathology, School of Medicine of São Paulo University and The Netherlands Brain Bank. Written informed consent for research purposes was obtained and ethical committees from the University of São Paulo, Brazil, the Netherlands Brain Bank and the University Medical Center Groningen, The Netherlands approved the procedure. Detailed data of the autopsy samples, such as age, gender, *post mortem* interval, cause of death, the number of sorted viable cells and RNA quality are listed in suppl. table 1.

Brain tissue biopsies were obtained from epilepsy patients subjected to temporal lobectomy by the Neurosurgery Group of the Department of Neurology at Hospital das Clínicas at the School of Medicine of the University of São Paulo, Brazil.

Microglia isolation

The procedure was carried out as described with a few modifications (Galatro et al., 2017). Samples from the right parietal cortex were collected in ice-cold HBBS (Lonza, Switzerland) supplemented with 15 mM HEPES (Lonza) and 0.6% glucose (Sigma-Aldrich, USA). The brain tissue was dissociated in a glass tissue homogenizer and filtered using a 300 µm sieve, followed by a 106 µm sieve to obtain a single cell suspension. Cells were pelleted by centrifugation at 220 rcf for 10 min (acc: 9, brake: 9, 4°C). The pellet was resuspended in 22% Percoll (GE Healthcare, UK), 40 mM NaCl and 77% myelin gradient buffer (5.6 mM NaH₂PO₄·H₂O, 20 mM Na₂HPO₄·2H₂O, 140 mM NaCl, 5.4 mM KCl, 11 mM Glucose, pH 7.4). A layer of PBS was added on top, and this gradient was centrifuged at 950 rcf for 20 min (acc: 4, brake: 0, 4°C). The myelin layer and the remaining supernatant were carefully removed and the pellet resuspended in a solution of 60% Percoll, which was overlaid with 30% Percoll and PBS respectively, and centrifuged at 800 rcf for 25 min (acc: 4, brake: 0, 4°C). The cell layer at the 60-30% Percoll interface was collected with a pre-wetted Pasteur pipette, washed and centrifuged at 600 rcf for 10 min (acc: 9, brake: 9, 4°C). The final pellet was resuspended in HBBS without phenol red (Lonza) supplemented with 15 mM HEPES

(Lonza) and 0.6% glucose (Sigma-Aldrich, USA). Fc receptors were blocked with human Fc receptor binding inhibitor (eBioscience, #14-9161-73, USA) for 10 min on ice. For sorting, cells were incubated for 20 min on ice with anti-human CD11b-PE (Biolegend, #301306, USA) and anti-human CD45-FITC (Biolegend, #304006) and subsequently washed with HBBS without phenol red. The cells were passed through a 35 µm nylon mesh and collected in round bottom tubes (Corning, USA) and sorted using either a BD Biosciences FACS Aria II cell sorter (Brazilian samples) or a Beckman Coulter MoFloAstrio cell sorter (Dutch samples). Cells were sorted based on CD11b^{high}/CD45^{int} expression and negative staining for DAPI, and collected in RNeasy Lysis Buffer (Qiagen, Germany). Sorted cells were centrifuged 5,000 rcf for 10 min and pellets were lysed in RLT-Plus buffer (Qiagen) for RNA extraction.

RNA extraction and RNA-Sequencing

Total RNA was extracted from flow cytometry-sorted cells using an RNeasy and AllPrep Micro Kit (Qiagen) and from whole brain tissue using RNeasy Lipid Tissue Mini kit (Qiagen), according to the manufacturer's protocol. RNA quality was checked with the Experion RNA HighSens Analysis Kit (Bio-Rad, USA) and RNA Screen Tape (Agilent Technologies, USA). RNA-Seq of all samples was performed at the next generation sequencing facility core (SELA - Sequenciamento em Larga Escala) at the University of São Paulo. TruSeq Stranded total RNA (Illumina, USA) cDNA libraries of 23 samples were prepared starting from 60 ng of total RNA. rRNAs were depleted with Ribo-zero Gold magnetic beads. SMARTer Stranded Total RNA-Seq Kit - Pico Input (Takara Bio, Japan) cDNA libraries were prepared for 16 samples starting with 500 pg of total RNA. rRNA fragments were captured and degraded with RiboGone probes and enzyme. For both protocols, remaining RNAs were fragmented by heat in the presence of divalent cations. The transcript for the first strand cDNA was prepared with reverse transcriptase and random primers. The second strand cDNA was synthesized by reverse transcriptase. Adaptors and index of unique sequence were added to cDNA fragments. The remaining library fragments were enriched by PCR. Final libraries were quantified by qPCR (Kappa Library Quantification Kit, Kappa Biosystems, USA), and the median size of the libraries determined by TapeStation 2200 (Agilent Technologies), using the High Sensitivity D1000 ScreenTape assay. Sequencing was performed as a 125 bp paired-end, dual index run, on a HiSeq 2500 (Illumina, USA) with V4 reagents.

RNA-Sequencing, data analysis and statistics

Human RNA samples generated in The Netherlands and Brazil were prepared and sequenced using similar protocols. Paired-end, 100 bp read length Illumina RNA sequencing was performed at the University of Sao Paulo. FAST-QC([CSL STYLE ERROR: reference with no printed form.]) quality checks were done to determine high quality base pairs, and *bbduk* (<https://sourceforge.net/projects/bbmap/>) was applied to trim low quality reads and adapters. Data was aligned using the STAR aligner Version 2.5 (Dobin et al., 2013) to the ensemble hg38 reference templates obtained from Ensembl and quantified with featureCounts (Liao et al., 2014). Quality check of aligned data was done with RNA-SEQC (DeLuca et al., 2012) and showed high quality alignment and data. Per sample, on average 17.6 million uniquely mapped reads were generated ranging between 6 and 61.1 million. Mouse cortex RNA samples were prepared with a Quantseq 3'mRNA-Seq kit (Lexogen, USA) and sequenced according to the manufacture's protocols. Non-expressed genes were flagged with DAFS(George and Chang, 2014) and removed from downstream analysis.

Data was loaded in R, annotated using BioMart (Durinck et al., 2009) and analyzed using the limma package from Bioconductor (Ritchie et al., 2015). Unwanted/hidden sources of variation, such as the use of different library preps (Clontech and Illumina) and different batches were removed using the *sva* package (Leek et al., 2012). To explore the spatial projection of the different types of samples and possible sources of batch effects such as age, gender, and country of origin, we performed principal component analysis and displayed the overlap of each variable as biplots (Figure 1). The expression values were adjusted according to the surrogate variables identified by *sva* using the function `removeBatchEffect` from the limma package. Next, three different types of supervised analyses were performed using limma: 1) microglia vs. cortex; 2) microglia: aging, gender and PMD analysis; and 3) microglia vs. monocytes and macrophages. For the first comparison two significance criteria were applied to determine the extended microglia signature (FDR-adjusted p values <0.001 and $\log_{2}FC > 3$) and core microglia signature (top 10% of the genes according to the adjusted p values). The defined microglia signature from humans was plotted in a volcano plot (Figure 2). We then compared this gene signature with different mouse studies. We used our own human and mouse datasets to calculate the average expression percentiles for each gene. In addition to our own data, mouse microglia signatures were obtained from previously published papers from (Grabert et

al., 2016; Matcovitch-Natan et al., 2016; Zhang et al., 2016). Two of these datasets consisted of RNA-Seq experiments. We downloaded the FASTQ files from SRA and performed the same procedures as we did with our own datasets to generate the expression data and calculate the average gene percentiles. The data by Grabert et al. was generated with Affymetrix arrays. We downloaded the raw CEL files and performed RMA normalization using the affy package from Bioconductor (Gautier et al., 2004). Expression percentiles were calculated similarly to our own mouse dataset. The percentiles the human genes and the other datasets were pairwise compared using the formula $1 - \text{absolute}(\text{human percentile} - \text{mouse percentile})$; supplemental tables). The absolute differences between the overlapping genes of the human microglia signature and the different mouse datasets were plotted as individual volcano plots. The second comparison was performed as a multivariate linear model that included gender as a binary variable, while age, post mortem delay and the surrogate variables calculated with sva were used as quantitative variables. In the different analyses and comparisons slightly different criteria were used to determine significance. For the quantitative variables only an FDR-adjusted p-value criteria was applied (<0.05), since the logFC values corresponded to estimate increase of the gene per year (for age) or per hr (for PMD). For the third comparison, differential gene expression analysis was performed for microglia vs macrophages, microglia vs monocytes, and monocytes vs macrophages. Raw data (FASTQ files) from a previous RNA-Seq study (Saeed et al., 2014) comparing macrophage and monocyte transcriptomes were downloaded and normalized following the same Bioinformatics approaches as described previously. Pairwise comparisons between microglia, macrophage, and monocytes were performed using limma after unknown sources of variance were removed with sva. The criteria for differential expression was set to FDR-adjusted p value <0.001 and $|\logFC| > 3$.

Enrichment for gene ontology (GO) terms for individual comparisons was performed by hypergeometric tests using the GOSTats package from Bioconductor (Falcon and Gentleman, 2007). Finally, we used the Bioconductor CoRegNet package (Nicolle et al., 2015) to identify the most influential regulatory elements (transcription factors) on the microglia transcriptome and to reconstruct the regulatory subnetwork. We selected the top 1000 most variable genes as inputs for the algorithm. The most influential transcription factors, their interactions, and their putative target genes are shown in Figure 2.

Heatmaps were made with CRAN package *pheatmap* (<https://CRAN.R-project.org/package=pheatmap>). Data is uploaded to GEO, RNA-Seq datasets published by Saeed et al.(Saeed et al., 2014) were obtained from GEO.

Immunohistochemistry

For immunohistochemical staining, snap-frozen brain tissue was cut on a cryostat and 6 µm thick sections were fixed for 10 min in acetone and rinsed with PBS. Sections were incubated for 24 hr at 4°C with primary antibodies diluted in BrightDiluent (09-500, ImmunoLogic, The Netherlands). The following antibodies were used: IBA1 (WAKO 019-19741, 1:750), CD32 (303201, 1:200, BioLegend), CD16 (302001, 1:200, BioLegend), HLA-DR (14-9956, 1:500, eBioscience), TMEM119 (HPA051870, 1:500, Atlas Antibodies, Sweden). On the next day, sections were incubated for 2 hr with the appropriate biotinylated secondary antibodies (anti-mouse or anti-rabbit 1:400 in PBS, both Vector Laboratories), rinsed and then immersed in ABC solution (Vectostain® Elite kit PK-6100, Vector Laboratories). The staining was visualized with 3,3 diaminobenzidine-tetrahydrochloride (Sigma-Aldrich) with H₂O₂. Finally, sections were dehydrated, embedded in DePeX (Merck, Germany) and images were acquired by the NanoZoomer 2.0-HT slide scanner (Hamamatsu, Japan).

In case of double immunofluorescence staining, above mentioned antibodies were used in various combinations and after the primary incubation, washed with PBS and incubated for 2 hr with horse anti-mouse-biotin (BA-2001, 1:400 in PBS; Vector Laboratories). After washing, sections were incubated for 1 hr in a mixture of donkey anti-rabbit-AF488 (A21202, 1:300 in PBS; Molecular Probes Thermo Fisher Scientific, USA) and streptavidin-AF594 (016-580-084, 1:400 in PBS; Jackson ImmunoResearch, USA). A Hoechst staining (14530, Sigma-Aldrich) was performed, followed by a 15 min incubation in 0.3% Sudan Black B (S-0393, Sigma-Aldrich) in 70% ethanol to reduce autofluorescence. Finally, sections were washed with demi-water and embedded in Mowiol (Sigma-Aldrich). Imaging was performed on a Zeiss LSM 780 confocal laser scanning microscope using a 20x Plan Apochromat NA=0,8 air objective or an 40x Plan-Neofluar NA 1.3 oil-immersion objective using 405 nm, 488nm and 594 nm lasers and appropriate filters (Carl Zeiss B.V., Sliedrecht, The Netherlands).

Western blotting

Cortex and sorted microglia was lysed in lysis buffer (CST#9803) and separated by SDS-PAGE and transferred to Immobilon®-FL membranes (IPFL00010, Millipore, Germany). The antibodies used were: β -actin (ab6276, 1:5000, Abcam, USA), Iba-1 (019-19741, 1:3000, WAKO, Japan), Vimentin (M0725, 1:1000, DAKO), β -III-tubulin (ab18207, 1:2000, Abcam), GFAP (Z0334, 1:3000, DAKO), and CNPase (C5922, 1:500, Sigma-Aldrich). Membranes were incubated with secondary antibodies: goat anti-rabbit IgG (H+L) IRDey800 CW and donkey anti-mouse IRDey680. Membranes were scanned and quantified on a LI-COR Odyssey® (LI-COR Biosciences, USA).

Proteome Profiler Array of FACS sorted microglia

FACS sorted microglia (200.000 - 400.000/donor; 4 donors/sample) were collected in lysis buffer with protein inhibitors. The proteins in these lysates were analyzed using the Human Soluble Receptor Array Kit (Catalog # ARY011, R&D Systems Inc., USA) according manufacturer's instructions. Membranes were imaged using an Imagequant LAS 4000 (GE Healthcare Life Sciences, USA). Quantification of the detected spots was performed using the Protein Array Analyzer plugin in ImageJ. Vimentin was used as in internal standard for membrane normalization.

RESULTS

Acute isolation of pure microglia from human *post-mortem* tissue samples

Human microglia samples were collected during the course of full body autopsy, by dissection of parietal cortex brain tissue, tissue processing and acute isolation of viable microglia by FACS sorting. Microglia isolations were performed within a 6 to 24 hr *post-mortem* delay (PMD) from donors without diagnosed brain diseases. 74 rapid microglia isolations were performed (33 in The Netherlands and 41 in Brazil). Ultimately, 39 samples from donors with a history of normal cognitive function and no apparent neuropathological abnormalities with sufficient levels of high quality RNA were selected for RNA-Sequencing. For donor information: sample ID, tissue type, sample origin, gender, age, PMD and cause of death see Suppl. Table 1.

Paired-end Illumina high quality deep sequencing was performed on 39 microglia, 16 corresponding superior parietal cortex tissue (further referred to as cortex) and 10 epilepsy surgery samples (referred to as biopsy). RNA-Seq data was pre-processed, quantified and differentially expressed genes were determined. The initial analysis focused on the expression of cell type-specific markers from microglia and other CNS cells to determine the purity of the samples and possible differences in gene expression between tissue with varying PMD and surgery tissue (Figure 1A). Human microglia highly expressed known microglia genes such as *CX3CR1*, *ITGAM*, *P2RY12*, and *TYROBP*. Genes characteristic for neurons, astrocytes, and oligodendrocytes were equally expressed in cortex and epilepsy biopsy samples but were low or not expressed in microglia. The monocyte marker *CCR2* was lowly expressed in microglia. These findings confirm that a highly pure population of microglia was collected and that PMD had little effect on gene expression. This is in agreement with various reports showing that PMD does not correlate with CNS tissue morphology, RNA quality or integrity (Chevyreva et al., 2008; Durrenberger et al., 2010; Ervin et al., 2007).

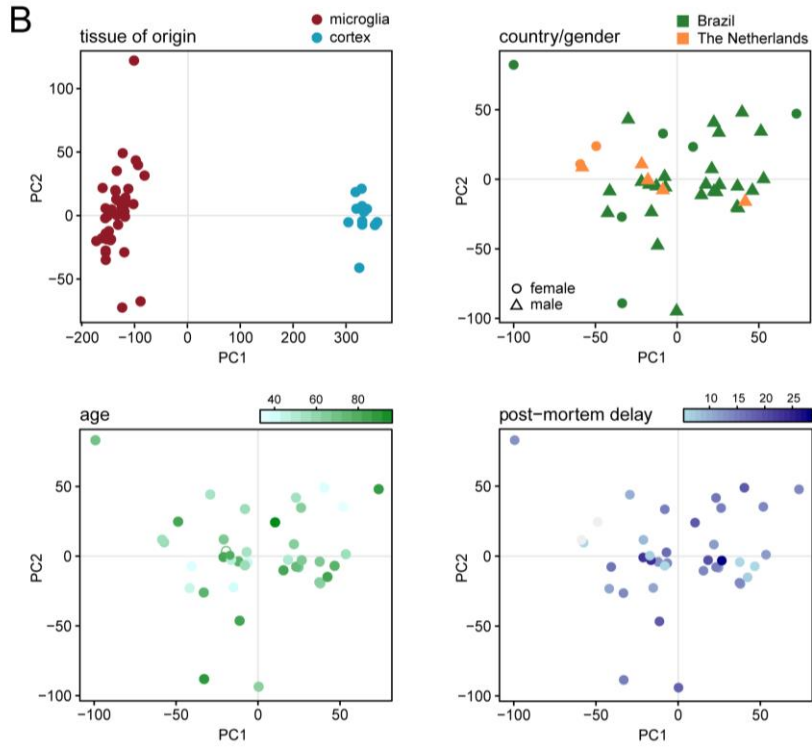
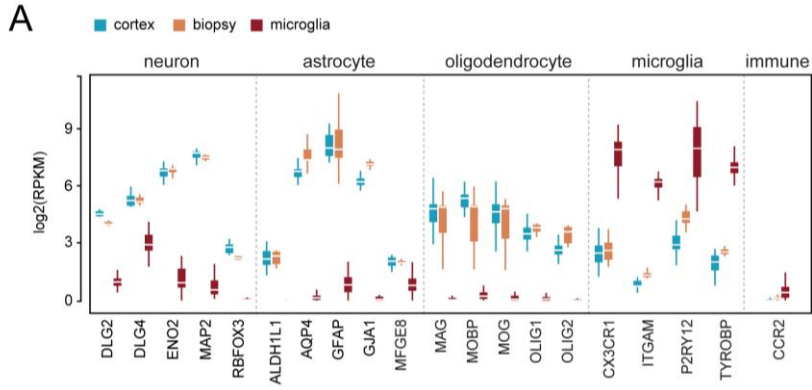


Figure 1: Comparison of human microglia and parietal cortex expression profiles. A) RNA-Sequencing of *ex-vivo* isolated microglia, corresponding parietal cortex tissue and epilepsy surgery biopsy samples revealed high and consistent expression of known genes in microglia, with low expression of genes for neurons, astrocytes, oligodendrocytes and potential immune infiltrates. As expected, expression of neural genes was detected in total parietal cortex tissue and epilepsy biopsy samples. This indicated that a highly pure microglia population was sorted from our cohort of human post-mortem brain samples. B) Principal component analysis of RNA-Seq samples showed that microglia were highly similar and very different from the unsorted superior parietal lobule (cortex) samples. Microglia samples did not segregate according to age, gender, country of sampling, or post mortem delay (PMD). The % variation in the data explained by the respective principal components is

Identification of the core human microglia gene signature

A principal component analysis (PCA) of RNA-Seq expression data of pure microglia and cortex samples with tissue of origin as a variable was performed. Microglia and cortex samples clearly segregated and were highly similar within each tissue group, indicating that microglia expression profiles are very different from unsorted parietal cortex tissue expression data. PCA of pure microglia samples with country of origin of the samples (The Netherlands and Brazil) as variables revealed no obvious segregation due to country of sampling or gender. For microglia isolations, the same reagents were used in both countries, and all samples were sequenced on the same sequencing platform to minimize variation. PCA based on age also did not indicate a clear age-associated effect on microglia gene expression. In case of human autopsy samples, *post-mortem* delay (PMD) is an inevitable factor. When the microglia expression data were analyzed using PMD as a variable, no effect of PMD was observed. This further corroborates the observation depicted in Figure 1A, where epilepsy surgery material was compared to parietal cortex tissue obtained during autopsy.

Extensive differences in gene expression between microglia and cortex tissue were detected and are visualized in a volcano plot (Figure 2A). A core human microglia signature of 1,297 genes, indicated by red dots, was generated with $\log_{2}FC > 3$ and $p < 10E-3$ as criteria (Figure 2A). In Suppl. Table 2, detailed gene expression data are provided; genes with no Entrez annotation were filtered out.

Gene ontology analysis was used to determine functional properties associated with the 1,297 genes of the human microglia core signature. As expected, many significantly enriched terms associated with the innate immune activity of microglia, like 'immune response', 'defense response', cytokine production'. The profile was also enriched for 'phagocytosis', 'cell migration', 'cell motility'. This data confirms that human microglia are the immunocompetent and phagocytic cells of the CNS that express a wide range of immune receptors and ligands, equipped to respond to a wide variety of pathogen- and damage-associated molecules. A full list of GO terms and p values is depicted in Suppl. Table 3.

Predicted protein-protein interactions in the core profile were analyzed using STRING. A network involved in cell motility and inflammation containment was detected with intracellular tyrosine kinase *SYK*, a gene involved in cell adhesion and cytoskeletal rearrangements. The human microglia core profile contains several members of this signaling pathway, such as CD11B (α -Integrin), CD18 (β -Integrin), FCGR and TYROBP (ITAM motif containing proteins). As microglia are highly motile cells that rapidly respond to stimuli and injury, it is only plausible that chemotaxis and cell motility signaling pathways are detected in these cells. Integrin-SYK signaling is also responsible for negatively regulating TLR signaling and the NF- κ B pathway by promoting the degradation of MYD88 (Kondo et al., 2012).

A protein-protein network involved in cell proliferation was also detected. CD74, highly expressed by human microglia, prevents MHC class II molecules from binding non-processed peptide and self-antigens (Stockinger et al., 1989). Its ligand, CXCR2/4 was also highly expressed by human microglia (Bernhagen et al., 2007). In monocytes, CXCR2/4-CD74 heterodimers induce PI3K/AKT signaling and P53 inhibition, leading to increased survival, proliferation and apoptosis evasion (Lue et al., 2007; Mitchell et al., 2002). CXCR2-CD74 leads to chemotactic signaling, which is activated by MIF (macrophage migration inhibitory factor), a gene expressed in cortical tissue.

Our human microglia expression profile was compared to a human CD45⁺ cell population, isolated using immunopanning from temporal lobe cortex tissue obtained during tumor or epilepsy surgery (Zhang et al., 2016). Genes were ranked based on their relative expression level in the respective data set. For the 1,297 human core genes, the respective percentiles of each gene in our human and the CD45⁺ data set were subtracted (Δ percentile). Genes similarly expressed in both datasets, a Δ percentile <20, are represented with bright blue dots, where genes much less

abundantly expressed in CD45⁺ cells are represented by black dots (Δ percentile >80; Figure 2B). Overall, a very extensive overlap in gene expression between these datasets was observed, the median Δ percentile was 10.065 indicating most genes are similarly expressed in both data sets.

To determine the overlap in gene expression between human and mouse microglia, a cortical mouse microglia gene expression profile was generated. The human transcriptome was compared to this data set as well as to recently published cortical microglia expression data sets (Grabert et al., 2016; Matcovitch-Natan et al., 2016) using the strategy explain above. An extensive overlap was observed between human and these three independent mouse microglia gene expression data sets. The median Δ percentiles were 14.31, 20.43, and 9.34 for our own expression data set, Grabert et al., and Matcovitch-Natan et al., respectively. Despite the fact these mouse expression data were generated using very different technologies (Lexogen 3' Quant Seq, Affymetrix arrays and RNA-Seq respectively), an extensive overlap with human microglia was observed. The Δ percentiles of all four datasets are depicted in the box plots (Figure 2D) and in supplemental Table 4.

Notably, several human microglia genes were much less abundant expressed in mouse microglia. Examples of human microglia-enriched genes are CD58, an adhesion molecule that plays a central part in the clustering of mature dendritic cells and T lymphocyte activation (Leitner et al., 2015). ERAP2, along with the closely related ERAP1, are peptide editing enzymes responsible for the trimming of N-terminal residues of MHC class I molecules (Chen et al., 2016). Granulysin (GNLY) is a cytolytic and proinflammatory molecule, largely cytolytic against tumors and microorganisms, including gram-positive and gram-negative bacteria (Krensky and Clayberger, 2005). GNLY acts also a chemoattractant for T lymphocytes, monocytes and other inflammatory cells, activating expression of several of cytokines, such as CCL5, MCP-1, and IL-10, IL-1, IL-6 and IFN- α . S100A12 has shown to be important for antimicrobial activity, its proinflammatory action involves recruitment of leukocytes, production of cytokines and chemokines, and regulation of leukocyte adhesion and migration. It also acts as an alarmin or a danger-associated molecular pattern (DAMP) molecule, stimulating innate immune cells. A recent study showed that S100A12 is sufficient to directly kill *Mycobacterium tuberculosis* and *Mycobacterium leprae* (Realegeno et al., 2016).

In short, an extensive overlap between human microglia gene expression and human CD45+ CNS cells and mouse cortical microglia was detected with some notable differences between human and mouse microglia.

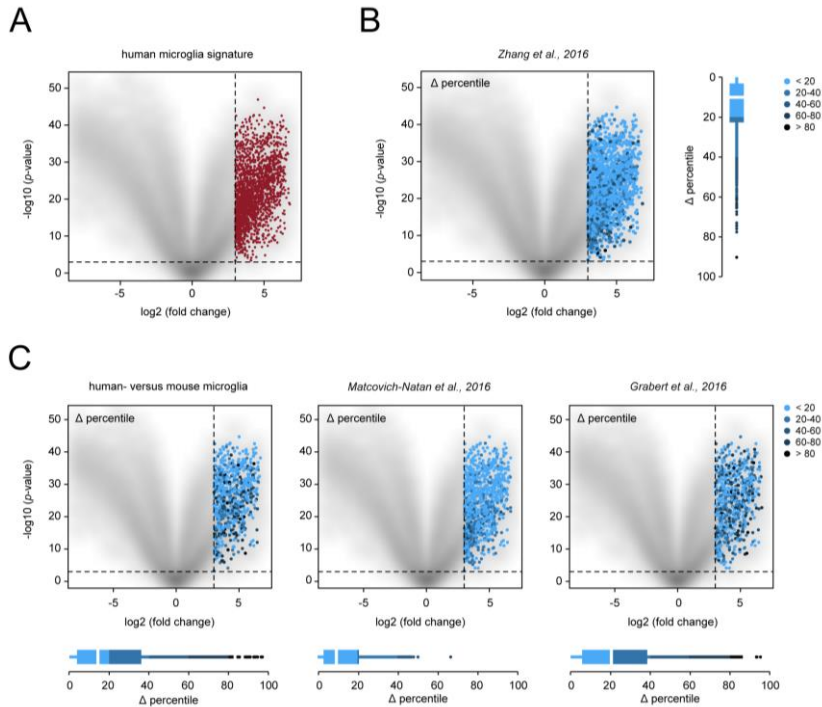


Figure 2: Comparison of the human microglia expression profile to cortex, human and mouse microglia signatures. A) Volcano plot illustrating differential expression of genes in microglia versus cortex samples. Genes with $\log_2FC > 3$ are depicted as red dots and comprise the human microglia core profile of 1285 genes. B) Volcano plots illustrating the overlap in gene expression of the human microglia core to CD45⁺ cells in the CNS (Zhang). Genes expressed to similar levels in both datasets are depicted as bright blue dots (Δ percentile <20), where genes much more abundantly expressed in microglia than in CD45⁺ cells are depicted by black dots (Δ percentile >80). The distribution of all detected human microglia core genes over the Δ percentile intervals (<20/20-40/40-60/60-80/>80) is shown in the box plot. C) Volcano plots illustrating the overlap in gene expression of the human microglia core to mouse cortex microglia. Genes expressed to similar levels in both datasets are depicted as bright blue dots (Δ percentile <20), where genes much more abundantly expressed in microglia than in mouse microglia cells are depicted by black dots (Δ percentile >80). Three independent mouse data sets are depicted: our own generated by 3'Quant seq, a RNA-Seq data set (Matcovitch-Natan et al., 2016)) and Affymetrix arrays (Grabert et al., 2016). The distribution of all detected human microglia core genes over the Δ percentile intervals (<20/20-40/40-60/60-80/>80) is shown in the box plot.

Under certain neuropathological conditions, i.e. glioma progression (Hambardzumyan et al., 2015) and multiple sclerosis (Dendrou et al., 2015), immune

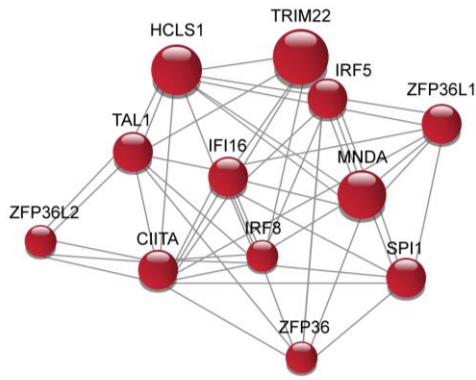
cells, such as macrophages and dendritic cells, infiltrate the CNS and contribute to disease progression. Microglia are often identified using *IBA1/AIF1*, *P2RY12* and *CX3CR1* as markers and differentiated from infiltrating immune cells based on *CCR2* (Mizutani et al., 2012). The expression levels of (some of) these markers are altered by microglia activation, priming and aging. PCA of our human microglia and published monocyte and macrophage data³¹ expression data indicated that these three datasets segregated, and that microglia were most distinct (Figure S1A). To determine differences in gene expression between microglia, monocytes and macrophages, three pair-wise comparisons were carried out. Differentially expressed genes were selected with a logFC of >3 and a p value <0.001 as depicted in suppl. Figure 1B, and suppl. Table 5.

In comparison to monocytes, microglia were enriched for GO terms synapse organization, neuron projection morphogenesis and cell projection morphogenesis; and hemophilic cell interactions, purine nucleotide metabolic process and sphingolipid metabolic process when compared to macrophages. This indicates that microglia, in comparison to monocytes, express many genes related to their CNS functions.

Transcription factors associated with the human microglia core gene expression

With the Bioconductor package CoRegNet, 12 microglia-specific transcriptional regulators of the human core genes were identified (Figure 3A). Two of these transcription factors are essential for microglia ontogeny: SPI-1 (or PU.1) and IRF8 (Kierdorf et al., 2013a). Additional transcriptional regulators identified were: CIITA, a positive regulator of MHC-II gene transcription; TRIM22, a transcription activator induced by interferon; MNDA, an interferon target gene; IRF5, a factor modulating inflammatory responses; TAL1, a transcription factor associated with microglia aging (Wehrspaun et al., 2015); IFI16, an interferon γ inducible gene; HCLS1, and ZPF36 with paralogs ZPF36L1 and ZPF36L2 were also detected. Genes that have been reported to be regulated by these proteins are indicated by red dots in the volcano plots in Figure 3B. The number and list of targets for each transcriptional regulator is provided in suppl. Table 6 and contains many established microglia genes, such as *CX3CR1*, *AIF-1/IBA1*, *P2RY12* and *P2RY13*.

A



B

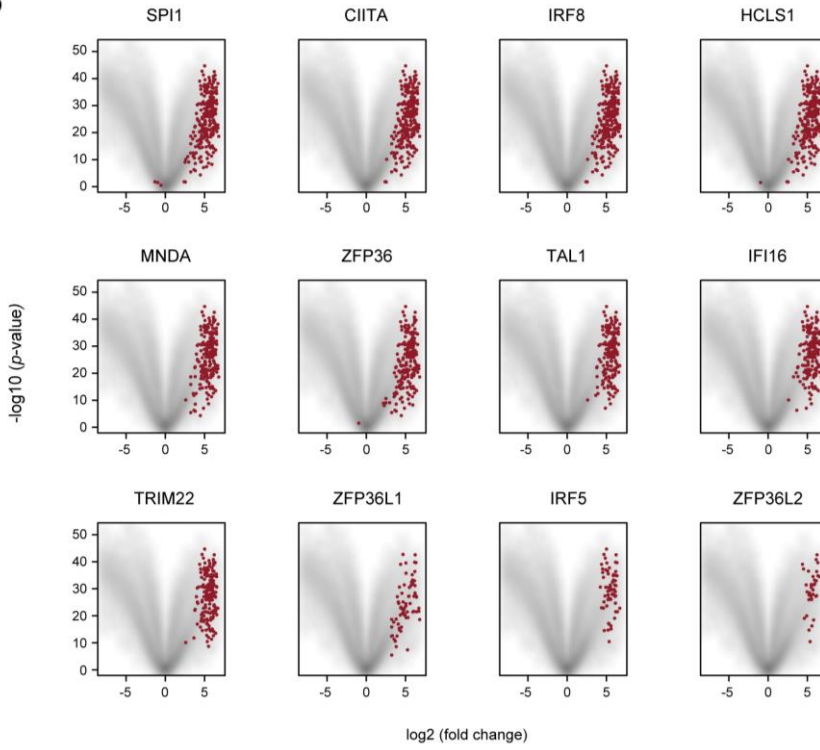


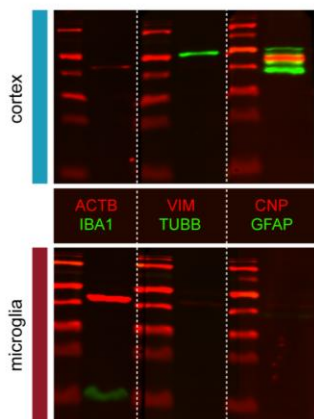
Figure 3: *Predicted transcriptional regulators of the human microglia core genes.* A) Using BioConductor package CoRegNet, transcriptional regulators of the 1,297 human microglia core genes were identified. B) Volcano plots depicting the genes of the human microglia core genes associated with the transcriptional regulators identified.

Microglia protein expression

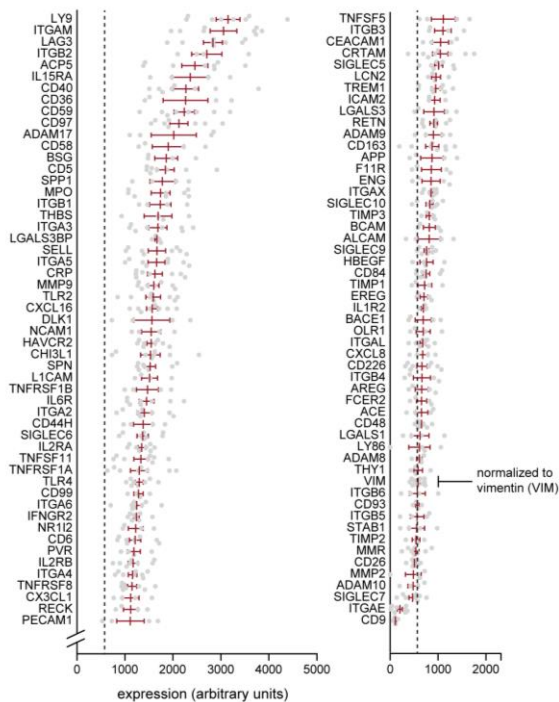
To confirm the RNA expression data at the protein level, human microglia were FACS isolated from parietal cortex and together with unsorted cortex tissue analyzed using western blot analysis, antibody arrays and immunohistochemistry. Microglia and cortex protein samples were separated using PAGE and detected with the indicated antibodies. IBA1 and vimentin were only detected in microglia protein lysates where β -III-tubulin, CNPase and GFAP, markers for neurons, oligodendrocytes and astrocytes, respectively, were only detected in cortex protein lysates. Next, arrays with antibodies against human hematopoietic proteins were incubated with microglia protein lysates. Parietal cortex microglia were isolated from autopsy tissue samples using FACS and pooled from 2x4 donors. Spot intensities on the membranes were normalized to vimentin and quantified. Expression of known microglia proteins, such as ITGAM (CD11B), SPP1 (Osteopontin), multiple TNF- α , SIGLEC, chemokine and TLR receptors was detected, confirming the RNA expression data.

Finally, human parietal cortex tissues were stained with antibodies against Iba1, HLA-DR, CD16, CD32 and TMEM119 either using immunohistochemistry and double immunofluorescence. Cells with clear microglia morphology were detected with the indicated antibodies and extensive co-localization with established microglia marker Iba1 was observed.

A



B



C

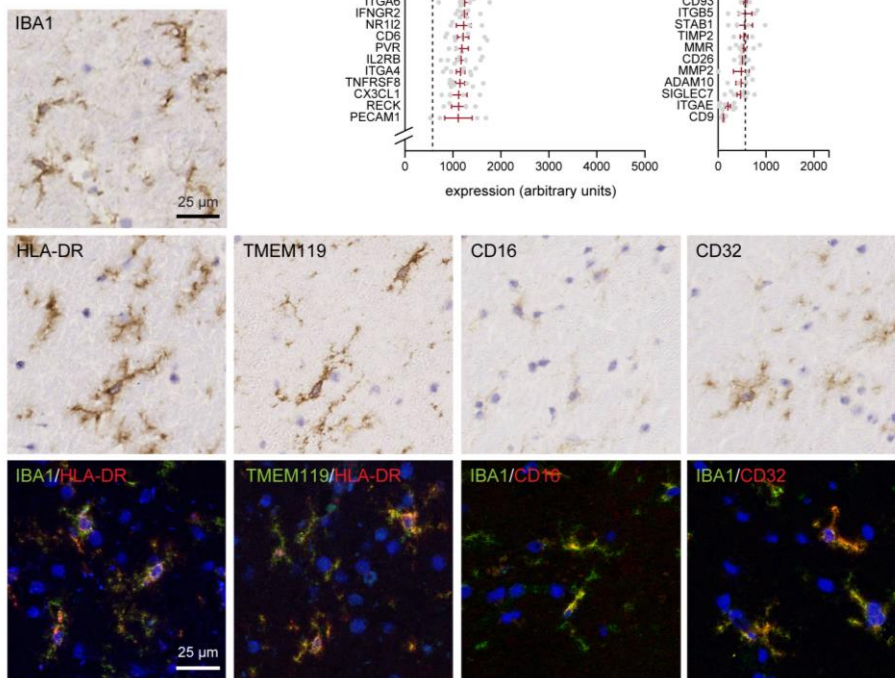


Figure 4: Protein validation microglia gene expression. A) Western blot analysis of sorted microglia and parietal cortex samples with the antibodies indicated. IBA1 was only detected in pure microglia, whereas proteins expressed by other CNS cells were only detected in unsorted parietal cortex protein samples. ACTB: β -actin, VIM: vimentin, TUBB: β -III-tubulin, CNP: CNPase. B) Proteome profiler antibody arrays directed against human hematopoietic proteins were incubated with pure parietal microglia protein samples. Spot intensities were quantified and normalized to vimentin. C) Microglia expressing Iba1, HLA-DR, CD16, CD32 and TMEM119 visualized by DAB staining and immunofluorescence. Extensive co-localization of these markers is observed. Scale bars are 25 μ m. Representative images of two independent experiments are shown.

Age-associated changes in microglia gene expression

Age-associated changes in gene expression are reported to occur in mouse microglia (Hickman et al., 2013; Ma et al., 2013). How these findings translate to human microglia aging is unknown. The age of our donors ranged between 34 and 102 years, allowing us to determine changes in microglia gene expression that occurred during aging. Using age as a quantitative variable, 212 genes increased and 360 genes decreased in expression ($p < 0.05$). In Figure 5A, a relative expression heatmap depicts the top 100 genes most significantly affected by age ($p < 0.01$). Hierarchical clustering of these genes resulted in two separate clusters, containing relatively younger and older samples, respectively. Noteworthy genes with reduced expression during aging included many actin cytoskeleton-associated genes like *TLN1*, *PFN1*, *EVL*, *ARPC1*, *CORO1A*, *CAP1*, *CTNNA2*, and *VASP*, some cell surface receptors *P2RY12*, *IL6R* and *TLR10*, and cell adhesion molecules and cell surface receptors as *ICAM3*, *ROBO2*, *SEMA3C*, *SEMA7A*. A comprehensive illustration of these genes is depicted in Figure 6B. Genes with relatively higher expression during aging included integrin modulators *DOCK1/5*, receptors *CXCR4*, *CD163* and *IGF2R*, growth factor *VEGFA* and transcription factor *RUNX3*. GO categories associated with the genes differentially expressed during aging (Figure 5B) were enriched for CNS development, with associated changes in cytoskeleton, immune response and motility (cell adhesion).

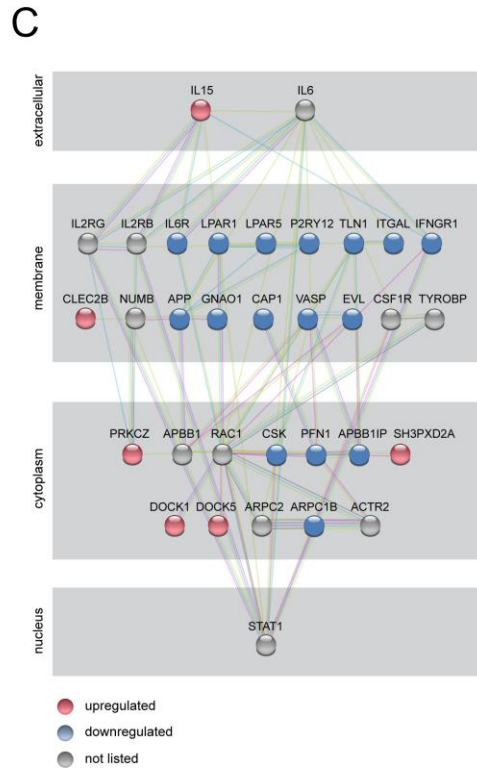
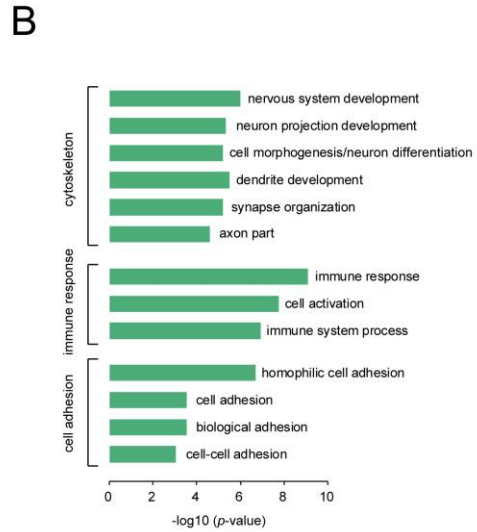
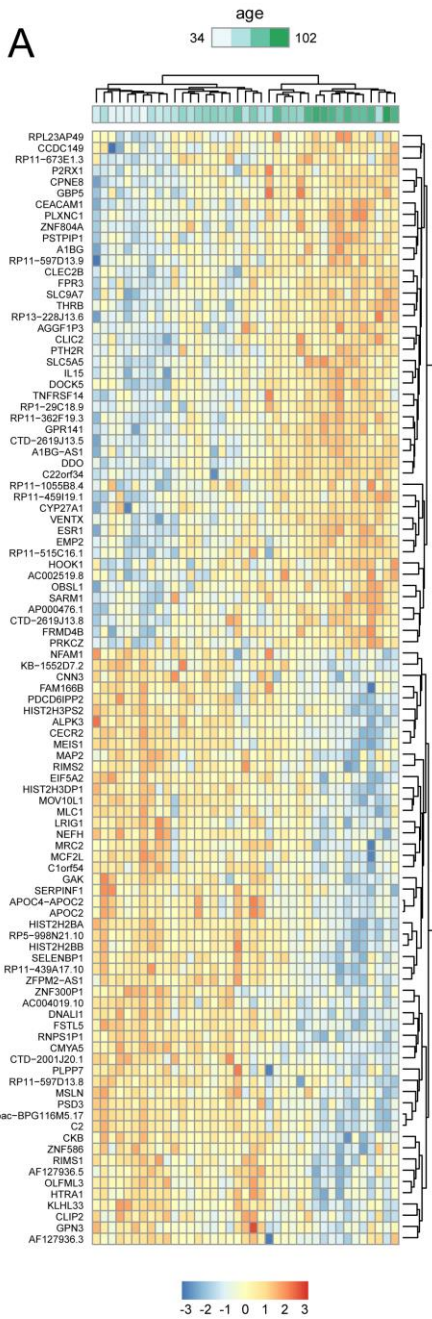
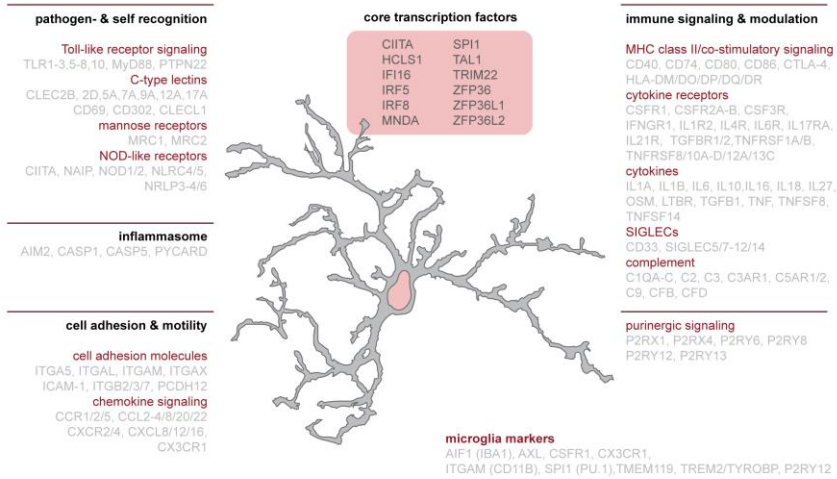


Figure 5: *Aging affects CNS-associated function and motility of human microglia.* A) Hierarchically clustered Z-score expression heat map of the 100 most affected genes by age showed a clear clustering separating older and younger samples. B) GO analysis showed enrichment for CNS development, immune response and motility of aging-associated genes. C) A predicted protein-protein interaction network of age-associated genes in microglia.

Comparison of the human microglia aging profile with a previously published mouse microglia aging study profiles (Grabert et al., 2016) revealed a small number of significantly overlapping genes. 14 genes were increased in both human and mouse microglia with aging, of which *CXCR4*, *VEGFA*, *TNFAIP2* and *GP2* have been previously identified by other aging or priming studies (Hickman et al., 2013; Holtman et al., 2015; Raj et al., 2015). The main biological pathway associated with these genes was “positive regulation of cell-matrix adhesion”. Nine genes with reduced expression in aging were overlapping between human and mouse cortical microglia, and included previously identified *ETS1*, along with *SEMA7A*, *MRC2*, *PSTPIP1* and *EMP2*, with no associated GO category. A Venn diagram depicting the overlap between aging cortical human and mouse (Grabert et al., 2016) microglia is depicted in suppl. Figure 2. The overlap in genes differentially expressed during aging between human and mouse is very limited, suggesting that the microglia of physiologically aged mice do not recapitulate the effect of aging on human microglia. The aging human microglia signature we have identified can be used as a benchmark to evaluate other model systems that intend to study the role of microglia in age-related neuroinflammation.

A. Human microglia core signature



B. Aging-associated changes in human microglia

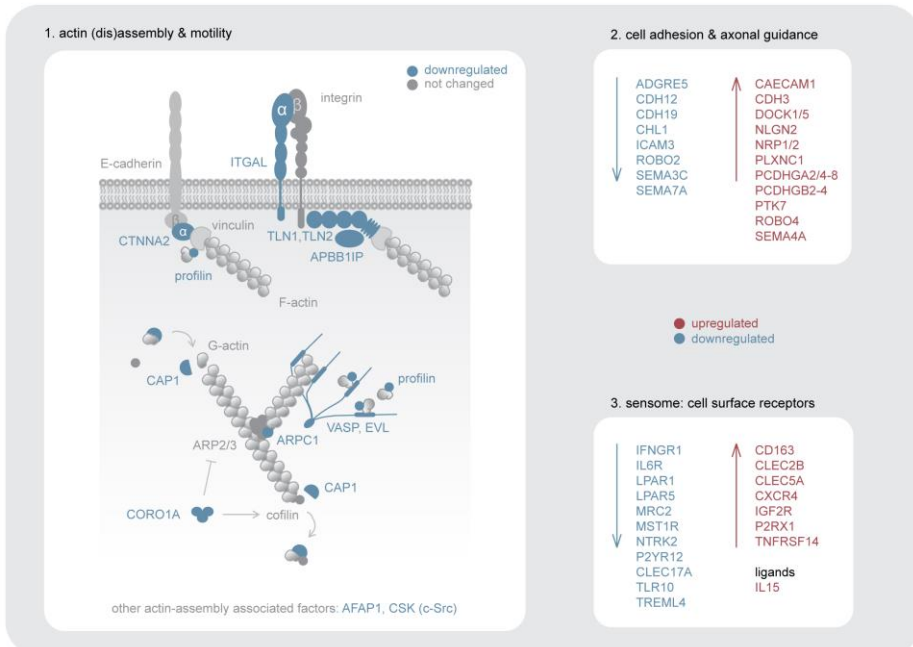


Figure 6: *Human microglia and the effect of aging.* A) Graphical summary of the human microglia core genes. Biological functions with associated gene families and representative gene names are depicted. B) Aging of microglia is associated with reduced expression of many genes involved in Actin dynamics. All genes with reduced expression in aged microglia are depicted in blue. Changes in genes involved in cell adhesion and axonal guidance as well as the sensome (cell surface receptors) are listed.

DISCUSSION

In this manuscript we present an extensive collection of human microglia transcriptome profiles and systematically compare them to previously published human and mouse profiles. Mice are frequently used for neuroscience research purposes but there is extensive debate about the validity of these mouse models to study microglia in aging and neurodegenerative conditions (Smith and Dragunow, 2014). We addressed two main questions: 1) what is the expression profile of human microglia and how does it relate to mouse microglia profiles?; 2) what age-related changes occur in aging human microglia and to what degree do they overlap with mouse microglia aging signatures?

To approximate the physiological human *in vivo* microglia expression profile, donors with overt CNS pathologies were excluded, viable microglia were FACS-sorted (DAPI-negative), and only high quality RNA samples were sequenced. Nonetheless, all donors suffered from a range of pathologies ultimately leading to their demise, potentially affecting the microglia gene expression profile. The effect of various parameters on gene expression, such as PMD, age, and gender was estimated. Our data indicate that a *post-mortem* delay between 4 and 24 hr had very little influence on the microglia gene expression profile. Numerous other studies already reported a poor correlation between PMD and CNS tissue morphology, RNA quality or integrity (Chevyreva et al., 2008; Durrenberger et al., 2010; Ervin et al., 2007).

The first aim of this study was to determine the similarities and differences between human and mouse microglia expression profiles. Considerable overlap between human and murine microglia gene expression was observed but interesting dissimilarities were also present. These dissimilarities could be caused by a range of factors, such as intrinsic differences between species, differences in environment, medical condition and differences in study design. For example, laboratory mice are, to a certain degree, kept under specified pathogen-free conditions and typically not exposed to a wide range of pathogens, which is in striking contrast to humans who are exposed to a range of pathogens during the course of their lives. In addition, mouse microglia were isolated from healthy animals, whereas the human microglia samples were obtained during the course of autopsies of donors that suffered from various pathologies. To minimize the reported effect of brain region on microglia gene expression (Grabert et al., 2016; Matcovitch-Natan et al., 2016; Zhang et al., 2016), only cortical microglia were included in our comparisons

A substantial number of the human microglia-specific genes are implicated in immune pathways, and could reflect functional characteristics of human microglia. Interesting examples are Granulysin, a protein present in cytotoxic granules and *Apobec3c*, a deaminase that inhibits retrovirus replication and retrotransposon mobility via deaminase-dependent and -independent mechanisms (Stenglein et al., 2010). Furthermore, immune response genes, such as *Clecl1*, a T-cell costimulatory molecule that enhances interleukin-4 production (Ryan et al., 2002), *FCAR/CD89*, a Fc- γ receptor mediator of cytokine production (Shimokawa and Ra, 2005), and inflammasome component *Card8*, were also observed in humans solely. It seems that human microglia-exclusive genes, despite not belonging to any specific biological pathway, are primarily implicated in host defense and the modulation of immune responses.

SIGLECs have an important role in immunosuppression and neuroprotection. SIGLECs regulate the effects of activation, phagocytosis and inflammasome formation via their immunoreceptor tyrosine-based inhibition motif (ITIM) (Macauley et al., 2014). *CD33* (SIGLEC3), a known microglia marker, is associated with the accumulation of amyloid beta plaques in mouse AD models due to diminished phagocytic capacity of microglial cells up-regulating this gene (Griciuc et al., 2013). Our finding that human microglia express many SIGLECs highlights their importance and the specialization of microglia for the maintenance of a homeostatic microenvironment.

NLR5 and *CIITA* are the respective master regulators of MHC class I and II gene expression (Meissner et al., 2010). While *CIITA* expression is restricted to antigen presenting cells (APCs), *NLR5* is constitutively expressed in various tissues, most highly in cells from the hematopoietic lineage (*CD4*⁺ T cells, *CD8*⁺ T cells, *CD19*⁺ B cells, natural killer (NK) cells and natural killer T cells). *NLR5* expression levels are intermediate in monocytic *CD14*⁺ cells and *CD11b*⁺ splenic myeloid cells (Kobayashi and van den Elsen, 2012). This data corroborates the notion that human microglia are potent APC and are able to interact with *CD4* and *CD8* T-helper cell subsets.

Using CoRegNet, regulators of the human core microglia genes were identified. Well-established microglia factors such as *SPI-1*, *CIITA*, *IRF8* were singled-out. *IRF8* is necessary for microglia genesis, along with *SPI-1* (Kierdorf et al., 2013b), and recent reports on the induction of human pluripotent stem cell-derived microglia-like cells demonstrated high levels of this transcription factor in such cells (Muffat et al., 2016). In addition to *IRF8*, human microglia expressed high levels of *IRF1*, *IRF5* and *IRF7*. *TAL1/SLC*, a basic helix-loop-helix transcription factor, is a master regulator of normal

and abnormal hematopoiesis and controls the expansion of primary monocyte progenitors (Dey et al., 2010). In adults, TAL1 is expressed in hematopoietic cells but also in specific regions of the midbrain, hindbrain, and spinal cord (van Eekelen et al., 2003; Sinclair et al., 1999). Chip-Seq analysis previously indicated that TAL1 forms a complex with RUNX1 and LYL1 (Wilson et al., 2009, 2010), and these transcription factors are abundantly expressed in the human microglia core. RUNX1 activates the transcription of SPI-1 (Huang et al., 2008), a bona fide microglia transcription factor.

IFI16 (p204), is associated with viral infection and the response to cytosolic double-stranded DNA (Gürtler and Bowie, 2013), performing an important role in regulating cell proliferation and transcription through different interactions with p53 (Liao et al., 2011) and STAT3. IFI16 is also involved in overcoming inhibitors of differentiation proteins (IDs) blocking of terminal cell differentiation (Luan et al., 2008), as exemplified by the down-regulation of ID4 in microglia. Interestingly, although human microglia seem to possess a highly activated pathway for proliferation (the aforementioned CXCR-CD74 axis), this pathway is dependent on extracellular signals, while genes involved in cell cycle are also highly expressed. IFI16 is possibly involved in regulating the relative microglia quiescence, which is observed under normal conditions.

The second aim of this study was to compare the human and mouse aging microglia expression profiles. Strikingly, no extensive overlap between the human and mouse aging signatures was detected. A small number of genes with increased/decreased expression during aging overlapped between human and mouse microglia. However, an almost equal number of genes displayed opposite directionalities in expression during aging, e.g. up in mouse and down in human or vice versa. Overall, the overlap in genes affected by aging in human and mouse microglia is relatively low, suggesting that microglia from both species age differently. A recent publication indicated that the microglia population in the brain is replaced approximately every 100 days in both mice and humans (Askew et al., 2017). This implies that the microglia population is replaced many more times in humans than in mice during their respective life spans, with possible ramifications for aging-induced alterations in gene expression of microglia function.

Age-induced changes in human microglia are enriched for a variety of genes involved in actin assembly and all these genes are less abundant in microglia during aging. For instance Talin1 (TLN1), a protein involved in actin remodeling and cell motility, Profilin (PFN1), a protein directly involved in actin binding and

polymerization, and VASP, a protein involved in actin filaments elongation are less abundant in microglia isolated from older donors (Siddiqui et al., 2012; Vincent et al., 2012). As actin (dis)assembly is essential for cellular motility and migration, this suggests that these functions might decrease during aging in microglia. Interestingly, a reduction of microglia process motility directed toward site of damage was significantly impaired in mice with A β plaques (Krabbe et al., 2013). Possibly, the observed changes in Actin assembly in human microglia during aging might be important in aging as such or in neurodegenerative conditions like Alzheimer's disease.

In addition, age-associated changes in genes involved in axonal guidance, cell adhesion and the sensome were observed. These receptors and their downstream signaling are implicated in chemotaxis and part of the microglia sensome (Ferrari et al., 2016; Hickman et al., 2013). Binding of chemoattractant ligands to their respective receptors on myeloid cells induces these cells to move towards injury sites, apoptotic cells or invading microorganisms. Movement of the fine microglial processes to sense the environment and initiate chemotaxis is primarily governed through these receptors and P2RY12, an established microglia marker (Butovsky et al., 2014; Hickman et al., 2013), is downregulated in our aging cohort, further highlighting the altered microglia sensing/motility with aging.

Little is known about microglia gender differences, but a few studies have identified a gender-specific role for microglia in the rat brain (Chen et al., 2014; Lenz et al., 2013). Sex differences in microglia function in the developing brain are associated with neurodevelopmental and psychiatric conditions (Lenz and McCarthy, 2015). We found that gender differences in humans were restricted to X and Y-chromosome genes. Since our donor population contained 7 females versus 32 males, more female donors would be required to identify possible gender-specific traits in human microglia.

In conclusion, here we present the first extensive human microglia gene expression profile. Critical differences with mouse microglia, especially in the context of aging, were observed which highlight the necessity to independently study human microglia. These data and analyses serve as a starting point to address human-specific microglia genes and functions under physiological and neuropathological conditions.

ACKNOWLEDGEMENTS

The authors want to thank Dr. I. Huitinga, the director of the Netherlands Brain Bank, for the Dutch brain samples. The authors thank Prof. Dr. E. G. Kallás for the use of the FACS facility at School of Medicine. The authors thank São Paulo Research Foundation (FAPESP), grants 2013/07704-3, 2013/06315-3, 2013/02162-8 and 2014-50137-5, CAPES-NUFFIC (062/15), Conselho Nacional de Pesquisa (CNPq 305730/2015-0) and Fundação Faculdade de Medicina (FFM) for financial support. The authors thank the Dutch MS Research Foundation and the Gemmy & Mibeth Tichelaar Foundation. The authors thank Geert Mesander, Henk Moes, Roelof Jan van der Lei and Priscilla Ramos Costa for their technical assistance with FACS sorting and Dr. Hilmar van Weering for artwork. The authors thank Isabele Moretti, Clarisse Silva, Mariana Molina, Vanessa Galdeno and Dr. C. E. Brantis for the assistance in laboratory work and library preparation.

REFERENCES

- Askew, K., Li, K., Olmos-Alonso, A., Garcia-Moreno, F., Liang, Y., Richardson, P., Tipton, T., Chapman, M.A., Riecken, K., Beccari, S., et al. (2017). Coupled Proliferation and Apoptosis Maintain the Rapid Turnover of Microglia in the Adult Brain. *Cell Rep.* *18*, 391–405.
- Bayés, A., Collins, M.O., Croning, M.D.R., van de Lagemaat, L.N., Choudhary, J.S., and Grant, S.G.N. (2012). Comparative study of human and mouse postsynaptic proteomes finds high compositional conservation and abundance differences for key synaptic proteins. *PLoS One* *7*, e46683.
- Bernhagen, J., Krohn, R., Lue, H., Gregory, J.L., Zernecke, A., Koenen, R.R., Dewor, M., Georgiev, I., Schober, A., Leng, L., et al. (2007). MIF is a noncognate ligand of CXC chemokine receptors in inflammatory and atherogenic cell recruitment. *Nat. Med.* *13*, 587–596.
- Bozek, K., Wei, Y., Yan, Z., Liu, X., Xiong, J., Sugimoto, M., Tomita, M., Pääbo, S., Sherwood, C.C., Hof, P.R., et al. (2015). Organization and Evolution of Brain Lipidome Revealed by Large-Scale Analysis of Human, Chimpanzee, Macaque, and Mouse Tissues. *Neuron* *85*, 695–702.
- Burns, T.C., Li, M.D., Mehta, S., Awad, A.J., and Morgan, A.A. (2015). Mouse models rarely mimic the transcriptome of human neurodegenerative diseases: A systematic bioinformatics-based critique of preclinical models. *Eur. J. Pharmacol.* *759*, 101–117.
- Butovsky, O., Jedrychowski, M.P., Moore, C.S., Cialic, R., Lanser, A.J., Gabriely, G., Koeglsperger, T., Dake, B., Wu, P.M., Doykan, C.E., et al. (2014). Identification of a unique TGF- β -dependent molecular and functional signature in microglia. *Nat. Neurosci.* *17*, 131–143.
- Buttgereit, A., Lelios, I., Yu, X., Vrohligs, M., Krakoski, N.R., Gautier, E.L., Nishinakamura, R., Becher, B., and Greter, M. (2016). *Sall1* is a transcriptional regulator defining microglia identity and function. *Nat. Immunol.* *17*, 1397–1406.
- Chen, H., Li, L., Weimershaus, M., Evnouchidou, I., van Endert, P., and Bouvier, M. (2016). ERAP1-ERAP2 dimers trim MHC I-bound precursor peptides; implications for understanding peptide editing. *Sci. Rep.* *6*, 28902.
- Chen, Y., Won, S.J., Xu, Y., and Swanson, R.A. (2014). Targeting microglial activation in stroke therapy: pharmacological tools and gender effects. *Curr. Med. Chem.* *21*, 2146–2155.

Chevryeva, I., Faull, R.L.M., Green, C.R., and Nicholson, L.F.B. (2008). Assessing RNA quality in postmortem human brain tissue. *Exp. Mol. Pathol.* *84*, 71–77.

Chiu, I.M., Morimoto, E.T.A., Goodarzi, H., Liao, J.T., O’Keeffe, S., Phatnani, H.P., Muratet, M., Carroll, M.C., Levy, S., Tavazoie, S., et al. (2013). A neurodegeneration-specific gene-expression signature of acutely isolated microglia from an amyotrophic lateral sclerosis mouse model. *Cell Rep.* *4*, 385–401.

Cribbs, D.H., Berchtold, N.C., Perreau, V., Coleman, P.D., Rogers, J., Tenner, A.J., and Cotman, C.W. (2012). Extensive innate immune gene activation accompanies brain aging, increasing vulnerability to cognitive decline and neurodegeneration: a microarray study. *J. Neuroinflammation* *9*, 179.

DeLuca, D.S., Levin, J.Z., Sivachenko, A., Fennell, T., Nazaire, M.-D., Williams, C., Reich, M., Winckler, W., and Getz, G. (2012). RNA-SeqQC: RNA-seq metrics for quality control and process optimization. *Bioinforma. Oxf. Engl.* *28*, 1530–1532.

Dendrou, C.A., Fugger, L., and Friese, M.A. (2015). Immunopathology of multiple sclerosis. *Nat. Rev. Immunol.* *15*, 545–558.

Dey, S., Curtis, D.J., Jane, S.M., and Brandt, S.J. (2010). The TAL1/SCL transcription factor regulates cell cycle progression and proliferation in differentiating murine bone marrow monocyte precursors. *Mol. Cell. Biol.* *30*, 2181–2192.

Dobin, A., Davis, C.A., Schlesinger, F., Drenkow, J., Zaleski, C., Jha, S., Batut, P., Chaisson, M., and Gingeras, T.R. (2013). STAR: ultrafast universal RNA-seq aligner. *Bioinforma. Oxf. Engl.* *29*, 15–21.

Durinck, S., Spellman, P.T., Birney, E., and Huber, W. (2009). Mapping identifiers for the integration of genomic datasets with the R/Bioconductor package biomaRt. *Nat. Protoc.* *4*, 1184–1191.

Durrenberger, P.F., Fernando, S., Kashefi, S.N., Ferrer, I., Hauw, J.-J., Seilhean, D., Smith, C., Walker, R., Al-Sarraj, S., Troakes, C., et al. (2010). Effects of antemortem and postmortem variables on human brain mRNA quality: a BrainNet Europe study. *J. Neuropathol. Exp. Neurol.* *69*, 70–81.

van Eekelen, J. a. M., Bradley, C.K., Göthert, J.R., Robb, L., Elefanty, A.G., Begley, C.G., and Harvey, A.R. (2003). Expression pattern of the stem cell leukaemia gene in the CNS of the embryonic and adult mouse. *Neuroscience* *122*, 421–436.

Ervin, J.F., Heinzen, E.L., Cronin, K.D., Goldstein, D., Szymanski, M.H., Burke, J.R., Welsh-Bohmer, K.A., and Hulette, C.M. (2007). Postmortem delay has minimal effect on brain RNA integrity. *J. Neuropathol. Exp. Neurol.* *66*, 1093–1099.

Falcon, S., and Gentleman, R. (2007). Using GOSTATS to test gene lists for GO term association. *Bioinforma. Oxf. Engl.* *23*, 257–258.

Ferrari, D., McNamee, E.N., Idzko, M., Gambari, R., and Eltzschig, H.K. (2016). Purinergic Signaling During Immune Cell Trafficking. *Trends Immunol.* *37*, 399–411.

Galatro, T.F., Vainchtein, I.D., Brouwer, N., Boddeke, E.W.G.M., and Eggen, B.J.L. (2017). Isolation of Microglia and Immune Infiltrates from Mouse and Primate Central Nervous System. *Methods Mol. Biol. Clifton NJ* *1559*, 333–342.

Gautier, L., Cope, L., Bolstad, B.M., and Irizarry, R.A. (2004). affy--analysis of Affymetrix GeneChip data at the probe level. *Bioinforma. Oxf. Engl.* *20*, 307–315.

George, N.I., and Chang, C.-W. (2014). DAFS: a data-adaptive flag method for RNA-sequencing data to differentiate genes with low and high expression. *BMC Bioinformatics* *15*, 92.

Gosselin, D., Link, V.M., Romanoski, C.E., Fonseca, G.J., Eichenfield, D.Z., Spann, N.J., Stender, J.D., Chun, H.B., Garner, H., Geissmann, F., et al. (2014). Environment Drives Selection and Function of Enhancers Controlling Tissue-Specific Macrophage Identities. *Cell* *159*, 1327–1340.

Grabert, K., Michoel, T., Karavolos, M.H., Clohisey, S., Baillie, J.K., Stevens, M.P., Freeman, T.C., Summers, K.M., and McColl, B.W. (2016). Microglial brain region-dependent diversity and selective regional sensitivities to aging. *Nat. Neurosci.* *19*, 504–516.

Griciuc, A., Serrano-Pozo, A., Parrado, A.R., Lesinski, A.N., Asselin, C.N., Mullin, K., Hooli, B., Choi, S.H., Hyman, B.T., and Tanzi, R.E. (2013). Alzheimer's Disease Risk Gene CD33 Inhibits Microglial Uptake of Amyloid Beta. *Neuron* *78*, 631–643.

Gürtler, C., and Bowie, A.G. (2013). Innate immune detection of microbial nucleic acids. *Trends Microbiol.* *21*, 413–420.

Hambardzumyan, D., Gutmann, D.H., and Kettenmann, H. (2015). The role of microglia and macrophages in glioma maintenance and progression. *Nat. Neurosci.* *19*, 20–27.

Hanisch, U.K., and Kettenmann, H. (2007). Microglia: active sensor and versatile effector cells in the normal and pathologic brain. *Nat. Neurosci.* *10*, 1387–1394.

Hawrylycz, M., Miller, J.A., Menon, V., Feng, D., Dolbeare, T., Guillozet-Bongaarts, A.L., Jegga, A.G., Aronow, B.J., Lee, C.-K., Bernard, A., et al. (2015). Canonical genetic signatures of the adult human brain. *Nat. Neurosci.* *18*, 1832–1844.

Hickman, S.E., Allison, E.K., and El Khoury, J. (2008). Microglial dysfunction and defective beta-amyloid clearance pathways in aging Alzheimer's disease mice. *J. Neurosci. Off. J. Soc. Neurosci.* *28*, 8354–8360.

Hickman, S.E., Kingery, N.D., Ohsumi, T.K., Borowsky, M.L., Wang, L., Means, T.K., and El Khoury, J. (2013). The microglial sensome revealed by direct RNA sequencing. *Nat. Neurosci.* *16*, 1896–1905.

Hoeffel, G., Chen, J., Lavin, Y., Low, D., Almeida, F.F., See, P., Beaudin, A.E., Lum, J., Low, I., Forsberg, E.C., et al. (2015). C-Myb(+) erythro-myeloid progenitor-derived fetal monocytes give rise to adult tissue-resident macrophages. *Immunity* *42*, 665–678.

Holtman, I.R., Raj, D.D., Miller, J.A., Schaafsma, W., Yin, Z., Brouwer, N., Wes, P.D., Möller, T., Orre, M., Kamphuis, W., et al. (2015). Induction of a common microglia gene expression signature by aging and neurodegenerative conditions: a co-expression meta-analysis. *Acta Neuropathol. Commun.* *3*, 31.

Huang, G., Zhang, P., Hirai, H., Elf, S., Yan, X., Chen, Z., Koschmieder, S., Okuno, Y., Dayaram, T., Gowney, J.D., et al. (2008). PU.1 is a major downstream target of AML1 (RUNX1) in adult mouse hematopoiesis. *Nat. Genet.* *40*, 51–60.

Kierdorf, K., Erny, D., Goldmann, T., Sander, V., Schulz, C., Perdiguero, E.G., Wieghofer, P., Heinrich, A., Riemke, P., Hölscher, C., et al. (2013a). Microglia emerge from erythromyeloid precursors via Pu.1- and Irf8-dependent pathways. *Nat. Neurosci.* *16*, 273–280.

Kierdorf, K., Erny, D., Goldmann, T., Sander, V., Schulz, C., Perdiguero, E.G., Wieghofer, P., Heinrich, A., Riemke, P., Hölscher, C., et al. (2013b). Microglia emerge from erythromyeloid precursors via Pu.1- and Irf8-dependent pathways. *Nat. Neurosci.* *16*, 273–280.

Kobayashi, K.S., and van den Elsen, P.J. (2012). NLR5: a key regulator of MHC class I-dependent immune responses. *Nat. Rev. Immunol.* *12*, 813–820.

Kondo, T., Kawai, T., and Akira, S. (2012). Dissecting negative regulation of Toll-like receptor signaling. *Trends Immunol.* *33*, 449–458.

Konopka, G., Friedrich, T., Davis-Turak, J., Winden, K., Oldham, M.C., Gao, F., Chen, L., Wang, G.-Z., Luo, R., Preuss, T.M., et al. (2012). Human-specific transcriptional networks in the brain. *Neuron* *75*, 601–617.

Krabbe, G., Halle, A., Matyash, V., Rinnenthal, J.L., Eom, G.D., Bernhardt, U., Miller, K.R., Prokop, S., Kettenmann, H., and Heppner, F.L. (2013). Functional impairment of microglia coincides with Beta-amyloid deposition in mice with Alzheimer-like pathology. *PloS One* *8*, e60921.

Krensky, A.M., and Clayberger, C. (2005). Granulysin: a novel host defense molecule. *Am. J. Transplant. Off. J. Am. Soc. Transplant. Am. Soc. Transpl. Surg.* 5, 1789–1792.

Lavin, Y., Winter, D., Blecher-Gonen, R., David, E., Keren-Shaul, H., Merad, M., Jung, S., and Amit, I. (2014). Tissue-Resident Macrophage Enhancer Landscapes Are Shaped by the Local Microenvironment. *Cell* 159, 1312–1326.

Leek, J.T., Johnson, W.E., Parker, H.S., Jaffe, A.E., and Storey, J.D. (2012). The sva package for removing batch effects and other unwanted variation in high-throughput experiments. *Bioinforma. Oxf. Engl.* 28, 882–883.

Leitner, J., Herndler-Brandstetter, D., Zlabinger, G.J., Grubeck-Loebenstien, B., and Steinberger, P. (2015). CD58/CD2 Is the Primary Costimulatory Pathway in Human CD28-CD8+ T Cells. *J. Immunol. Baltim. Md 1950* 195, 477–487.

Lenz, K.M., and McCarthy, M.M. (2015). A starring role for microglia in brain sex differences. *Neurosci. Rev. J. Bringing Neurobiol. Neurol. Psychiatry* 21, 306–321.

Lenz, K.M., Nugent, B.M., Haliyur, R., and McCarthy, M.M. (2013). Microglia are essential to masculinization of brain and behavior. *J. Neurosci. Off. J. Soc. Neurosci.* 33, 2761–2772.

Liao, J.C.C., Lam, R., Brazda, V., Duan, S., Ravichandran, M., Ma, J., Xiao, T., Tempel, W., Zuo, X., Wang, Y.-X., et al. (2011). Interferon-Inducible Protein 16: Insight into the Interaction with Tumor Suppressor p53. *Structure* 19, 418–429.

Liao, Y., Smyth, G.K., and Shi, W. (2014). featureCounts: an efficient general purpose program for assigning sequence reads to genomic features. *Bioinforma. Oxf. Engl.* 30, 923–930.

Loerch, P.M., Lu, T., Dakin, K.A., Vann, J.M., Isaacs, A., Geula, C., Wang, J., Pan, Y., Gabuzda, D.H., Li, C., et al. (2008). Evolution of the aging brain transcriptome and synaptic regulation. *PLoS One* 3, e3329.

Luan, Y., Lengyel, P., and Liu, C.-J. (2008). p204, a p200 family protein, as a multifunctional regulator of cell proliferation and differentiation. *Cytokine Growth Factor Rev.* 19, 357–369.

Lue, H., Thiele, M., Franz, J., Dahl, E., Speckgens, S., Leng, L., Fingerle-Rowson, G., Bucala, R., Lüscher, B., and Bernhagen, J. (2007). Macrophage migration inhibitory factor (MIF) promotes cell survival by activation of the Akt pathway and role for CSN5/JAB1 in the control of autocrine MIF activity. *Oncogene* 26, 5046–5059.

Ma, W., Cojocaru, R., Gotoh, N., Gieser, L., Villasmil, R., Cogliati, T., Swaroop, A., and Wong, W.T. (2013). Gene expression changes in aging retinal microglia:

relationship to microglial support functions and regulation of activation. *Neurobiol. Aging* 34, 2310–2321.

Macauley, M.S., Crocker, P.R., and Paulson, J.C. (2014). Siglec-mediated regulation of immune cell function in disease. *Nat. Rev. Immunol.* 14, 653–666.

Matcovitch-Natan, O., Winter, D.R., Giladi, A., Vargas Aguilar, S., Spinrad, A., Sarrazin, S., Ben-Yehuda, H., David, E., Zelada González, F., Perrin, P., et al. (2016). Microglia development follows a stepwise program to regulate brain homeostasis. *Science* 353, aad8670.

Meissner, T.B., Li, A., Biswas, A., Lee, K.-H., Liu, Y.-J., Bayir, E., Iliopoulos, D., van den Elsen, P.J., and Kobayashi, K.S. (2010). NLR family member NLRC5 is a transcriptional regulator of MHC class I genes. *Proc. Natl. Acad. Sci. U. S. A.* 107, 13794–13799.

Miller, J.A., Horvath, S., and Geschwind, D.H. (2010). Divergence of human and mouse brain transcriptome highlights Alzheimer disease pathways. *Proc. Natl. Acad. Sci. U. S. A.* 107, 12698–12703.

Mitchell, R.A., Liao, H., Chesney, J., Fingerle-Rowson, G., Baugh, J., David, J., and Bucala, R. (2002). Macrophage migration inhibitory factor (MIF) sustains macrophage proinflammatory function by inhibiting p53: regulatory role in the innate immune response. *Proc. Natl. Acad. Sci. U. S. A.* 99, 345–350.

Mizutani, M., Pino, P.A., Saederup, N., Charo, I.F., Ransohoff, R.M., and Cardona, A.E. (2012). The fractalkine receptor but not CCR2 is present on microglia from embryonic development throughout adulthood. *J. Immunol. Baltim. Md 1950* 188, 29–36.

Muffat, J., Li, Y., Yuan, B., Mitalipova, M., Omer, A., Corcoran, S., Bakiasi, G., Tsai, L.-H., Aubourg, P., Ransohoff, R.M., et al. (2016). Efficient derivation of microglia-like cells from human pluripotent stem cells. *Nat. Med.* 22, 1358–1367.

Nicolle, R., Radvanyi, F., and Elati, M. (2015). CoRegNet: reconstruction and integrated analysis of co-regulatory networks. *Bioinforma. Oxf. Engl.* 31, 3066–3068.

Orre, M., Kamphuis, W., Osborn, L.M., Melief, J., Kooijman, L., Huitinga, I., Klooster, J., Bossers, K., and Hol, E.M. (2014b). Acute isolation and transcriptome characterization of cortical astrocytes and microglia from young and aged mice. *Neurobiol. Aging* 35, 1–14.

Orre, M., Kamphuis, W., Osborn, L.M., Jansen, A.H.P., Kooijman, L., Bossers, K., and Hol, E.M. (2014a). Isolation of glia from Alzheimer's mice reveals inflammation and dysfunction. *Neurobiol. Aging*.

Perry, V.H., and Holmes, C. (2014). Microglial priming in neurodegenerative disease. *Nat. Rev. Neurol.* *10*, 217–224.

Raj, D.D.A., Moser, J., van der Pol, S.M.A., van Os, R.P., Holtman, I.R., Brouwer, N., Oeseburg, H., Schaafsma, W., Wesseling, E.M., den Dunnen, W., et al. (2015). Enhanced microglial pro-inflammatory response to lipopolysaccharide correlates with brain infiltration and blood-brain barrier dysregulation in a mouse model of telomere shortening. *Aging Cell*.

Realegeno, S., Kelly-Scumpia, K.M., Dang, A.T., Lu, J., Teles, R., Liu, P.T., Schenk, M., Lee, E.Y., Schmidt, N.W., Wong, G.C.L., et al. (2016). S100A12 Is Part of the Antimicrobial Network against *Mycobacterium leprae* in Human Macrophages. *PLoS Pathog.* *12*, e1005705.

Ritchie, M.E., Phipson, B., Wu, D., Hu, Y., Law, C.W., Shi, W., and Smyth, G.K. (2015). limma powers differential expression analyses for RNA-sequencing and microarray studies. *Nucleic Acids Res.* *43*, e47.

Ryan, E.J., Marshall, A.J., Magaletti, D., Floyd, H., Draves, K.E., Olson, N.E., and Clark, E.A. (2002). Dendritic cell-associated lectin-1: a novel dendritic cell-associated, C-type lectin-like molecule enhances T cell secretion of IL-4. *J. Immunol. Baltim. Md 1950* *169*, 5638–5648.

Saeed, S., Quintin, J., Kerstens, H.H.D., Rao, N.A., Aghajani-refah, A., Matarese, F., Cheng, S.-C., Ratter, J., Berentsen, K., van der Ent, M.A., et al. (2014). Epigenetic programming of monocyte-to-macrophage differentiation and trained innate immunity. *Science* *345*, 1251086–1251086.

Salter, M.W., and Beggs, S. (2014). Sublime Microglia: Expanding Roles for the Guardians of the CNS. *Cell* *158*, 15–24.

Schulz, C., Gomez Perdiguero, E., Chorro, L., Szabo-Rogers, H., Cagnard, N., Kierdorf, K., Prinz, M., Wu, B., Jacobsen, S.E.W., Pollard, J.W., et al. (2012). A lineage of myeloid cells independent of Myb and hematopoietic stem cells. *Science* *336*, 86–90.

Shimokawa, T., and Ra, C. (2005). C/EBPalpha functionally and physically interacts with GABP to activate the human myeloid IgA Fc receptor (Fc alphaR, CD89) gene promoter. *Blood* *106*, 2534–2542.

Siddiqui, T.A., Lively, S., Vincent, C., and Schlichter, L.C. (2012). Regulation of podosome formation, microglial migration and invasion by Ca²⁺-signaling molecules expressed in podosomes. *J. Neuroinflammation* *9*, 250.

Sinclair, A.M., Göttgens, B., Barton, L.M., Stanley, M.L., Pardanaud, L., Klaine, M., Gering, M., Bahn, S., Sanchez, M., Bench, A.J., et al. (1999). Distinct 5' SCL enhancers

direct transcription to developing brain, spinal cord, and endothelium: neural expression is mediated by GATA factor binding sites. *Dev. Biol.* 209, 128–142.

Smith, A.M., and Dragunow, M. (2014). The human side of microglia. *Trends Neurosci.* 37, 125–135.

Stenglein, M.D., Burns, M.B., Li, M., Lengyel, J., and Harris, R.S. (2010). APOBEC3 proteins mediate the clearance of foreign DNA from human cells. *Nat. Struct. Mol. Biol.* 17, 222–229.

Stockinger, B., Pessara, U., Lin, R.H., Habicht, J., Grez, M., and Koch, N. (1989). A role of Ia-associated invariant chains in antigen processing and presentation. *Cell* 56, 683–689.

Vincent, C., Siddiqui, T.A., and Schlichter, L.C. (2012). Podosomes in migrating microglia: components and matrix degradation. *J. Neuroinflammation* 9, 190.

Wehrspaun, C.C., Haerty, W., and Ponting, C.P. (2015). Microglia recapitulate a hematopoietic master regulator network in the aging human frontal cortex. *Neurobiol. Aging* 36, 2443.e9-2443.e20.

Wilson, N.K., Miranda-Saavedra, D., Kinston, S., Bonadies, N., Foster, S.D., Calero-Nieto, F., Dawson, M.A., Donaldson, I.J., Dumon, S., Frampton, J., et al. (2009). The transcriptional program controlled by the stem cell leukemia gene *Scl/Tal1* during early embryonic hematopoietic development. *Blood* 113, 5456–5465.

Wilson, N.K., Foster, S.D., Wang, X., Knezevic, K., Schütte, J., Kaimakis, P., Chilarska, P.M., Kinston, S., Ouwehand, W.H., Dzierzak, E., et al. (2010). Combinatorial Transcriptional Control In Blood Stem/Progenitor Cells: Genome-wide Analysis of Ten Major Transcriptional Regulators. *Cell Stem Cell* 7, 532–544.

Zhang, Y., Chen, K., Sloan, S.A., Bennett, M.L., Scholze, A.R., O’Keeffe, S., Phatnani, H.P., Guarnieri, P., Caneda, C., Ruderisch, N., et al. (2014). An RNA-Sequencing Transcriptome and Splicing Database of Glia, Neurons, and Vascular Cells of the Cerebral Cortex. *J. Neurosci. Off. J. Soc. Neurosci.* 34, 11929–11947.

Zhang, Y., Sloan, S.A., Clarke, L.E., Caneda, C., Plaza, C.A., Blumenthal, P.D., Vogel, H., Steinberg, G.K., Edwards, M.S.B., Li, G., et al. (2016). Purification and Characterization of Progenitor and Mature Human Astrocytes Reveals Transcriptional and Functional Differences with Mouse. *Neuron* 89, 37–53.

Babraham Bioinformatics - FastQC A Quality Control tool for High Throughput Sequence Data.

CHAPTER 7

Microglia molecular signature in diffuse gliomas

Thais F. Galatro^{1,2*}, Antonio M Lerario^{3,4,7*}, Paula Sola¹, Ester RM Bertoldi⁵, Vanessa G Freitas¹, Isabele F Moretti¹, Tulio Pereira⁶, Bart J. Eggen², Suely K.N. Marie^{1,6}

¹Department of Neurology, Laboratory of Molecular and Cellular Biology, LIM15, School of Medicine, University of São Paulo, São Paulo, Brazil

²Department of Neuroscience, section Medical Physiology, University of Groningen, University Medical Center Groningen, Groningen, 9713 AV, The Netherlands.

³Departments of Cell & Developmental Biology, Pathology, Molecular & Integrative Physiology, Internal Medicine, University of Michigan, Ann Arbor, MI 48109, USA

⁴University of Michigan Comprehensive Cancer Center, University of Michigan, Ann Arbor, MI 48109, USA

⁵Bioinformatics Postgraduate Interunit Program, University of São Paulo, Brazil

⁶Center for Studies of Cellular and Molecular Therapy (NETCEM) University of Sao Paulo, São Paulo, Brazil

⁷Bioinformatics coordinator of SELA (NGS facility core), School of Medicine, University of São Paulo.

*shared first authors

Manuscript in preparation

SUMMARY

Diffuse gliomas are primary brain tumors characterized by infiltrative growth and high heterogeneity, rendering the disease mostly incurable. Advances in genetic analysis have characterized molecular alterations affecting patients' overall survival and clinical outcome, particularly in glioblastoma (GBM). However, glioma tumorigenicity is not exclusively controlled by its genetic alterations. The crosstalk between tumor cells and the surrounding microenvironment plays a pivotal role in modulating glioma growth and aggressiveness. Resident microglia, with central nervous system (CNS)-tailored functions, and infiltrating tumor-associated monocytes/macrophages (iTAMs) from the bone marrow, comprise the most abundant non-neoplastic cells in this microenvironment. Recently, we have identified the human microglia molecular signature in homeostatic conditions. Here, we propose to determine the global changes microglia underwent during glioma progression, correlating them to the oncogenic molecular alterations in the tumor, particularly GBM. Fresh microglia were isolated from human lower grade gliomas (astrocytoma and oligodendroglioma, LGG) and GBMs and RNA sequenced. Our data suggests not only an immune-suppressive profile for tumor microglia, but also alterations largely related to a highly proliferative and mobile phenotype for microglia, that increases with disease progression. In agreement with this, we observed overexpression of genes coding for extracellular matrix proteins, which were shown to correlate to the mesenchymal GBM subtype. Further exploring the characteristics and dynamics of microglia within different grades and subtypes of glioma is crucial for a better understanding of the role of the microenvironment in disease etiology.

INTRODUCTION

Gliomas are a heterogeneous group of primary neuroectodermal tumors, originating from glial cells – such as astrocytes and oligodendrocytes, or their progenitors. The current classification of the World Health Organization (WHO) associates clinical and histological information with mutational data, classifying diffuse astrocytomas, oligodendrogliomas and glioblastomas (Louis et al., 2016; Parsons et al., 2008). Glioblastomas are extremely aggressive, highly malignant, and the most frequent of gliomas. Their main features include high mitotic and vascular proliferation rates, necrosis and resistance to both chemotherapy and radiotherapy treatments (Cloughesy et al., 2014). Advances in integrated large scale strategies, as exome and transcriptome approaches, allowed the identification of genetic alterations singular to GBM's genesis and progression (Brennan et al., 2013a; Phillips et al., 2006; Stieber et al., 2014; Verhaak et al., 2010). These genetic studies have identified four molecular subtypes of GBM: proneural, classical, neural and mesenchymal; this last subtype has the worst prognosis.

Glioma tumorigenicity is not exclusively the result of its genetic alterations. The crosstalk between tumor cells and their surrounding microenvironment plays a crucial role in modulating glioma growth and aggressiveness. This microenvironment includes cancer stem cells, endothelial cells, pericytes and normal CNS cells, such as glial cells, neurons and microglia (Charles et al., 2011). The most abundant, non-neoplastic cells in this microenvironment belong to the myeloid lineage, comprising of resident microglia, and infiltrating tumor-associated monocytes/macrophages (further called iTAMs) originating in the bone marrow (Hambardzumyan et al., 2015). There are conflicting studies regarding the role of such cells in tumor progression. While some claim better outcomes for patients with high levels of immune cells, either infiltrates or CNS resident cells, many others have assessed the same phenomena and related it to poorer prognosis (reviewed by Fridman *et al* (Fridman et al., 2012)). Such divergence in results seems to originate from the different functional and activation states innate immune cells can adopt within a tumor and at different time points. Historically, microglia and iTAM activation has been classified as classic (M1) and alternative (M2) (Galdiero et al., 2013; Hao et al., 2012; Mantovani et al., 2002). However, considering their ability to respond readily to stimuli, changes the microenvironment can lead both to anti or pro-tumoral responses.

In this study, we aim to characterize the gene expression profile of microglia isolated from human gliomas (glioblastoma and lower grade gliomas) and to compare it to a normal microglia set from *post-mortem* cortical tissue. We observed that changes in microglial cells exceed the M1/M2 polarization, and display gene expression alterations in signaling pathways of proliferation, migration and invasiveness. We also analyzed the expression of the selected targets in the tumor-microglia transcriptome in a RNA-Seq database of TCGA cohort of GBM cases with molecular stratification, and demonstrated that these overexpressed tumor-microglia targets associated to the most invasive mesenchymal subtype with the worst prognosis. Taken together, our data provides a set of targets involved in the crosstalk between the tumor cell and microenvironment cell that might determine tumor aggressiveness, and potential drugable targets.

METHODOLOGY

Human Brain Tissue and Ethical Statement

Six glioma samples were obtained during therapeutic surgery of patients treated by the Neurosurgery Group of the Department of Neurology at Hospital das Clínicas at the School of Medicine of the University of São Paulo, in the period of 2000 to 2015. Diagnosis were confirmed by neuropathologists from the Division of Pathological Anatomy of the same institution, according to the WHO grading system. Patient information and clinical findings are presented in Supplemental Table 1. Samples were macrodissected and immediately snap-frozen in liquid nitrogen upon surgical removal. A 4µm-thick cryosection of each sample was analyzed under a light microscope after hematoxylin-eosin staining for assessment of necrotic, cellular debris and non-neoplastic areas, followed by removal from the frozen block by macrodissection prior to RNA extractions. Written informed consent was obtained from all patients according to the ethical guidelines approved by the Department of Neurology, School of Medicine, University of São Paulo (0599/10).

Human brain tissue was collected from the right parietal cortex during the course of full body autopsy. This cohort is part of our previous study *The human microglia transcriptome and age-associated changes in actin dynamics and cell function* (Galatro et al, *submitted*. Refer to **Chapter 6**).

Microglia isolation from glioma surgical resected tissue and post mortem parietal cortex

Pure human microglia population was isolated from glioma surgical resection (n=6, of which: 3 GBMs, 1 AGII, 1 AGIII and 1 ODII; herein called lower-grades gliomas, LGG), according to our recently published protocol (Galatro et al., 2017). Briefly, samples were collected either during the course of brain surgery or full body autopsy (right parietal cortex) and collected in ice-cold HBBS (Lonza, Switzerland) supplemented with 15 mM HEPES (Lonza) and 0.6% glucose (Sigma-Aldrich, USA). The brain tissue was dissociated in a glass tissue homogenizer and filtered using a 300 µm sieve, followed by a 106 µm sieve to obtain a single cell suspension. Cells were pelleted by centrifugation at 220 rcf for 10 min. (acc: 9, brake: 9, 4°C). The pellet was resuspended in 22% Percoll (GE Healthcare, UK), 40 mM NaCl and 77% myelin gradient

buffer (5.6 mM NaH₂PO₄·H₂O, 20 mM Na₂HPO₄·2H₂O, 140 mM NaCl, 5.4 mM KCl, 11 mM Glucose, pH 7.4). A layer of PBS was added on top, and this gradient was centrifuged at 950 rcf for 20 min. (acc: 4, brake: 0, 4°C). The myelin layer and the remaining supernatant were carefully removed and the pellet resuspended in a solution of 60% Percoll, which was overlaid with 30% Percoll and PBS respectively, and centrifuged at 800 rcf for 25 min (acc: 4, brake: 0, 4°C). The cell layer at the 60-30% Percoll interface was collected with a pre-wetted Pasteur pipette, washed and centrifuged at 600 rcf for 10 min (acc:9, brake: 9, 4°C). The final pellet was resuspended in HBBS without phenol red (Lonza) supplemented with 15 mM HEPES (Lonza) and 0.6% glucose (Sigma-Aldrich). Fc receptors were blocked with human Fc receptor binding inhibitor (eBioscience, Affymetrix, USA) for 10 min on ice. For sorting, cells were incubated for 20 min on ice with anti-human CD11b-PE (Biolegend, USA) and anti-human CD45-FITC (Biolegend) and subsequently washed with HBBS without phenol red. The cells were passed through a 35-µm nylon mesh and collected in round bottom tubes (Corning, USA) and sorted using a BD Biosciences FACS Aria II cell sorter. Cells were sorted based on CD11b^{high}/CD45^{int} expression and negative staining for DAPI and collected in RNeasy Lysis Buffer (Qiagen). Cells with the profile of myeloid infiltrates were collected separately. Sorted cells were centrifuged 5,000 rcf for 10 min and pellets were lysed in RLT-Plus buffer (Qiagen) for RNA extraction.

RNA extraction and RNA sequencing (RNA-seq)

Total RNA was extracted from flow cytometry-sorted cells using an RNeasy and AllPrep Micro Kit (Qiagen, Germany), according to the manufacturer's protocol. RNA quality was checked with RNA Screen Tape (Agilent technologies, USA). RNA-Seq were performed at the next generation sequencing facility core (SELA - Sequenciamento em Larga Escala) at the University of São Paulo. SMARTer Stranded Total RNA-Seq Kit - Pico Input (Takara Bio, JP) cDNA libraries were prepared starting from 500 pg of total RNA. RNAs were fragmented by heat in the presence of divalent cations. The transcript for the first strand cDNA was prepared with reverse transcriptase and random primers. The second strand cDNA was synthesized by reverse transcriptase. Adaptors and index of unique sequence were added to cDNA fragments by PCR. rRNA fragments were captured and degraded with RiboGone probes and enzyme and the remaining library fragments were enriched by PCR. Final libraries

were quantified by qPCR (Kappa Library Quantification Kit, Illumina, Kappa Biosystems, USA), and the median size of the libraries determined by TapeStation 2200 (Agilent Technologies, USA), using the High Sensitivity D1000 ScreenTape assay. Sequencing was performed as a 2x126 paired-end, dual index run, on a HiSeq 2500 (Illumina, USA) with V4 reagents.

RNA-Seq data analysis

RNA-Seq data analysis of six tumor microglia samples was done using the hereinafter described pipeline, developed in the SELA facility. Metrics for FASTQ files were done using the FastQC program. All samples presented sufficient quality, with >95% of reads presenting quality above Q30. Despite sufficient quality with .FASTQ files, we decided to remove possible traces of adapter sequences. We also removed low quality bases from extremities and excessive short reads. These procedures were executed using the software `bbduk` (BBMap - Bushnell B. - www.ourcourceforge.net/projects/bbmap/). FASTQ files post-processing were aligned to hg38 version of human genome, acquired from the website www.ensembl.org. Reads were aligned to the reference-genome using the STAR aligner (Dobin et al., 2013) software. The resulting .BAM files (reads aligned to genomic coordinates) were submitted to metric analysis through RNA-SEQC software (DeLuca et al., 2012).

All the following steps were done using R program, with the exception of the generation of the raw counts spreadsheet. The .BAM files, aligned to the genomic coordinates, were quantified by the RSEM software (Li and Dewey, 2011). Quantification was done considering gene's full extension. Genes that were not expressed in at least 20% of samples were removed from the matrix. After this step, 22070 genes were considered as expressed.

Data normalization was done using the `limma-voom` pipeline, obtained through the R-Bioconductor package (Ritchie et al., 2015). Annotation of each gene was done using the `biomaRt` (R-Bioconductor) software. Class comparison consisted of: tumor microglia *versus* autopsy microglia. The Benjamini-Hochberg procedure was used for false-positive controls. Using this pipeline, we identified 10462 differentially expressed genes.

For gene set enrichment and pathway analysis, we used the *ROAST* (Wu et al., 2010) tool from the *limma* package. Unsupervised analysis consisted of the Independent Component Analysis (ICA) and the co-regulatory network analysis

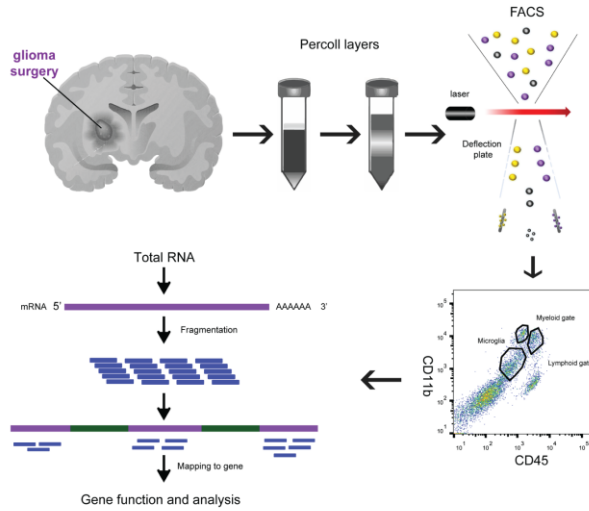
CoRegNet (Nicolle et al., 2015). ICA was used to determine the differentially expressed genes according to the molecular signature found in samples. CoRegNet analysis provided a set of genes representing the active transcriptional programs in our analyzed cohort.

RESULTS

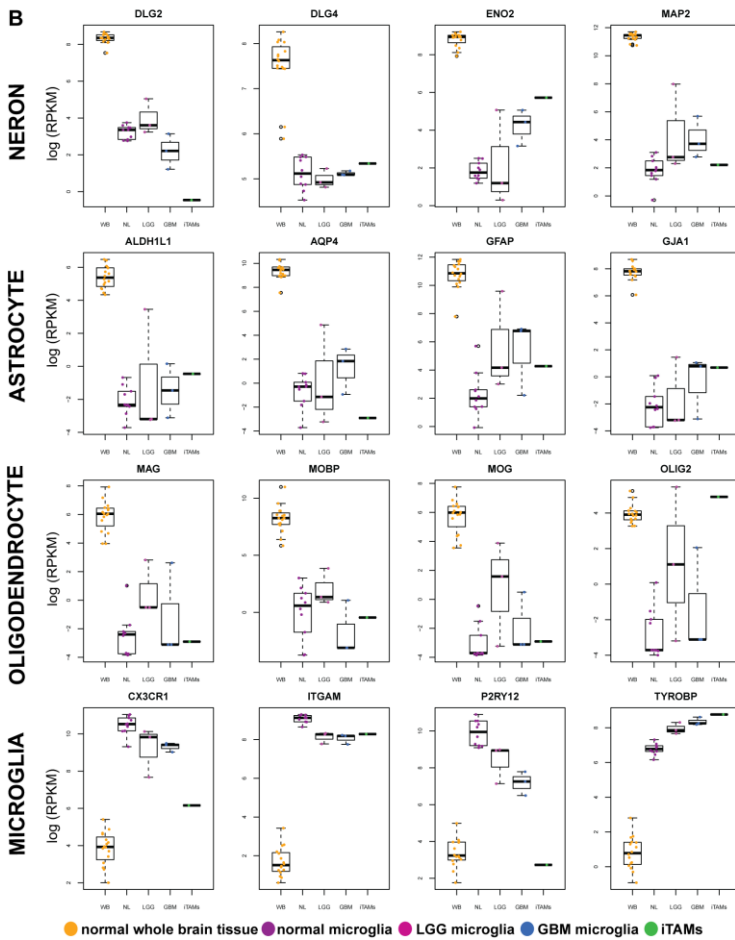
Isolation of pure microglia population from human glioma samples

Human glioma samples were collected during the course brain surgery, followed by tissue processing and acute isolation of viable microglia by FACS sorting. The sorting strategy followed was previously described (Galatro et al., 2017), with particular care to avoid contamination of the microglia population with other myeloid infiltrates. Figure 1A depicts the isolation workflow and in Figure 1B the expressions of known microglia genes *versus* genes specific for other CNS cells are depicted, in order to assess purity. For one GBM sample, it was possible to collect samples in the myeloid infiltrates gates (further referred to as iTAM). RNAs were extracted and their quality analyzed. In total, 6 samples of microglia were obtained from glioma surgery (3 GBMs and 3 LGG) and one of iTAMs. Paired-end Illumina high quality deep sequencing was performed and the generated data was analyzed conjointly with n=10 samples of microglia isolated from autopsy cortical brain tissue. These samples are part of our work, *The human microglia transcriptome and age-associated changes in actin dynamics and cell function* (Galatro et al, submitted. Refer to **Chapter 6**). RNA-Seq data was pre-processed, quantified and differentially expressed genes were determined.

Figure 1: Illustration of the course of glioma surgery, followed by RNA sequencing and expression analysis. Refer to the supplementary information for a detailed description of the difference between normal microglia and glioma-associated microglia.



glioma. A) during the glioma resection. B) RNA-sequencing of very low tumor burden samples. Comparison of normal microglia and glioma-associated microglia. Submitted. I will indicate the glioma-pure samples.



Genes differentially expressed between tumor and normal microglia

Gene expression analysis revealed major differences between tumor and normal cortical microglia. Principal component analysis (PCA) plots (Figure 2A) showed that iTAMs differed from both normal and tumor microglia samples; also, normal microglia segregated from tumor microglia. Tumor microglia samples did not segregate according to tumor subtype, possibly reflecting the intrinsic heterogeneity in those samples. The pathways associated with genes expressed in tumor (GBM and LGG) microglia were determined with GSEA enrichment analysis. GBM microglia gene expression profile (Figure 2B) was enriched for general processes, such as proliferation related pathways (“cell proliferation” and “cytoskeleton organization and biogenesis”); and motility related pathways (“extracellular matrix”, “cell migration” and “locomotory behavior”), but also for CNS specific pathways, like “synaptic transmission”, “brain development” and “CNS development”. The oncogenic-related pathways were represented by “angiogenesis”, “epithelial to mesenchymal transition”, “hypoxia” and “myc targets”. In LGG microglia, inflammatory-specific pathway “TNF signaling via NFkB”, “chromatin remodeling process” and transcription related “transcription factor binding” and “regulation of transcription DNA dependent” (Figure 2C) were significantly enriched. The most notable pathways when we compared the profile of GBM and LGG microglia were “response to hypoxia”, “extracellular matrix”, “basement membrane” and “positive regulation of response to stimulus” (Figure 2C). These results point to a possible involvement of microglia in glioma progression.

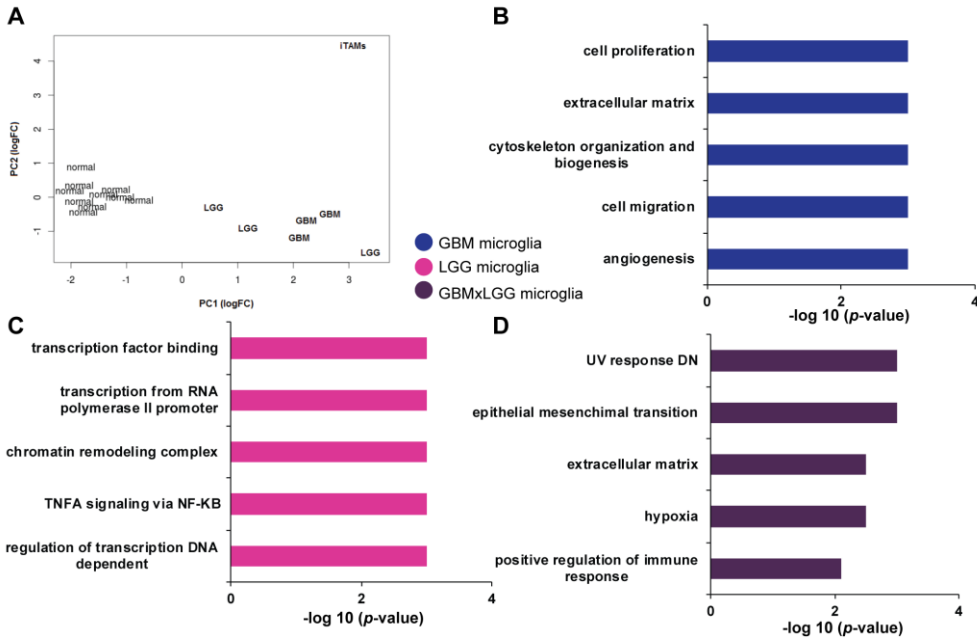


Figure 2: PCA analysis and biological pathways in glioma microglia. A) Principal component analysis of RNA-Seq showed that normal microglia were highly similar while tumor microglia segregated differentially and further. iTAMs were the most different sample. GO analysis for GBM (B), LGG (C) and the comparison between GBM versus LGG (D) microglia showed biological pathways related to proliferation, migration, and cell cycle control.

GBM and LGG microglia signature

We next established a representative gene set for both GBM and LGG microglia. The differentially expressed genes between both tumors types and normal microglia were filtered with the following criteria: $\log_{2}FC > 3$ (for upregulated genes), $\log_{2}FC < -3$ (for downregulated genes) and $p < 0.001$. With these stringent criteria, the GBM microglia signature consisted of 332 genes, while the LGG microglia signature consisted of 90 genes (Figure 3). 213 genes were upregulated in GBM microglia in comparison to LGG microglia. In our previous work, we determined a core signature for human microglia gene expression from cortical autopsy samples using stringent variables. We compared the overlap between the core signatures of normal, GBM and LGG microglia and, surprisingly, detected no overlap.

GBM μglia versus Normal μglia	UP 332 genes
	DOWN 84 genes
LGG μglia versus Normal μglia	UP 90 genes
	DOWN 24 genes
GBM μglia versus LGG μglia	UP 213 genes
	DOWN 36 genes

Figure 3: Core genes in glioma microglia. Differentially expressed genes from the comparison between both tumors types to normal microglia were filtered with the following criteria: $\log_{2}FC > 3$ (for upregulation), $\log_{2}FC < -3$ (for downregulation) and $p < 0.001$ for both cases. The GBM microglia signature contained 332 genes, the LGG microglia signature consisted of 90 genes

Most genes in the LGG microglia core were also present in GBM microglia signature, even at higher levels. We highlight *FCMR*, *IER2*, and the *AP-1* transcription factor complex members *FOS* and *JUND* as genes exclusive for the LGG microglia signature. GBM microglia core genes comprised inflammation-related gene families, such as chemokines (*CCL3*, *CCL4*, *CCL8*, *CXCL2*, *CXCL3*, *CXCL8*, *CXCL9*, *CCR7*), interleukins (*IL15*, *IL2RA*, *IL7R*), antigens (*CD72*, *CD109* and *CD209*), and anti-inflammatory markers (*CD163* and *ANXA1*). Receptors of growth factors, like *EGFR* and *PDGFRA*, developmental genes, like *NES* and *POU3F2/3*, extracellular matrix (ECM) genes - *FN1*, *TNC*, *THBS*, *BCAN*, and members of the *SRY* (sex determining region Y) family of genes - *SOX1*, *SOX2*, *SOX11*, *SOX21* were also present in GBM microglia core.

We were also able to collect one sample of iTAMs from a GBM case. Despite being statistically underpowered, iTAMs was more similar to GBM/LGG microglia than control microglia. However, major differences between iTAMs and GBM microglia signature were also identified as differentially expressed surface receptors like *ROBO1* and *PDGFRA* in GBM microglia, *MARCO* and *MET* in iTAMs.

We next aimed to evaluate the expressions of the human normal microglia core genes in tumor microglia. Figure 4 depicts the expressions 30 genes from the core of normal human microglia in the tumor microglia cohort. The majority of the analyzed

genes was differentially expressed between the LGG and GBM microglia demonstrating changes in the expression profile of the microglia in the tumor environment.

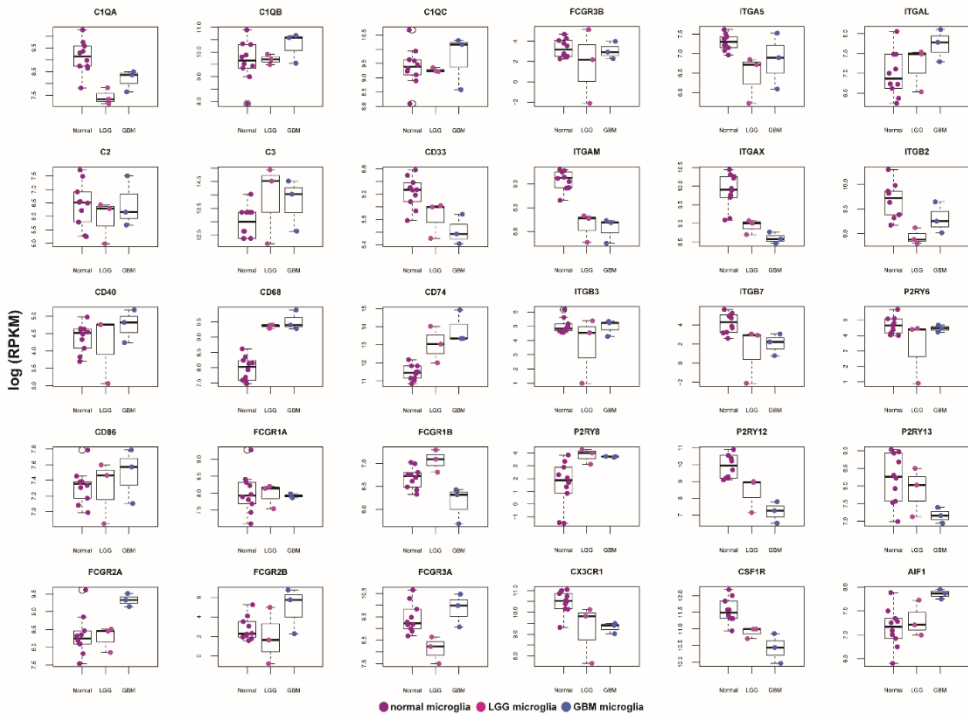


Figure 4: Expression of human normal microglia core genes in glioma microglia. Genes from the normal microglia core presented differentially expressed in tumor microglia, and also when compared LGG to GBM microglia, demonstrating significant changes of the normal microglia core gene expression profile in the tumor environment.

Independent Component Analysis and pathways in tumor microglia

In order to determine the set of genes presenting significant expression alterations between the two groups, normal and tumor microglia, studied, we applied Independent Component Analysis (ICA) to the RNA-Seq data distributed in 6 components. We then selected the best component that segregated normal from tumor microglia, and the LGG from GBM microglia. Components 1 showed the best separation between normal and tumor microglia, and component 6 for LGG and GBM microglia. (Figure 5).

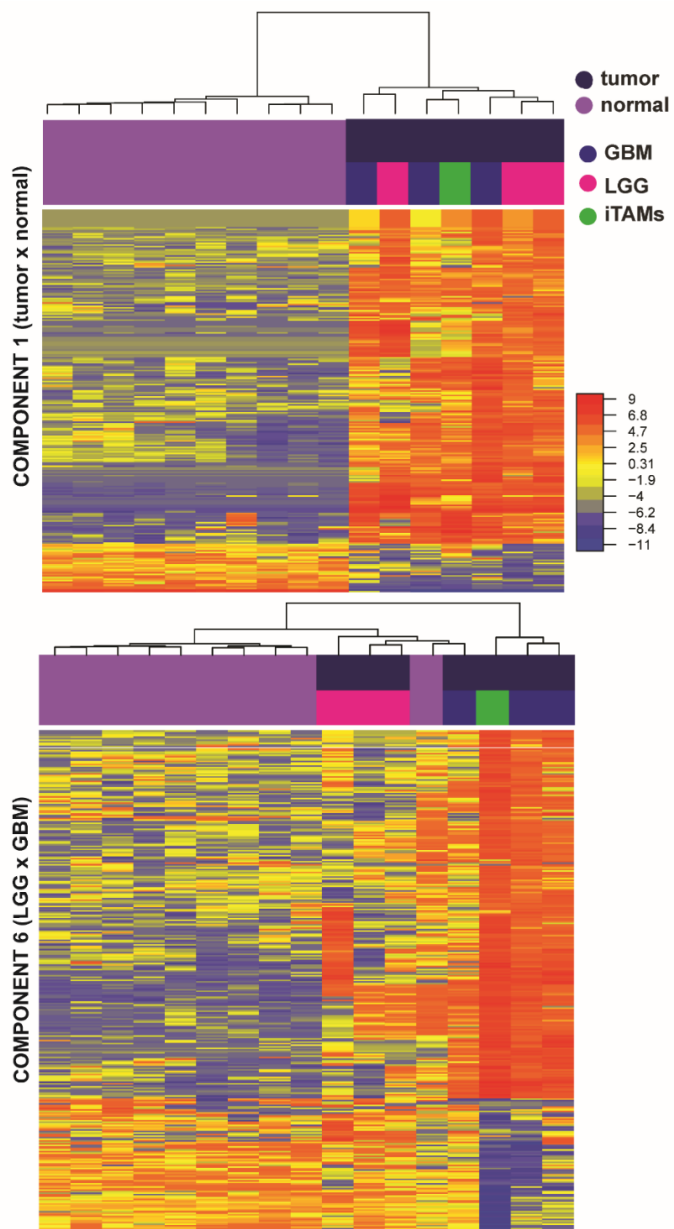


Figure 5: Hierarchically clustered Z-score expression heatmap of the differentially expressed genes of Components 1 and 6 from the Independent Component Analysis (ICA).

In component 1, the upregulated genes in tumor microglia relative to normal microglia included: chemokines *CXCL2/8*, *CCL3/4/5* and receptor *CCR7*; genes related to mitotic stimuli responses *ASPM* and *EGR1-4*; to development *SOX2/10* and *KLF2/4/10*; metalloproteinase *MMP19* (Figure 6). GSEA analysis of the set of upregulated genes in the component 1 revealed signaling pathways related to proliferation (“regulation of cell proliferation”, “regulation of cell cycle”), and to motility (“regulation of granulocyte chemotaxis”, “positive regulation of leukocyte chemotaxis”). Additionally, were also observed pathways associated to “response to hormone” and “regulation of apoptotic process”. Downregulated genes in this component 1 included *LTB*, *PPP1RC3* and *CA13*.

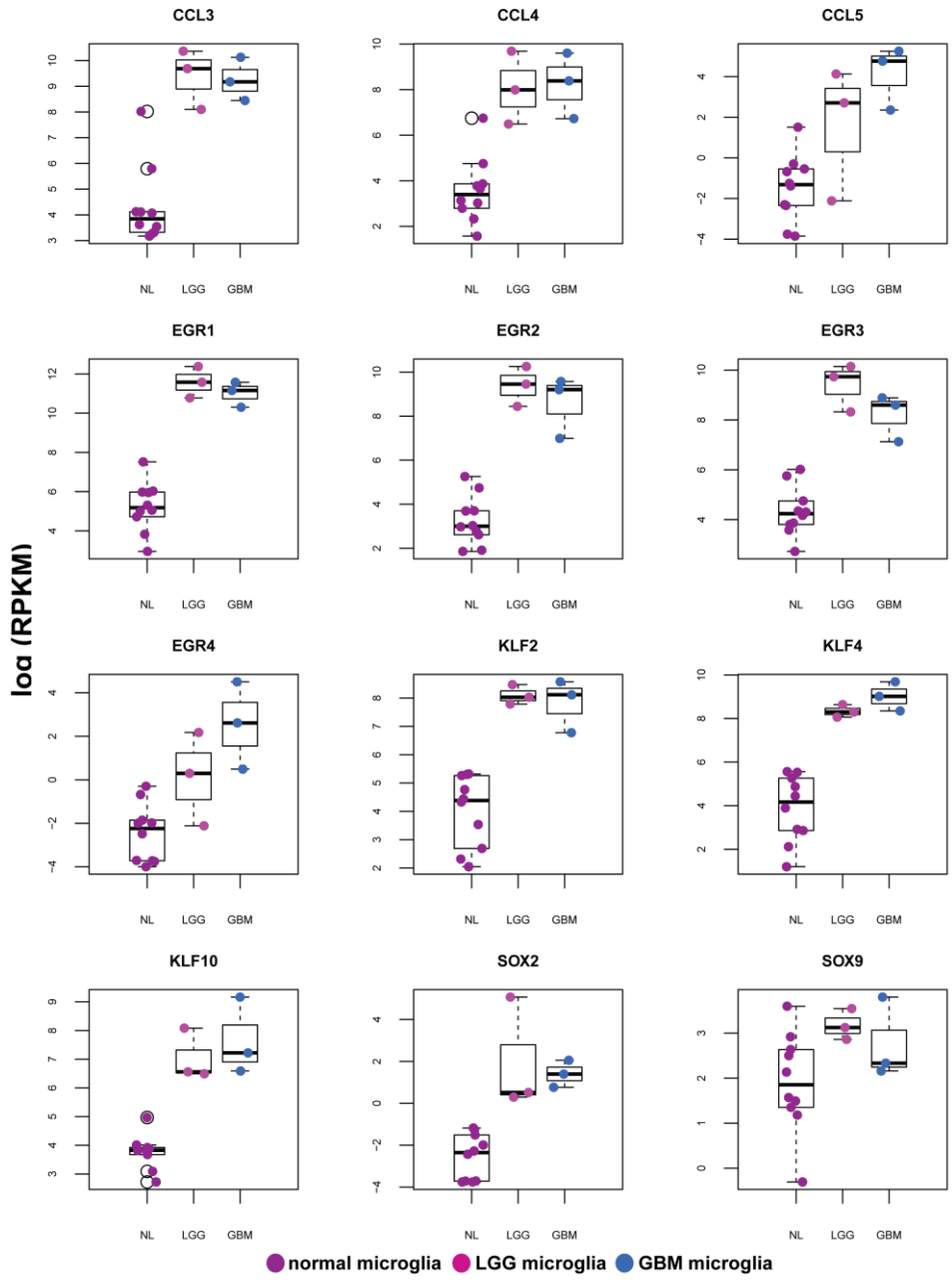


Figure 6: *Upregulated genes in tumor microglia in the Component 1 which segregated normal from glioma microglia are presented, including chemokines CXCL2/8 and CCL3/4/5; mitotic stimuli responses related genes ASPM, EGR1-4 and CDK1; development related genes SOX2/10 and KLF2/4/10; metalloproteinase MMP19; and LMNA. Despite separating tumor from normal microglia, no significant difference of their expressions were detected between GBM and LGG microglia.*

Component 6 of the ICA analysis separated GBM from LGG microglia. The analysis of this component has also shown a very similar expression profile between iTAMs and GBM microglia. The downregulated genes in GBM microglia compared to LGG microglia in this component 6 fitted to any particular pathway, however, we highlighted the significant differential expression of *HIST2H2AA3*, *CXCL12*, *P2RY14*, *TAL1* and *FOXP2* between these two groups, LGG and GBM microglia. On the other hand, the upregulated genes associated to pathways related to proliferation (such as “regulation of transcription involved in G1/S transition of mitotic cell cycle”, “mitotic spindle assembly” and “microtubule cytoskeleton organization involved in mitosis”), and, also related to extracellular matrix organization and leukocyte migration. Among those upregulated genes in GBM microglia compared to LGG microglia *NES*, *MELK* (development), *FOXM1* (cell cycle), *CXCL3* (chemoattractant chemokines), *IL2RA*, *IL7R* (interleukin receptors), *FN1*, *THBS1*, *TNC* and *VCAN* (ECM), *ITGA4* (integrin) presented interesting increment of their expression in parallel to the progression of malignancy (Figure 7).

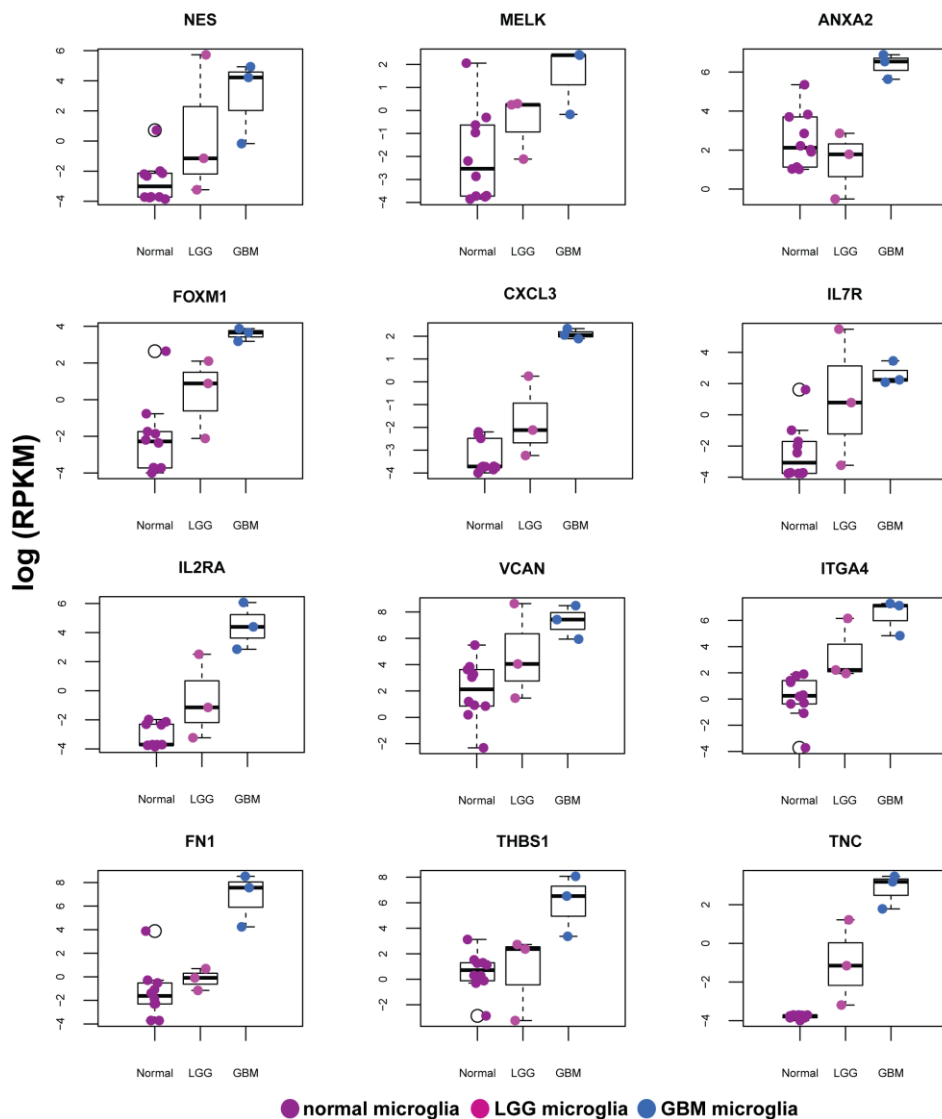


Figure 7: *Upregulated genes of Component 6* associated to pathways related to proliferation, extracellular matrix organization and leukocyte migration. *NES*, *MELK* (development related genes), *FOXM1*(cell cycle control), *CXCL3* (chemoattractant chemokine), *IL2RA* (interleukin receptors), *FN1*, *THBS1*, *TNC*, *VCAN* (ECM) and *ITGA4* (integrin) present increase in their expressions according to the increment of malignancy.

Figure 8 shows the functional protein association network resulting from upregulated genes in the Component 6 analysis, when compared LGG to GBM microglia transcriptome.

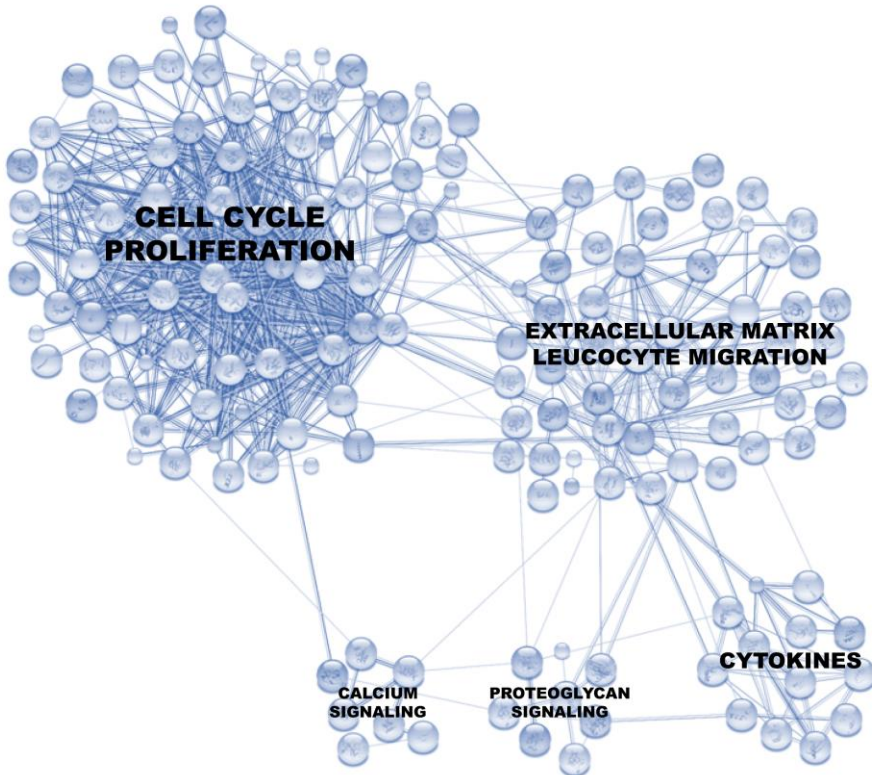


Figure 8: A predicted protein-protein interaction network of the upregulated genes of Components 6 analysis, comparing LGG to GBM microglia expression profile.

Transcription network in tumor microglia

CoRegNet analysis provided a set of genes representing the co-operative regulators and the active transcriptional programs in our analyzed cohort. Figure 9 displays the results from this analysis. It is interesting to notice that *TAL1*, *ID1* and *ID3*, three coding genes for bHLH proteins, *MEIS1* and *ZNF556* presented low regulation activity in tumor-microglia compared to normal microglia. Active transcription factors add up to 43, including the previously mentioned *EGR1-3* and *KLF2/4/6/10*, histone

acetylating *CREBBP*, along with FOS family (*FOS*, *FOSB*, *FOSL1*, *FOSL2*), *VDR*, *RUNX3*, *BCL6*, *NFKB1A*, *MAFF* and *MITF*. The heat map on Figure 9 displays how these transcription factors were distributed in our cohort.

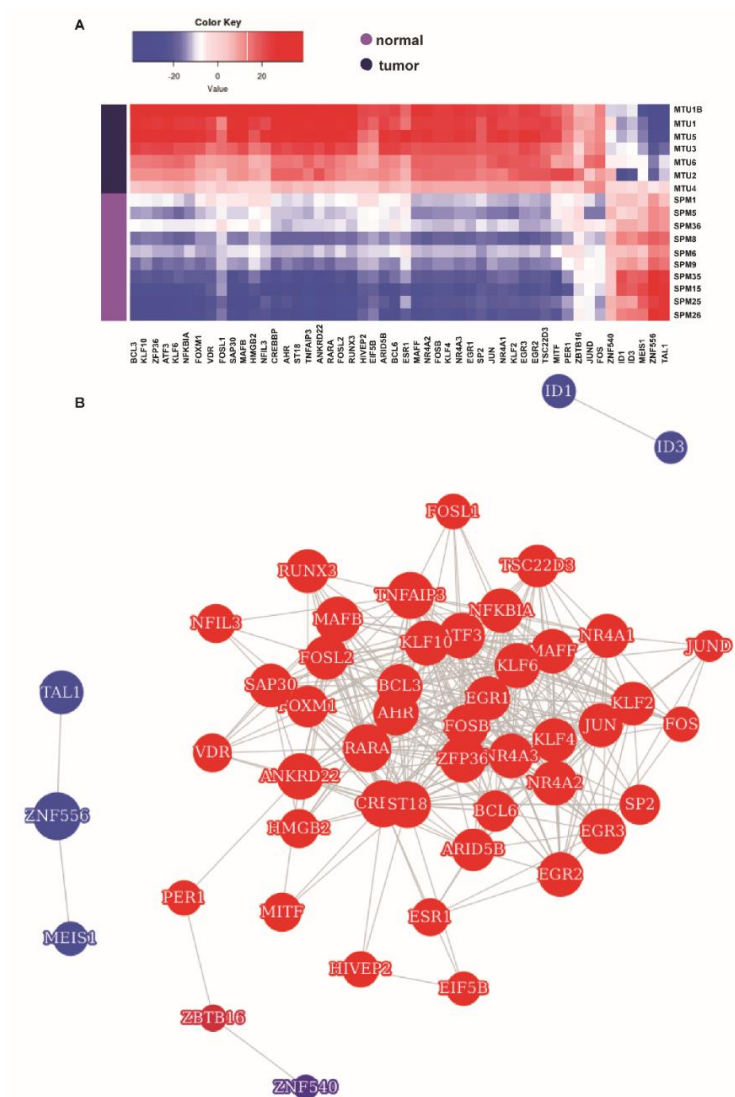


Figure 9: CoRegNet analysis. Using BioConductor package CoRegNet, transcriptional regulators of human glioma microglia were identified. A) A heat map displaying the expression of these transcription factors in our cohort. B) The predicted glioma microglia transcriptional network. In red the active transcription regulators, and in blue the transcription factor with low activity.

TCGA validation

A set of differentially expressed genes were detected within GBM microglia samples. This led us to question whether these were related to the previously described GBM subtypes (Brennan et al., 2013b; Cloughesy et al., 2014; Phillips et al., 2006; Verhaak et al., 2010). The genetic alterations within these tumors might influence the surrounding microenvironment and influence the microglia transcriptome. We previously assessed the genetic alterations of the corresponding bulk tumors of our GBM microglia cases (refer to **Chapter 3**). In the present tumor-microglia series, two samples were classified as classical GBM and one as mesenchymal. Our cohort is underpowered to make any inference if GBM subtypes somehow impact on microglia and iTAMs gene expression. Hence, we proceeded to investigate how this set of genes was expressed in a TCGA cohort of GBM samples stratified by molecular alteration.

A TCGA-GBM analyzed cohort contained samples from whole-tissue RNA-Seq. Our inquiry was to which GBM subtype (mesenchymal, classical, neural or proneural) was enriched for microglia. For that, we evaluated a gene set of membrane associated proteins from the normal microglia core signature previously mentioned (refer to Chapter 6). Members of the FC-gamma receptor family, integrins and purinergic receptors were selected (Figure 10). We observed a clear upregulation of these markers in the mesenchymal subtype of GBM. This observation agrees with current data reporting mesenchymal GBM enriched for myeloid activation/inflammation markers (Engler et al., 2012; Rutledge et al., 2013; de Vrij et al., 2015; Zanotto-Filho et al., 2016). Interestingly, the most notable genes with lower expression in the Mesenchymal subtype were known microglial markers *P2RY12*, *CX3CR1* and *AIF1*.

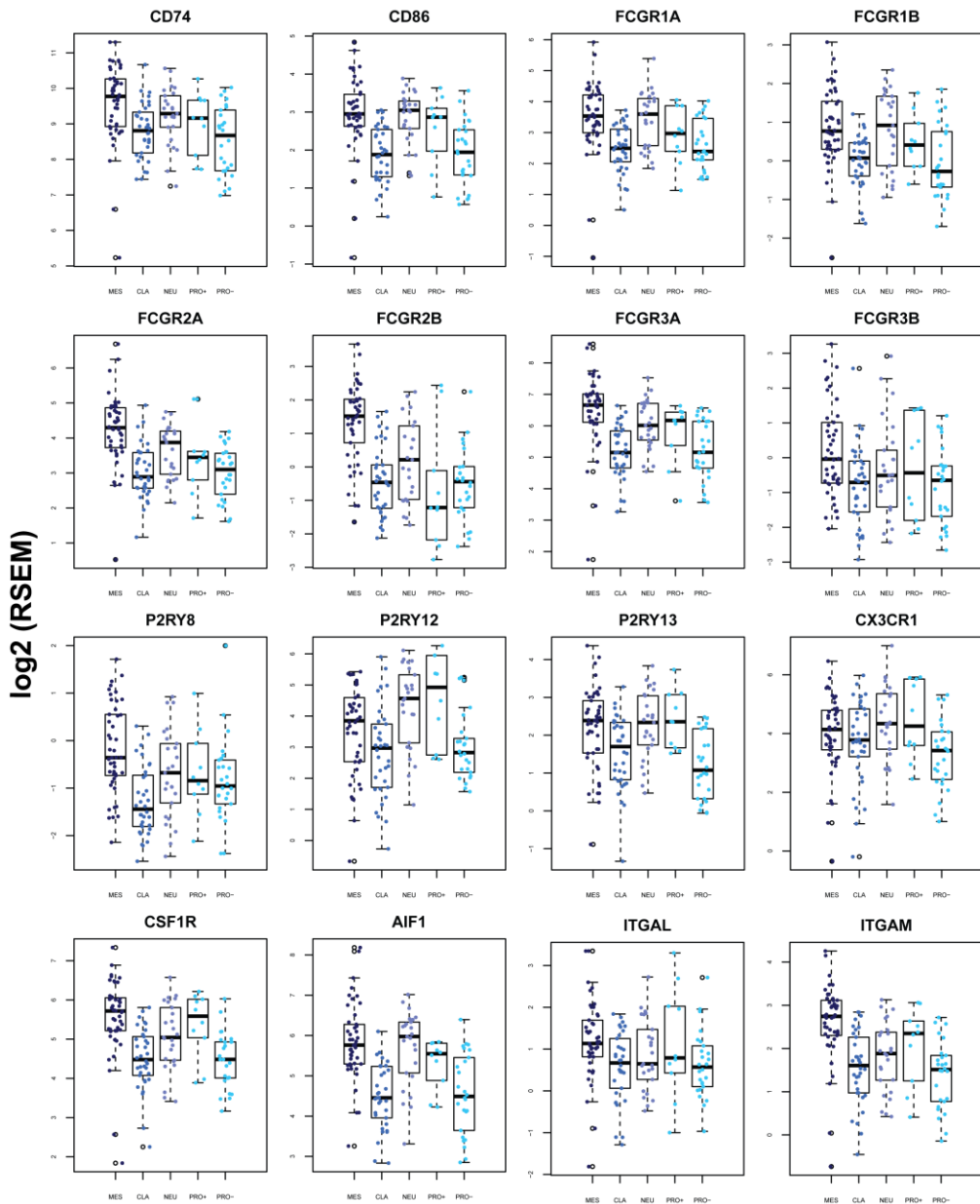


Figure 10: Normal microglia core genes are upregulated in the Mesenchymal GBM subtype. Members of the FC-gamma receptor family, integrins, complement and purinergic receptors were selected for this analysis. Noteworthy exceptions include *P2RY12* and *CX3CR1*. MES, mesenchymal; CLA, classical; NEU, neural, PRO, proneural (+) *IDH1* mutated and (-) *IDH1* wild-type.

Genes that were upregulated in tumor-microglia from the above analysis did not present any specific pattern and their expressions varied among GBM subtypes (Supplemental Figure 1). However, we noticed that genes encoding ECM proteins from Component 6 analysis, with the exception of *VCAN*, were significantly higher expressed in the mesenchymal GBM subtype (Figure 11). This data indicates that the increased expression of these genes in GBM might be related to a microglial source.

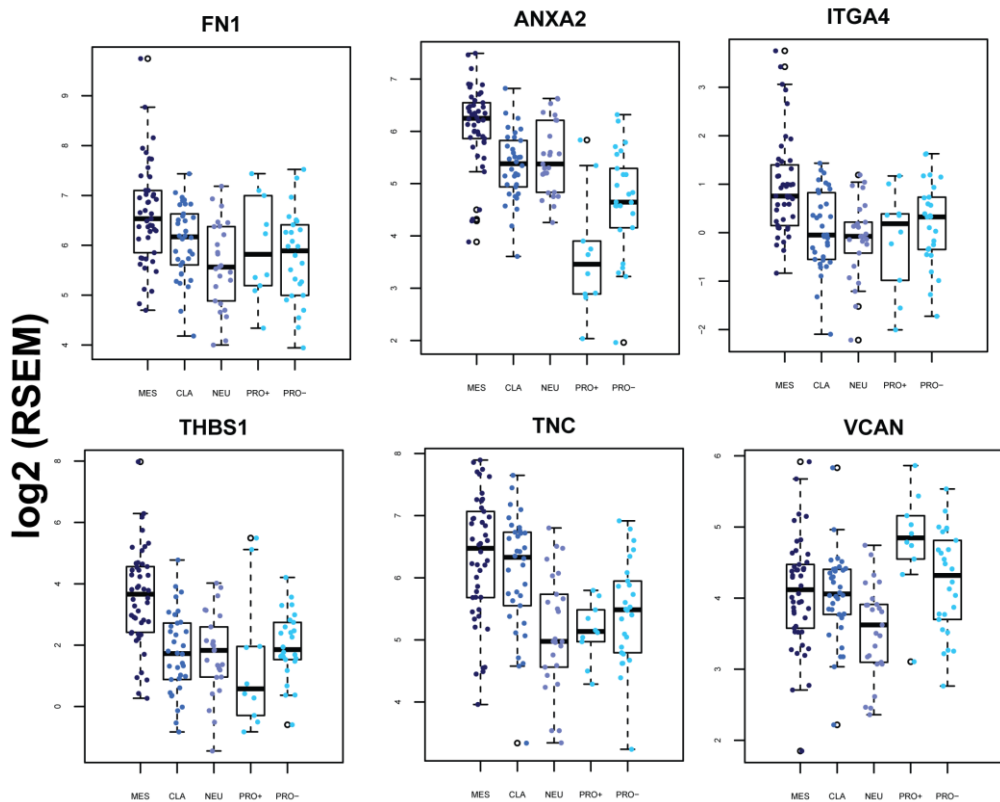


Figure 11: ECM proteins coding genes are upregulated in the Mesenchymal GBM subtype. Despite not present any specific pattern and their hyper-expression varying among GBM subtypes, we observed higher levels of ECM proteins coding genes from component 6 in mesenchymal GBMs. MES, mesenchymal; CLA, classical; NEU, neural, PRO, proneural (+) *IDH1* mutated and (-) *IDH1* wild-type.

DISCUSSION

In this study, we report differential gene expression profile between glioma-derived and normal microglia, as well as the differences found between microglia derived from lower grade gliomas and from glioblastomas. Most studies regarding human microglia lack an appropriate control population for comparison, relying on samples from epilepsy surgeries, which display inflammatory alterations intrinsic to the disease (Devinsky et al., 2013; Eyo et al., 2016). Our control population consists of microglia isolated from cortical *post-mortem* tissue, whose transcriptome has been extensively analyzed (refer to Chapter 6). Our tumor microglia analysis was based on the comparison to a set of normal microglia samples from this study, allowing for a comparison between tumor and normal microglia, and between LGG and GBM microglia.

Isolation of pure human microglia in the presence of myeloid infiltrates is difficult. Several protocols have been published, by our group and others (Olah et al., 2012; Rustenhoven et al., 2016), aiming to diminish contamination with other leucocytes or brain cells. Our latest protocol (Galatro et al., 2017) (refer to **Chapter 5**) focuses on high purity population (above 98% of microglial purity) and employs a sorting strategy that clearly separates microglia cells from myeloid infiltrates. Further transcriptome analysis corroborates this claim, as markers for neurons, astrocytes, oligodendrocytes and immune infiltrate were low or not present at all in our data (Figure 1).

Human tumor microglia display changes that go beyond an inflammatory phenotype

Comparison of tumor *versus* normal microglia indicated that tumor microglia samples are not as homogenous as normal microglia. Heterogeneity in gliomas, under histological and molecular parameters, is a known fact (reviewed by (Filbin and Suvà, 2016)). If and how these intrinsic differences affect the microenvironment and as a consequence influence microglia gene expression is unclear. It is clear, however, that both tumor grade (LGG and GBM) and molecular subtype (in the case of GBM subtypes) have major influences on the myeloid cells in the microenvironment.

While assessing which biological pathways were associated with the differentially expressed genes in tumor *versus* normal microglia, we observed that,

while inflammation related pathways were altered, the most prominent changes were related to other pathways. Proliferation, cell cycle control and motility (the last one includes extracellular matrix-related changes) were most affected in tumor-microglia. It also seems that, even if markers previously identified in non-neoplastic microglia are still expressed, tumor-microglia undergo such drastic changes upon glioma stimuli, that a different set of markers were hyperexpressed in tumor-microglia.

Despite the high levels of anti-inflammatory markers, such as *CD163*, *CD209* and *ANXA1*, the set of chemokines and other secreted factors differentially expressed that characterize a polarized M1 or M2 phenotype was difficult to recognize in tumor microglia. A recent report where the transcriptome of a mixed population of microglia and iTAMs from human GBMs was analyzed (Szulzewsky et al., 2016) also showed a lack of an inflammatory profile for those cells. In that study, one possible explanation raised was the fact that normal and tumor samples were not age-matched, as is the case with our study. An intrinsic inflammation in normal (older) microglia samples would be the cause for such result. As we demonstrated in **Chapter 6**, aging in human microglia does not present an inflammatory profile, but is related to changes in actin dynamics. In our tumor microglia analysis, we observed a plethora of genes, involved in unexpected biological pathways, discussed below.

Transcriptome signature for glioma microglia

With stringent criteria, we could determine core genes for both GBM and LGG microglia, and through ICA analysis, we were able to further identify differentially expressed genes and to associate them to specific biological functions. Interestingly, we identified a set of genes by both analysis: class comparison and independent component analyses. A considerable number of genes selected as differentially expressed in LGG microglia compared to normal microglia were also present in GBM microglia, although at higher levels, suggesting the participation of these genes in the malignant progression of the tumor. This finding corroborate a previous observation (Hambardzumyan et al., 2016), that microglia play a crucial role in the progression of gliomas.

Transcriptional regulators

EGR1-4 genes were differentially expressed in both LGG and GBM microglia and the lower expression in normal microglia suggest that they might also be important for the shift from normal to tumor microglia. EGRs are zinc finger-containing transcription factors first discovered in the search for genes whose expression was induced by growth factors; they have been associated to both lymphoid and myeloid hematopoiesis (Gashler and Sukhatme, 1995; Gómez-Martín et al., 2010). Further studies postulated EGR1 as central for the regulation of mitotic processes, ensuring that weak signals did not trigger cell proliferation (Zwang et al., 2011). EGR1 also mediates responses to ischemia in mononuclear phagocytes (Bosco et al., 2008), has been recently associated with tumor-specific education of microglial cells in mice (Bowman et al., 2016), and induces the expression of IL6, promoting protective effects in the CNS upon stimuli with anti-inflammatory molecules (Casella et al., 2016). Along with EGR1, EGR2 promotes differentiation of monocytes into macrophage (Laslo et al., 2006) and is essential for CSFR1 expression in the course of macrophage differentiation from myeloid progenitors by forming an active enhancer complex with PU.1 and RUNX1 (Krysinska et al., 2007). Their roles myeloid specific and in proliferation/cell cycle control as tracked by ICA components 1 and 6 analyses highlight EGRs as regulators for the microglia response to glioma stimuli.

Krüppel-like transcription factors (KLFs) have been previously associated with monocyte/macrophage differentiation or activation (Cao et al., 2010). KLF4, a major downstream target of IRF8 and PU.1, is critical for development of the monocyte lineage (Terry and Miller, 2014), but not for microglia development (Kierdorf et al., 2013). In addition, KLF4 has been associated with IL1 β expression and the regulation of neuro-inflammation and immunomodulatory activities in murine microglia cell line (Kaushik et al., 2010, 2013). KLF6 has been associated to macrophage polarization towards a pro-inflammatory phenotype (Bi et al., 2016; Date et al., 2014), while KLF2 and KLF10 were proposed as promoters of a supportive and anti-inflammatory phenotype (Das et al., 2012; Mahabeleshwar et al., 2011; Papadakis et al., 2015). In our evaluation, KLF2/6 levels were upregulated in LGG microglia, and their expression levels were also high in GBM microglia. Interestingly, *KLF4/10* expression levels increased with tumor grade.

Activator-protein 1 (AP-1 complex), encoded by genes from both the FOS and JUN families, is also related to the activation of pro-inflammatory responses (Waetzig et al., 2005). In our cohort, their members showed a similar pattern to KLFs.

Although a specific inflammatory phenotype was lacking in the tumor-microglia expression profile in the present study, a disbalance in the regulatory network of the inflammatory response of microglia along glioma progression was detected. A single cell approach may clarify the major players of the tumor-microglia during the progression from LGG to GBM.

Among the lower active transcription factors in tumor-microglia, we highlighted genes coding for basic helix-loop-helix proteins (bHLH), *TAL1* and *ID1/3*. *TAL1* is one of the transcriptional regulators in adult microglia, possibly forming a complex with *RUNX1* and *LYL1* (Wilson et al., 2009, 2010), and activating the transcription of many microglia specific genes. The loss of the “normal” microglia identity in gliomas might be explained by the downregulation of a factor such as *TAL1*. ID proteins are dominant negative transcription factors, a highly evolutionarily conserved group of proteins that play crucial roles in cellular process ranging from cell cycle control, differentiation and tumorigenesis (Benezra et al., 1990; Lasorella et al., 2014). We have recently characterized ID proteins expression in human glioma whole tissue (refer to **Chapter 3**), assessing their differential expression according to tissue of origin (astro or oligocytic) and GBM subtype. It now becomes clear that the differences found in IDs expression in our previous work are not related to the inflammatory microenvironment in gliomas, and are mostly related to tumor cells.

Extracellular matrix modulation and invasiveness

Our analysis revealed that tumor-microglia express high levels of genes related to extracellular matrix remodeling, such as fibronectin (*FN1*), tenascin-C (TNC) and thrombospondin-1 (*THBS1*), along with invasiveness related *ANXA2*. *FN1* is known to be highly expressed in GBM, in comparison to non-invasive pilocytic astrocytoma (AGI). Functional studies in GBM cell lines have correlated this overexpression to increased tumor cell proliferation, invasion, resistance to ionizing irradiation and enhanced *in vivo* angiogenic potential (Blandin et al., 2016; Colin et al., 2006; Serres et al., 2014). Tenascin-C has been shown to limit the pro-inflammatory response, as well as to increase the invasive phenotype of iTAMs and to control the “go or grow” switch in glioma *in vivo* (Brellier and Chiquet-Ehrismann, 2011; Van Obberghen-Schilling et al., 2011; Xia et al., 2016). The role of *THBS1* in gliomas is unclear, as it has been associated to tumor suppression given its anti-angiogenic properties (Kazerounian et al., 2008), but also to increased invasiveness at the border of gliomas (Gritsenko et al., 2012).

Recent studies have demonstrated that ANXA2, a calcium-binding cytoskeletal protein expressed on the surface of several cell types, stands out as an epigenetically controlled master regulator of mesenchymal transformation in glioma (Kling et al., 2016), associated with patient survival. Also, it has been shown that GBM cell migration and invasion are sustained by *ANXA2* (Maule et al., 2016). While these previous studies focused on tumor cells, we detected microglia as a major source for these proteins.

Among GBM subtypes, the above mentioned targets related to ECM modulation were highest in mesenchymal subtype, presenting the highest invasive rate and the worst prognosis (Balbous et al., 2014; Carro et al., 2010).

The present findings shed new light on the changes human microglia undergo upon glioma stimuli and open questions about the regulatory processes between tumor and microglia compartments. Addressing these questions in additional studies may lead to potential new strategies to control gliomagenesis and malignant progression.

REFERENCES

Balbous, A., Cortes, U., Guilloteau, K., Villalva, C., Flamant, S., Gaillard, A., Milin, S., Wager, M., Sorel, N., Guilhot, J., et al. (2014). A mesenchymal glioma stem cell profile is related to clinical outcome. *Oncogenesis* 3, e91.

Benezra, R., Davis, R.L., Lockshon, D., Turner, D.L., and Weintraub, H. (1990). The protein Id: a negative regulator of helix-loop-helix DNA binding proteins. *Cell* 61, 49–59.

Bi, J., Zeng, X., Zhao, L., Wei, Q., Yu, L., Wang, X., Yu, Z., Cao, Y., Shan, F., and Wei, M. (2016). miR-181a Induces Macrophage Polarized to M2 Phenotype and Promotes M2 Macrophage-mediated Tumor Cell Metastasis by Targeting KLF6 and C/EBP α . *Mol. Ther. Nucleic Acids* 5, e368.

Blandin, A.-F., Noulet, F., Renner, G., Mercier, M.-C., Choulier, L., Vauchelles, R., Ronde, P., Carreiras, F., Etienne-Selloum, N., Vereb, G., et al. (2016). Glioma cell dispersion is driven by α 5 integrin-mediated cell-matrix and cell-cell interactions. *Cancer Lett.* 376, 328–338.

Bosco, M.C., Puppo, M., Blengio, F., Fraone, T., Cappello, P., Giovarelli, M., and Varesio, L. (2008). Monocytes and dendritic cells in a hypoxic environment: Spotlights on chemotaxis and migration. *Immunobiology* 213, 733–749.

Bowman, R.L., Klemm, F., Akkari, L., Pyonteck, S.M., Sevenich, L., Quail, D.F., Dhara, S., Simpson, K., Gardner, E.E., Iacobuzio-Donahue, C.A., et al. (2016). Macrophage Ontogeny Underlies Differences in Tumor-Specific Education in Brain Malignancies. *Cell Rep.* 17, 2445–2459.

Brellier, F., and Chiquet-Ehrismann, R. (2011). Function of Tenascins in the Tumor Stroma. In *Tumor-Associated Fibroblasts and Their Matrix*, M.M. Mueller, and N.E. Fusenig, eds. (Springer Netherlands), pp. 145–158.

Brennan, C.W., Verhaak, R.G.W., McKenna, A., Campos, B., Noushmehr, H., Salama, S.R., Zheng, S., Chakravarty, D., Sanborn, J.Z., Berman, S.H., et al. (2013a). The somatic genomic landscape of glioblastoma. *Cell* 155, 462–477.

Brennan, C.W., Verhaak, R.G.W., McKenna, A., Campos, B., Noushmehr, H., Salama, S.R., Zheng, S., Chakravarty, D., Sanborn, J.Z., Berman, S.H., et al. (2013b). The Somatic Genomic Landscape of Glioblastoma. *Cell* 155, 462–477.

Cao, Z., Sun, X., Icli, B., Wara, A.K., and Feinberg, M.W. (2010). Role of Krüppel-like factors in leukocyte development, function, and disease. *Blood* 116, 4404–4414.

Carro, M.S., Lim, W.K., Alvarez, M.J., Bollo, R.J., Zhao, X., Snyder, E.Y., Sulman, E.P., Anne, S.L., Doetsch, F., Colman, H., et al. (2010). The transcriptional network for mesenchymal transformation of brain tumours. *Nature* 463, 318–325.

Casella, G., Garzetti, L., Gatta, A.T., Finardi, A., Maiorino, C., Ruffini, F., Martino, G., Muzio, L., and Furlan, R. (2016). IL4 induces IL6-producing M2 macrophages associated to inhibition of neuroinflammation in vitro and in vivo. *J. Neuroinflammation* 13.

Charles, N.A., Holland, E.C., Gilbertson, R., Glass, R., and Kettenmann, H. (2011). The brain tumor microenvironment. *Glia* 59, 1169–1180.

Cloughesy, T.F., Cavenee, W.K., and Mischel, P.S. (2014). Glioblastoma: from molecular pathology to targeted treatment. *Annu. Rev. Pathol.* 9, 1–25.

Colin, C., Baeza, N., Bartoli, C., Fina, F., Eudes, N., Nanni, I., Martin, P.-M., Ouafik, L., and Figarella-Branger, D. (2006). Identification of genes differentially expressed in glioblastoma versus pilocytic astrocytoma using Suppression Subtractive Hybridization. *Oncogene* 25, 2818–2826.

Das, M., Lu, J., Joseph, M., Aggarwal, R., Kanji, S., McMichael, B.K., Lee, B.S., Agarwal, S., Ray-Chaudhury, A., Iwenofu, O.H., et al. (2012). Kruppel-Like Factor 2 (KLF2) Regulates Monocyte Differentiation and Functions in mBSA and IL-1 β -Induced Arthritis. *Curr. Mol. Med.* 12, 113–125.

Date, D., Das, R., Narla, G., Simon, D.I., Jain, M.K., and Mahabeleshwar, G.H. (2014). Kruppel-like Transcription Factor 6 Regulates Inflammatory Macrophage Polarization. *J. Biol. Chem.* 289, 10318–10329.

DeLuca, D.S., Levin, J.Z., Sivachenko, A., Fennell, T., Nazaire, M.-D., Williams, C., Reich, M., Winckler, W., and Getz, G. (2012). RNA-SeQC: RNA-seq metrics for quality control and process optimization. *Bioinforma. Oxf. Engl.* 28, 1530–1532.

Devinsky, O., Vezzani, A., Najjar, S., Lanerolle, N.C.D., and Rogawski, M.A. (2013). Glia and epilepsy: excitability and inflammation. *Trends Neurosci.* 36, 174–184.

Dobin, A., Davis, C.A., Schlesinger, F., Drenkow, J., Zaleski, C., Jha, S., Batut, P., Chaisson, M., and Gingeras, T.R. (2013). STAR: ultrafast universal RNA-seq aligner. *Bioinforma. Oxf. Engl.* 29, 15–21.

Engler, J.R., Robinson, A.E., Smirnov, I., Hodgson, J.G., Berger, M.S., Gupta, N., James, C.D., Molinaro, A., and Phillips, J.J. (2012). Increased microglia/macrophage gene expression in a subset of adult and pediatric astrocytomas. *PloS One* 7, e43339.

Eyo, U.B., Murugan, M., and Wu, L.-J. (2016). Microglia-Neuron Communication in Epilepsy. *Glia*.

Filbin, M.G., and Suvà, M.L. (2016). Gliomas Genomics and Epigenomics: Arriving at the Start and Knowing It for the First Time. *Annu. Rev. Pathol.* *11*, 497–521.

Fridman, W.H., Pagès, F., Sautès-Fridman, C., and Galon, J. (2012). The immune contexture in human tumours: impact on clinical outcome. *Nat. Rev. Cancer* *12*, 298–306.

Galatro, T.F., Vainchtein, I.D., Brouwer, N., Boddeke, E.W.G.M., and Eggen, B.J.L. (2017). Isolation of Microglia and Immune Infiltrates from Mouse and Primate Central Nervous System. *Methods Mol. Biol. Clifton NJ* *1559*, 333–342.

Galdiero, M.R., Garlanda, C., Jaillon, S., Marone, G., and Mantovani, A. (2013). Tumor associated macrophages and neutrophils in tumor progression. *J. Cell. Physiol.* *228*, 1404–1412.

Gashler, A., and Sukhatme, V.P. (1995). Early growth response protein 1 (Egr-1): prototype of a zinc-finger family of transcription factors. *Prog. Nucleic Acid Res. Mol. Biol.* *50*, 191–224.

Gómez-Martín, D., Díaz-Zamudio, M., Galindo-Campos, M., and Alcocer-Varela, J. (2010). Early growth response transcription factors and the modulation of immune response: implications towards autoimmunity. *Autoimmun. Rev.* *9*, 454–458.

Gritsenko, P.G., Ilina, O., and Friedl, P. (2012). Interstitial guidance of cancer invasion. *J. Pathol.* *226*, 185–199.

Hambardzumyan, D., Gutmann, D.H., and Kettenmann, H. (2015). The role of microglia and macrophages in glioma maintenance and progression. *Nat. Neurosci.* *19*, 20–27.

Hambardzumyan, D., Gutmann, D.H., and Kettenmann, H. (2016). The role of microglia and macrophages in glioma maintenance and progression. *Nat. Neurosci.* *19*, 20–27.

Hao, N.-B., Lü, M.-H., Fan, Y.-H., Cao, Y.-L., Zhang, Z.-R., and Yang, S.-M. (2012). Macrophages in tumor microenvironments and the progression of tumors. *Clin. Dev. Immunol.* *2012*, 948098.

Kaushik, D.K., Gupta, M., Das, S., and Basu, A. (2010). Krüppel-like factor 4, a novel transcription factor regulates microglial activation and subsequent neuroinflammation. *J. Neuroinflammation* *7*, 68.

Kaushik, D.K., Thounaojam, M.C., Kumawat, K.L., Gupta, M., and Basu, A. (2013). Interleukin-1 β orchestrates underlying inflammatory responses in microglia via Krüppel-like factor 4. *J. Neurochem.* *127*, 233–244.

Kazerounian, S., Yee, K.O., and Lawler, J. (2008). Thrombospondins in cancer. *Cell. Mol. Life Sci. CMLS* 65, 700–712.

Kierdorf, K., Erny, D., Goldmann, T., Sander, V., Schulz, C., Perdiguero, E.G., Wieghofer, P., Heinrich, A., Riemke, P., Hölscher, C., et al. (2013). Microglia emerge from erythromyeloid precursors via Pu.1- and Irf8-dependent pathways. *Nat. Neurosci.* 16, 273–280.

Kling, T., Ferrarese, R., Ó hAilín, D., Johansson, P., Heiland, D.H., Dai, F., Vasilikos, I., Weyerbrock, A., Jörnsten, R., Carro, M.S., et al. (2016). Integrative Modeling Reveals Annexin A2-mediated Epigenetic Control of Mesenchymal Glioblastoma. *EBioMedicine* 12, 72–85.

Krysinska, H., Hoogenkamp, M., Ingram, R., Wilson, N., Tagoh, H., Laslo, P., Singh, H., and Bonifer, C. (2007). A Two-Step, PU.1-Dependent Mechanism for Developmentally Regulated Chromatin Remodeling and Transcription of the *c-fms* Gene. *Mol. Cell. Biol.* 27, 878–887.

Laslo, P., Spooner, C.J., Warmflash, A., Lancki, D.W., Lee, H.-J., Sciammas, R., Gantner, B.N., Dinner, A.R., and Singh, H. (2006). Multilineage Transcriptional Priming and Determination of Alternate Hematopoietic Cell Fates. *Cell* 126, 755–766.

Lasorella, A., Benzera, R., and Iavarone, A. (2014). The ID proteins: master regulators of cancer stem cells and tumour aggressiveness. *Nat. Rev. Cancer* 14, 77–91.

Li, B., and Dewey, C.N. (2011). RSEM: accurate transcript quantification from RNA-Seq data with or without a reference genome. *BMC Bioinformatics* 12, 323.

Louis, D.N., Perry, A., Reifenberger, G., von Deimling, A., Figarella-Branger, D., Cavenee, W.K., Ohgaki, H., Wiestler, O.D., Kleihues, P., and Ellison, D.W. (2016). The 2016 World Health Organization Classification of Tumors of the Central Nervous System: a summary. *Acta Neuropathol. (Berl.)* 131, 803–820.

Mahabeleshwar, G.H., Kawanami, D., Sharma, N., Takami, Y., Zhou, G., Shi, H., Nayak, L., Jeyaraj, D., Grealy, R., White, M., et al. (2011). The Myeloid Transcription Factor KLF2 Regulates the Host Response to Polymicrobial Infection and Endotoxic Shock. *Immunity* 34, 715–728.

Mantovani, A., Sozzani, S., Locati, M., Allavena, P., and Sica, A. (2002). Macrophage polarization: tumor-associated macrophages as a paradigm for polarized M2 mononuclear phagocytes. *Trends Immunol.* 23, 549–555.

Maule, F., Bresolin, S., Rampazzo, E., Boso, D., Della Puppa, A., Esposito, G., Porcù, E., Mitola, S., Lombardi, G., Accordi, B., et al. (2016). Annexin 2A sustains glioblastoma cell dissemination and proliferation. *Oncotarget* 7, 54632–54649.

Nicolle, R., Radvanyi, F., and Elati, M. (2015). CoRegNet: reconstruction and integrated analysis of co-regulatory networks. *Bioinforma. Oxf. Engl.* *31*, 3066–3068.

Olah, M., Raj, D., Brouwer, N., De Haas, A.H., Eggen, B.J.L., Den Dunnen, W.F.A., Biber, K.P.H., and Boddeke, H.W.G.M. (2012). An optimized protocol for the acute isolation of human microglia from autopsy brain samples. *Glia* *60*, 96–111.

Papadakis, K.A., Krempsi, J., Svingen, P., Xiong, Y., Sarmiento, O.F., Lomberg, G.A., Urrutia, R.A., and Faubion, W.A. (2015). Krüppel-like factor KLF10 deficiency predisposes to colitis through colonic macrophage dysregulation. *Am. J. Physiol. - Gastrointest. Liver Physiol.* *309*, G900–G909.

Parsons, D.W., Jones, S., Zhang, X., Lin, J.C.-H., Leary, R.J., Angenendt, P., Mankoo, P., Carter, H., Siu, I.-M., Gallia, G.L., et al. (2008). An integrated genomic analysis of human glioblastoma multiforme. *Science* *321*, 1807–1812.

Phillips, H.S., Kharbanda, S., Chen, R., Forrest, W.F., Soriano, R.H., Wu, T.D., Misra, A., Nigro, J.M., Colman, H., Soroceanu, L., et al. (2006). Molecular subclasses of high-grade glioma predict prognosis, delineate a pattern of disease progression, and resemble stages in neurogenesis. *Cancer Cell* *9*, 157–173.

Ritchie, M.E., Phipson, B., Wu, D., Hu, Y., Law, C.W., Shi, W., and Smyth, G.K. (2015). limma powers differential expression analyses for RNA-sequencing and microarray studies. *43*.

Rustenhoven, J., Park, T.I.-H., Schweder, P., Scotter, J., Correia, J., Smith, A.M., Gibbons, H.M., Oldfield, R.L., Bergin, P.S., Mee, E.W., et al. (2016). Isolation of highly enriched primary human microglia for functional studies. *Sci. Rep.* *6*, 19371.

Rutledge, W.C., Kong, J., Gao, J., Gutman, D.A., Cooper, L.A.D., Appin, C., Park, Y., Scarpace, L., Mikkelsen, T., Cohen, M.L., et al. (2013). Tumor-infiltrating lymphocytes in glioblastoma are associated with specific genomic alterations and related to transcriptional class. *Clin. Cancer Res. Off. J. Am. Assoc. Cancer Res.* *19*, 4951–4960.

Serres, E., Debarbieux, F., Stanchi, F., Maggiorella, L., Grall, D., Turchi, L., Burel-Vandenbos, F., Figarella-Branger, D., Virolle, T., Rougon, G., et al. (2014). Fibronectin expression in glioblastomas promotes cell cohesion, collective invasion of basement membrane in vitro and orthotopic tumor growth in mice. *Oncogene* *33*, 3451–3462.

Stieber, D., Golebiewska, A., Evers, L., Lenkiewicz, E., Brons, N.H.C., Nicot, N., Oudin, A., Bougnaud, S., Hertel, F., Bjerkvig, R., et al. (2014). Glioblastomas are composed of genetically divergent clones with distinct tumorigenic potential and variable stem cell-associated phenotypes. *Acta Neuropathol. (Berl.)* *127*, 203–219.

Szulzewsky, F., Arora, S., de Witte, L., Ulas, T., Markovic, D., Schultze, J.L., Holland, E.C., Synowitz, M., Wolf, S.A., and Kettenmann, H. (2016). Human glioblastoma-associated microglia/monocytes express a distinct RNA profile compared to human control and murine samples. *Glia* 64, 1416–1436.

Terry, R.L., and Miller, S.D. (2014). Molecular control of monocyte development. *Cell. Immunol.* 291, 16–21.

Van Obberghen-Schilling, E., Tucker, R.P., Saupe, F., Gasser, I., Cseh, B., and Orend, G. (2011). Fibronectin and tenascin-C: accomplices in vascular morphogenesis during development and tumor growth. *Int. J. Dev. Biol.* 55, 511–525.

Verhaak, R.G.W., Hoadley, K.A., Purdom, E., Wang, V., Qi, Y., Wilkerson, M.D., Miller, C.R., Ding, L., Golub, T., Mesirov, J.P., et al. (2010). Integrated genomic analysis identifies clinically relevant subtypes of glioblastoma characterized by abnormalities in PDGFRA, IDH1, EGFR, and NF1. *Cancer Cell* 17, 98–110.

de Vrij, J., Maas, S.L.N., Kwappenberg, K.M.C., Schnoor, R., Kleijn, A., Dekker, L., Luider, T.M., de Witte, L.D., Litjens, M., van Strien, M.E., et al. (2015). Glioblastoma-derived extracellular vesicles modify the phenotype of monocytic cells. *Int. J. Cancer* n/a-n/a.

Waetzig, V., Czeloth, K., Hidding, U., Mielke, K., Kanzow, M., Brecht, S., Goetz, M., Lucius, R., Herdegen, T., and Hanisch, U.-K. (2005). c-Jun N-terminal kinases (JNKs) mediate pro-inflammatory actions of microglia. *Glia* 50, 235–246.

Wilson, N.K., Miranda-Saavedra, D., Kinston, S., Bonadies, N., Foster, S.D., Calero-Nieto, F., Dawson, M.A., Donaldson, I.J., Dumon, S., Frampton, J., et al. (2009). The transcriptional program controlled by the stem cell leukemia gene *Scl/Tal1* during early embryonic hematopoietic development. *Blood* 113, 5456–5465.

Wilson, N.K., Foster, S.D., Wang, X., Knezevic, K., Schütte, J., Kaimakis, P., Chilarska, P.M., Kinston, S., Ouwehand, W.H., Dzierzak, E., et al. (2010). Combinatorial Transcriptional Control In Blood Stem/Progenitor Cells: Genome-wide Analysis of Ten Major Transcriptional Regulators. *Cell Stem Cell* 7, 532–544.

Wu, D., Lim, E., Vaillant, F., Asselin-Labat, M.-L., Visvader, J.E., and Smyth, G.K. (2010). ROAST: rotation gene set tests for complex microarray experiments. *Bioinforma. Oxf. Engl.* 26, 2176–2182.

Xia, S., Lal, B., Tung, B., Wang, S., Goodwin, C.R., and Lattera, J. (2016). Tumor microenvironment tenascin-C promotes glioblastoma invasion and negatively regulates tumor proliferation. *Neuro-Oncol.* 18, 507–517.

Zanotto-Filho, A., Gonçalves, R.M., Klafke, K., de Souza, P.O., Dillenburg, F.C., Carro, L., Gelain, D.P., and Moreira, J.C.F. (2016). Inflammatory landscape of human brain tumors reveals an NFκB dependent cytokine pathway associated with mesenchymal glioblastoma. *Cancer Lett.*

Zwang, Y., Sas-Chen, A., Drier, Y., Shay, T., Avraham, R., Lauriola, M., Shema, E., Lidor-Nili, E., Jacob-Hirsch, J., Amariglio, N., et al. (2011). Two phases of mitogenic signaling unveil roles for p53 and EGR1 in elimination of inconsistent growth signals. *Mol. Cell* 42, 524–535.

CHAPTER 8

Summary and General Discussion

This doctoral thesis presents the analysis and tools for genomic exploration in glioma cell compartments, particularly tumor and immune cells. This section summarizes the findings in each chapter and further discuss them, focusing on future perspectives.

Summary

Malignant brain tumors are highly aggressive cancers. Their diffuse forms are infiltrative neoplasms, invading the surrounding normal tissue and hampering surgical resection. Among gliomas, glioblastomas (GBMs) are the most frequent and aggressive subtype (Ostrom et al., 2015).

Studies on the heterogeneity – both intertumoral and intratumoral – of GBMs showed that these brain tumors, although histologically similar, GBMs are a heterogeneous diseases regarding both its cells and its genetic alterations (Dunn et al., 2012; Filbin and Suvà, 2016). This conclusion was only possible due to advances in large-scale molecular analysis through next generation sequencing (NGS) over the last decade. Molecular alterations predicting patients' response to treatment, overall survival and clinical outcome have been proposed and new GBM subtypes: proneural, classical and mesenchymal were identified (Brennan et al., 2013; Cancer Genome Atlas Research Network et al., 2015; Ceccarelli et al., 2016; Parsons et al., 2008; Phillips et al., 2006; Stieber et al., 2014; Verhaak et al., 2010). In **Chapter 2**, we explored the differential expression of genes associated with glioma stem cells (ID4, SOX4 and OCT-4) and showed their association with a worsening on the overall survival of GBM patients in the advent of conjoint hyper expression of these markers. In **Chapter 3**, we applied NGS technology to classify a Brazilian cohort of GBM samples. We also aimed to assess the correlation of our molecular findings using a more feasible proteomic immunohistochemistry-based approach. Our results, however, indicate the need for a genetic approach to further classify GBMs, particularly the mesenchymal subtype, as the IHC approach failed to do so. In **Chapter 4**, we explored the role of a family of transcription factors, inhibitors of differentiation (IDs) in gliomas from different origins (astrocytic and oligodendrocytic) and grades (I-IV), as well as the different GBM subtypes classified in Chapter 3. We showed an association between IDs and the proneural subtype of GBM, as well as their usefulness in differentiating between astrocytomas and oligodendrogliomas. The response to treatment between astro- and oligodendrogliomas varies, with the latter proving to be more sensitive to the standard

of care and to present a better prognosis (recently reviewed by Otani et al., 2016), highlighting the importance to differentiate both tumors. With the aim of analyzing the different cell compartments of glioma, we investigated the immune myeloid cell compartment, which comprises up to 30% of brain tumors (Roggendorf et al., 1996). In **Chapter 5**, we describe a protocol for *ex vivo* isolation of pure populations of microglia and myeloid infiltrates from the CNS, based on mechanical dissociation followed by FACS-sorting. In **Chapter 6**, we describe the use of this methodology to isolate human microglia from cortical *post-mortem* tissue. We then identified the human microglia transcriptome and assessed how these cells are affected by aging. Aside from stipulating a core of genes associated with human microglia identity, we demonstrated that genes related to actin modulation are affected during aging, possibly hampering cell motility. In **Chapter 7**, we reported the differences found in the transcriptome of glioma and normal human microglia, as well as the differences between microglia derived from lower grade gliomas and glioblastomas. We identified a transcriptional network of regulators related to cell proliferation and motility processes, as well as related to extracellular matrix, which genes presented overexpressed among the most malignant subtype of GBM (mesenchymal subtype). Our findings propose a role for microglia in GBM invasiveness and highlight their potential to be an optional complementary treatment target as a step forward to a precision medicine.

General discussion and future perspectives

GBM sub classification and its applicability

Diffuse gliomas, which include astrocytomas, oligodendrogliomas and glioblastomas, (Louis et al., 2016) are invasive CNS tumors. Complete surgical resection of these tumors is hence very difficult to achieve. The presence of residual tumor cells results in recurrence and malignant progression, albeit at different intervals. Some of lower grade tumors will either recur or progress to a GBM within months, while others will remain stable for years; the same is true for GBMs, with recurrence occurring at different rates (Cancer Genome Atlas Research Network et al., 2015; Ceccarelli et al., 2016; Foote et al., 2015; Kamoun et al., 2016). The determinant factors for one behavior or another are not yet completely understood. For GBMs, despite surgery, radiotherapy

and temozolomide chemotherapy, patient median survival is of 14.6 months, where only 10.7% of the patients is disease-free after two years (Stupp et al., 2005).

The advent of next generation sequencing and large-scale molecular analysis in the last decade has revealed that molecular alterations predict patients' response to treatment, overall survival and clinical outcome. A new light was shed on the high level of GBM heterogeneity and new subclassifications have emerged. For GBM, several studies have singled out specific determinant mutations of the main, newly identified subtypes: proneural, neural, classical and mesenchymal (Brennan et al., 2013; Cloughesy et al., 2014; Parsons et al., 2008; Phillips et al., 2006; Stieber et al., 2014; Verhaak et al., 2010).

We have performed a somatic mutation analysis in a GBM cohort utilizing a customized gene panel for next-generation sequencing (**Chapter 3**). This gene panel included all coding regions of the target genes, as well as their splicing regions. The analysis of our results made clear that the identification of GBM subtypes is not possible by targeting point mutations alone, particularly in the case of the mesenchymal subtype. The identification of mesenchymal subtype of GBM is important because it demands an aggressive treatment to improve the poor prognosis (Phillips et al., 2006; Verhaak et al., 2010). Although patients with classical and mesenchymal GBM subtype display similar overall survival, the latter also present resistance to treatment. By implementing the correct approaches to identify GBM subtypes, new discoveries leading to better clinical approaches and precision medicine might be developed.

Studies on glioma progression could also benefit from GBM subclassification. In **Chapter 4**, we analyzed a family of genes, inhibitors of differentiation (IDs), associated to specific low-grade gliomas and to the proneural GBM subtype. As prognostic markers, this family of genes could help guide treatment course in the long run, as proneural GBMs were also shown to progress to a mesenchymal GBM profile (Segerman et al., 2016). More recent studies have focused on the identification of genetic profiles for low-grade gliomas (Cancer Genome Atlas Research Network et al., 2015; Ceccarelli et al., 2016), also concluding that genetic status was more reflective of the disease subtypes than was histologic class. The genetic pathways leading to glioma progression are progressively being unraveled, providing possible intervention targets. Although still costly and sometimes laborious, genetic profiling has proven its value as an overall survival predictor and to the understanding of glioma biology.

Immune microenvironment in the treatment of gliomas

Innate immune cells, such as microglia are major components of the glioma microenvironment. There are conflicting studies regarding the role of such cells in tumor progression. While some claim better outcomes for patients with high levels of immune cells, either by peripheral infiltration or from resident cells in the tissue, many others have assessed the same phenomena to be related to a poorer prognosis (reviewed by Fridman et al., 2012). Such divergence in results seems to arise from the different functional and activation states that innate immune cells can adopt within the same tumor at different time points. Considering their ability to respond readily to stimuli, changes in microenvironment can lead to both anti- or pro-tumoral responses. Immune evasion, one of the hallmarks of cancer (Hanahan, 2014), is characterized by the ability tumor cells have to manipulate the immune system via secretion of cytokines and growth factors. This process may promote tumor progression and escape from destruction, and it is crucially dependent on the crosstalk between these two types of cells. In the scope of glioma, in addition to target highly heterogeneous tumor cells, also targeting non-neoplastic cells, particularly microglia and iTAMs, seems an attractive gambit to overcome the mechanisms associated with recurrence and therapeutic resistance. New insights on how the immune cells respond to tumor signals and which molecules they release to support tumor growth and progression will prove valuable.

New perspectives for cancer treatment have risen with the onset of immunotherapy-based treatments. For gliomas, however, there are several issues to be resolved, the main of which is the blood-brain barrier (BBB) which prevents CNS entry of certain macromolecules and hampers drug delivery (Preusser et al., 2015). Nonetheless, there are immune checkpoints in the crosstalk between glioma cells and leucocytes that can be approached. The first of which is the uptake of antigens released by tumor cells by APCs (microglia and iTAMs), as well as the initial changes in phenotype these cells undergo. The early interaction between APCs and tumor cells has been particularly difficult to track in human gliomas so far. The process is followed by migration of APCs to lymph nodes and presentation of antigens to T cells. When T cells infiltrate the brain, their interaction with tumor cells and tumor supportive microglia/iTAMs results in the release of immunosuppressive factors, leading to tumor cell immune evasion instead of immune destruction.

The most successful immunotherapy drugs have targeted the mid to late phases of immune checkpoints, namely the presentation of antigens to T cells and the

interactions between activated T cells and tumor/myeloid cells. By further and thoroughly exploring early immune checkpoints, such as the early interaction between tumor cells and APCs, new potential complimentary targets may be revealed.

Paving the way for glioma-microenvironment interaction studies: human microglia profile in homeostasis and glioma

The human CNS immune cells transcriptome is necessary to address their functional changes upon stimuli from glioma cells. While there are several reports on mouse microglia gene expression profiles, both under physiological and disease conditions (recently reviewed by (Hambardzumyan et al., 2016; Prinz and Priller, 2017), reports on human microglia transcriptome data were still scarce due to several reasons.

The first challenge was to achieve an isolation protocol preserving homeostatic features of microglia and CNS infiltrative cells. In **Chapter 5**, we describe such protocol with adapted improvements from previous publications (Becher and Antel, 1996; Melief et al., 2012; Olah et al., 2012). Subsequent flow cytometry and gene expression analysis showed that isolated cells through our developed protocol retained their steady state features.

The next challenge was related to what kind of brain sample to use as starting point to profile microglia. Recent studies on human microglia have reported the transcriptome findings in cells derived from either epilepsy or tumor surgery, and in a restricted number of samples (Bennett et al., 2016; Spaethling et al., 2017; Zhang et al., 2016b). In **Chapter 6**, we present the characterization of an extensive cohort of human microglia derived from *postmortem* cortical brain tissue. We compared the human microglia to a mouse microglia transcriptome profile generated in our groups and to the previously reported human and mouse microglia datasets. The analysis of these datasets using the same bioinformatics pipeline allowed to elucidate the (dis)similarities between microglia profile between these species. Recent studies have reexamined the validity of mouse models to study microglia in aging and neurodegenerative conditions (Smith and Dragunow, 2014). As our cohort comprised individuals with ages ranging from late thirties to over 100 years old, our dataset also allowed to address what age-related changes occur in human microglia during aging and to what degree they overlap with mouse microglia aging and priming signatures.

We established a core human microglia gene signature and the functional properties associated with these genes by gene ontology analysis. As expected, many significantly enriched terms associated with the innate immune activity of microglia, like 'immune response', 'defense response', cytokine production' were present. The profile was also enriched for 'phagocytosis', 'cell migration', 'cell motility', confirming that human microglia are the immunocompetent and phagocytic cells of the CNS that express a wide range of immune receptors and ligands, equipped to respond to a wide variety of pathogen- and damage-associated molecules. Interestingly, although human microglia seem to possess a highly activated pathway for proliferation with genes involved in cell cycle highly expressed, this pathway seems to be dependent on extracellular signals. This data corroborates the recently reported findings regarding the turnover rate of microglia in both mouse and humans (Askew et al., 2017), in which the authors concluded that microglia cell levels are maintained throughout adult life in a tightly regulated mechanism alternating between proliferation and apoptosis.

Microglia-specific transcriptional regulators were also identified in the human microglia core genes. These include transcription factors required for microglia ontogeny SPI-1 (or PU.1) and IRF8 (Kierdorf et al., 2013), along with CIITA, a positive regulator of MHC-II gene transcription; TRIM22, a transcription activator induced by interferon; MNDA, an interferon target gene; IRF5, a factor modulating inflammatory responses; TAL1, a transcription factor associated with microglia aging (Wehrspaun et al., 2015); and IFI16, an interferon gamma inducible gene. A large number of members of the core microglia signature were regulated by these transcription factors, suggesting their critical role in human microglia identity.

An extensive overlap between the transcriptome of human and mouse microglia was found, however, few genes were exclusively represented in human microglia, without any mouse orthologues. Despite the absence of any specific associated biological pathways, significant roles as host defense and modulation of immune responses can be attributed to these human-exclusive genes. This might indicate a possible evolutionary role for these genes in the immune development of the brain.

Microglia are highly ramified and with motile processes that constantly survey their immediate surroundings (Davalos et al., 2005; Nimmerjahn et al., 2005). Gene expression changes in these processes, like integrins and actin (de)polymerization and remodeling were observed in the microglia profile when age was considered as a variable. Purinergic receptors and their downstream signaling are implicated in

chemotaxis and part of the microglia sensome (Ferrari et al., 2016; Hickman et al., 2013). Movement of the fine microglial processes to sense the environment and initiate chemotaxis is primarily governed through the activation of P2Y12 receptors. P2RY12, is an established microglia marker (Butovsky et al., 2014; Hickman et al., 2013). This gene was also downregulated with aging in our cohort, further highlighting the impairment of microglia motility with aging.

Genes varying with age related to inflammation/priming as previously reported in mouse aging models (Holtman et al., 2015; Raj et al., 2015) were not observed in the present study. Instead, important immune regulators participating in cell adhesion were detected. In our analysis, human and mouse microglia transcriptome similarities were mostly associated to a disequilibrium in cell adhesion and motility related pathways.

Another noteworthy result from our analysis of human microglia was that *postmortem* delay (PMD), ranging from 4-24h interval, had no effect on the transcriptome, corroborating previous reports that PMD does not correlate with RNA quality or integrity (Chevyreva et al., 2008; Durrenberger et al., 2010; Ervin et al., 2007). This confirmation is highly relevant allowing the use of this source of human specimens for future studies.

In **Chapter 7**, we demonstrated the differences found between glioma and normal microglia, as well as the comparison between microglia derived from lower grade gliomas (LGG) and from glioblastomas (GBM). We compared our tumor microglia to a set of normal microglia samples from the study in Chapter 6. The comparison to post-mortem brain derived microglia permitted to avoid the already known bias of comparisons to microglia derived from epilepsy cases.

Tumor microglia showed an expected heterogeneity in their gene expression, just as heterogeneity is demonstrated in tumor tissue (Filbin and Suvà, 2016). These results led us to speculate that different activation signaling pathways occur within the same tumor sample. Microglia are subject to a number of signals from different clones of tumor cells, driving different responses along the progression of neoplasia, increasing its tumorigenicity. One alternative to elucidate how human microglia respond to stimuli from cells in each of glioma niches is to focus on single cell sequencing analysis. Such studies have been conducted on glioma cells in recent works (Meyer et al., 2015; Patel et al., 2014; Tirosh et al., 2016), revealing important mechanisms of drug response, growth, and differentiation potential related to specific

genetic alterations. Using the same approach to microglia would elucidate their definitive role in tumorigenesis and progression.

The biological pathways associated with the differentially expressed genes in tumor *versus* normal microglia were not restricted to inflammation related pathways, neither to the M1/M2 paradigm (Glass and Synowitz, 2014). Prominent changes in proliferation, cell cycle control and motility, including extracellular matrix related pathways were also detected. It also seems that, even if markers previously identified in non-neoplastic microglia are still expressed, tumor microglia undergo such drastic changes upon glioma stimuli, that the “quiescence” markers are supplanted by others.

With stringent criteria, we determined the core genes for both GBM and LGG microglia, and through independent component analysis, we were able to assess the differentially expressed genes according to the molecular stratification of the analyzed gliomas. A great portion of signature genes from LGG microglia were also present in GBM microglia, but at higher levels. This increased expression might reflect the progression in malignancy as previously described (Hambardzumyan et al., 2016), reinforcing the hypothesis that microglia play a crucial role in the progression of gliomas.

An explicitly inflammatory phenotype was not detected in tumor microglia. Previous murine studies (a Dzaye et al., 2016; Sielska et al., 2013; Zhang et al., 2016a) revealed that microglia display an inflammatory profile – either pro- or anti-inflammatory – upon interaction with glioma cells, and speculation on how each of these phenotypes promote or hamper tumor growth have been made. However, our dataset depicted a balance in the expression of chemokines and secreted factors that characterize both phenotypes, not permitting any determination of a specific inflammatory profile for human microglia along glioma progression.

Our analysis revealed that tumor microglia express high levels of genes related to extracellular matrix (ECM) remodeling, such as fibronectin (*FN1*), tenascin-C (TNC) and thrombospondin-1 (*THBS1*), along with invasiveness-related genes as *ANXA2*. The proteins encoded by these genes have been previously associated to glioma tumorigenicity and invasiveness (Blandin et al., 2016; Colin et al., 2006; Kling et al., 2016; Maule et al., 2016; Serres et al., 2014; Van Obberghen-Schilling et al., 2011; Xia et al., 2016). However, these previous studies focused on tumor cells, while the present analysis identified microglia as presenting high expression levels for these genes.

Among GBM subtypes, genes encoding ECM proteins were most abundant in mesenchymal subtypes, associated to the highest invasive rate and the worst prognosis

(Balbous et al., 2014; Carro et al., 2010). These genes highly expressed in microglia are attractive targets for treatment options to prevent invasion of the surrounding CNS parenchyma by tumor cells. Microglia are extremely mobile cells, needing to migrate to exert their function, both in homeostatic and pathological conditions. It is interesting then, that the main biological processes affected in microglia in both aging – a physiological process – and by glioma were related to motility, migration and invasion.

Functional studies focusing on the early changes that human microglia undergo upon interaction with glioma will further elucidate the results presented herein. Recent reports have advanced in the culturing of human microglia, allowing for newer approaches on the manipulation of these cells. It is now possible to derive microglia-like cells from both iPS and embryonic stem cells, and culture them for longer periods (Muffat et al., 2016; Rustenhoven et al., 2016), creating new opportunities for assessing the crosstalk between tumor cells and microglia.

Final considerations

We explored the current genetic approaches for glioma studies, and demonstrated the relevant role of molecular profiling. We had also expanded our study to the innate immune compartment, first analyzing a pure population of non-neoplastic cohort of microglia and further comparing them to glioma-derived cells. Our data sheds new light on the transcriptome changes that human microglia undergoes upon both aging and glioma stimuli towards tumor progression. These findings will guide the next step studies to further deepen the knowledge on this domain.

Many aspects regarding the players in glioma progression remain to be elucidated. We showed here that heterogeneity within the tumor is not restricted to cancer cells, but also to microglia. Other cells from the tumor microenvironment, such as endothelial cells, astrocytes and pericytes, could also present such intrinsic populational differences. Single-cell sequencing analysis of diverse cell types could further aid understanding how they affect / are affected by glioma cells. Recent report on mass cytometry used for single cell analysis in solid tumors (including glioma) demonstrated the possibility to isolate several populations from the same human sample (Leelatian et al., 2017). Along with next generation sequencing analysis, these would be elegant approaches to tumor heterogeneity.

A recent molecular study using a large cohort of human glioma samples revealed discrete pathways in tumor progression to be associated with epigenetic

mechanisms of control (Ceccarelli et al., 2016). Epigenetic changes, such as histone modifications and chromatin-remodeling complexes, play a role in gene transcription following stimuli, from either pathogens, injuries or tumor cells. This phenomenon involves a series of proteins that “read”, “write” and “erase” epigenetic signals, either by inherited characteristics or by stimuli response (Mehta and Jeffrey, 2015). These changes have been included in glioma classification and are now considered crucial for determining therapeutic strategies (recently reviewed by (Reifenberger et al., 2016). In myeloid cells, these changes occur within hours and are tightly associated with the microenvironment, as observed by studies using mouse microglia and tissue macrophages (Gosselin et al., 2014; Lavin et al., 2014) and, more recently, human macrophages differentiated from blood monocytes (Schmidt et al., 2016). Studies on human microglia or iTAMs epigenetic changes upon stimuli are still lacking. Functional co-culturing experiments with glioma and microglia cells would allow to assess these early changes.

Another aspect to be assessed is whether microglia from different regions in human brain display different transcriptional profiles. In mice, this has been previously shown (Grabert et al., 2016), as well as for human total brain tissue (Hawrylycz et al., 2012; Oldham et al., 2008). Considering different tumor can rise in different regions of the brain, understanding what is the “quiescent” profile of the local immune cells would help explore how these cells would respond to tumorigenesis.

The scientific field is experiencing an era in which the discoveries made today can reach clinical application much faster than in previous times. Cancer biology research has expanded its interest from just looking into tumor cells, but also focusing on the microenvironment. The results of such approach will much benefit future and innovative treatment options.

REFERENCES

Askew, K., Li, K., Olmos-Alonso, A., Garcia-Moreno, F., Liang, Y., Richardson, P., Tipton, T., Chapman, M.A., Riecken, K., Beccari, S., et al. (2017). Coupled Proliferation and Apoptosis Maintain the Rapid Turnover of Microglia in the Adult Brain. *Cell Rep.* *18*, 391–405.

Balbous, A., Cortes, U., Guilloteau, K., Villalva, C., Flamant, S., Gaillard, A., Milin, S., Wager, M., Sorel, N., Guilhot, J., et al. (2014). A mesenchymal glioma stem cell profile is related to clinical outcome. *Oncogenesis* *3*, e91.

Becher, B., and Antel, J.P. (1996). Comparison of phenotypic and functional properties of immediately ex vivo and cultured human adult microglia. *Glia* *18*, 1–10.

Bennett, M.L., Bennett, F.C., Liddelow, S.A., Ajami, B., Zamanian, J.L., Fernhoff, N.B., Mulinyawe, S.B., Bohlen, C.J., Adil, A., Tucker, A., et al. (2016). New tools for studying microglia in the mouse and human CNS. *Proc. Natl. Acad. Sci. U. S. A.* *113*, E1738–E1746.

Blandin, A.-F., Noulet, F., Renner, G., Mercier, M.-C., Choulier, L., Vauchelles, R., Ronde, P., Carreiras, F., Etienne-Selloum, N., Vereb, G., et al. (2016). Glioma cell dispersion is driven by $\alpha 5$ integrin-mediated cell-matrix and cell-cell interactions. *Cancer Lett.* *376*, 328–338.

Brennan, C.W., Verhaak, R.G.W., McKenna, A., Campos, B., Noushmehr, H., Salama, S.R., Zheng, S., Chakravarty, D., Sanborn, J.Z., Berman, S.H., et al. (2013). The somatic genomic landscape of glioblastoma. *Cell* *155*, 462–477.

Butovsky, O., Jedrychowski, M.P., Moore, C.S., Cialic, R., Lanser, A.J., Gabriely, G., Koeglsperger, T., Dake, B., Wu, P.M., Doykan, C.E., et al. (2014). Identification of a unique TGF- β -dependent molecular and functional signature in microglia. *Nat. Neurosci.* *17*, 131–143.

Cancer Genome Atlas Research Network, Brat, D.J., Verhaak, R.G.W., Aldape, K.D., Yung, W.K.A., Salama, S.R., Cooper, L.A.D., Rheinbay, E., Miller, C.R., Vitucci, M., et al. (2015). Comprehensive, Integrative Genomic Analysis of Diffuse Lower-Grade Gliomas. *N. Engl. J. Med.* *372*, 2481–2498.

Carro, M.S., Lim, W.K., Alvarez, M.J., Bollo, R.J., Zhao, X., Snyder, E.Y., Sulman, E.P., Anne, S.L., Doetsch, F., Colman, H., et al. (2010). The transcriptional network for mesenchymal transformation of brain tumours. *Nature* *463*, 318–325.

Ceccarelli, M., Barthel, F.P., Malta, T.M., Sabedot, T.S., Salama, S.R., Murray, B.A., Morozova, O., Newton, Y., Radenbaugh, A., Pagnotta, S.M., et al. (2016). Molecular

Profiling Reveals Biologically Discrete Subsets and Pathways of Progression in Diffuse Glioma. *Cell* 164, 550–563.

Chevyreva, I., Faull, R.L.M., Green, C.R., and Nicholson, L.F.B. (2008). Assessing RNA quality in postmortem human brain tissue. *Exp. Mol. Pathol.* 84, 71–77.

Cloughesy, T.F., Cavenee, W.K., and Mischel, P.S. (2014). Glioblastoma: from molecular pathology to targeted treatment. *Annu. Rev. Pathol.* 9, 1–25.

Colin, C., Baeza, N., Bartoli, C., Fina, F., Eudes, N., Nanni, I., Martin, P.-M., Ouafik, L., and Figarella-Branger, D. (2006). Identification of genes differentially expressed in glioblastoma versus pilocytic astrocytoma using Suppression Subtractive Hybridization. *Oncogene* 25, 2818–2826.

Davalos, D., Grutzendler, J., Yang, G., Kim, J.V., Zuo, Y., Jung, S., Littman, D.R., Dustin, M.L., and Gan, W.-B. (2005). ATP mediates rapid microglial response to local brain injury in vivo. *Nat. Neurosci.* 8, 752–758.

Dunn, G.P., Rinne, M.L., Wykosky, J., Genovese, G., Quayle, S.N., Dunn, I.F., Agarwalla, P.K., Chheda, M.G., Campos, B., Wang, A., et al. (2012). Emerging insights into the molecular and cellular basis of glioblastoma. *Genes Dev.* 26, 756–784.

Durrenberger, P.F., Fernando, S., Kashefi, S.N., Ferrer, I., Hauw, J.-J., Seilhean, D., Smith, C., Walker, R., Al-Sarraj, S., Troakes, C., et al. (2010). Effects of antemortem and postmortem variables on human brain mRNA quality: a BrainNet Europe study. *J. Neuropathol. Exp. Neurol.* 69, 70–81.

a Dzaye, O.D., Hu, F., Derkow, K., Haage, V., Euskirchen, P., Harms, C., Lehnardt, S., Synowitz, M., Wolf, S.A., and Kettenmann, H. (2016). Glioma Stem Cells but Not Bulk Glioma Cells Upregulate IL-6 Secretion in Microglia/Brain Macrophages via Toll-like Receptor 4 Signaling. *J. Neuropathol. Exp. Neurol.* 75, 429–440.

Ervin, J.F., Heinzen, E.L., Cronin, K.D., Goldstein, D., Szymanski, M.H., Burke, J.R., Welsh-Bohmer, K.A., and Hulette, C.M. (2007). Postmortem delay has minimal effect on brain RNA integrity. *J. Neuropathol. Exp. Neurol.* 66, 1093–1099.

Ferrari, D., McNamee, E.N., Idzko, M., Gambari, R., and Eltzschig, H.K. (2016). Purinergic Signaling During Immune Cell Trafficking. *Trends Immunol.* 37, 399–411.

Filbin, M.G., and Suvà, M.L. (2016). Gliomas Genomics and Epigenomics: Arriving at the Start and Knowing It for the First Time. *Annu. Rev. Pathol.* 11, 497–521.

Foote, M.B., Papadopoulos, N., and Diaz, L.A. (2015). Genetic Classification of Gliomas: Refining Histopathology. *Cancer Cell* 28, 9–11.

Fridman, W.H., Pagès, F., Sautès-Fridman, C., and Galon, J. (2012). The immune contexture in human tumours: impact on clinical outcome. *Nat. Rev. Cancer* 12, 298–306.

Glass, R., and Synowitz, M. (2014). CNS macrophages and peripheral myeloid cells in brain tumours. *Acta Neuropathol. (Berl.)* 128, 347–362.

Gosselin, D., Link, V.M., Romanoski, C.E., Fonseca, G.J., Eichenfield, D.Z., Spann, N.J., Stender, J.D., Chun, H.B., Garner, H., Geissmann, F., et al. (2014). Environment Drives Selection and Function of Enhancers Controlling Tissue-Specific Macrophage Identities. *Cell* 159, 1327–1340.

Grabert, K., Michoel, T., Karavolos, M.H., Clohisey, S., Baillie, J.K., Stevens, M.P., Freeman, T.C., Summers, K.M., and McColl, B.W. (2016). Microglial brain region-dependent diversity and selective regional sensitivities to aging. *Nat. Neurosci.* 19, 504–516.

Hambardzumyan, D., Gutmann, D.H., and Kettenmann, H. (2016). The role of microglia and macrophages in glioma maintenance and progression. *Nat. Neurosci.* 19, 20–27.

Hanahan, D. (2014). Rethinking the war on cancer. *Lancet Lond. Engl.* 383, 558–563.

Hawrylycz, M.J., Lein, E.S., Guillozet-Bongaarts, A.L., Shen, E.H., Ng, L., Miller, J.A., van de Lagemaat, L.N., Smith, K.A., Ebbert, A., Riley, Z.L., et al. (2012). An anatomically comprehensive atlas of the adult human brain transcriptome. *Nature* 489, 391–399.

Hickman, S.E., Kingery, N.D., Ohsumi, T.K., Borowsky, M.L., Wang, L., Means, T.K., and El Khoury, J. (2013). The microglial sensome revealed by direct RNA sequencing. *Nat. Neurosci.* 16, 1896–1905.

Holtman, I.R., Raj, D.D., Miller, J.A., Schaafsma, W., Yin, Z., Brouwer, N., Wes, P.D., Möller, T., Orre, M., Kamphuis, W., et al. (2015). Induction of a common microglia gene expression signature by aging and neurodegenerative conditions: a co-expression meta-analysis. *Acta Neuropathol. Commun.* 3, 31.

Kamoun, A., Idbah, A., Dehais, C., Elarouci, N., Carpentier, C., Letouzé, E., Colin, C., Mokhtari, K., Jouvet, A., Uro-Coste, E., et al. (2016). Integrated multi-omics analysis of oligodendroglial tumours identifies three subgroups of 1p/19q co-deleted gliomas. *Nat. Commun.* 7, 11263.

Kierdorf, K., Erny, D., Goldmann, T., Sander, V., Schulz, C., Perdiguero, E.G., Wieghofer, P., Heinrich, A., Riemke, P., Hölscher, C., et al. (2013). Microglia emerge from

erythromyeloid precursors via Pu.1- and Irf8-dependent pathways. *Nat. Neurosci.* *16*, 273–280.

Kling, T., Ferrarese, R., Ó hAilín, D., Johansson, P., Heiland, D.H., Dai, F., Vasilikos, I., Weyerbrock, A., Jörnsten, R., Carro, M.S., et al. (2016). Integrative Modeling Reveals Annexin A2-mediated Epigenetic Control of Mesenchymal Glioblastoma. *EBioMedicine* *12*, 72–85.

Lavin, Y., Winter, D., Blecher-Gonen, R., David, E., Keren-Shaul, H., Merad, M., Jung, S., and Amit, I. (2014). Tissue-Resident Macrophage Enhancer Landscapes Are Shaped by the Local Microenvironment. *Cell* *159*, 1312–1326.

Leelatian, N., Doxie, D.B., Greenplate, A.R., Mobley, B.C., Lehman, J.M., Sinnaeve, J., Kauffmann, R.M., Werkhaven, J.A., Mistry, A.M., Weaver, K.D., et al. (2017). Single cell analysis of human tissues and solid tumors with mass cytometry. *Cytometry B Clin. Cytom.* *92*, 68–78.

Louis, D.N., Perry, A., Reifenberger, G., von Deimling, A., Figarella-Branger, D., Cavenee, W.K., Ohgaki, H., Wiestler, O.D., Kleihues, P., and Ellison, D.W. (2016). The 2016 World Health Organization Classification of Tumors of the Central Nervous System: a summary. *Acta Neuropathol. (Berl.)* *131*, 803–820.

Maule, F., Bresolin, S., Rampazzo, E., Boso, D., Della Puppa, A., Esposito, G., Porcù, E., Mitola, S., Lombardi, G., Accordi, B., et al. (2016). Annexin 2A sustains glioblastoma cell dissemination and proliferation. *Oncotarget* *7*, 54632–54649.

Mehta, S., and Jeffrey, K.L. (2015). Beyond receptors and signaling: epigenetic factors in the regulation of innate immunity. *Immunol. Cell Biol.* *93*, 233–244.

Melief, J., Koning, N., Schuurman, K.G., Van De Garde, M.D.B., Smolders, J., Hoek, R.M., Van Eijk, M., Hamann, J., and Huitinga, I. (2012). Phenotyping primary human microglia: tight regulation of LPS responsiveness. *Glia* *60*, 1506–1517.

Meyer, M., Reimand, J., Lan, X., Head, R., Zhu, X., Kushida, M., Bayani, J., Pressey, J.C., Lionel, A.C., Clarke, I.D., et al. (2015). Single cell-derived clonal analysis of human glioblastoma links functional and genomic heterogeneity. *Proc. Natl. Acad. Sci.* *112*, 851–856.

Muffat, J., Li, Y., Yuan, B., Mitalipova, M., Omer, A., Corcoran, S., Bakiasi, G., Tsai, L.-H., Aubourg, P., Ransohoff, R.M., et al. (2016). Efficient derivation of microglia-like cells from human pluripotent stem cells. *Nat. Med.* *22*, 1358–1367.

Nimmerjahn, A., Kirchhoff, F., and Helmchen, F. (2005). Resting microglial cells are highly dynamic surveillants of brain parenchyma in vivo. *Science* *308*, 1314–1318.

Olah, M., Raj, D., Brouwer, N., De Haas, A.H., Eggen, B.J.L., Den Dunnen, W.F.A., Biber, K.P.H., and Boddeke, H.W.G.M. (2012). An optimized protocol for the acute isolation of human microglia from autopsy brain samples. *Glia* 60, 96–111.

Oldham, M.C., Konopka, G., Iwamoto, K., Langfelder, P., Kato, T., Horvath, S., and Geschwind, D.H. (2008). Functional organization of the transcriptome in human brain. *Nat. Neurosci.* 11, 1271–1282.

Ostrom, Q.T., Gittleman, H., Fulop, J., Liu, M., Blanda, R., Kromer, C., Wolinsky, Y., Kruchko, C., and Barnholtz-Sloan, J.S. (2015). CBTRUS Statistical Report: Primary Brain and Central Nervous System Tumors Diagnosed in the United States in 2008-2012. *Neuro-Oncol.* 17 Suppl 4, iv1-iv62.

Otani, R., Uzuka, T., and Ueki, K. (2016). Classification of adult diffuse gliomas by molecular markers-a short review with historical footnote. *Jpn. J. Clin. Oncol.*

Parsons, D.W., Jones, S., Zhang, X., Lin, J.C.-H., Leary, R.J., Angenendt, P., Mankoo, P., Carter, H., Siu, I.-M., Gallia, G.L., et al. (2008). An integrated genomic analysis of human glioblastoma multiforme. *Science* 321, 1807–1812.

Patel, A.P., Tirosch, I., Trombetta, J.J., Shalek, A.K., Gillespie, S.M., Wakimoto, H., Cahill, D.P., Nahed, B.V., Curry, W.T., Martuza, R.L., et al. (2014). Single-cell RNA-seq highlights intratumoral heterogeneity in primary glioblastoma. *Science* 344, 1396–1401.

Phillips, H.S., Kharbanda, S., Chen, R., Forrest, W.F., Soriano, R.H., Wu, T.D., Misra, A., Nigro, J.M., Colman, H., Soroceanu, L., et al. (2006). Molecular subclasses of high-grade glioma predict prognosis, delineate a pattern of disease progression, and resemble stages in neurogenesis. *Cancer Cell* 9, 157–173.

Preusser, M., Lim, M., Hafler, D.A., Reardon, D.A., and Sampson, J.H. (2015). Prospects of immune checkpoint modulators in the treatment of glioblastoma. *Nat. Rev. Neurol.* 11, 504–514.

Prinz, M., and Priller, J. (2017). The role of peripheral immune cells in the CNS in steady state and disease. *Nat. Neurosci.* 20, 136–144.

Raj, D.D.A., Moser, J., van der Pol, S.M.A., van Os, R.P., Holtman, I.R., Brouwer, N., Oeseburg, H., Schaafsma, W., Wesseling, E.M., den Dunnen, W., et al. (2015). Enhanced microglial pro-inflammatory response to lipopolysaccharide correlates with brain infiltration and blood-brain barrier dysregulation in a mouse model of telomere shortening. *Aging Cell.*

Reifenberger, G., Wirsching, H.-G., Knobbe-Thomsen, C.B., and Weller, M. (2016). Advances in the molecular genetics of gliomas - implications for classification and therapy. *Nat. Rev. Clin. Oncol.*

Roggendorf, W., Strupp, S., and Paulus, W. (1996). Distribution and characterization of microglia/macrophages in human brain tumors. *Acta Neuropathol. (Berl.)* 92, 288–293.

Rustenhoven, J., Park, T.I.-H., Schweder, P., Scotter, J., Correia, J., Smith, A.M., Gibbons, H.M., Oldfield, R.L., Bergin, P.S., Mee, E.W., et al. (2016). Isolation of highly enriched primary human microglia for functional studies. *Sci. Rep.* 6, 19371.

Schmidt, S.V., Krebs, W., Ulas, T., Xue, J., Baßler, K., Günther, P., Hardt, A.-L., Schultze, H., Sander, J., Klee, K., et al. (2016). The transcriptional regulator network of human inflammatory macrophages is defined by open chromatin. *Cell Res.* 26, 151–170.

Segerman, A., Niklasson, M., Haglund, C., Bergström, T., Jarvius, M., Xie, Y., Westermark, A., Sönmez, D., Hermansson, A., Kastemar, M., et al. (2016). Clonal Variation in Drug and Radiation Response among Glioma-Initiating Cells Is Linked to Proneural-Mesenchymal Transition. *Cell Rep.* 17, 2994–3009.

Serres, E., Debarbieux, F., Stanchi, F., Maggiorella, L., Grall, D., Turchi, L., Burel-Vandenbos, F., Figarella-Branger, D., Virolle, T., Rougon, G., et al. (2014). Fibronectin expression in glioblastomas promotes cell cohesion, collective invasion of basement membrane in vitro and orthotopic tumor growth in mice. *Oncogene* 33, 3451–3462.

Sielska, M., Przanowski, P., Wylot, B., Gabrusiewicz, K., Maleszewska, M., Kijewska, M., Zawadzka, M., Kucharska, J., Vinnakota, K., Kettenmann, H., et al. (2013). Distinct roles of CSF family cytokines in macrophage infiltration and activation in glioma progression and injury response. *J. Pathol.* 230, 310–321.

Smith, A.M., and Dragunow, M. (2014). The human side of microglia. *Trends Neurosci.* 37, 125–135.

Spaethling, J.M., Na, Y.-J., Lee, J., Ulyanova, A.V., Baltuch, G.H., Bell, T.J., Brem, S., Chen, H.I., Dueck, H., Fisher, S.A., et al. (2017). Primary Cell Culture of Live Neurosurgically Resected Aged Adult Human Brain Cells and Single Cell Transcriptomics. *Cell Rep.* 18, 791–803.

Stieber, D., Golebiewska, A., Evers, L., Lenkiewicz, E., Brons, N.H.C., Nicot, N., Oudin, A., Bougnaud, S., Hertel, F., Bjerkvig, R., et al. (2014). Glioblastomas are composed of genetically divergent clones with distinct tumourigenic potential and variable stem cell-associated phenotypes. *Acta Neuropathol. (Berl.)* 127, 203–219.

Stupp, R., Mason, W.P., van den Bent, M.J., Weller, M., Fisher, B., Taphoorn, M.J.B., Belanger, K., Brandes, A.A., Marosi, C., Bogdahn, U., et al. (2005). Radiotherapy plus concomitant and adjuvant temozolomide for glioblastoma. *N. Engl. J. Med.* *352*, 987–996.

Tirosh, I., Venteicher, A.S., Hebert, C., Escalante, L.E., Patel, A.P., Yizhak, K., Fisher, J.M., Rodman, C., Mount, C., Filbin, M.G., et al. (2016). Single-cell RNA-seq supports a developmental hierarchy in human oligodendroglioma. *Nature* *539*, 309–313.

Van Obberghen-Schilling, E., Tucker, R.P., Saupe, F., Gasser, I., Cseh, B., and Orend, G. (2011). Fibronectin and tenascin-C: accomplices in vascular morphogenesis during development and tumor growth. *Int. J. Dev. Biol.* *55*, 511–525.

Verhaak, R.G.W., Hoadley, K.A., Purdom, E., Wang, V., Qi, Y., Wilkerson, M.D., Miller, C.R., Ding, L., Golub, T., Mesirov, J.P., et al. (2010). Integrated genomic analysis identifies clinically relevant subtypes of glioblastoma characterized by abnormalities in PDGFRA, IDH1, EGFR, and NF1. *Cancer Cell* *17*, 98–110.

Wehrspaun, C.C., Haerty, W., and Ponting, C.P. (2015). Microglia recapitulate a hematopoietic master regulator network in the aging human frontal cortex. *Neurobiol. Aging* *36*, 2443.e9-2443.e20.

Xia, S., Lal, B., Tung, B., Wang, S., Goodwin, C.R., and Laterra, J. (2016). Tumor microenvironment tenascin-C promotes glioblastoma invasion and negatively regulates tumor proliferation. *Neuro-Oncol.* *18*, 507–517.

Zhang, I., Alizadeh, D., Liang, J., Zhang, L., Gao, H., Song, Y., Ren, H., Ouyang, M., Wu, X., D'Apuzzo, M., et al. (2016a). Characterization of Arginase Expression in Glioma-Associated Microglia and Macrophages. *PloS One* *11*, e0165118.

Zhang, Y., Sloan, S.A., Clarke, L.E., Caneda, C., Plaza, C.A., Blumenthal, P.D., Vogel, H., Steinberg, G.K., Edwards, M.S.B., Li, G., et al. (2016b). Purification and Characterization of Progenitor and Mature Human Astrocytes Reveals Transcriptional and Functional Differences with Mouse. *Neuron* *89*, 37–53.

HOOFDSTUK 9

Nederlandse samenvatting

Nederlandse samenvatting

Kwaadaardige hersentumoren zijn zeer agressief, ze dringen het omliggende normale hersenweefsel binnen en zijn daardoor chirurgisch moeilijk te verwijderen. Van de kwaadaardige hersentumoren is glioblastoma multiforme (GBM) de meest voorkomende en het meest agressieve subtype (Ostrom et al., 2015).

Studies naar de diversiteit van GBM, – zowel binnen een tumor als tussen verschillende tumoren- heeft aangetoond dat deze hersentumoren, terwijl ze microscopisch erg op elkaar lijken, erg heterogeen zijn op moleculair niveau (Dunn et al., 2012; Filbin and Suvà, 2016). Dit inzicht is gedurende het afgelopen decennium tot stand gekomen door grootschalige moleculaire analyses van deze tumoren met behulp van next generation sequencing (NGS). Deze moleculaire veranderingen hebben een voorspellende waarde voor de werkzaamheid van bepaalde behandelingen, en de overlevingskans en overlevingsduur van de patiënt. Op grond van deze analyses zijn de volgende GBM subtypes zijn vastgesteld: proneuraal, klassiek en mesenchymaal (Brennan et al., 2013; Cancer Genome Atlas Research Network et al., 2015; Ceccarelli et al., 2016; Parsons et al., 2008; Phillips et al., 2006; Stieber et al., 2014; Verhaak et al., 2010).

In dit proefschrift hebben we NGS technologie toegepast om een Braziliaans cohort van GBM tumoren te classificeren. Het doel was de moleculaire classificatie door middel van gen sequensen te bevestigen met een eenvoudiger en handzamer methode, namelijk door microscopische analyse van tumorweefsel, aangekleurd met specifieke antilichamen. Onze data lieten echter zien, dat een moleculair genetische classificatie momenteel noodzakelijk is, vooral voor het mesenchymale GBM subtype (Hoofdstuk 2).

Een familie van transcriptie factoren, inhibitors of differentiation (IDs), speelt een rol in verschillende subtypen gliomen. Onderzoek is verricht naar IDs in astrocytomen en oligodendrogliomas, van verschillende gradaties (I-IV). We lieten een verband zien tussen IDs en het proneurale GBM subtype, en dat met IDs onderscheid gemaakt kon worden tussen astrocytomen en oligodendrogliomas. Astrocytomen and oligodendrogliomas reageren anders op behandelingen, waarbij oligodendrogliomas gevoeliger zijn voor gebruikelijke therapieën en een betere prognose hebben (recent beschreven in Otani et al., 2016), wat het belang onderschrijft van de mogelijkheid onderscheid te kunnen maken tussen beide typen tumoren (Hoofdstuk 3).

Hersentumoren bestaan naast hersenweefsel ook uit witte bloedcellen, die verantwoordelijk zijn voor soms wel 30% van de tumormassa (Roggendorf et al.,

1996). Deze cellen (myeloïde infiltraten) lijken erg op microglia, cellen die al in de hersenen aanwezig zijn. In dit proefschrift is een protocol beschreven om microglia en geïnfiltrateerde myeloïde cellen te isoleren en op te zuiveren tot pure cel populaties (Hoofdstuk 4). Met behulp van deze methode is uit een groot cohort mensen, na overlijden, de microglia geïsoleerd. Van deze microglia is een gen expressie profiel gegenereerd (Hoofdstuk 5). De expressie van microglia genen is in kaart gebracht door middel van RNA sequencing. Humane microglia lijken erg op microglia van muizen, maar hebben een zeer ander verouderingsprofiel. Menselijke microglia laten een verandering zien in genen die betrokken zijn bij cel beweging. Mogelijk verminderd bij menselijke microglia tijdens veroudering het vermogen te bewegen, naar bijvoorbeeld gebieden met schade. In hersentumoren, worden behalve microglia ook witte bloedcellen aangetroffen. Of en hoe deze cellen bijdragen aan de tumor is onduidelijk. Met behulp van de in Hoofdstuk 4 beschreven methode zijn microglia en myeloïde infiltraten geïsoleerd uit verschillende typen hersentumoren en hun gen expressie profielen in kaart gebracht. De verschillen in genexpressie tussen gliomen humane microglia zijn bepaald, evenals verschillen in gen expressie in microglia verkregen uit laaggradige gliomen enerzijds en glioblastomen anderzijds. We hebben een netwerk van transcriptie regulatoren geïdentificeerd dat betrokken is bij cel proliferatie, cel beweging, en bij extracellulaire matrix, in het meest kwaadaardige, mesenchymale, GBM subtype. Onze bevindingen wijzen op een rol voor microglia in de invasieve eigenschappen van GBM en belichten hun potentie als complementaire doelwitten in de behandeling van GBM.

In dit proefschrift zijn de gangbare genetische methoden voor het bestuderen van gliomen onderzocht, en de belangrijke rol van moleculair karakteriseren is bevestigd. Daarnaast hebben we onze studies uitgebreid naar microglia, door eerst microglia uit menselijke hersenen zonder tumoren te bestuderen en later door microglia te bestuderen die uit gliomen zijn verkregen. Onze data tonen aan dat gen expressie profielen van humane microglia veranderen als gevolg van veroudering en in hersentumoren.

Vele aspecten van de progressie van gliomen zijn nog onbekend. Wij hebben hier aangetoond dat de heterogeniteit in deze tumoren niet beperkt is tot de tumor cellen zelf maar dat ook andere cellen, zoals de microglia, in de tumor heterogeen zijn. Het genereren van gen expressie profielen op individueel cel niveau zou leiden tot een beter begrip hoe deze cellen beïnvloedt zijn door de tumor cellen en hoe ze op hun

beurt de tumor cellen beïnvloeden. Recente proteomics (eiwit) data van individuele cellen van solide tumoren, waaronder gliomen, toonden aan dat verschillende cel populaties in een tumor aanwezig waren (Leelatian et al., 2017). Een combinatie van next generation sequencing en proteomics zou een elegante en complementaire strategie zijn om tumor heterogeniteit nader en preciezer in kaart te brengen.

In een recente moleculaire studie aan een groot cohort gliomen zijn specifieke signaleringsroutes gevonden die aan epigenetische controle mechanismen gelinkt lijken (Ceccarelli et al., 2016). Epigenetische veranderingen, zoals histon modificaties en complexen die chromatine structuren moduleren, spelen een rol in gen expressie regulatie. Bij dit mechanisme zijn eiwitten betrokken die epigenetische veranderingen “lezen”, “schrijven” en “verwijderen” (Mehta and Jeffrey, 2015). Deze veranderingen zijn relevant voor glioom classificatie en worden gezien als essentieel om therapeutische strategieën te bepalen (Reifenberger et al., 2016). In myeloïde cellen zijn epigenetische veranderingen nauw gerelateerd met het micromilieu, zoals is waargenomen bij microglia en andere weefselmacrofagen (Gosselin et al., 2014; Lavin et al., 2014), en meer recent, bij humane macrofagen (Schmidt et al., 2016). Studies naar epigenetische veranderingen in humane microglia of tumor-geassocieerde macrofagen zijn nog niet uitgevoerd.

Een andere, nog niet geadresseerde vraag, is hoe verschillend microglia zijn in verschillende menselijke hersengebieden. In de muis zijn regionale verschillen in microglia vastgesteld (Grabert et al., 2016), en ook in de mens is hersenweefsel van verschillende gebieden heterogeen (Hawrylycz et al., 2012; Oldham et al., 2008). Omdat tumoren kunnen ontstaan in verschillende hersengebieden, zou een beter begrip van de eigenschappen van microglia in verschillende hersengebieden kunnen bijdragen aan inzicht in de wijze en mate waarin deze cellen bijdragen aan tumorvorming en groei.

Het wetenschappelijke veld is in een tijd aangekomen waarin bevindingen sneller tot klinische toepassingen kunnen leiden. De focus in kankeronderzoek is nu naast de tumorcellen zelf, ook gericht op de rol van het micromilieu. De resultaten van deze aanpak zal ons fundamentele begrip van het ontstaan en groei van tumoren doen toenemen met mogelijke nieuwe en innovatieve therapieën als gevolg.

REFERENTIES

Askew, K., Li, K., Olmos-Alonso, A., Garcia-Moreno, F., Liang, Y., Richardson, P., Tipton, T., Chapman, M.A., Riecken, K., Beccari, S., et al. (2017). Coupled Proliferation and Apoptosis Maintain the Rapid Turnover of Microglia in the Adult Brain. *Cell Rep.* *18*, 391–405.

Balbous, A., Cortes, U., Guilloteau, K., Villalva, C., Flamant, S., Gaillard, A., Milin, S., Wager, M., Sorel, N., Guilhot, J., et al. (2014). A mesenchymal glioma stem cell profile is related to clinical outcome. *Oncogenesis* *3*, e91.

Becher, B., and Antel, J.P. (1996). Comparison of phenotypic and functional properties of immediately ex vivo and cultured human adult microglia. *Glia* *18*, 1–10.

Bennett, M.L., Bennett, F.C., Liddelow, S.A., Ajami, B., Zamanian, J.L., Fernhoff, N.B., Mulinyawe, S.B., Bohlen, C.J., Adil, A., Tucker, A., et al. (2016). New tools for studying microglia in the mouse and human CNS. *Proc. Natl. Acad. Sci. U. S. A.* *113*, E1738–E1746.

Blandin, A.-F., Noulet, F., Renner, G., Mercier, M.-C., Choulier, L., Vauchelles, R., Ronde, P., Carreiras, F., Etienne-Selloum, N., Vereb, G., et al. (2016). Glioma cell dispersion is driven by $\alpha 5$ integrin-mediated cell-matrix and cell-cell interactions. *Cancer Lett.* *376*, 328–338.

Brennan, C.W., Verhaak, R.G.W., McKenna, A., Campos, B., Noushmehr, H., Salama, S.R., Zheng, S., Chakravarty, D., Sanborn, J.Z., Berman, S.H., et al. (2013). The somatic genomic landscape of glioblastoma. *Cell* *155*, 462–477.

Butovsky, O., Jedrychowski, M.P., Moore, C.S., Cialic, R., Lanser, A.J., Gabriely, G., Koeglsperger, T., Dake, B., Wu, P.M., Doykan, C.E., et al. (2014). Identification of a unique TGF- β -dependent molecular and functional signature in microglia. *Nat. Neurosci.* *17*, 131–143.

Cancer Genome Atlas Research Network, Brat, D.J., Verhaak, R.G.W., Aldape, K.D., Yung, W.K.A., Salama, S.R., Cooper, L.A.D., Rheinbay, E., Miller, C.R., Vitucci, M., et al. (2015). Comprehensive, Integrative Genomic Analysis of Diffuse Lower-Grade Gliomas. *N. Engl. J. Med.* *372*, 2481–2498.

Carro, M.S., Lim, W.K., Alvarez, M.J., Bollo, R.J., Zhao, X., Snyder, E.Y., Sulman, E.P., Anne, S.L., Doetsch, F., Colman, H., et al. (2010). The transcriptional network for mesenchymal transformation of brain tumours. *Nature* *463*, 318–325.

Ceccarelli, M., Barthel, F.P., Malta, T.M., Sabedot, T.S., Salama, S.R., Murray, B.A., Morozova, O., Newton, Y., Radenbaugh, A., Pagnotta, S.M., et al. (2016). Molecular

Profiling Reveals Biologically Discrete Subsets and Pathways of Progression in Diffuse Glioma. *Cell* 164, 550–563.

Chevyreva, I., Faull, R.L.M., Green, C.R., and Nicholson, L.F.B. (2008). Assessing RNA quality in postmortem human brain tissue. *Exp. Mol. Pathol.* 84, 71–77.

Cloughesy, T.F., Cavenee, W.K., and Mischel, P.S. (2014). Glioblastoma: from molecular pathology to targeted treatment. *Annu. Rev. Pathol.* 9, 1–25.

Colin, C., Baeza, N., Bartoli, C., Fina, F., Eudes, N., Nanni, I., Martin, P.-M., Ouafik, L., and Figarella-Branger, D. (2006). Identification of genes differentially expressed in glioblastoma versus pilocytic astrocytoma using Suppression Subtractive Hybridization. *Oncogene* 25, 2818–2826.

Davalos, D., Grutzendler, J., Yang, G., Kim, J.V., Zuo, Y., Jung, S., Littman, D.R., Dustin, M.L., and Gan, W.-B. (2005). ATP mediates rapid microglial response to local brain injury in vivo. *Nat. Neurosci.* 8, 752–758.

Dunn, G.P., Rinne, M.L., Wykosky, J., Genovese, G., Quayle, S.N., Dunn, I.F., Agarwalla, P.K., Chheda, M.G., Campos, B., Wang, A., et al. (2012). Emerging insights into the molecular and cellular basis of glioblastoma. *Genes Dev.* 26, 756–784.

Durrenberger, P.F., Fernando, S., Kashefi, S.N., Ferrer, I., Hauw, J.-J., Seilhean, D., Smith, C., Walker, R., Al-Sarraj, S., Troakes, C., et al. (2010). Effects of antemortem and postmortem variables on human brain mRNA quality: a BrainNet Europe study. *J. Neuropathol. Exp. Neurol.* 69, 70–81.

a Dzaye, O.D., Hu, F., Derkow, K., Haage, V., Euskirchen, P., Harms, C., Lehnardt, S., Synowitz, M., Wolf, S.A., and Kettenmann, H. (2016). Glioma Stem Cells but Not Bulk Glioma Cells Upregulate IL-6 Secretion in Microglia/Brain Macrophages via Toll-like Receptor 4 Signaling. *J. Neuropathol. Exp. Neurol.* 75, 429–440.

Ervin, J.F., Heinzen, E.L., Cronin, K.D., Goldstein, D., Szymanski, M.H., Burke, J.R., Welsh-Bohmer, K.A., and Hulette, C.M. (2007). Postmortem delay has minimal effect on brain RNA integrity. *J. Neuropathol. Exp. Neurol.* 66, 1093–1099.

Ferrari, D., McNamee, E.N., Idzko, M., Gambari, R., and Eltzschig, H.K. (2016). Purinergic Signaling During Immune Cell Trafficking. *Trends Immunol.* 37, 399–411.

Filbin, M.G., and Suvà, M.L. (2016). Gliomas Genomics and Epigenomics: Arriving at the Start and Knowing It for the First Time. *Annu. Rev. Pathol.* 11, 497–521.

Foote, M.B., Papadopoulos, N., and Diaz, L.A. (2015). Genetic Classification of Gliomas: Refining Histopathology. *Cancer Cell* 28, 9–11.

Fridman, W.H., Pagès, F., Sautès-Fridman, C., and Galon, J. (2012). The immune contexture in human tumours: impact on clinical outcome. *Nat. Rev. Cancer* 12, 298–306.

Glass, R., and Synowitz, M. (2014). CNS macrophages and peripheral myeloid cells in brain tumours. *Acta Neuropathol. (Berl.)* 128, 347–362.

Gosselin, D., Link, V.M., Romanoski, C.E., Fonseca, G.J., Eichenfield, D.Z., Spann, N.J., Stender, J.D., Chun, H.B., Garner, H., Geissmann, F., et al. (2014). Environment Drives Selection and Function of Enhancers Controlling Tissue-Specific Macrophage Identities. *Cell* 159, 1327–1340.

Grabert, K., Michoel, T., Karavolos, M.H., Clohisey, S., Baillie, J.K., Stevens, M.P., Freeman, T.C., Summers, K.M., and McColl, B.W. (2016). Microglial brain region-dependent diversity and selective regional sensitivities to aging. *Nat. Neurosci.* 19, 504–516.

Hambardzumyan, D., Gutmann, D.H., and Kettenmann, H. (2016). The role of microglia and macrophages in glioma maintenance and progression. *Nat. Neurosci.* 19, 20–27.

Hanahan, D. (2014). Rethinking the war on cancer. *Lancet Lond. Engl.* 383, 558–563.

Hawrylycz, M.J., Lein, E.S., Guillozet-Bongaarts, A.L., Shen, E.H., Ng, L., Miller, J.A., van de Lagemaat, L.N., Smith, K.A., Ebbert, A., Riley, Z.L., et al. (2012). An anatomically comprehensive atlas of the adult human brain transcriptome. *Nature* 489, 391–399.

Hickman, S.E., Kingery, N.D., Ohsumi, T.K., Borowsky, M.L., Wang, L., Means, T.K., and El Khoury, J. (2013). The microglial sensome revealed by direct RNA sequencing. *Nat. Neurosci.* 16, 1896–1905.

Holtman, I.R., Raj, D.D., Miller, J.A., Schaafsma, W., Yin, Z., Brouwer, N., Wes, P.D., Möller, T., Orre, M., Kamphuis, W., et al. (2015). Induction of a common microglia gene expression signature by aging and neurodegenerative conditions: a co-expression meta-analysis. *Acta Neuropathol. Commun.* 3, 31.

Kamoun, A., Idbah, A., Dehais, C., Elarouci, N., Carpentier, C., Letouzé, E., Colin, C., Mokhtari, K., Jouvet, A., Uro-Coste, E., et al. (2016). Integrated multi-omics analysis of oligodendroglial tumours identifies three subgroups of 1p/19q co-deleted gliomas. *Nat. Commun.* 7, 11263.

Kierdorf, K., Erny, D., Goldmann, T., Sander, V., Schulz, C., Perdiguero, E.G., Wieghofer, P., Heinrich, A., Riemke, P., Hölscher, C., et al. (2013). Microglia emerge from

erythromyeloid precursors via Pu.1- and Irf8-dependent pathways. *Nat. Neurosci.* *16*, 273–280.

Kling, T., Ferrarese, R., Ó hAilín, D., Johansson, P., Heiland, D.H., Dai, F., Vasilikos, I., Weyerbrock, A., Jörnsten, R., Carro, M.S., et al. (2016). Integrative Modeling Reveals Annexin A2-mediated Epigenetic Control of Mesenchymal Glioblastoma. *EBioMedicine* *12*, 72–85.

Lavin, Y., Winter, D., Blecher-Gonen, R., David, E., Keren-Shaul, H., Merad, M., Jung, S., and Amit, I. (2014). Tissue-Resident Macrophage Enhancer Landscapes Are Shaped by the Local Microenvironment. *Cell* *159*, 1312–1326.

Leelatian, N., Doxie, D.B., Greenplate, A.R., Mobley, B.C., Lehman, J.M., Sinnaeve, J., Kauffmann, R.M., Werkhaven, J.A., Mistry, A.M., Weaver, K.D., et al. (2017). Single cell analysis of human tissues and solid tumors with mass cytometry. *Cytometry B Clin. Cytom.* *92*, 68–78.

Louis, D.N., Perry, A., Reifenberger, G., von Deimling, A., Figarella-Branger, D., Cavenee, W.K., Ohgaki, H., Wiestler, O.D., Kleihues, P., and Ellison, D.W. (2016). The 2016 World Health Organization Classification of Tumors of the Central Nervous System: a summary. *Acta Neuropathol. (Berl.)* *131*, 803–820.

Maule, F., Bresolin, S., Rampazzo, E., Boso, D., Della Puppa, A., Esposito, G., Porcù, E., Mitola, S., Lombardi, G., Accordi, B., et al. (2016). Annexin 2A sustains glioblastoma cell dissemination and proliferation. *Oncotarget* *7*, 54632–54649.

Mehta, S., and Jeffrey, K.L. (2015). Beyond receptors and signaling: epigenetic factors in the regulation of innate immunity. *Immunol. Cell Biol.* *93*, 233–244.

Melief, J., Koning, N., Schuurman, K.G., Van De Garde, M.D.B., Smolders, J., Hoek, R.M., Van Eijk, M., Hamann, J., and Huitinga, I. (2012). Phenotyping primary human microglia: tight regulation of LPS responsiveness. *Glia* *60*, 1506–1517.

Meyer, M., Reimand, J., Lan, X., Head, R., Zhu, X., Kushida, M., Bayani, J., Pressey, J.C., Lionel, A.C., Clarke, I.D., et al. (2015). Single cell-derived clonal analysis of human glioblastoma links functional and genomic heterogeneity. *Proc. Natl. Acad. Sci.* *112*, 851–856.

Muffat, J., Li, Y., Yuan, B., Mitalipova, M., Omer, A., Corcoran, S., Bakiasi, G., Tsai, L.-H., Aubourg, P., Ransohoff, R.M., et al. (2016). Efficient derivation of microglia-like cells from human pluripotent stem cells. *Nat. Med.* *22*, 1358–1367.

Nimmerjahn, A., Kirchhoff, F., and Helmchen, F. (2005). Resting microglial cells are highly dynamic surveillants of brain parenchyma in vivo. *Science* *308*, 1314–1318.

Olah, M., Raj, D., Brouwer, N., De Haas, A.H., Eggen, B.J.L., Den Dunnen, W.F.A., Biber, K.P.H., and Boddeke, H.W.G.M. (2012). An optimized protocol for the acute isolation of human microglia from autopsy brain samples. *Glia* 60, 96–111.

Oldham, M.C., Konopka, G., Iwamoto, K., Langfelder, P., Kato, T., Horvath, S., and Geschwind, D.H. (2008). Functional organization of the transcriptome in human brain. *Nat. Neurosci.* 11, 1271–1282.

Ostrom, Q.T., Gittleman, H., Fulop, J., Liu, M., Blanda, R., Kromer, C., Wolinsky, Y., Kruchko, C., and Barnholtz-Sloan, J.S. (2015). CBTRUS Statistical Report: Primary Brain and Central Nervous System Tumors Diagnosed in the United States in 2008-2012. *Neuro-Oncol.* 17 Suppl 4, iv1-iv62.

Otani, R., Uzuka, T., and Ueki, K. (2016). Classification of adult diffuse gliomas by molecular markers-a short review with historical footnote. *Jpn. J. Clin. Oncol.*

Parsons, D.W., Jones, S., Zhang, X., Lin, J.C.-H., Leary, R.J., Angenendt, P., Mankoo, P., Carter, H., Siu, I.-M., Gallia, G.L., et al. (2008). An integrated genomic analysis of human glioblastoma multiforme. *Science* 321, 1807–1812.

Patel, A.P., Tirosch, I., Trombetta, J.J., Shalek, A.K., Gillespie, S.M., Wakimoto, H., Cahill, D.P., Nahed, B.V., Curry, W.T., Martuza, R.L., et al. (2014). Single-cell RNA-seq highlights intratumoral heterogeneity in primary glioblastoma. *Science* 344, 1396–1401.

Phillips, H.S., Kharbanda, S., Chen, R., Forrest, W.F., Soriano, R.H., Wu, T.D., Misra, A., Nigro, J.M., Colman, H., Soroceanu, L., et al. (2006). Molecular subclasses of high-grade glioma predict prognosis, delineate a pattern of disease progression, and resemble stages in neurogenesis. *Cancer Cell* 9, 157–173.

Preusser, M., Lim, M., Hafler, D.A., Reardon, D.A., and Sampson, J.H. (2015). Prospects of immune checkpoint modulators in the treatment of glioblastoma. *Nat. Rev. Neurol.* 11, 504–514.

Prinz, M., and Priller, J. (2017). The role of peripheral immune cells in the CNS in steady state and disease. *Nat. Neurosci.* 20, 136–144.

Raj, D.D.A., Moser, J., van der Pol, S.M.A., van Os, R.P., Holtman, I.R., Brouwer, N., Oeseburg, H., Schaafsma, W., Wesseling, E.M., den Dunnen, W., et al. (2015). Enhanced microglial pro-inflammatory response to lipopolysaccharide correlates with brain infiltration and blood-brain barrier dysregulation in a mouse model of telomere shortening. *Aging Cell.*

Reifenberger, G., Wirsching, H.-G., Knobbe-Thomsen, C.B., and Weller, M. (2016). Advances in the molecular genetics of gliomas - implications for classification and therapy. *Nat. Rev. Clin. Oncol.*

Roggendorf, W., Strupp, S., and Paulus, W. (1996). Distribution and characterization of microglia/macrophages in human brain tumors. *Acta Neuropathol. (Berl.)* 92, 288–293.

Rustenhoven, J., Park, T.I.-H., Schweder, P., Scotter, J., Correia, J., Smith, A.M., Gibbons, H.M., Oldfield, R.L., Bergin, P.S., Mee, E.W., et al. (2016). Isolation of highly enriched primary human microglia for functional studies. *Sci. Rep.* 6, 19371.

Schmidt, S.V., Krebs, W., Ulas, T., Xue, J., Baßler, K., Günther, P., Hardt, A.-L., Schultze, H., Sander, J., Klee, K., et al. (2016). The transcriptional regulator network of human inflammatory macrophages is defined by open chromatin. *Cell Res.* 26, 151–170.

Segerman, A., Niklasson, M., Haglund, C., Bergström, T., Jarvius, M., Xie, Y., Westermark, A., Sönmez, D., Hermansson, A., Kastemar, M., et al. (2016). Clonal Variation in Drug and Radiation Response among Glioma-Initiating Cells Is Linked to Proneural-Mesenchymal Transition. *Cell Rep.* 17, 2994–3009.

Serres, E., Debarbieux, F., Stanchi, F., Maggiorella, L., Grall, D., Turchi, L., Burel-Vandenbos, F., Figarella-Branger, D., Virolle, T., Rougon, G., et al. (2014). Fibronectin expression in glioblastomas promotes cell cohesion, collective invasion of basement membrane in vitro and orthotopic tumor growth in mice. *Oncogene* 33, 3451–3462.

Sielska, M., Przanowski, P., Wylot, B., Gabrusiewicz, K., Maleszewska, M., Kijewska, M., Zawadzka, M., Kucharska, J., Vinnakota, K., Kettenmann, H., et al. (2013). Distinct roles of CSF family cytokines in macrophage infiltration and activation in glioma progression and injury response. *J. Pathol.* 230, 310–321.

Smith, A.M., and Dragunow, M. (2014). The human side of microglia. *Trends Neurosci.* 37, 125–135.

Spaethling, J.M., Na, Y.-J., Lee, J., Ulyanova, A.V., Baltuch, G.H., Bell, T.J., Brem, S., Chen, H.I., Dueck, H., Fisher, S.A., et al. (2017). Primary Cell Culture of Live Neurosurgically Resected Aged Adult Human Brain Cells and Single Cell Transcriptomics. *Cell Rep.* 18, 791–803.

Stieber, D., Golebiewska, A., Evers, L., Lenkiewicz, E., Brons, N.H.C., Nicot, N., Oudin, A., Bougnaud, S., Hertel, F., Bjerkvig, R., et al. (2014). Glioblastomas are composed of genetically divergent clones with distinct tumourigenic potential and variable stem cell-associated phenotypes. *Acta Neuropathol. (Berl.)* 127, 203–219.

Stupp, R., Mason, W.P., van den Bent, M.J., Weller, M., Fisher, B., Taphoorn, M.J.B., Belanger, K., Brandes, A.A., Marosi, C., Bogdahn, U., et al. (2005). Radiotherapy plus concomitant and adjuvant temozolomide for glioblastoma. *N. Engl. J. Med.* *352*, 987–996.

Tirosh, I., Venteicher, A.S., Hebert, C., Escalante, L.E., Patel, A.P., Yizhak, K., Fisher, J.M., Rodman, C., Mount, C., Filbin, M.G., et al. (2016). Single-cell RNA-seq supports a developmental hierarchy in human oligodendroglioma. *Nature* *539*, 309–313.

Van Obberghen-Schilling, E., Tucker, R.P., Saupe, F., Gasser, I., Cseh, B., and Orend, G. (2011). Fibronectin and tenascin-C: accomplices in vascular morphogenesis during development and tumor growth. *Int. J. Dev. Biol.* *55*, 511–525.

Verhaak, R.G.W., Hoadley, K.A., Purdom, E., Wang, V., Qi, Y., Wilkerson, M.D., Miller, C.R., Ding, L., Golub, T., Mesirov, J.P., et al. (2010). Integrated genomic analysis identifies clinically relevant subtypes of glioblastoma characterized by abnormalities in PDGFRA, IDH1, EGFR, and NF1. *Cancer Cell* *17*, 98–110.

Wehrspaun, C.C., Haerty, W., and Ponting, C.P. (2015). Microglia recapitulate a hematopoietic master regulator network in the aging human frontal cortex. *Neurobiol. Aging* *36*, 2443.e9-2443.e20.

Xia, S., Lal, B., Tung, B., Wang, S., Goodwin, C.R., and Laterra, J. (2016). Tumor microenvironment tenascin-C promotes glioblastoma invasion and negatively regulates tumor proliferation. *Neuro-Oncol.* *18*, 507–517.

Zhang, I., Alizadeh, D., Liang, J., Zhang, L., Gao, H., Song, Y., Ren, H., Ouyang, M., Wu, X., D'Apuzzo, M., et al. (2016a). Characterization of Arginase Expression in Glioma-Associated Microglia and Macrophages. *PloS One* *11*, e0165118.

Zhang, Y., Sloan, S.A., Clarke, L.E., Caneda, C., Plaza, C.A., Blumenthal, P.D., Vogel, H., Steinberg, G.K., Edwards, M.S.B., Li, G., et al. (2016b). Purification and Characterization of Progenitor and Mature Human Astrocytes Reveals Transcriptional and Functional Differences with Mouse. *Neuron* *89*, 37–53.

ACKNOWLEDGEMENTS

The end of this journey is also the time to appreciate and be thankful to all the amazing people that were part of my life during this period. PhD can be an arduous affair, made even harder for someone so far from home. For me, having the people from the Medical Physiology by my side was crucial for the success of this ordeal. Nonetheless, none of this would be possible if it was not for the unconditional support I had from back home. I would like to show my gratitude towards my promoters, colleagues, co-workers, collaborators, friends and family.

Dear **dr. Bart Eggen**, the title of supervisor does not suit you at all. You were much more than that. You assured my well-being and provided all that was necessary to ensure the best of environments for us all. I value all of our talks, the professional and the not-so-professional ones. Thank you for the spot-on advices, for being an example to be followed, for your trust and the great time we had together. I am glad to see that our relationship has developed into friendship.

Dear **Prof. dr. Erik Boddeke**, I would like to begin thanking you for all the support you always gave me. My successful time here in The Netherlands was only possible due to your encouragement and acceptance. Your trust in the potential of our collaboration was the key for all the current accomplishments. I hope we can continue on this track. Once again, thank you.

Dear **Prof. dr. Suely Marie**, you were the great supporter of this odyssey. Without your faith in me and everlasting backup, we would have never gotten this far. I thank you for all the past opportunities that helped build the foundations of my career. I particularly would like to thank you for the chance to develop myself professionally and personally in an international environment. I am very grateful to have been given the chance and I hope to have represented your lab and your precepts of more than ten years accordingly.

Dear **Nieske Brouwer**, what would I have done without you? Thank you for your great support and understanding on all matters. You once said you fill your days with helping students, that you are happy when others are happy. There isn't a truer statement. You have welcomed my family and has helped me on both sides of the Atlantic. You (and **Jan!**) are great individuals, very special to me and I am sure we will meet many times again for more fruitful projects.

Dear **Prof. dr. Jon Laman**, it was a pleasure having met you and working with you. Thank you for all your valuable lessons, for making yourself always available and

ready to assist, and for your contagious enthusiasm for sharing knowledge. I hope we keep in touch and expand our collaboration.

Dear **dr. Sueli Mieko Oba-Shinjo**, you have also been with me for more than ten years and a part of my professional formation. Thank you for your patience, guidance and assistance with all associated matters. I owe you a few “ghostly souls” from all your help. I am certain that you will overcome yet this other obstacle in your life and will come out of it successful. I wish that you stay well.

Dear **dr. Antonio Marcondes Lerario**, I thank you for your crucial assistance when we needed the most. Your willingness to help and your patience have made this work what it is today. Thank you.

I would like to show my appreciation for all the staff members and colleagues of the Medical Physiology department that, somehow, made the development of this work possible and even more pleasant. **dr. Armagan Kocer**, it was great to share witty comments and laughs with you. Thank you for opening your house for us and for introducing your family. **dr. Sjef Copray**, it was great to see your enthusiasm with your trip to Brasil. I hope you are enjoying your retirement and that you never lose your sense of dark humor. **dr. Rob Bakels**, our meetings in the hallway always caused me to smile. Thank you for always being such a nice, understanding person with this “peculiar” Brazilian. **Ellie Eggens-Meijer**, dear Ellie, I enjoyed working with you a lot. I think we made a great team. Thank you for teaching me the first steps into the microglia world. Having you by my side early on made all the difference. I wish you all the best! **Evelyn Wesseling**, Eef, it was great to follow you on your path to motherhood and see you become the mother of two gorgeous children. I thank you for all the assistance you gave me whenever it was needed. **dr. Hilmar van Weering**, our nerdy talks were wonderful, and your talents with Adobe Illustrator still amaze me. Thank you for sharing the passion with coffee, the extensive ebook list you provided me and all the support on editing the figures for our publication. **Michel Meijer**, you were for times the only one who understood my taste in (loud) rock music. I really enjoyed these moments, your support on day-to-day life in the lab and the laughs we shared during breaks and lunch hours. **Harry Moes** and **Hank Heidekamp**, thank you for your essential support on all administration matters, and for always handling such things with humor and lightness. **Trix van der Sluis**, my dearest Trix, you were great and welcoming from day one. You were always available and eager to help when help was needed. Thanks for all your smiles and laughs, and for putting up with all the noise from our room! I would also like to recognize **Loes Drenth**, **Tjalling Nijboer**, **dr. Inge**

Zijdewind, dr. Wieb Patberg, Ietje Manting-Otter, Roelof Jan, Geert and Henk and dr. Hiske van Duinen. Thank you for being part of this important period of my professional and personal life.

From the Neurology Department in Brazil, I would like to recognize staff members **Amanda, Luiz, Rosa, Nice, Eliene** and **Marcia**. I particularly want to thank **Gisele Reis** and **Paula Sola**. Gisele, your help with preparing and organizing the tumor samples for genotyping was crucial for the execution of this work. You are an excellent professional a dear friend. Paula “conjuja”, your help with library prep has made this study possible. Your presence in the lab was important for me and I miss our daily interactions. I hope you have found yourself in your new career and I wish you the best

As mentioned before, I am a believer that science is, above all else, about people. As a PhD, the closest people are your fellow PhDs, post-docs and students – both in The Netherlands and in Brazil – that share the lab, the experiments, the good and the bad of our work routine. My most genuine gratitude goes to these people. **dr. Ilia Vainchtein**, Illia, Microllia, and so many others, my co-author, lab and mischief partner, I owe much of what I have accomplished to you. You were the best of colleagues and now a great friend. We are oceans apart, completely different individuals, and still can keep a conversation about basically everything and anything. My days in the Netherlands were amazing and you were an important part of it. Thank you for your friendship, understanding, patience and assistance. **Koen van Zomeren**, aka the Batman, also a partner in mischief, my personal superhero for all associated matters. We had loads of fun, sharing both jokes and experiment tips. You are someone who is always willing to help and teach and I appreciate that. You’ve been through some dark times, facing it with strength and dignity. I hope to have been of some support to you, and that you find happiness and success. **dr. Duco Schriemer**, the constant presence during our tea/hot chocolate breaks. Our talks were always a pleasure to me, and our exchanges very therapeutic. Thank you for showing me that so different people can share so much. I hope you are doing great and I wish you all the best. **dr. Inge Holtman**, also my co-author and collaborator. I’ll miss popping up in your room and calling you “my darling”, only to hear “sweety” in return. It was an enlightening experience working with you. I appreciate our long talks and the time we spent together. I wish you all the success! **dr. Divya Raj**, you were very important when I had just gotten to the lab, I hope you have found fulfillment on both your personal and professional life. **dr. Su Ping Peng**, you were always kind and very easy-going person. I enjoyed our talks and social gatherings very much. Thank you for your help with the

first pilot of our animal model experiment! **dr. Zhuoran Yin**, dear Zhu, you are one of the nicest people I have ever known. It is always easy to talk to you and I enjoyed all the moments we shared. Good luck on your career and all the best to your growing family. **Marissa Dubbelaar**, I had the feeling you were going to be a great professional, I think I was right. You are a lovely person and the little time we spent together was a blast. Good luck and I hope we get to collaborate in the future. **Betty Hornix**, the Master Minion, I always thought you were a prodigy. It is great to see you succeeding. I had a lot of fun with our nerdy talks during breaks and social gatherings. I wish you all the best. **Wandert Schaafsma**, your humor and positive attitude are contagious. I had lots of fun with you. Best of luck in Spain! **dr. Marcin Czepiel**, you were also a source of great fun and mischief for the time we spent together. Your stories still make me laugh, and your PhD party was one to remember. Best of luck in Poland! **dr. Susanne Kooistra**, it was great meeting and sharing the lab with you. Thank you for the advices you gave me and for setting an example of women in Science. **dr. Thaiany Quevedo Melo**, amiga! This road would have been a lot harder if it wasn't for you. Your presence grounded me on many occasions and gave that warm feeling we only get when we are back home. Thank you for all your support and friendship. **Clarissa Haas**, I appreciate the moments we shared a lot. It was a lot of fun and important for me. I wish you all the best and good luck with finishing your PhD! **dr. Kumar Balasubramanian**, thank you for all your support and assistance with the early phases of this PhD project. I wish you the best of luck in your career. **Xiaoming Zhang**, you were always a friendly colleague and a nice person. Your innocent humor was the source of lots of fun along the way. I wish you all the happiness to you and your family. **dr. Ria Wolkorte**, our talks were always fun and light. You are a very agreeable person and I hope we meet again. **Claudio Tiecher**, one of the funniest additions to the lab, your sharp humor made my days more enjoyable. Good luck with everything! **Javier Villamil**, we also had a great time on the short period we were together at the lab. I wish you all the success with finishing your PhD. **dr. Ming-san Ma**, **dr. Zhilin Luan**, **dr. Duygu Yilmaz**, **Sabrina Jacobs**, **Martjin** and **Linda Hoes**, thank you for making this experience so great! **Isabele Moretti**, the queen of elves, you have made possible for me to teach as much as to learn. You have a brilliant future ahead of you. I am a great supporter and enthusiast of your work. Thank you for the essential help you always gave and give me, and for making the lab routine so fun. **Mariana Molina**, your eagerness to help and to learn will get you far. Your empathy to people around you are captivating. Keep on spreading good vibes around you and your good work. Your assistance has been imperative in all

senses. **Stella Gonçalves**, another little (very little) prodigy, your enthusiasm with all things Science-related is contagious. You bring new energy to our daily routine. Future is bright and I hope to be there to applaud. **Vanessa Galdeno**, your calm demeanor has brushed a little on me. I admire your ability to not let yourself be affected by stress. You have assisted me on many occasions and was a part of the execution of this work. Thank you very much and I am sure you will have a very successful career ahead of you! **dr. Carlos E. Brantis**, you have tremendously helped people the moment you entered the lab. Your willingness to do so is admirable. Thank you for all your support. **Tulio Pereira** and **dr. Priscilla Costa**, your help with the FACs experiments was crucial. Thank you for always being so excited about the experiments, and for making the long hours much funnier. My sincere gratitude to **dr. Roseli Silva**, **dr. Daiane Franco**, **Lais Cavalca**, **Fernanda Serachi**, **Clarisse Nunes**, **Talita Laurentino**, **Ticiane Batista**, **Samuel Leith** and **Tawany Carvalho** you have made the working environment a place we feel at ease and have fun. Thank you for your daily support.

My paranympths, **Rianne van der Pijl** and **Corien Grit** (and the three of us together: **the holy Trinity**, **the Minion Girls**). Dearest Rianne, you are one of those friends that makes distance matter very little. You have made me feel welcome and at ease, and always found a way to make me (and others) feel good about themselves. I hold you very dearly in my heart and I hope you find happiness in your life as much as you bring to others. Dearest Corien, I am thankful for the familiarity and friendship we share. We had so, so much fun together, an easy connection that is hard to find. You also have a special place in my heart and I wish you everything that best in your future. I have tried before to express my appreciation for all you have done for me and I'll try again: **thank you**, I could not have done this without you. I miss you!

Friendship is one of the foundations upon which we build our lives on. I immensely appreciate the friends that have supported me on this road, mostly without fully grasping what it all meant, but just happy to see me accomplishing a dream. **Rodrigo Farah**, my partner in crime for more than twenty years, I thank you for unconditional and everlasting support. I came back, you see! **Franciele Machado**, you always know when I need a friendly word and your understanding – sometimes almost telekinetic – of the ordeals that I faced were crucial for my well-being. Thank you for your support decades-old friendship. **Miri Becker**, my roommate, you were the best surprise when I arrived in Holland. Your openness and welcoming demeanor gave the support I needed to go on with this plan. I am very proud of all you have accomplished, of your courage and your enthusiasm with the world and, mostly, of our friendship. We

will meet again many times. Thank you for being such a great person! **Daniele Barbosa, Bruna Carvalho, Diego Melo, Matheus Ramires, Thiago Veloso, Rafael Lopes**, the times we spent together gave me the necessary energy to continue with the work. Thank You! **Ester Bertoldi**, you were also one of the great enthusiasts of this dream, encouraging me to move forward and helping me with many of the little (and big) problems that came along the way. Thank you for the times you were there when I needed, there were plenty. I did it! I wish only good things in your life.

And finally, my family. Ever present and always, always supportive. You make my life feel like a gift every day. I am today what you have taught and allowed me to teach through all these years. Words are very little to express how much I am thankful and love you. My aunts and uncles, my cousins and godson, all in my heart. My bother-in-law, **Omar Curi**, always enthusiastic about traveling, thank you for all your help and tips! My niece, **Nasta Curi**, future lawyer, thank you for all the fun and the much-needed relaxation you provided. The lightness with which you take life inspires me to see life that way as well. My sisters, **Quica** and **Babinha**, you were strong supporters from the start. You have reassured me when I needed and have been with me every step of the way. **My mother**, mom, you did the hardest part: accepting my choices and being supportive without restrain. You once said I was very brave: it was only due to you. You were as courageous with me all the way. Without you, there would be nothing. And **my father**, my eternal inspiration. Thank you from the bottom of my heart. I love you all.

Thais Galatro
26th April 2017.